Hadrons in a finite volume and in a background field

Dissertation
zur
Erlangung des Doktorgrades (Dr. rer. nat.)
der
Mathematisch-Naturwissenschaftlichen Fakultät
der
Rheinischen Friedrich-Wilhelms-Universität Bonn

von
Jonathan Lozano de la Parra
aus
Ensenada, Mexiko

Bonn, 2023

Acknowledgements

Agradecimientos

Me gustaría agradecer al PD Dr. Akaki Rusetsky por dejarme ser parte de su grupo de investigación durante todos estos años. Sin duda ha sido una experiencia muy enriquecedora, no solo en el aspecto profesional sino también en el de vida. Su guía me ha servido para formarme en esta cautivadora área de la ciencia que es la física de partículas. De igual manera me encuentro agradecido con el Prof. Dr. Ulf-G. Meißner por apoyarme durante todo este trayecto que he tomado en mis estudios de posgrado. Le doy también las gracias a los doctores Andria Agadjanov, Jambul Gegelia y Fernando Romero-López por siempre estar al tanto de cualquier inconveniente que surgiera durante los proyectos que desarrollamos en conjunto.

Aprovecho también para darle las gracias a mi familia que siempre estuvo ahí desde el inicio de esta travesía en Alemania que ha tomado más de seis años. A mis padres, que desde joven apoyaron mi curiosidad de estudiar esta disciplina y que nunca dudaron en que podría realizar este sueño. A mi hermano, por auxiliar a mis padres en estos años de ausencia que no han sido fáciles, pero que hemos logrado superar con tu ayuda.

Muchísimas gracias a todas las amigas y amigos con los que compartí esta etapa de crecimiento y aprendizaje. Sin ustedes la vida aquí hubiera sido muy complicada, y seguramente muy aburrida. Estoy contento de poder haber coincidido con todos ustedes durante este breve tiempo y compartir incontables momentos que ahora se han convertido en lindas memorias que guardo con mucho cariño en el corazón. Saludos especiales a Juan, Daniel, Jula, Sven, Davit, Luca, Simon, Max, y por último a Cesar, que sin su invitación a la maestría en Bonn nada de esto hubiera sucedido.

Por último, agradezco produndamente al Consejo Nacional de Ciencia y Tecnología (CONACyT) y al Deutscher Akademischer Austauschdienst (DAAD) por financiar en conjunto mis estudios de posgrado en Alemania.

Abstract

In this cumulative thesis, we study various properties of hadrons in a finite volume. The motivation of this work is the following: The Quantum Chromodynamics (QCD) is a fundamental theory describing hadrons. The crucial property of QCD is that it is non-perturbative, i.e., the well-established method of perturbation theory cannot be fully applied, as in Quantum Electrodynamics. For this reason, an alternative framework must be put forward in order to address this subtlety of the theory. Lattice field theory provides a first-principle non-perturbative approach to solving QCD, where simulations of particle interactions take place on a lattice of finite size. Of course, working in a finite-sized box comes with its challenges, which must be addressed accordingly. Calculating the mismatch between the finite- and infinite-volume results is the main objective of this thesis.

Chapter 1 briefly introduces the reader to the main subjects that are discussed in the following chapters. In Chapter 2 the findings of our study of the doubly virtual nucleon Compton scattering in a finite volume are presented. In particular, we were interested in calculating the errors induced by working in a finite-sized box to certain physical quantities, e.g. the electric and magnetic polarizabilities and the so-called subtraction function. Since we started our calculations in an infinite volume, we were also able to extract infinite-volume results. To this end, Chiral Perturbation Theory, which is well suited for the study of this problem, was employed. The results of this study are of importance for the solving of long-standing physics problems, such as the proton-neutron mass difference.

The second work, presented in Chapter 3, deals with the study of resonance form factors on the lattice. These particles are unstable under the strong interactions and present a challenge when studied in a finite volume. For instance, the well-understood lattice quantum chromodynamics techniques for a single particle cannot be applied here. Development in this area has been very substantial in recent years, which can be attributed to the so-called Lüscher method and its extensions. The advantage of this approach is that it relates the QCD spectrum in a finite volume to the scattering amplitudes that are defined in the infinite volume. This powerful technique is what we used to study the form factors of resonances. In fact, we were able to expand this prescription to the case where an external field is present. With this, the calculation of the form factor of an unstable particle was performed.

Contents

Hadrons in a finite volume and in a background field

1.1 Introduction

In the last century, physics has been able to answer some of the most fundamental questions in nature. For example, what are the elementary constituents of matter? What is the nature of forces between them? Throughout the years, many models have been proposed to answer these challenging questions, but only a few managed to accurately explain what we observe in experiments. Currently, the most outstanding and successful of all the attempts to describe the very nature of our Universe are the Standard Model (SM) [1–6] and General Relativity (GR) [7, 8]. The dynamics of elementary particles and its interactions is well described by the SM while the deformation of space-time due to massive objects and its consequences can be understood using the tools that GR provides. Currently, these two are the theories that lead the research in theoretical physics. In recent years, attempts have been made to combine them into one [9]. So far, no success is at sight [10, 11]. While it might seem tempting to pursue the so-called theory of everything, there are still topics that can be studied by applying the currently available framework in physics, which has been undeniable quite accurate in its predictions. For instance, gravitational waves were recently detected by the LIGO Collaboration [12], just one hundred years after they were predicted by Albert Einstein. Nevertheless, there are still phenomena which, up to now, cannot be thoroughly described using this modern apparatus of knowledge. For instance, a recent test to the SM has been done via the Muon $g - 2$ experiment [13–16]. Deviations from the theoretical value might point to yet undiscovered subatomic particles. Finally, the endeavor of working a solution to these remaining problems in our fundamental theories is what might lead to finding alternatives or extensions of the physical models. We can conclude that physics is a fascinating subject that is slowly, but constantly, evolving towards a better understanding of how our Universe and its contents work.

Nowadays, the SM is regarded as the most successful theory to describe the dynamics of elementary particles. This work is the culmination of several decades of research in both theoretical and experimental particle physics. From the lightest to the heaviest particle, all constituents of matter that were theorized or discovered in experiments have found a place within the SM. About a decade ago, the existence of the last missing piece was confirmed, when the LHC collaboration announced that the Higgs boson was detected [17, 18]. Thus, the theory was able to pass one of the most difficult tests to
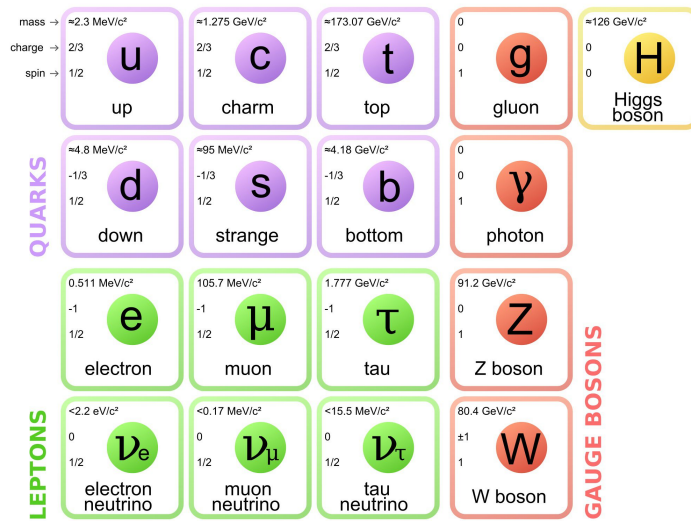
Figure 1.1: Elementary particles in the Standard Model. Figure taken from [19].

date: finding a particle that was first proposed half a century ago and is a crucial part of the model.

The particles that participate in the interactions allowed by this theory are the fermions and bosons. The first type, divided into leptons and quarks, are the constituents of matter, while the second kind, also known as gauge bosons, are the force carriers, see Fig. 1.1. Let us briefly discuss the categories in which the fermions can be categorized. Quarks are allowed to come together and form bigger particles called hadrons. Depending on the number of quarks, hadrons can be divided into two categories: the baryons, which have an odd number of quarks and the mesons, containing an even number. A couple of well-known examples of baryons are the proton and neutron. The lightest mesons, with two quarks, are the pions. Hadrons can be further categorized depending on their quantum numbers. This is known as the eightfold way. For example, mesons can be accommodated into what is called the meson octet, see Fig. 1.2. Furthermore, baryons can also be organized based on their spin. For instance, those with spin-$\frac{1}{2}$ go into the octet while the spin-$\frac{3}{2}$ baryons are part of the decuplet. Now, let us shortly discuss, how the gauge bosons are classified. For the three fundamental forces, electromagnetic, strong and weak, the particles that carry the interactions are the photon, gluon and the W together with the Z, respectively. As already mentioned, space-time effects are not included in this framework. Because of this, a force-carrier particle of gravity is not present. In fact, a spin-2 boson known as the graviton has been proposed as a candidate to mediate gravitational interactions. Yet again, no particle with such characteristics has been detected.

It might seem rather complicated to write down a single theory where all particles come together and follow a set of rules that dictate how they can interact with each other. This was indeed a great endeavor that lead to what we know as the SM. This theory incorporates special relativity and quantum mechanics, therefore it is a quantum field theory that respects the internal symmetries of the product group

$$SU(3)_C \times SU(2)_W \times U(1)_Y, \tag{1.1}$$

where the subscripts C, W and Y denote color, weak isospin and hypercharge, respectively. The $SU(2)_W \times U(1)_Y$ subgroup describes the interactions of photons and the weak bosons (the W and Z)

with matter particles. This is the underlying symmetry group of the electroweak model, which is a unified description of the electromagnetic and weak forces. Moreover, the theory that describes the strong interactions of quarks and gluons is a quantum field theory, more specifically a non-Abelian gauge theory, called Quantum Chromodynamics (QCD) [20, 21], is based upon the Lie algebra of the $SU(3)$ gauge group. Certainly, there is a nice and convenient way to write down all possible interactions in the SM. This done through a Lagrangian, which obeys all symmetries of the SM group. It can be written in a rather compact way

$$\mathcal{L}_{SM} = -\frac{1}{4} F_{\mu\nu} F^{\mu\nu} + i\bar{\psi} \slashed{D}\psi + \psi_i y_{ij} \psi_j \phi + |D_\mu \phi|^2 - V(\phi) + h.c, \tag{1.2}$$

where D_μ denotes the covariant derivative, $F_{\mu\nu}$ is the field strength tensor, ψ_i are the fermion fields, the scalar field ϕ represents the Higgs boson and y_{ij} are the Yukawa couplings through which the Higgs couples to the massless quarks and leptons. Notice that there are no mass terms for any of the fermions and gauge bosons. The masses are generated through the Higgs mechanism in which the Higgs field acquires a vacuum expectation value. For instance, the electroweak group gets broken down by the Higgs mechanism to $U(1)_{em}$ of QED, leading to massive W and Z bosons. So far, we are not aware of the existence of a fundamental force other than gravitation that is not included in this framework. The same applies to the fermion sector in the SM. Nevertheless, as already discussed, there exists phenomena which the model cannot successfully describe. To mention one example of this, the SM does not incorporate the neutrino masses even though it is known that these particles have non-zero mass. Still, the accomplishments of this theory are undeniable exceptional.

The tools used in this work are mainly applied to the strong sector of the SM. Because of this, we will introduce this topic in more detail in the following subsections. For this, a brief introduction to the main aspects of QCD is presented next. Furthermore, a couple of approaches to study this theory at low-energies are discussed. Finally, a short review of the methods employed in the subsequent chapters is given.

1.2 Quantum Chromodynamics

The non-abelian gauge theory that defines the interaction between fermions mediated by gluons is QCD. Quarks come in six different flavors (up, down, charm, strange, top and bottom) each with the property of having one of the three possible colors (red, green and blue). These fermions come with an additional quantum number, called color charge. The extra degree of freedom accounts for the Pauli principle in the description of baryons as three-quark states. This is the so-called quark model, proposed by M. Gell-Mann [23], and G. Zweig [24] in 1964. This modern theory of quarks has been able to successfully describe the phenomena observed in experiments, where the strong force plays a role. For example, an accurate prediction of the QCD coupling constant, the quantity that determines the strength of interactions between quarks and gluons, has been achieved [25]. Even though the theory has been quite successful in its predictions, some fundamental questions remain open. For instance, the strong CP problem stands as one of the most intriguing topics in QCD [26]. Furthermore, this theory requires particular care while studying it at different energy regimes. The latter is discussed by the end this subsection.

As a brief introduction to the topic, we will present the mathematical framework developed in order to understand the nature of strong interactions in terms of quark and gluon as degrees of freedom. The
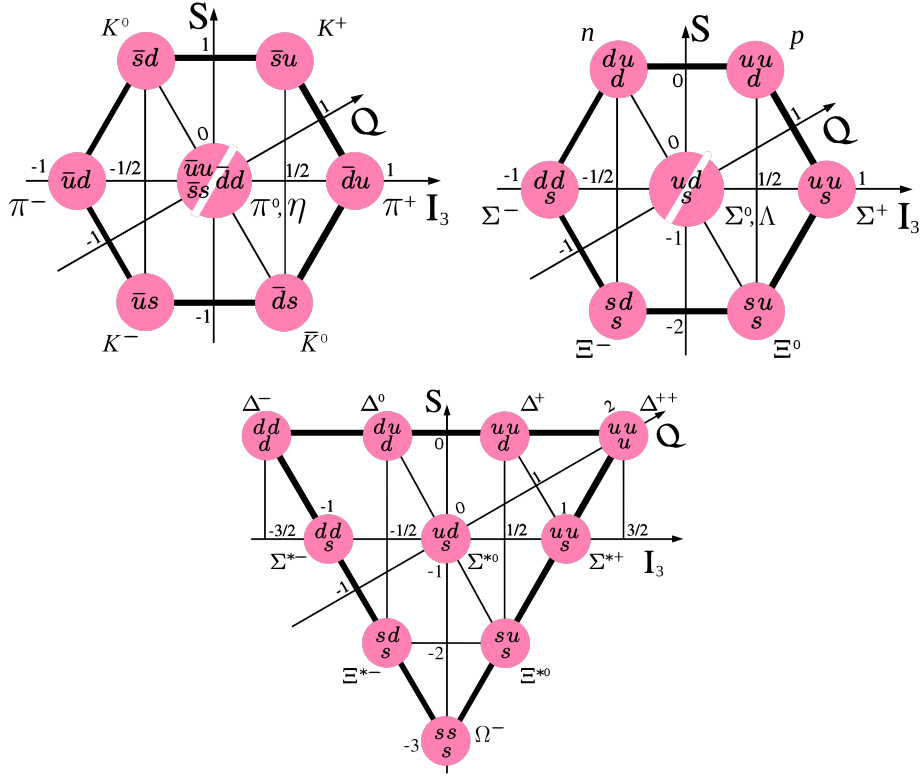
Figure 1.2: Classification of hadrons based on the eightfold way. The component axis labeled by S, Q and I_3 denote the strangeness, electric charge and isospin component, respectively. The main quark content is indicated within the pink circles. The pink circle split in two represents the two baryons indicated besides. Figure taken from [22].

QCD Lagrangian can be obtained by applying SU(3) gauge invariance to the free fermion Lagrangian, i.e. no interacting particles, which is the well-known Dirac Lagrangian

$$\mathcal{L}_{free} = \bar{q}(i\gamma^{\mu}\partial_{\mu} - \mathcal{M})q. \tag{1.3}$$

Here, q is a quark spinor, $\mathcal{M}$ is the mass matrix of the fermions, and ∂_{μ} denotes the partial derivative. If we impose the color $SU(3)$ gauge invariance on $\mathcal{L}_{free}$, the fermion field will transform as $q \rightarrow Uq$ with $U = \exp(-i\theta_a \frac{\lambda_a}{2})$, where λ_a are the well-known Gell-Mann matrices and $a = 1, \ldots, 8$. With this prescription we will notice that an extra term arises from the partial derivative on the quark field, spoiling the gauge symmetry. To solve this problem, eight four-vector gauge potentials A_{μ} are added to the theory to keep the invariance of the Lagrangian under $SU(3)$ local transformations. This will also lead to a modification of the partial derivative of the Lagrangian, namely

$$\partial_{\mu}q \longrightarrow D_{\mu}q \equiv (\partial_{\mu} + ig_s A_{\mu})q, \tag{1.4}$$

where g_s is the coupling constant of the theory. This is how the gauge bosons interact with the fermions. It is important to mention that the interaction between the eight gluons and the quarks is independent of the flavor, as only one coupling constant appears. In other words, the gluons are

"flavor blind". In order to add the gluons as dynamical degrees of freedom, a generalization of the field-strength tensor to non-abelian algebras is needed. This is defined as follows

$$G_{a\mu\nu} \equiv \partial_\mu A_{a\nu} - \partial_\nu A_{a\mu} - g_s f_{abc} A_{b\mu} A_{c\nu}, \tag{1.5}$$

where f_{abc} are the structure constants of the $SU(3)$ Lie algebra. In the case of QED, the structure constants are zero as $U(1)$ is an Abelian group.

Finally, we are in position of writing the full QCD Lagrangian after imposing color $SU(3)$ gauge invariance. It reads (assuming exact CP invariance):

$$\mathcal{L}_{QCD} = \bar{q}(i\gamma^\mu D_\mu - m)q - \frac{1}{4}G_a^{\mu\nu}G_{\mu\nu a}. \tag{1.6}$$

Note also that gluons are massless, i.e. there is no $m_g^2 A^\mu A_\mu$ term in the Lagrangian as this would explicitly break the desired gauge invariance. As a reminder, the masses are generated through the Higgs mechanism. Another important observation about the structure of the Lagrangian is that the QCD Lagrangian gives rise to self-interaction terms of the gauge fields with three and four vertices with strength g_s and g_s^2, respectively. This is characteristic of non-Abelian gauge theories and makes them even more difficult to study. For example, these extra terms do not exist in QED because this theory is based on the Abelian group.

An interesting property of QCD is how the coupling constant changes for different values of the energy. To understand how g_s varies, it is more convenient to define the bare coupling of QCD as

$$\alpha_s = \frac{g_s^2}{4\pi}. \tag{1.7}$$

This is the bare coupling, meaning that it is subject to renormalization. The renormalized coupling depends on the renormalization scale μ. At lowest order in perturbation theory, this dependence is given by

$$\alpha_s(q^2) = \frac{\alpha_s(\mu^2)}{1 + \beta_0 \alpha_s(\mu^2) \ln \frac{q^2}{\mu^2}}, \qquad \beta_0 = \frac{33 - 2N_f}{12\pi}, \tag{1.8}$$

where μ is some fixed renormalization scale and N_f is the number of flavor contained in the theory. One can conclude that the strength of the QCD coupling varies significantly at different energy scales, as can be seen in Fig 1.3. At low energies, perturbation theory is no longer applicable due to the magnitude of the coupling constant. On the other hand, for very large momenta, α_s is small enough, so perturbation theory can again be used. This phenomena exhibited by non-Abelian gauge theories is called asymptotic freedom [28, 29]. Another interesting phenomena observed in QCD is called color confinement. This means that the color-charged particles cannot be isolated. For this reason, quarks and gluons cannot be directly observed. Instead, colorless combinations of these particles are detected: the hadrons.

Due to the fact that QCD cannot be investigated using the traditional approach of perturbation theory at low energies, as in QED, we must employ an alternative way to describe the interactions in this regime. The non-perturbative approach that will be used in the following is called Chiral Perturbation Theory (ChPT). This is the effective field theory of QCD at the energies way below 1 GeV and it will allow us to replace quarks and gluons by hadronic degrees of freedom such as, for example, the pion,
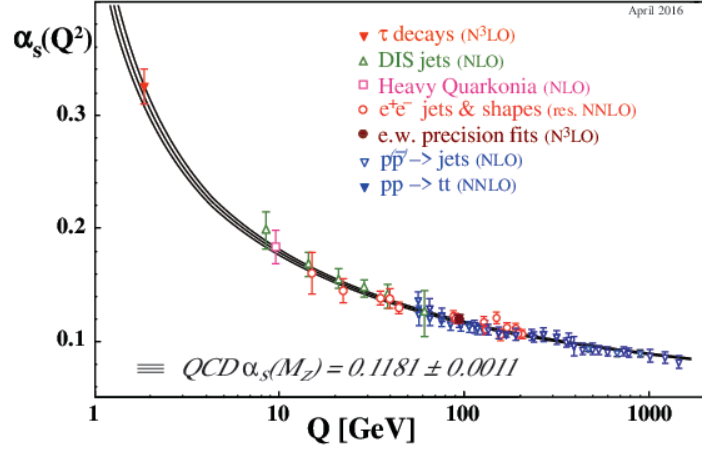
Figure 1.3: Summary of measurements of α_s as a function of the energy scale Q. Figure taken from [27].

neutron and proton fields. After introducing ChPT, we will make a brief introduction to Lattice QCD, which is one of the most popular numerical tools to study the low-energy regime of this theory.

1.3 Effective field theories

The effective field theory of QCD is ChPT. Here, the building blocks are the hadrons, instead of quarks and gluons. To begin this section, let us first briefly motivate the idea of considering the chiral symmetry of the QCD Lagrangian. If we would like to study the QCD spectrum at low energies, it is then appropriate to concentrate our attention only to the light quark flavors; up, down and strange. This choice of quarks is due to the fact that their masses are small compared to the typical hadron masses. For instance, the proton and neutron share a similar mass of approximately 940 MeV, then

$$m_u < m_d < m_s \ll m_{\text{hadrons}}.$$

Next, we can focus on the region of energies where heavy particles can be integrated out. As a starting point, the masses of the light quarks are taken to zero

$$m_u, m_d, m_s \longrightarrow 0.$$

This is the so-called chiral limit. At the last stage, one could turn on the quark masses, which are considered as perturbations towards the chiral limit.

We will start with the QCD Lagrangian and work with only three flavors, while taking their masses to zero

$$\mathcal{L}_{QCD}^0 = \sum_{f=1}^{3} i \bar{q}_f \gamma^\mu D_\mu q_f - \frac{1}{4} G^{a\mu\nu} G_{a\mu\nu}. \tag{1.9}$$

This Lagrangian exhibits chiral symmetry, which can be seen by taking an element of the flavor group $(L, R) \in SU(3)_L \times SU(3)_R$ and looking at its action on the left- and right-handed quarks defined as $q_{R,L} = \frac{1}{2}(1 \pm \gamma_5)q$ and transforming as $q_L \to Lq_L = q'_L$, $q_R \to Rq_R = q'_R$

$$\bar{q}i\gamma^\mu D_\mu q \longrightarrow \bar{q}'_L i\gamma^\mu D_\mu q'_L + \bar{q}'_R i\gamma^\mu D_\mu q'_R$$
$$= \bar{q}' i\gamma^\mu D_\mu q'.$$

Invoking Noether's theorem, the existence of a continuous symmetry of the Lagrangian represents the conservation of a current J_μ, i.e. $\partial_\mu J^\mu = 0$ with the corresponding charge $Q(t) = \int d^3x J_0(t, \vec{x})$. In the chiral limit, the conserved currents of the chiral symmetry are

$$L_\mu^a = \sum_{q=u,d,s} \bar{q}_L \gamma_\mu \frac{\lambda^a}{2} q_L, \tag{1.10a}$$

$$R_\mu^a = \sum_{q=u,d,s} \bar{q}_R \gamma_\mu \frac{\lambda^a}{2} q_R. \tag{1.10b}$$

The charges Q_L^a and Q_R^a generate the algebra for the $SU(3)_L$ and $SU(3)_R$ groups, respectively. It is convenient to define a combination of both charges

$$Q_A^a = Q_R^a + Q_L^a, \tag{1.11a}$$
$$Q_V^a = Q_R^a - Q_L^a. \tag{1.11b}$$

Now consider an eigenstate $|\psi\rangle$ of the QCD Hamiltonian, $H_{QCD}|\psi\rangle = E|\psi\rangle$. Then, the states $Q_V^a|\psi\rangle$ and $Q_A^a|\psi\rangle$ have the same energy but opposite parity. The later observation means that for each positive parity multiplet, corresponding to the non-trivial representation of the $SU(3)_V$, there must exist a negative-parity multiplet with the same mass (not necessarily corresponding to the same irreducible representation). This is not the case in nature, as such states haven't been observed [30]. This problem was later solved by the Nambu-Goldstone realization of chiral symmetry [31] which asserts that the vacuum, $|0\rangle$, is not invariant under the action of the axial charge

$$Q_V^a|0\rangle = 0, \quad Q_A^a|0\rangle \neq 0. \tag{1.12}$$

This leads to the spontaneous breaking of the chiral symmetry group in the following fashion

$$SU(3)_L \times SU(3)_R \xrightarrow{\text{SSB}} SU(3)_V.$$

Invoking Goldstone's theorem, we will find that there are eight massless spinless particles, each for every broken generator. These are the lightest hadrons in the spectrum: $\pi^\pm$, π^0, K^0, $K^\pm$, $\bar{K}$ and η. In reality, these bosons are not massless and adding the mass term for their components will explicitly break the chiral symmetry. Nonetheless, this addition of a mass can be treated as a small perturbation. Before constructing the Lagrangian describing the eight Goldstone bosons, let us take a look at the non-vanishing matrix elements of the axial vector current

$$\langle 0| A_\mu^a |\phi^b(p)\rangle = ie^{-ip\cdot x} p_\mu \delta^{ab} f, \tag{1.13}$$

where $f = 93$ MeV is the leptonic decay constant of the Goldstone bosons. We can conclude that a non-zero value of f is a necessary and sufficient criterion for spontaneous chiral symmetry breaking.

The dynamics of the eight Goldstone bosons are described by the effective Lagrangian and the matter field can be collected in an unitary matrix field $U \in SU(3)$, with the following behavior under chiral transformations

$$U \longrightarrow g_R U g_L^\dagger, \quad g_R, g_L \in SU(3).$$

By Lorentz invariance, the effective Lagrangian can only contain even powers in the derivatives

$$\mathcal{L} = \mathcal{L}^{(2)} + \mathcal{L}^{(4)} + \dots \tag{1.14}$$

where $\mathcal{L}^{(2)}$ is given by

$$\mathcal{L}^{(2)} = \frac{f^2}{4} Tr[\partial_\mu U \partial^\mu U^\dagger]. \tag{1.15}$$

Let us consider a parametrization of U, given by

$$U = \exp\left(\frac{i\phi}{f}\right), \quad \phi = \sqrt{2} \begin{bmatrix} \frac{\pi^0}{\sqrt{2}} + \frac{\eta}{\sqrt{6}} & \pi^+ & K^+ \\ \pi^- & \frac{-\pi^0}{\sqrt{2}} + \frac{\eta}{\sqrt{6}} & K^0 \\ K^- & \bar{K}^0 & -\frac{2\eta}{\sqrt{6}} \end{bmatrix}. \tag{1.16}$$

Taking the expansion of U in powers of ϕ, $U = 1 + i\phi/f - \phi^2/(2f^2) + \dots$ and plugging it back into $\mathcal{L}^{(2)}$ yields the kinetic terms of the eight massless Goldstone bosons

$$\mathcal{L}^{(2)} = \frac{1}{2}\partial_\mu \pi^0 \partial^\mu \pi^0 + \frac{1}{2}\partial_\mu \eta \partial^\mu \eta + \partial_\mu \pi^+ \partial^\mu \pi^- + \partial_\mu K^+ \partial^\mu K^- + \partial_\mu K_0 \partial^\mu \bar{K}_0 + \dots. \tag{1.17}$$

As we mentioned, the masses of the light quarks are small but certainly not zero. However, the inclusion of a quark mass term would explicitly break the chiral symmetry of the fermionic Lagrangian. In order to address this issue, one could use the spurion technique described e.g. in Refs. [32, 33]. Namely, the Lagrangian is equipped with a set of external sources. The fermionic part of the QCD Lagrangian is therefore

$$\mathcal{L}_F(s, p, v, a) = \bar{q}\left(\gamma^\mu\left(iD_\mu + v_\mu + \gamma^5 a_\mu\right) - s + i\gamma^5 p\right)q. \tag{1.18}$$

The external sources are the classical scalar s, pseudoscalar p, vector v_μ and axial-vector a_μ ones. In this manner, the generating functional now depends on the introduced sources

$$Z(s, p, v, a) = \int dq d\bar{q} dG_\mu \exp\left\{i \int d^4x \left(\mathcal{L}_G + \mathcal{L}_F(s, p, v, a)\right)\right\}, \tag{1.19}$$

where $\mathcal{L}_G$ contains the gauge boson terms of $\mathcal{L}_{QCD}$. The key feature of this procedure is the following: the Green's functions with massive quarks can be obtained by expanding $Z(s, p, v, a)$ at the point $s = \mathcal{M}$, $p = v = a = 0$, where $\mathcal{M}$ is the quark mass matrix, whereas QCD in the chiral limit is obtained by expanding the same generating functional at $s = p = a = v = 0$.

Furthermore, the QCD generating functional equipped with the external sources can be shown to be invariant under local $SU(3)_R \times SU(3)_L$ group transformations. For instance, the covariant derivative

of U transforms under the group action as

$$D_\mu U \rightarrow g_R(x) D_\mu U g_L^\dagger(x), \tag{1.20}$$

where $D_\mu U = \partial_\mu - i r_\mu U + i U l_\mu$. Here, the vector and axial currents, v_μ, a_μ are combined into $r_\mu = v_\mu + a_\mu$ and $l_\mu = v_\mu - a_\mu$. Further, $g_R(x)$ and $g_L(x)$ are elements of $SU(3)_R$ and $SU(3)_L$, respectively. Moreover, the quantity $D_\mu \chi$, where $\chi = 2B_0(s+ip)$, also follows the same transformation law. Here, B_0 is one of the two low-energy constants and it is related to the quark condensate by $3f^2 B_0 = - < \bar{q}q >_0 = - < \bar{u}u + \bar{d}d + \bar{s}s >_0$.

Finally, having considered the local invariance of the Lagrangian under $SU(3)_R \times SU(3)_L$ transformations and the counting rules for the operators

$$U = O(p^0), \quad D_\mu U = O(p), \quad r_\mu = O(p), \quad l_\mu = O(p), \quad \chi = O(p^2), \tag{1.21}$$

where the momenta p the momenta of the lightest Goldstone bosons, assumed to be small compared to the hadronic scale of 1 GeV, the leading order Lagrangian can be written down as [34]:

$$\mathcal{L}_{\pi\pi}^{(2)} = \frac{f^2}{4} \text{Tr} \left[D^\mu U^\dagger D_\mu U + \chi^\dagger U + U^\dagger \chi \right], \tag{1.22}$$

where the traces is taken over flavor space. Setting all external sources to zero, one recovers Eq. 1.15, whereas setting $s = \mathcal{M}$, $p = v = a = 0$, one gets the Lagrangian describing pions with non-zero mass.

With the most general, chirally invariant, effective Lagrangian at lowest chiral order it is possible to describe phenomena at low energies without explicitly taking into account the quarks or gluons. For example, one can describe the $\pi\pi$ scattering by also including the baryon fields in a chiral-symmetric fashion. Adding the photon field in the Lagrangian, the Compton scattering can be then studied.

1.3.1 Power Counting Scheme

The so-called Weinberg's theorem states that a perturbative description of the most general effective Lagrangian containing all terms compatible with assumed symmetry principles yields the most general S-matrix consistent with the fundamental principles of quantum field theory [35]. This is, the effective Lagrangian contains an infinite number of terms and free parameters. Applying this theorem requires from us to find a scheme to organize the terms of the Lagrangian and a method to determine the importance of a diagram as compared to others.

We have already seen that the mesonic Lagrangian is composed of a string of terms containing increasing powers of the momenta and quark masses. Now, in order to determine the importance of a diagram contributing to a process, we do a rescaling of the external momenta and the light-quark masses, $p \rightarrow tp$ and $\mathcal{M} \rightarrow t^2 \mathcal{M}$, respectively. This leads to a rescaling of the amplitude $\mathbf{M}$ in the following way

$$\mathbf{M}(tp, t^2 \mathcal{M}) = t_\chi^D \mathbf{M}(p, \mathcal{M}), \tag{1.23}$$

where D_χ is called the chiral dimension of the diagram given by

$$D_\chi = 2 + (D - 2)N_L + \sum_{k=1}^{\infty} 2(k-1)N_{2k}, \tag{1.24}$$

where D is the dimension of space-time ($D \to 4$), N_L is the number of independent loop momenta and N_{2k} is the number of vertices coming from the effective mesonic Lagrangian. Note that going to lower momenta represents a rescaling with $0 < t < 1$. This means that in this regime diagrams with small D_χ should dominate.

1.3.2 The $O(p^4)$ Effective Lagrangian

Since ChPT is not a renormalizable theory like QED or QCD, an infinite number of terms are to be added to the Lagrangian in order to compensate for this. One-loop diagrams will generate divergences that can only be absorbed by a redefinition of the LECs of the next order Lagrangian. This means, a vertex generated by $\mathcal{L}_2$ that produces a divergence can be cured by a counterterm from $\mathcal{L}_4$.

For this, one can follow the main ideas of the previous subsections to construct the $SU(3)_L \times SU(3)_R$ locally invariant Lagrangian at $O(p^4)$. In the following, we quote the result of Gasser and Leutwyler [34]

$$
\begin{aligned}
\mathcal{L}_4 &= L_1 \left(Tr\left[D_\mu U (D^\mu U)^\dagger \right] \right)^2 + L_2 Tr\left[D_\mu U (D_\nu U)^\dagger \right] Tr\left[D^\mu U (D^\nu U)^\dagger \right] \\
&+ L_3 Tr\left[D_\mu U (D^\mu U)^\dagger D_\nu U (D^\nu U)^\dagger \right] + L_4 Tr\left[D_\mu U (D^\mu U)^\dagger \right] Tr\left(\chi U^\dagger + U \chi^\dagger \right) \\
&+ L_5 Tr\left[D_\mu U (D^\mu)^\dagger \left(\chi U^\dagger + U \chi^\dagger \right) \right] + L_6 \left[Tr\left(\chi U^\dagger + U \chi^\dagger \right) \right]^2 \\
&+ L_7 \left[Tr\left(\chi U^\dagger - U \chi^\dagger \right) \right]^2 + L_8 Tr\left(U \chi^\dagger U \chi^\dagger + \chi U^\dagger \chi U^\dagger \right) \\
&- i L_9 Tr\left[f_{\mu\nu}^R D^\mu U (D^\nu U)^\dagger + f_{\mu\nu}^L (D^\mu)^\dagger D^\nu U \right] + L_{10} Tr\left(U f_{\mu\nu}^L U^\dagger U^\dagger f_R^{\mu\nu} \right) \\
&+ H_1 Tr\left(f_{\mu\nu}^R f_R^{\mu\nu} + f_{\mu\nu}^L f_L^{\mu\nu} \right) + H_2 Tr[\chi \chi^\dagger].
\end{aligned}
\tag{1.25}
$$

The vector and axial currents, v_μ, a_μ are combined into r_μ and l_μ to form the tensors $f_L^{\mu\nu} = \partial^\mu l^\nu - \partial^\nu l^\mu - i[l^\mu, l^\nu]$, $f_R^{\mu\nu} = \partial^\mu r^\nu - \partial^\nu r^\mu - i[r^\mu, r^\nu]$. As in the leading order case, the low-energy constants L_i are not determined by chiral symmetry but by the remaining QCD parameters (heavy quark masses and the QCD scale). They can be calculated, for example, by fitting numerical data using LQCD.

Now, it is possible to absorb all the one-loop divergences coming from the $\mathcal{L}_2$ Lagrangian by an appropriate renormalization of the LECs L_i and high-energy constants H_i

$$
L_i = L_i^r + \frac{\Gamma_i}{32\pi^2}\lambda \quad i = 1, \ldots 10,
\tag{1.26a}
$$

$$
H_i = H_i^r + \frac{\Delta_i}{32\pi^2}\lambda \quad i = 1, 2,
\tag{1.26b}
$$

where R is defined as

$$
\lambda = \frac{\mu^{D-4}}{16\pi^2}\left[\frac{1}{D-4} - \frac{1}{2}\left(\Gamma'(1) + \ln 4\pi + 1 \right) \right].
\tag{1.27}
$$

Here, D is the number of space-time dimensions.

1.3.3 The Baryon Sector

Having discussed the effective Lagrangian for the (pseudo) Goldstone bosons, one might wonder if the extension to the baryon sector, following the same steps as before, is possible[1]. To begin with, let us take a look at the masses of the lightest baryons; proton and neutron: $m_{p,n} \sim 1$ GeV. The main concern here is that in the chiral limit the masses remain almost the same, that is:

$$\lim_{m_q \to 0} m_N \sim m_N, \tag{1.28}$$

where m_q and m_N are the quark masses and of the nucleon, respectively. As we will see, the naive power counting used in the mesonic sector is broken due to the new (massive) scale introduced by the nucleon mass. This will force us to look for alternative ways to circumnavigate this problem, which we will see it is not a trivial matter.

Now, the construction of the meson-baryon Lagrangian follows as in the previous case: we choose a convenient representation of the $SU(N)_L \times SU(N)_R$ group, as well as the transformation law for the baryons. Then, the terms of the Lagrangian are organized in increasing powers of momenta.

In this work we will restrict ourselves to the nucleon, i.e. proton and neutron. Consequently, we stick to the $SU(2)$ version of chiral perturbation theory, where the contribution from the strange quark is included into the low-energy constants. For this, we define the field that embodies both of these particles

$$\Psi = \begin{pmatrix} p \\ n \end{pmatrix}, \tag{1.29}$$

where p and n are the proton and neutron fields, respectively. The matrix U in the two-flavor case, analogous to Eq. (1.21), is given by

$$u^2(x) = U(x) = \begin{pmatrix} \frac{1}{\sqrt{2}}\pi^0 & \pi^+ \\ \pi^- & \frac{1}{\sqrt{2}}\pi^0 \end{pmatrix} \tag{1.30}$$

The transformation law for ψ is as follows $\Psi \longmapsto \Psi' = K\psi$ where $K = K(g_L, g_R, U) \in SU(N)$ is called the compensator field. Furthermore, we define the covariant derivative $D^\mu = \partial^\mu + \Gamma^\mu$ where Γ^μ is the chiral connection defined as

$$\Gamma^\mu = \frac{1}{2}\left(u^\dagger(\partial^\mu - ir^\mu)u + u(\partial^\mu - il^\mu)u^\dagger\right), \tag{1.31}$$

where l^μ and r^μ are external fields. This connection is chosen in way such that the covariant derivative transforms in the desired way

$$D^\mu\Psi \longmapsto KD^\mu\Psi. \tag{1.32}$$

The chiral vielbein is also introduced in the form

$$u^\mu = i\left(u^\dagger(\partial^\mu - ir^\mu)u - u(\partial^\mu - il^\mu)u^\dagger\right), \tag{1.33}$$

transforming as $u^\mu \longmapsto Ku^\mu K^\dagger$. These building blocks are used to write the most general effective

---

[1] For a deeper review on this topic, we refer the reader to [36].

πN Lagrangian describing a process with a nucleon in the initial and final state. At leading order, it is given by [37]

$$\mathcal{L}_{\pi\Psi}^{(1)} = \bar{\Psi}\left(i\slashed{D} - \overset{\circ}{m} + \frac{g_A}{2}\gamma^\mu\gamma_5 u_\mu\right)\Psi. \tag{1.34}$$

The Lagrangian contains two parameters that are yet to be fixed: $\overset{\circ}{m}$, the nucleon mass in the chiral limit and g_A, the axial-vector coupling also in the chiral limit. Below, we shall not make a difference between $\overset{\circ}{m}$ and the physical nucleon mass, m, since this difference does not play a role at the order we are working.

Furthermore, in the baryonic sector both odd and even powers of momenta are allowed, contrary to the mesonic one where only even powers are allowed:

$$\mathcal{L}_{\pi N} = \mathcal{L}_{\pi N}^{(1)} + \mathcal{L}_{\pi N}^{(2)} + \mathcal{L}_{\pi N}^{(3)} + \mathcal{L}_{\pi N}^{(4)} + \dots. \tag{1.35}$$

As it was also done in the mesonic sector, we present the next-to-leading order Lagrangian which contains seven LEC c_i. The second order Lagrangian includes terms with quark mass insertions that explicitly break the chiral symmetry, terms with two vielbeins u_μ, and terms with external currents such as $f_{L\mu\nu}$ and $f_{R\mu\nu}$ [37, 38]

$$\begin{aligned}
\mathcal{L}_{\pi N}^{(2)} =\,& c_1 \operatorname{Tr}(\chi_+)\bar{\Psi}\Psi - \frac{c_2}{4m^2}\operatorname{Tr}(u_\mu u_\nu)\left(\bar{\Psi}D^\mu D^\nu\Psi + \text{H.c.}\right) \\
&+ \frac{c_3}{2}\operatorname{Tr}(u^\mu u_\mu)\bar{\Psi}\Psi - \frac{c_4}{4}\bar{\Psi}\gamma^\mu\gamma^\nu[u_\mu, u_\nu]\Psi + c_5\bar{\Psi}\left[\chi_+ - \frac{1}{2}\operatorname{Tr}(\chi_+)\right]\Psi \\
&+ \bar{\Psi}\sigma^{\mu\nu}\left[\frac{c_6}{2}f_{\mu\nu}^+ + \frac{c_7}{2}v_{\mu\nu}^{(s)}\right]\Psi,
\end{aligned} \tag{1.36}$$

where H.c. refers to Hermitian conjugate and

$$\begin{aligned}
\chi_\pm &= u^\dagger\chi u^\dagger \pm u\chi^\dagger u, \\
v_{\mu\nu}^{(s)} &= \partial_\mu v_\nu^{(s)} - \partial_\nu v_\mu^{(s)}, \\
f_{\mu\nu}^{(\pm)} &= u f_{L\mu\nu} u^\dagger \pm u^\dagger f_{R\mu\nu} u.
\end{aligned}$$

To make predictions using this model, the values of the LECs have to be determined by comparing them with experiments. Values for the πN LECs at NLO are given in [39]

$$c_1 = -.74(2)\text{ GeV}^{-1}, \quad c_2 = 1.81\text{ GeV}^{-1}, \quad c_3 = -3.61(5)\text{ GeV}^{-1}, \quad c_4 = 2.17(3)\text{ GeV}^{-1}. \tag{1.37}$$

One might wonder if the naive power counting is still viable here, which is the most natural assumption that can be made. To verify this, we will now introduce a power counting scheme similar to the one in the mesonic sector for the tree-level and loop diagrams for baryons. It is important to notice that the power counting applies only to renormalized diagrams, that is, the sum of diagrams coming from the effective Lagrangian and also from the counter-term Lagrangian. Now, the power D of a diagram can be written as

$$D_\chi = DN_L - 2I_\pi - I_N + \sum_{k=1}^\infty 2k N_{2k}^\pi + \sum_{k=1}^\infty k N_k^N, \tag{1.38}$$

where D is the dimension of the integration (dimension of space-time), N_L, I_π, I_N, N_{2k}^π and N_k^N are

the independent loop momenta, internal pion lines, internal nucleon lines, vertices originating from the effective pion Lagrangian and vertices from the baryon one, respectively. Taking the case where only one nucleon is on the initial and final state, the formula can be further simplified into

$$D_\chi = 1 + (D - 2)N_L + \sum_{k=1}^{\infty} 2(k - 1)N_{2k}^\pi + \sum_{k=1}^{\infty} (k - 1)N_k^N. \tag{1.39}$$

From here we can conclude that loop calculations start counting at $O(q^{n-1})$, where q is a small parameter, for example, the pion mass.

Recalling what was said at the beginning of this subsection, the mass scale introduced by the (heavy) baryon spoils the power counting for loop diagrams. This is because the integration over all energy scales can also pick up the momenta of the same order as the nucleon mass, i.e. $p \sim m_N$. This is an issue, that can be fixed by applying different regularization and renormalization prescriptions. Each of these have their on advantages and disadvantages, which will depend on the kind of processes being studied. Here, we will shortly introduce three of the most popular schemes.

Heavy-Baryon Approach

The first method to cure this power counting violation due to the nucleon mass goes by the name of heavy-baryon approach [40, 41]. The basic idea is to separate nucleon four-momenta p into a large piece close to on-shell kinematics plus a residual momentum obeying

$$p_\mu = \mathring{m}v_\mu + l_\mu, \tag{1.40}$$

which has the properties

$$v^2 = 1,$$
$$v \cdot l \ll \mathring{m}.$$

As we will see below, this explicitly eliminates the nucleon mass m from the propagator. Furthermore, the nucleon field ψ is decomposed into two velocity-dependent fields

$$H_v(x) = e^{i\mathring{m}v \cdot x} P_v^+ \psi(x), \quad h_v(x) = e^{i\mathring{m}v \cdot x} P_v^- \psi(x), \tag{1.41}$$

where the projection operators $P_v^\pm = \frac{1}{2}(1 \pm \slashed{v})$ are introduced. One can proceed to rewrite the leading order Lagrangian $\mathcal{L}_{\pi N}^{(1)}$ using the decomposition of the nucleon four-momenta and the nucleon field redefinition as

$$\mathcal{L}_{\pi N}^{(1)} = \bar{H}_v \left(iv \cdot D + g_A S \cdot u \right) H_v + O(1/\mathring{m}), \tag{1.42}$$

where the Pauli-Lubanski spin vector $S_\mu = \frac{i}{2}\gamma_5\sigma_{\mu\nu}v^\nu$ is introduced. Now, we see that the nucleon mass has disappeared from the Lagrangian, in contrast to the relativistic one. The terms not explicitly shown in Eq. (1.42) are suppressed by $1/\mathring{m}$.

A consequence of this is that in the heavy-baryon limit the nucleon propagator S_F is modified in the following form (see Eq. (1.42))

$$S_F \longrightarrow S_F^{HB} = \frac{P_v^+}{v \cdot k + i0^+} \tag{1.43}$$
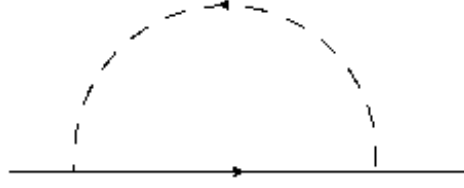
Figure 1.4: Nucleon self energy diagram. The solid line represents the nucleon and the dashed line the pion.

Using this heavy-baryon propagator in the loop calculations will restore the naive power counting, since the mass scale $\mathring{m}$ does not appear.

Infrared Regularization

Another method to fix the naive power counting in the baryon sector is called infrared regularization [42] and relies on the analytic structure of the loop integrals in D dimensions. It allows a manifestly covariant way of calculating loops in ChPT. To illustrate this, we will give the example of the nucleon self energy. The diagram of this process can be seen in Fig. 1.4 and the integral part of the amplitude (omitting prefactors for simplicity and using physical masses of the nucleon and pion, denoted by m and M respectively, in the propagators) is

$$H = \int \frac{d^D k}{(2\pi)^D} \frac{1}{[(k-p)^2 - m^2 + i0^+](k^2 - M^2 + i0^+)}. \tag{1.44}$$

One can show that after evaluating this integral in D-dimensions at threshold $p_{\text{thr}}^2 = (m+M)^2$ we get

$$H = \frac{\Gamma(2 - \frac{D}{2})}{(4\pi)^{D/2}(D-3)} \left(\frac{M^{D-3}}{m+M} + \frac{m^{D-3}}{m+M} \right). \tag{1.45}$$

The first term in Eq. (1.45) proportional to M^{D-3} is called the infrared-singular part of H, while the second term is called the infrared-regular part. The regular part scales with fractional powers of m, but has a regular expansion in M and momenta. This part of the integrals is the one that violates the naive power counting. Due to the fact that it can be expanded as a polynomial, these terms can be absorbed by a redefinition of the contact terms of the Lagrangian. Opposite to the previous case, the infrared part is the one that obeys the naive power counting.

Now, one would like to find the infrared part of the integral H, since it is the one that we want to keep. A simple method was introduced in [42] to achieve this. The scalar integral H can be written in terms of the Feynman parameter z as

$$H = \int_0^1 dz \int \frac{d^D k}{(2\pi)^D} \frac{1}{[(1-z)a + zb]^2}. \tag{1.46}$$

With $a = k^2 - M^2 + i0^+$ and $b = (k-p)^2 - m^2 + i0^+$ it can be seen that the integration around $z = 1$ does not lead to a singularity at $m^2 = 0$. By this, one can obtain the infrared part I of H by extending

the integration limit of z to infinity.

$$I = \int_0^\infty dz \int \frac{d^D k}{(2\pi)^D} \frac{1}{[(1-z)a + zb]^2}. \tag{1.47}$$

Thus, one writes H as the sum of the infrared singular and regular parts

$$H = I + R, \tag{1.48}$$

where R is the regular part, corresponding to the integral over z from infinity to one.

Extended-On-Mass Shell Scheme

Although the infrared regularization is one of the most popular methods to recover the naive power counting in the baryon sector, it is not the only one to deal directly with the loop integrals. The extended-on-mass shell (EOMS) [43, 44] scheme is also another approach to solve this problem. In the infrared regularization, the infrared-regular part of the integral is the one that contains the terms that violate power counting. Nonetheless, this part of the integral can also contain an infinite number of terms that actually do not violate the power counting. It is possible to reabsorb these problematic parts into counter terms of the Lagrangian, but this is not necessary, as described by the EOMS method. The main idea behind this technique is that in addition to the $\bar{M}S$ scheme, finite subtraction to the result are to be performed in order to remove the terms that break power counting.

We again consider the integral H but now in the chiral limit, to illustrate the idea behind the EOMS approach

$$H = \int \frac{d^D k}{(2\pi)^D} \frac{1}{[(k-p)^2 - m^2 + i0^+](k^2 + i0^+)}. \tag{1.49}$$

Taking into consideration that the nucleon momentum is close to the mass shell, $p^2 \approx m^2$, one can show that when taking the limit $D \to 4$ one gets

$$H = \frac{m^{D-4}}{(4\pi)^{\frac{D}{2}}} \left[\frac{\Gamma(2 - \frac{D}{2})}{D - 3} + \left(1 - \frac{p^2}{m^2}\right) \ln\left(1 - \frac{p^2}{m^2}\right) \right.$$
$$\left. + \left(1 - \frac{p^2}{m^2}\right)^2 \ln\left(1 - \frac{p^2}{m^2}\right) + \dots \right]. \tag{1.50}$$

The terms in Eq. (1.50), which contain logarithmic dependence of the nucleon momentum do not break the power counting. The term that violates the power counting is local in the external momentum, and so it can be absorbed in a finite number of counter terms. Thus, the following term is subtracted

$$H_s = \frac{m^{D-4}}{(4\pi)^{\frac{D}{2}}} \frac{\Gamma(2 - \frac{D}{2})}{D - 3}, \tag{1.51}$$

15

yielding the renormalized integral

$$
\begin{aligned}
H_R = \frac{m^{D-4}}{(4\pi)^{\frac{D}{2}}} \Bigg[&\left(1 - \frac{p^2}{m^2}\right) \ln\left(1 - \frac{p^2}{m^2}\right) \\
&+ \left(1 - \frac{p^2}{m^2}\right)^2 \ln\left(1 - \frac{p^2}{m^2}\right) + \ldots \Bigg].
\end{aligned}
\tag{1.52}
$$

This can be extended beyond the chiral limit as well.

1.4 Lattice QCD

So far, we have discussed a method that allows us to explore the low-energy regime of QCD, where the traditional approach of perturbation theory cannot be applied. This is ChPT, the effective field theory of QCD that, in recent years, has been an indispensable framework to the particle physics community. Another popular method is Lattice QCD (LQCD), which is a non-perturvative tool used to study the properties of the low-energy regime of QCD. At present, LQCD is the only method that allows one to investigate the properties of the strong interactions directly from the underlying theory. It was formulated in an attempt to solve the confinement problem by K. Wilson [45]. This theory is confined to a finite volume on a discrete hyper-cubic lattice with spacing a, where the quarks fields are placed on sites and the gluons on the links between them. The lattice spacing provides a natural ultraviolet regulator, rendering the theory finite. In practice, LQCD calculations are limited by the computational power currently available and the efficiency of the algorithms employed. Thus, results are bound to yield statistical and systematic errors due to the numerical method employed and by the fact that the lattice spacing is non-zero. In the end, the continuum limit, $a \to 0$, must be recovered.

Let us now introduce some of the main ideas in LQCD. First, we shall discuss, how fermions and bosons are managed on the lattice by studying the gauge action on discretized space-time. Taking QCD to a discrete space-time grid and to a finite-volume can be easily done, but one has to be careful on how to interpret the results given by these kind of calculations. This is more notable in the fermion sector, where subtle issues arise. There are several proposals on how to account for these complications, each one with their own advantages and disadvantages. Regardless of these complications, LQCD has proven to be an essential theoretical tool to study QCD at low energies.

To study how the QCD action is modified by this framework, let us consider a finite Euclidean space-time where the quarks are only allowed to interact with each other via a gauge link. Under gauge group, quarks and gluons transform as

$$
q(x) \to V(x)q(x), \quad \bar{q}(x) \to \bar{q}(x)V^\dagger(x), \quad U_\mu(x) \to V(x)U_\mu(x)V(x + a\hat{\mu}),
\tag{1.53}
$$

where $U_\mu(x)$ is the gluon field, $V(x)$ is an element of $SU(3)$ and $\hat{\mu}$ is a unit vector in the μ'th direction. It is important to notice that $U_\mu(x)$ is also an element of $SU(3)$, in contrast to its continuum analog A_μ, which takes values in the Lie algebra $\mathfrak{su}(3)$. The simplest possible action can be constructed from the gauge links around a plaquette, illustrated in Fig. 1.5. This is the well-known Wilson action,

$$
S_g = \beta \sum_{x,\mu,\nu} \left\{ 1 - \frac{1}{3} \mathrm{Re}\, \mathrm{Tr}\left[U_\mu(x) U_\nu(x + a\hat{\mu}) U_\mu^\dagger(x + a\hat{\mu}) U_\nu^\dagger(x) \right] \right\},
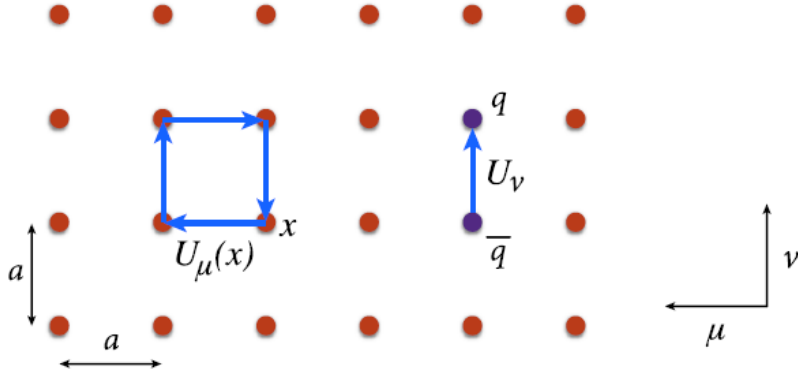\tag{1.54}
$$

Figure 1.5: Gluon and quark fields on the lattice. Figure taken from [30].

with $\beta = 6/g_{\text{lat}}^2$, where g_{lat} is the bare coupling constant in the lattice scheme. Parametrizing now the expression for the gauge link in terms of the gluon field A_μ as $U_\mu(x) = \exp(-iaA_\mu(x))$. With this, one recovers the $G_{\mu\nu}^2$ term of the QCD Lagrangian in Eq. 1.6 in the limit $a \to 0$. In practice, the lattice spacing is not zero. This leads to the discretization error of $O(a^2)$ in numerical results. To reduce the errors, one can apply the Symanzik improvement program [46, 47]. This leads to a modification of the action S_g in the following fashion

$$S_g \longrightarrow S_g + a^2 \sum_j c_j O_6^{(j)}, \tag{1.55}$$

where $O_6^{(j)}$ are operators of dimension 6 allowed by the lattice symmetries and c_j are unknown coefficients. The Symanzik program can either lead to tree-level correction, proportional to $\alpha_s a^2$, or a one-loop correction where errors go as $\alpha_s^2 a^2$. Another popular choice of numerical improvement in the lattice is the so-called Iwasaki action [48].

So far, we have only considered the gauge boson part of the action. Now, we shall briefly discuss about the fermionic sector. For instance, the discretization of the gauge-covariant derivative in the following way

$$D_\mu q(x) \to \frac{1}{2a} \left[U_\mu(x)q(x + a\hat{\mu}) - U_\mu(x - a\hat{\mu})^\dagger q(x - a\hat{\mu}) \right], \tag{1.56}$$

leads to the so-called naive fermion action, which in the continuum describes 16 fermion fields. This is a consequence of the Nielsen-Ninomiya theorem [49], which states that one cannot define lattice fermions with exact, continuum-like chiral symmetry without producing doublers. This issue can be tackled in several ways. One solution for the doubling problem is to add new terms to the Lagrangian, which explicitly break chiral symmetry. This will lead to what are known as Wilson fermions [50]. The consequence of adding chiral-breaking terms is that the doublers acquire the mass of order $O(1/a)$ and become heavy in the limit $a \to 0$, decoupling from the theory. This term, however, introduces discretization errors of order $O(a)$. The improvement is achieved by considering the $O(a)$-improved Wilson fermion [51], which is an application of the already introduced Symanzik improvement program [52]. The main advantage of this method is that it is relatively cheap (does not require large amount of computational resources) [53, 54].

A variant of the Wilson method is known as twisted-mass fermions [55]. Here, two flavors of quarks are treated together with a twisted-mass term which breaks isospin. The advantage of this method is that all leading-order errors proportional to the lattice spacing automatically vanish by a clever choice of the twisting angle [56]. An issue of this method is the emergence of isospin breaking effects. These, however, go as $a^2\Lambda^2$ in the continuum limit, where Λ is the momentum scale for the quantity being calculated.

Other formulations of fermions on the lattice exist (see, e.g. [57–68]). As with the previously introduced methods, these also have their own advantages and disadvantages. Thus, the choice of technique will depend on what is being studied. For instance, if the object of study does not require a near-exact chiral symmetry, there is no need to make use of the methods which are very expensive. On the contrary, there are applications where exact chiral symmetry is required and the expensive formulations (e.g., domain wall fermions, overlap fermions) are heavily favored.

1.5 Finite volume formalism

Until now, we have briefly introduced a couple of approaches that allow us to study the QCD spectrum in the low-energy regime. The first method relies on the fact that quarks have never been seen isolated, i.e. only colorless states are observed in experiments. Thus, in a certain energy domain, we could consider these states as relevant degrees of freedom, neglecting the effects of their inner structure. As already mentioned in previous sections, these composite particles are the hadrons. Further, considering the scale separation that naturally arises in this sector, one could construct an effective Lagrangian where the lightest particles are the dynamic degrees of freedom. Roughly speaking, the heavy particles can be integrated out from the effective theory. Of course, the effect of these particles is still present in the low-energy constants (LECs) that parametrize the low-energy Lagrangian. Nevertheless, these parameters can be fitted to experimental data, deeming the theory free of any direct influence from the heavy sector. In the case at hand, the degrees of freedom are the lightest mesons (pions, kaons and eta). With this, one can then proceed to compute the scattering of hadrons in the low-energy regime and investigate their properties, without any knowledge of their inner constituents, i.e., quarks and gluons. This framework is known as ChPT, introduced in Sec. 1.3.

Another way of accessing information in the low-energy regime of QCD is Lattice Quantum Chromodynamics. This is, until now, the only model-independent approach to study, from first principles, the effects of strong interactions between particles that are color charged. Within this scheme, several proposals on how to introduce the gauge bosons and fermions to the lattice have been discussed in the latter Section. Furthermore, it was also briefly mentioned that errors due to discretization and finite volume are to be expected in the results within this framework. Namely, these are a consequence of working in a finite lattice spacing a and in a finite volume, i.e., $a \neq 0$ and $L \neq \infty$, where L is the size of a cubic box in which we work in the following. Fortunately, both of these can be studied with the help of EFTs. For instance, a program that deals with errors that emerge from a non-vanishing lattice spacing was briefly introduced in Sec.1.4, the so-called Symanzik improvement program, where the Symanzik effective Lagrangian is used. Furthermore, an important characteristic of finite-volume effects is that they are considerably smaller than the hadronic scale Λ, i.e., $1/L \ll \Lambda$. Because of this, the effective theory of QCD, the already introduced ChPT, can be employed to calculate finite-volume effects in this low-energy domain.

Furthermore, it is important to note that these two effects can be studied separately. This can be seen

if we look at the scales at which these artifacts emerge. For example, the discretization of space-time naturally introduces an ultraviolet cutoff of order $1/a \sim \Lambda$. Taking $L \gg 1/\Lambda$ we can conclude that the artifacts arising as a consequence of the volume dependence can be studied independently from the other effects. A peculiar outcome of this conclusion is that one can work in the continuum, $a \rightarrow 0$, in order to calculate effects introduced by the volume.

Since our main objective is the extraction of physical quantities from a finite volume, the question now is whether we can apply both of the introduced methods, effective theories and lattice QCD, to extract the maximum information possible from the system under investigation. As previously mentioned, the key feature in this case is that the scale at which the finite-volume artifacts arise are of order $1/L$, far away from Λ which is of order 1 GeV. Moreover, the effective field theory of QCD in this momenta regime is already known to us. The conclusion that can be drawn from both these facts is the following: owing to the fact that $1/L \ll \Lambda$, the effective Lagrangians in a finite and in the infinite volume are the same. In this manner, one can consistently make use of effective field theories to analyze the finite-volume effects that arise in lattice QCD.

In short, the transition from an infinite- to a finite-volume is straightforward. The crucial point is that the effective Lagrangians are the same both in a finite and in the infinite volume. Furthermore, the low-energy constants that parametrize the effects from the heavy sector are not affected by the volume. Hence, the only L-dependence in this case stems from the loops. This means that, in order to work in a finite volume, one has to apply the boundary conditions to the fields and rewrite the integrals as sums over the loop momenta. With this, it is possible to compare the values of physical quantities of interest calculated both in an infinite-volume and on the lattice.

Additionally, the region in which the effective theory is valid poses an interesting question. Namely, the value of the product $M_\pi L$ will lead to regimes where distinct methods are applicable. Consider for example the case where $M_\pi L$ is of order one. This is the so-called p-regime. Here, the already introduced finite-volume methods are still valid. That is, we have to replace the integrals by sums over the allowed discrete values of momenta. This will lead to finite-volume corrections that are exponentially suppressed in the argument $M_\pi L$. Another case that can be considered is when $M_\pi L$ is small. This is known as the δ-regime and it is accessed when the chiral limit is considered. Here, ChPT is no longer applicable as the finite-volume artifacts become non-perturbative in this regime. Note also that the exponential suppression does not emerge in case of the so-called "gapless" diagrams, in which the intermediate particles can go on shell. Such diagrams emerge in certain kinematical regimes (e.g. in the scattering process). In such cases, it is convenient to work in large volumes, $M_\pi L \gg 1$, and neglect the exponentially suppressed contributions vs. power-law suppressed ones, emerging from "gapless" diagrams. Since the characteristic momenta are of order $1/L$, one may conclude that the non-relativistic EFTs are the most natural way to describe this energy domain. For instance, an equation for the extraction of scattering data from the lattice can be derived by implementing this prescription. In later sections this formalism is described in detail. Finally, one an also consider a box in a finite temperature, i.e., the time extension is considered finite. This case is known as the ϵ-regime. In the following we will focus our attention to the p-regime, which is relevant to study we want to perform in later Chapters.

Before we dwell into how to calculate these artifacts, let us see what are the consequences of working in a cubic space. One of these is that space-time boundary conditions for the fields have to be introduced. For instance, the most common choice of these conditions is to have all fields periodic in the spatial coordinates. These periodic boundary conditions mean that the three-momenta can only
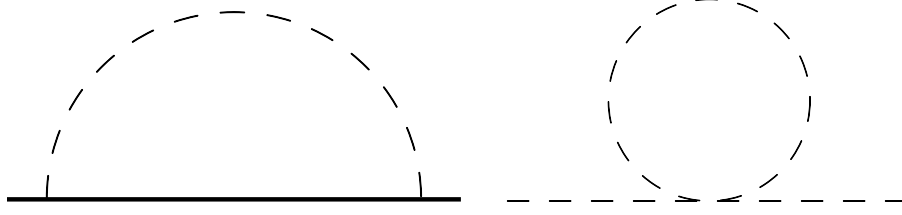
Figure 1.6: Loop diagrams that contribute to the mass in a finite volume of the nucleon and pion, respectively. Solid and dashed lines denote the nucleon and pion propagators, respectively.

take discrete values

$$\vec{p} = \frac{2\pi}{L}\left(n_1, n_2, n_3\right), \qquad n_i \in \mathbb{Z}. \tag{1.57}$$

Moreover, the finite size in the temporal coordinate, denoted by T, puts the system at a finite temperature. This effect is suppressed, provided that $m_\pi T \gg 1$, where m_π is the mass of the lightest meson. $T \to \infty$ is assumed in the following.

For now, let us give a concrete example on how to proceed in a finite volume. It is natural to ask how the structure of the loop integrals is modified in this scheme. In practice, this is done by constraining the arbitrary values of the momenta to discrete ones, as in Eq. 1.57. Thus, the only difference consists in replacing the three-dimensional integrals with the sums over discrete lattice momenta. Assuming periodic boundary conditions, loop integrals are modified in the following way:

$$\frac{1}{i}\int \frac{d^4k}{(2\pi)^4} \to \frac{1}{i}\int_V \frac{d^4k}{(2\pi)^4} \equiv \int \frac{dk_0}{2\pi}\frac{1}{L^3}\sum_{\vec{k}}, \quad \vec{k} = \frac{2\pi}{L}\vec{n}, \ \vec{n} = \mathbb{Z}^3. \tag{1.58}$$

Depending on their momentum dimension, some of the loop integrals in the infinite volume diverge. In the continuum this divergence is tamed by using dimensional regularization. The question now is whether this procedure also works on the lattice. Indeed, this methodology works both in the finite- and infinite-volume prescription, as the counterterms that remove the divergences are the same in both cases. Let us now consider a simple case where this prescription is applied. We will briefly sketch the calculation of the pion mass in a finite volume. To this end, we will make use of the finite-volume pion mass calculated in ChPT to fourth order in p, where p is a small momentum/mass. The physical mass is [69]

$$M^2_{\text{phys}} = M^2 + \frac{M^2}{2F^2}I_0 + \frac{2M^4}{F^2}l_3, \tag{1.59}$$

where M is related to the quark condensate through $M^2 = 2B\hat{m}$ and $\hat{m} = \frac{1}{2}(m_u + m_d)$. Furthermore, I_0 is a one-loop integral of the form $\int \frac{d^D k}{(2\pi)^D i}\frac{1}{M^2-k^2}$ and l_3 is a low-energy constant stemming from the fourth-order ChPT Lagrangian for the case of two flavors, $N_f = 2$. As already mentioned, the finite-volume corrections arise solely through the pion loops. Also, recall that the low-energy constant is not modified on the lattice, i.e., it remains the same in both a finite and in an infinite volume. Hence, to find the mass of the pion and its effects due to the lattice, we must replace I_0 by $I_{0,L}$ (note that we

perform the calculations on Euclidean space), where

$$I_{0,L} = \frac{1}{L^d} \sum_{\vec{p}} \int \frac{dp_4}{2\pi} \frac{1}{M^2 + p_4^2 + \vec{p}^2}, \quad d = D - 1. \tag{1.60}$$

This result can be conveniently simplified by applying the Poisson's summation formula to the integrand. The obtained expression is:

$$I_{0,L} = \sum_{\vec{n}} \int \frac{dp_4}{2\pi} \int \frac{d^d \vec{p}}{(2\pi)^d} \frac{e^{iL\vec{n}\vec{p}}}{M^2 + p_4^2 + \vec{p}^2}. \tag{1.61}$$

Here, the case when is considered $\vec{n} = \vec{0}$ gives back the infinite-volume result, I_0. Therefore, the subsequent terms in the sum are the finite-volume corrections to the loop integral. In this case, $\vec{n} \neq \vec{0}$, we notice that the integrals are finite. Thus, we can write the finite-volume result as

$$I_{0,L} = I_0 + \Delta I_{0,L},$$
$$\Delta I_{0,L} = \sum_{\vec{n} \neq \vec{0}} \frac{M}{4\pi^2 Ln} K_1(nLM), \tag{1.62}$$

where $n = |\vec{n}|$ and K_1 is the modified Bessel function of the second kind. Finally, we can write the correction to the pion mass as

$$M_L^2 = M^2 + \sum_{\vec{n} \neq \vec{0}} \frac{M^3}{8\pi^2 F^2 Ln} K_1(nLM). \tag{1.63}$$

The asymptotic behavior of the Bessel functions for large arguments allows us to further simplify this result

$$M_L^2 = M^2 + \frac{M^4}{2F^2} \sum_{\vec{n} \neq \vec{0}} \frac{e^{-nLM}}{2(2\pi nLM)^{\frac{3}{2}}} + \dots . \tag{1.64}$$

From here, it can be easily seen that the effects induced by the lattice are exponentially suppressed by an argument of ML.

To end this section, let us consider the case of the nucleon mass and briefly discuss the corrections in a finite volume. The steps to determine the effects induced by the lattice closely follow the ones taken for the pion case; corrections to the mass arise from the loops, see Fig. 1.6. In this case, however, the heavy particle mass is also present in the integrals. As discussed in previous sections, this gives rise to the breaking of power counting in the infinite volume. We shall see that this does not occur in a finite volume. To illustrate this, consider the nucleon self energy integral in Eq. 1.44 in Euclidean space on the lattice

$$I_{\pi N,L} = \frac{1}{L^d} \sum_{\vec{k}} \int \frac{dk_4}{2\pi} \frac{1}{\left[(k-p)^2 + m^2\right](k^2 + M^2)}, \tag{1.65}$$

where p and m are the nucleon momentum and mass, respectively. The integral can be rewritten as

$$\Delta I_{\pi N,L} = \sum_{\vec{n}\neq 0} \int \frac{d^4 k}{(2\pi)^4} \int_0^1 \frac{dx\, e^{iL\vec{n}\vec{k}}}{(k_4^2 + \vec{k}^2 + \Delta)^2}. \tag{1.66}$$

Here, the Poisson's summation formula was used together with the Feynman trick to simplify the integral. Further, $\Delta = (1-x)M^2 + xm^2 - x(1-x)p_4^2$. This can also be brought to a compact form by writing it in terms of Bessel functions. In this case we have:

$$\begin{aligned}
\Delta I_{\pi N,L} &= \frac{1}{8\pi^2} \sum_{\vec{n}\neq 0} \int_0^1 K_0(nL\sqrt{\Delta}) e^{iLx\vec{n}\vec{p}} \\
&= \frac{1}{8\pi^2} \sum_{\vec{n}\neq 0} \int_0^1 \sqrt{\frac{\pi}{2nL\Delta^{1/2}}} e^{-nL\sqrt{\Delta}} e^{iLx\vec{n}\vec{p}} + \dots,
\end{aligned} \tag{1.67}$$

where the ellipses denote terms of order $O(\Delta^{-1})$. In the end, we see that in $I_{\pi N,L}$ the contribution from the region $x \equiv 1$, which is responsible for the breaking of the power counting rules, is highly suppressed by the presence of the nucleon mass in the exponential. This happens because the power counting breaks down when $p \sim m$, which leads to finite-volume effects proportional to e^{-mL}. However, since $m \sim \Lambda$ and $m\lambda L \gg 1$, these terms can be safely neglected. Because of this, only the infinite volume part has to be taken care of. Thus, finite-volume contributions to the nucleon mass automatically respects the power counting scheme.

1.6 External field method

The external field method states that the three- and four-point correlation functions can be obtained from considering the two-point function of the nucleon in a weak background electromagnetic field, A_μ. This technique is quite versatile and it has been used to determine several properties of baryons on the lattice. For example, the magnetic moments, axial-vector matrix elements and polarizabilities of hadrons have been measured by making use of a constant background field [70–75]. If the case of a non-uniform field is considered, further hadronic quantities such as form-factors and structure functions can be evaluated [76–78].

The implementation of this method on to the lattice is relatively simple. Namely, the gauge link $SU(3)$ between the lattice sites is replaced by

$$U_\mu(x) \to U_\mu(x) \exp\left[ieaA_\mu\right], \tag{1.68}$$

where a is the lattice spacing. Supposing that the field is small, a perturbative expansion on the field can be performed, corresponding to Fig. 1.7. Thus, by considering certain configurations of A^μ, different parameters can be accessed by means of this technique [79]. Let us now consider an application in the context of low-energy scattering.

Recently, the authors in [80, 81] implemented this method to investigate the Compton amplitude on the lattice. They noted that the Compton tensor emerges as a second-order term in the external field strength. This allows one to study the Compton amplitude from the nucleon two-point function in a
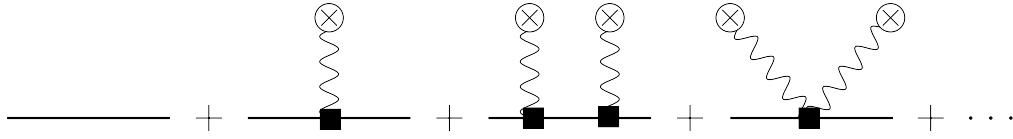
Figure 1.7: Expansion of the two-point function in the external field. Notice that the Compton tensor appears as a second-order term in the expansion. Figure adapted from [79]

weak external field, avoiding the direct computation of the four-point function, which is computationally quite burdensome. In the following Section the implications of the findings in these works are further discussed. In short, the authors were able to extract the so-called subtraction function by using a non-relativistic effective field theory.

Motivated by this result, one could attempt to extend the findings to the case where unstable particles are present. This is further discuss in the following sections, where resonances and the Lüscher's method are introduced.

1.7 Compton scattering

The Compton scattering plays an important role in the study of physical properties of hadrons. For example, the low-energy Compton scattering takes part in the determination of the nucleon electromagnetic polarizabilities, which quantify the quadratic response to an applied external field. These quantities can be calculated, for example, in the context of ChPT, see, e.g. [82] were able to determine the electric and magnetic polarizabilities of the nucleon to great accuracy. More recently, several works that also consider and further develop this study have been published [83–86]. Another way of studying the Compton tensor is through lattice QCD. The advantage of doing so, is that it offers a model-independent approach to analyze certain aspects of the system, e.g., the structure functions, which have played an important role in the determination of the muonic Lamb shift [87], as well as the proton-neutron mass difference [88].

Let us formally define the Compton scattering in an infinite volume. Here, we will consider the forward Compton scattering off the nucleon. More specifically, the doubly virtual case is investigated in what follows. To begin, let us define the Compton scattering amplitude:

$$\hat{T}^{\mu\nu}(p', s', q'|p, s, q) = \frac{i}{2} \int d^4x \, e^{iq \cdot x} \langle p', s'|T j^\mu(x) j^\nu(0)|p, s\rangle \,, \qquad (1.69)$$

where p and q denote the incoming nucleon and photon four-momenta, respectively. Similarly, p' and q' are the outgoing ones. Additionally, s and s' are the spin projections of the in- and out-going nucleon. Moreover, j^μ denotes the electromagnetic current. The spin-averaged forward scattering amplitude is defined as

$$T^{\mu\nu}(p, q) = \frac{1}{2} \sum_s \hat{T}^{\mu\nu}(p, s, q|p, s, q) \,. \qquad (1.70)$$

Owing to Lorenz invariance, current conservation and parity, the amplitude can be written in terms of
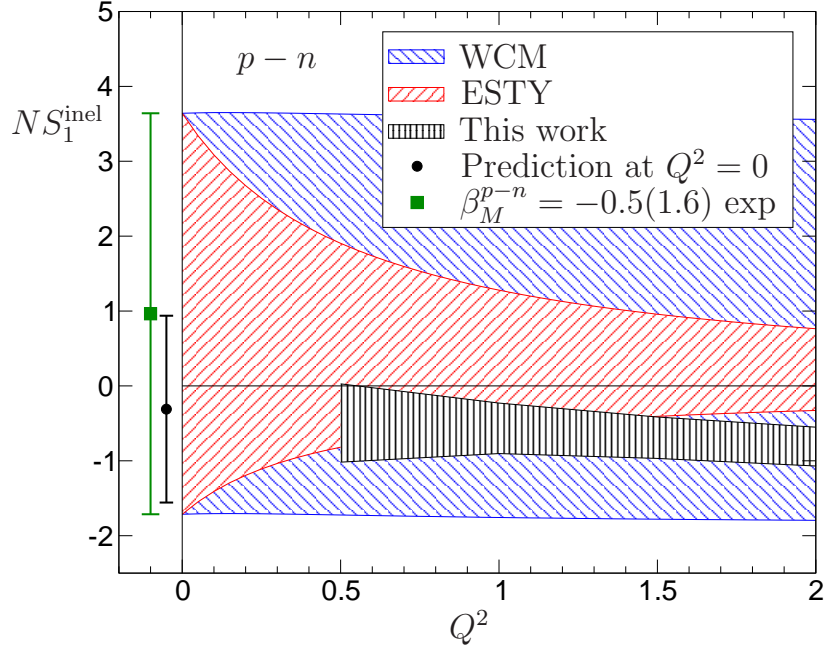
Figure 1.8: Proton minus neutron subtraction function in terms of momentum transfer Q^2 in GeV units. The vertical axis is stretched by the inverse of the dipole form factor, $N = (1 + Q^2/M_d^2)^2$, $M_d^2 = 0.71$ GeV^2. The blue and red shadowed areas represent the phenomenological parametrizations given in [89] (WCM) and in [90] (ESTY), respectively. The gray band is obtained from the Reggeon dominance hypothesis [91], where the prediction of the subtraction at Q^2 is displaced for visibility purposes.

the invariant amplitudes T_1 and T_2:

$$T^{\mu\nu}(p,q) = T_1(\nu, q^2) K_1^{\mu\nu} + T_2(\nu, q^2) K_2^{\mu\nu}, \qquad (1.71)$$

where $\nu = p \cdot q/m$ and m is the nucleon mass. Both structure functions can be split into elastic and inelastic parts. The first are given by:

$$
\begin{aligned}
T_1^{\text{el}}(\nu, q^2) &= \frac{4m^2 q^2 \left\{ G_E^2(q^2) - G_M^2(q^2) \right\}}{(4m^2\nu^2 - q^4)(4m^2 - q^2)}, \\
T_2^{\text{el}}(\nu, q^2) &= -\frac{4m^2 \left\{ 4m^2 G_E^2(q^2) - q^2 G_M^2(q^2) \right\}}{(4m^2\nu^2 - q^4)(4m^2 - q^2)},
\end{aligned}
\qquad (1.72)
$$

where G_E, G_M denote the electric and magnetic form factors of the nucleon. Furthermore, the

inelastic parts obey the following dispersion relations

$$T_1^{\text{inel}}(\nu, q^2) = T_1^{\text{inel}}(\nu_0, q^2) + 2(\nu^2 - \nu_0^2) \int_{\nu_{\text{th}}}^{\infty} \frac{\nu' d\nu' \, V_1(\nu', q^2)}{(\nu'^2 - \nu_0^2)(\nu'^2 - \nu^2 - i\varepsilon)} \, ,$$

$$T_2^{\text{inel}}(\nu, q^2) = 2 \int_{\nu_{\text{th}}}^{\infty} \frac{\nu' d\nu' \, V_2(\nu', q^2)}{\nu'^2 - \nu^2 - i\varepsilon} \, . \tag{1.73}$$

The lower integration limit is $\nu_{\text{th}} = (W_{\text{th}}^2 - m^2 - q^2)/(2m)$, with $W_{\text{th}} = m + M$, where M is the pion mass. Further, V_1, V_2 denote the absorptive parts of T_1^{inel}, T_2^{inel}. These can be expressed through experimental data of the observed total electroproduction cross sections $\sigma_T(\nu, q^2)$, $\sigma_L(\nu, q^2)$, where the subscripts T and L denote the transverse and longitudinal parts, respectively.

The amplitude T_2 is fully determined through the experimental data. However, the dispersion relation for T_1 requires a subtraction. Choosing $\nu_0 = 0$ for simplicity, the subtraction function, defined as $S_1 \equiv T_1(0, q^2)$, is not determined by experimental data without further dynamical assumptions. To this end, several approaches have been proposed in an attempt to resolve this problem. For instance, effective field theories and phenomenological considerations were used to fix this function [89, 90]. More recently, the Reggeon dominance hypothesis was used to estimate the value of S_1 [92, 93]. In the later, it is assumed that the high-energy limit of the Compton amplitude is determined by the Reggeon exchange. The results in the context of the Reggeon dominance hypothesis from the available experimental data are displayed in Fig.1.8. From the plot, it is clear that the uncertainties are sizable and difficult to estimate. Hence, a model-independent approach must be put forward to test this hypothesis. Lattice QCD represents such a tool. If the behavior of the subtraction function, measured on the lattice, will be very much different from the one determined phenomenologically, this would testify in favor of the existence of a fixed pole in the Compton amplitude and will lead to important ramification on our present understanding of the asymptotic behavior of the QCD amplitude.

The exercise of designing a framework for evaluating the Compton amplitude on the lattice has been done recently [80, 81]. The authors made use of a non-relativistic effective field theory to compute the two-point correlation function in a background field. More specifically, they considered the case of a nucleon in a static periodic magnetic field $\vec{B} = (0, 0, B^3)$ with $B^3 = -B\cos(\vec{\omega}\vec{x})$ and $\vec{\omega} = (0, \omega, 0)$. Summarizing their findings, the authors were able to demonstrate that energy shift of the nucleon in an external field is directly related to the subtraction function. Namely,

$$\delta E = \frac{(eB)^2}{4m} S_1(-\vec{\omega}^2), \tag{1.74}$$

where δE denotes the spin-averaged energy shift and m is the mass of the nucleon. As this expression was obtained in the infinite-volume limit, a re-formulation starting from a finite-volume setup was necessary to take into account the finite-volume corrections in the presence of an external field. Their final result was:

$$\delta E = -\frac{1}{4\pi} \left(\frac{eB}{\omega} \right)^2 T^{11}(p, q) + O(B^3). \tag{1.75}$$

This expression contains the "11" component of the Compton tensor in a finite-volume given in Eq. 1.71. Before actually extracting this quantity on the lattice, it would be important to estimate where there are large finite-volume artifacts in this quantity. This can be done with the use of ChPT. With this
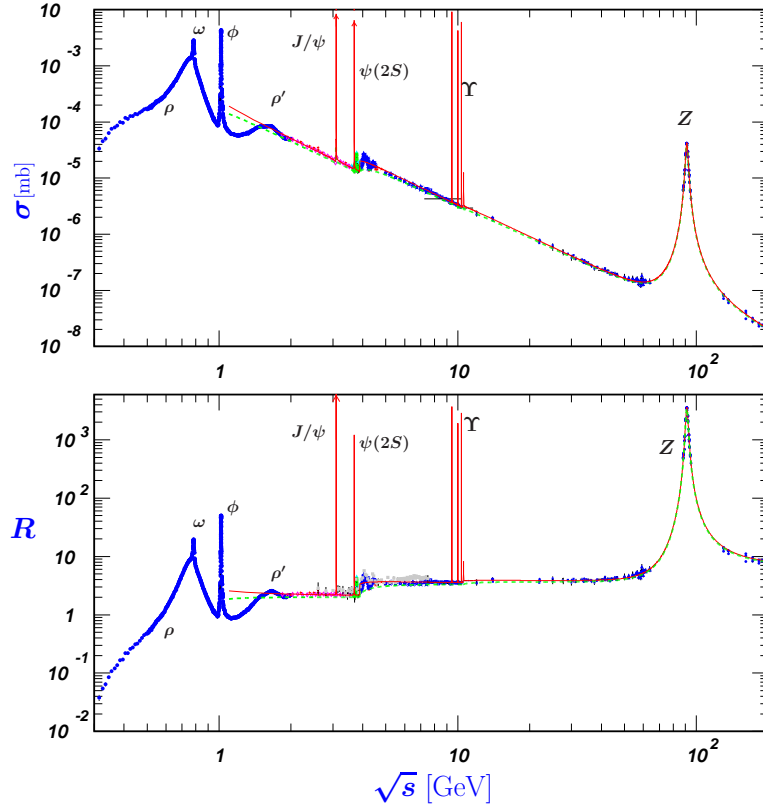
Figure 1.9: Hadronic annihilation cross-section in e^+e^- collisions [94].

result, it is possible to estimate the exponentially suppressed corrections to the subtraction function.

To summarize, the determination of the subtraction function $S_1(q^2)$ remains an interesting and topical research topic. Finding this function is of great interest to the nuclear physics community.

1.8 Resonances

A fascinating feature of QCD is that most of the hadrons are resonances. One particular aspect of these states is that they will eventually decay into other strongly interacting particles, i.e. they are unstable within QCD. Usually, two-particle resonances are seen as poles in the cross-sections of a given process when plotted as a function of the energy, see Fig. 1.9. Examples of such a behavior are the ρ-meson, primarily decaying via $\rho \to \pi\pi$, the $\Delta(1232) \to N\pi$, and so on.

Resonances can be identified as poles in the scattering amplitude. In particular, consider the case of two interacting particles of mass m, $p_1 + p_2 \to p_3 + p_4$. The amplitude is a function the Mandelstam variables $s = (p_1 + p_2)^2$ and $t = (p_1 - p_3)^2$. Further, the elastic scattering amplitude $\mathcal{T}$ of the system can be decomposed in terms of partial-wave amplitudes as

$$\mathcal{T} = 4\pi \sum_{l=0}^{\infty} \sum_{m=-l}^{l} \mathcal{Y}_{lm}(\vec{p}')\mathcal{Y}_{lm}^*(\vec{p})T_l, \tag{1.76}$$

where $\mathcal{Y}_{lm} = |\vec{p}|^l Y^{lm}(\hat{p})$ and $\hat{p} = \vec{p}/|\vec{p}|$. In this expression l denotes the angular momentum contributions to the amplitude.

The elastic unitarity condition is

$$\text{Im}\,\mathcal{T}_l^{-1} = -\frac{2q(s)}{\sqrt{s}}\Theta(\sqrt{s} - 2m). \tag{1.77}$$

Here, $q(s) = \sqrt{s/4 - m^2}$. The presence of $q(s)$ in the unitary relations means that, at threshold, $\mathcal{T}_l$ has a branch cut starting at $\sqrt{s} = \sqrt{2m}$. A direct consequence of the latter is that the elastic scattering amplitude features two Riemann sheets. In this framework, bound-states can be identified as poles on the real axis of the physical sheet below threshold. Furthermore, resonances appear as poles off the real axis on the unphysical sheet. In particular, resonances come in conjugate pairs where the real part, m_R is related to the mass, and the imaginary part to its width, Γ_R. The above given definition is exact. In the literature, we find various phenomenological parametrizations of the resonant amplitudes as well. A well-known way of describing narrow resonances is through the Breit-Wigner parametrization [95, 96]:

$$T_{BW} \propto \frac{1}{m_R^2 - im_R\Gamma_R - s}, \tag{1.78}$$

which is valid near $s = m_R^2$.

It is convenient to find the resonance pole by employing the K-matrix parametrization of the amplitude. For instance, the partial-wave amplitude $\mathcal{T}_l$ can be parameterized by making use of the so-called K-matrix as

$$\mathcal{T}_l = \frac{\sqrt{s}}{2}\frac{1}{K_l^{-1}(s) - iq(s)}, \tag{1.79}$$

with $K_l^{-1}(s) = q(s)\cot\delta_l$. Here, δ_l denotes the phase-shifts of the two-particle system. This particular parametrization of the amplitude facilitates the determination of the resonance pole position, q_R, on the complex plane. As the parameters m_R and Γ_R are formally defined on the second Riemann sheet, an analytic continuation is necessary. Namely, one has to find a solution to the equation

$$q_R(s)\cot\delta_l - iq_R(s) = 0. \tag{1.80}$$

To achieve this, the effective range expansion, valid near the threshold can be used [96, 97]:

$$q\cot\delta_l = -\frac{1}{a} + \frac{1}{2}rq^2 + O(q^4), \tag{1.81}$$

where a and r are the S-wave scattering length and the effective range, respectively. These parameters can be determined, e.g., through a fit to lattice energy levels.

Resonances exhibit a peculiar behavior on the lattice. Namely, their presence in scattering data has a distinctive influence on the energy levels. For instance, let us briefly consider a resonance in a finite volume and the energy spectrum as a function of the box length. When a narrow resonance is present, the energy levels behave in a distinctive way. Namely, the curves tend to a particular energy in the spectrum, which is identified as the resonance mass, $E = E_R$, see Fig. 1.10. Thus, the avoided level crossing in the lattice spectrum provides a solid indication of the presence of such a resonance in the
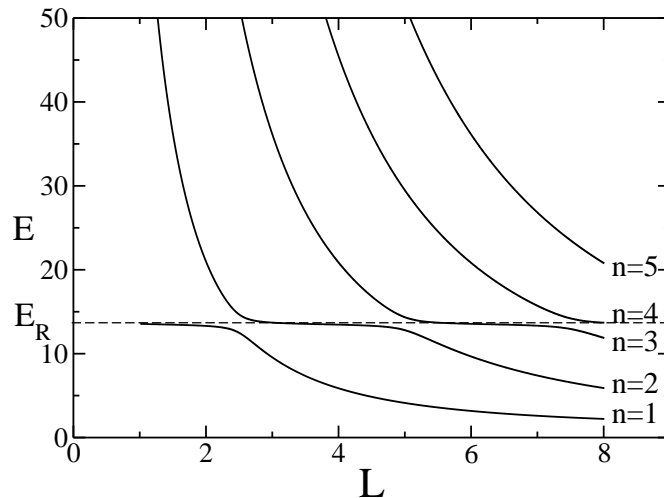
Figure 1.10: Spectrum of the two-particle system in a finite box of size L. The energy levels reach a plateau at the resonance mass, E_R. Figure taken from [100].

scattering amplitude.

Configurations where resonances are present turn the analysis of physical observables on the lattice into quite a challenging task. Fortunately, the Lüscher's method facilitates the access to scattering data of unstable particles in a finite volume. By relating the discrete finite-volume spectrum of QCD to the infinite-volume scattering amplitude of resonances, physical information can be extracted from the lattice through the determination of partial-wave phase shifts.

In-depth descriptions of the main tools here presented and alternative ways to categorize and study resonances can be found in the following comprehensive reviews [98, 99].

1.9 Lüscher's method

It is natural to ask whether one can extract physical information of a scattering process in a finite volume. The answer to this question is positive, as it was shown by M. Lüscher in his seminal works [101, 102]. In the following, we will briefly discuss how one can obtain scattering data from the discrete energy spectrum in a finite volume, more specifically from its volume dependence. The main ingredients of this prescription are the scattering phase-shift, denoted by $\delta(p)$, and the extension of the box, L. Let us now discuss how these two quantities come together to create a bridge between the infinite- and finite-volume prescriptions.

To illustrate this, consider for simplicity the scattering of two identical bosons in an infinite volume with one spatial dimension, where relativistic effects can be neglected. Here, all values of momenta, p, are allowed and the scattering amplitude is described by the phase-shift, $\delta(p)$. Now, let us examine what happens when the system is put in a box. As we know, the allowed momenta now are restricted to discrete values, as in Eq. 1.57. Additionally, the asymptotic form of the wave function goes as

$$\Psi(x) \propto e^{-ip|x|} + e^{2i\delta(x)}e^{ip|x|}, \tag{1.82}$$

where x is the distance between the particles. Imposing the periodic boundary conditions of the box on the wave function, $\Psi(0) = \Psi(L)$, it can be showed that the momenta will exhibit the following behavior

$$p = \frac{2\pi}{L} - \frac{2}{L}\delta(p). \tag{1.83}$$

From this result it can be concluded that, when the particles interact, the spectrum depends on the finite-volume box size and the infinite-volume phase-shift. If we set $\delta = 0$, i.e. no scattering, the free energy spectrum is recovered. The main consequence of this expression is that it is possible to extract infinite-volume information from the discrete energy spectrum. We note that Eq. 1.83 is the one-dimensional equivalent of the well-known Lüscher equation. Although this example was done in a one-dimensional setup, the procedure can be generalized to three dimensions within a cubic box. In this derivation we will take advantage of the perks that non-relativistic effective field theories have to offer. Namely, this method will enable us to derive the quantitation condition in a relatively easy manner.

In the following, we closely follow the derivation from [103]. Here, we will consider the case of non-identical scalar particles in a moving frame. For this, it is convenient to use the NREFT Lagrangian in its covariant form given by [104, 105]:

$$\begin{aligned}
\mathcal{L} = &\sum_{i=1,2} \Phi_i^\dagger 2W_i(i\partial_t - W_i)\Phi_i + C_0\Phi_1^\dagger\Phi_1\Phi_2^\dagger\Phi_2 \\
&+ C_1\left((\Phi_1^\dagger)^\mu(\Phi_2^\dagger)_\mu\Phi_1\Phi_2 - m_1m_2\Phi_1^\dagger\Phi_1\Phi_2^\dagger\Phi_2 + h.c.\right) \\
&+ C_2\left(\Phi_1^\dagger(\Phi_2^\dagger)^\mu - (\Phi_1^\dagger)^\mu\Phi_2^\dagger\right)\left((\Phi_1)_\mu\Phi_2 - \Phi_1(\Phi_2)_\mu\right) + \dots,
\end{aligned} \tag{1.84}$$

where ellipses denote terms with higher order derivatives and C_0, C_1 and C_2 are related to the effective-range expansion parameters for $1 + 2 \to 1 + 2$ elastic scattering. Further, Φ_i, $i = 1, 2$ denote two scalar fields with masses m_1 and m_2. The energies of the particles are denoted by $W_i = \sqrt{m_i^2 + \nabla^2}$, and

$$(\Phi_i)_\mu = (\mathcal{P}_i)_\mu\Phi_i, \quad (\Phi_i^\dagger)_\mu = (\mathcal{P}_i^\dagger)_\mu\Phi_i^\dagger, \quad (\mathcal{P}_i)_\mu = (W_i, -i\nabla), \quad (\mathcal{P}_i^\dagger)_\mu = (W_i, i\nabla). \tag{1.85}$$

Now, let us write down the scattering T-matrix in the infinite volume with the help of the Lagrangian in Eq. 1.84. It can be shown that the T-matrix obeys the Lippmann-Schwinger (LS) equation:

$$\begin{aligned}
T(\vec{p}_1.\vec{p}_2; \vec{q}_1, \vec{q}_2) = &-V(\vec{p}_1, \vec{p}_2; \vec{q}_1, \vec{q}_2) - \int \frac{d^D\vec{k}_1}{(2\pi)^D 2w_1(\vec{k}_2)}\frac{d^D\vec{k}_2}{(2\pi)^D 2w_2(\vec{k}_2)} \\
&\times (2\pi)^D\delta^D(\vec{p}_1 + \vec{p}_2 - \vec{k}_1 - \vec{k}_2)\frac{V(\vec{p}_1, \vec{p}_2; \vec{k}_1, \vec{k}_2)T(\vec{k}_1.\vec{k}_2; \vec{q}_1, \vec{q}_2)}{w_1(\vec{k}_1) + w_2(\vec{k}_2) - w_1(\vec{p}_1) - w_2(\vec{p}_2) - i0},
\end{aligned} \tag{1.86}$$

where D denotes the space-time dimension and $w_i(\vec{p}) = \sqrt{m_i^2 + \vec{p}^2}$. Further, the potential V is given by the matrix element of the interaction Hamiltonian between the two-particle states

$$\langle\vec{p}_1, \vec{p}_2| H_1 |\vec{q}_1, \vec{q}_2\rangle = (2\pi)^3\delta^3(\vec{p}_1 + \vec{p}_2 - \vec{q}_1 - \vec{q}_2)V(\vec{p}_1, \vec{p}_2; \vec{q}_1, \vec{q}_2). \tag{1.87}$$

Now, let us consider the partial-wave expansion of the amplitude. The expression is given by

$$T(\vec{p}_1.\vec{p}_2; \vec{q}_1, \vec{q}_2) = 4\pi \sum_{lm} t_l(|\vec{p}^*|, |\vec{q}^*|) \mathcal{Y}_{lm}(\vec{p}^*) \mathcal{Y}_{lm}^*(\vec{q}^*),$$

$$V(\vec{p}_1.\vec{p}_2; \vec{q}_1, \vec{q}_2) = 4\pi \sum_{lm} v_l(|\vec{p}^*|, |\vec{q}^*|) \mathcal{Y}_{lm}(\vec{p}^*) \mathcal{Y}_{lm}^*(\vec{q}^*), \tag{1.88}$$

where $\mathcal{Y} = |\vec{p}|^l Y_{lm}(\hat{p})$ and Y_{lm} are spherical harmonics. Here, $\vec{p}^*$ denotes the momenta boosted to the CM frame. Next, we substitute Eq. 1.88 into Eq. 1.86 to obtain

$$t_l(s) = -v_l(s) - v_l(s)|\vec{p}^*|^{2l} G(s) t_l(s). \tag{1.89}$$

Here, $t_l(s) = t_l(|\vec{p}^*|, |\vec{p}^*|)$ and $v_l(s) = v_l(|\vec{p}^*|, |\vec{p}^*|)$ where v_l denotes the Hermitian potential. Further, $G(s)$ is [104, 105]

$$G(s) = \frac{i|\vec{p}^*|}{8\pi\sqrt{s}}. \tag{1.90}$$

Finally, unitarity dictates the following relations for the amplitude and the potential:

$$t_l(s) = \frac{8\pi\sqrt{s}}{|\vec{p}^*|^{2l+1}} e^{i\delta_l(s)} \sin \delta_l(s), \tag{1.91}$$

$$v_l(s) = -\frac{8\pi\sqrt{s}}{|\vec{p}^*|^{2l+1}} \tan \delta_l(s). \tag{1.92}$$

Next, let us consider the system in a finite volume. In this case, rotational invariance is broken, which leads to partial-wave mixing. Because of this, the scattering amplitude has to be modified in the following way:

$$T(\vec{p}_1.\vec{p}_2; \vec{q}_1, \vec{q}_2) = 4\pi \sum_{lm,l'm'} \mathcal{Y}_{lm}(\vec{p}^*) \mathcal{Y}_{l'm'}^*(\vec{q}^*) t_{lm,l'm'}(|\vec{p}^*|, |\vec{q}^*|). \tag{1.93}$$

The partial-wave expansion of the potential is again give by Eq. 1.88, because only exponential corrections arise there and these are consistently neglected. Furthermore, the partial-wave expanded amplitude is substituted into the LS equation. This yields:

$$t_{lm,l'm'}(s; \vec{P}) = -\delta_{lm,l'm'} v_l(s) - 4\pi \sum_{l''m''} v_l(s) X_{lm,l''m''}(s; \vec{P}) t_{l''m'',l'm'}(s; \vec{P}), \tag{1.94}$$

where $X_{lm,l''m''}(s; \vec{P})$ takes the form

$$X_{lm,l''m''}(s; \vec{P}) = \frac{|\vec{p}|^{l+l'+1}}{32\pi^2\sqrt{s}} i^{l-l'} M_{lm,l'm'} \tag{1.95}$$

$$M_{lm,l'm'} = \frac{(-1)^l}{\pi^{3/2}\gamma} \sum_{j=|l-l'|}^{l+l'} \sum_{s=-j}^{j} \frac{i^j}{\eta^{j+1}} \mathcal{Z}_{js}^{\vec{d}}(1; s) C_{lm,js,l'm'}, \tag{1.96}$$

and $\gamma = \sqrt{1 + \vec{P}^2/s}$, $\vec{d} = 2\pi/L\vec{P}$, $\eta = |\vec{p}|L/2\pi$ and $C_{lm,js,l'm'}$ are the Wigner $3 - j$ symbols. Additionally, the function $\mathcal{Z}$ is defined as

$$\mathcal{Z}_{lm}^{\vec{p}}(1;s) = \sum_{\vec{r} \in P_d} \frac{\mathcal{Y}_{lm}(\vec{r})}{\vec{r}^2 - \eta^2}, \qquad P_d = \left\{ \vec{r} | \vec{r} = \gamma^{-1}\left(\vec{n} - \frac{1}{2}\vec{\Delta}\right), \vec{n} \in \mathbb{Z}^3 \right\}, \qquad \vec{\Delta} = \vec{d}\left(1 + \frac{m_1^2 - m_2^2}{s}\right)$$

(1.97)

The finite-volume spectrum is determined by locating the poles of the scattering matrix T. These appear when the determinant of the system of linear equations in Eq. 1.94 vanishes.

The so-called Lüscher quantization condition for the case of two non-identical particles is finally given by:

$$\det\left[\delta_{ll'}\delta_{mm'} - \tan\delta_l(s)\mathcal{M}_{lm,l'm'} \right] = 0.$$

(1.98)

Through this equation, it is possible to relate the infinite-volume scattering data with the finite-volume energy spectrum of the system. In particular, given a set of energy levels calculated in the lattice, Eq. 1.98 can be fitted to the spectrum in order to obtain the scattering phase-shift. This is, in practice, the primary use of the quantization condition.

It is important to note that the derived expression holds only for the two-particle system. However, most of the resonances have decay channels that involve three or more hadrons in the final state. Well-known examples of these are the $a_1(1260)$ and Roper resonances, which decay into multiparticle stable states. In this case, the introduced formalism is not suited to extract the information one is interested in. Because of this, an extension to the well-understood Lüscher formalism must be put forward, e.g. a three-particle quantization condition.

In recent years, three equivalent formulations have been introduced in regards of the three-particle quantization condition. These are known as the non-relativistic Effective-Field-Theory (NREFT) [106, 107], Relativist Field Theory (RFT) [108–114] and Finite-Volume Unitarity (FVU) [115, 116] approaches. These formulations are not covered in the following, as this work only deals with the two-body case. Nonetheless, a reader is referred to [117] for an in-depth analysis of the methods mentioned here. In particular, the three-particle quantization condition is thoroughly discussed there. In the review, it is concluded that the three formulations are conceptually equivalent, although each of them has their own advantages and disadvantages.

The main benefit of the NREFT approach is that the derivation of the quantization condition is dramatically simplified. This due to the fact that there is no particle creation in the non-relativistic regime, leading to a reduced number of diagrams to be calculated. This, in turn, allows the easy computation of such. There have been recent developments in the three-particle sector. For instance, a formula for the three-body s-wave decay amplitude was derived [118]. Furthermore, an extension to all partial-waves was recently made available [119]. These examples demonstrate that NREFTs are indeed a very efficient method of extracting information from the lattice. The interested reader is further referred to [120] for a detailed summary on EFTs and their implementation on a finite volume.

1.10 Resonance Form Factors

The study of resonances through the Lüscher's method has further applications. For instance, one could consider the case where the system is placed in a weak background field. This allows one to study the structure of resonances through its interaction with an external source. This information in
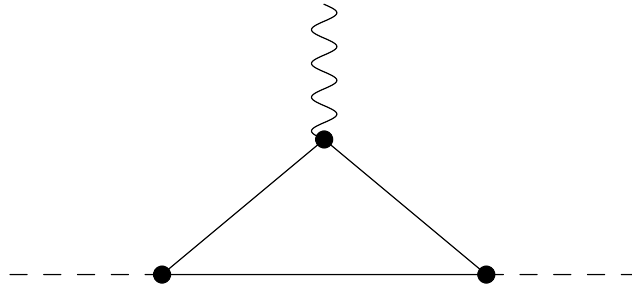
Figure 1.11: The triangle diagram. Here, the dashed lines denote a resonance. Further, solid and wiggled lines are the constituents of the resonance and the external current, respectively.

particular is encoded in the so-called resonance form factors (RFF). Through their determination, one can have access to information about the inner structure of such particles.

It is important to calculate RFF on the lattice. To formally define it, one must take the obtained finite-volume result into the infinite volume. Such a procedure requires an analytic continuation into the complex plane. For matrix elements between one-particle states, the extraction of the form factors from a finite volume is rather straightforward. However, this mapping is non-trivial for the resonance case. The study can get complicated by the presence of a rather problematic diagram, the so-called triangle diagram, where one of the resonance constituents couples to the external source, see Fig. 1.11.

This issue has been tackled in [103, 110, 121, 122]. Here, however, we aim to circumnavigate the problematic situation that arises by the presence of the triangle diagram in a different way. Namely, we take the result from [78] and extend it to the case of resonances. In short, the authors of that paper made use of the Feynman-Hellmann theorem [123, 124] to compute the form factor of a stable hadron in a static, spatially periodic field. They showed that the mass of the particle can be determined by computing the two-point correlation function in the Breit frame in an external field. It was further showed that the form factor can be derived by taking the derivative of the mass with respect to the coupling of the external field to leading order. In the unstable particle case, the pole position, P_R, will play the role of the mass parameter. Thus, the aim is to calculate it on the lattice and take its derivative with respect to the external field coupling, e. Namely,

$$\frac{dP_R(e)}{de}\bigg|_{e=0} \propto F, \tag{1.99}$$

where F is the RFF.

To achieve this, the NREFT formalism can be employed. As mentioned already, an advantage of this method is that the number of diagrams to be calculated is small when compared to other formalisms.

The Lagrangian, for the case of two scalar fields ϕ of mass m in an external field A^μ, can be written as:

$$\mathcal{L} = \phi^\dagger \left(i\partial_t - m + eA^0 + \frac{eC_R}{6m^2} \triangle A^0 + \frac{\nabla^2}{2m} \right) \phi + C_0 \phi^\dagger \phi^\dagger \phi \phi$$

$$+ C_2 \left(\phi^\dagger \phi^\dagger (\phi \overset{\leftrightarrow}{\nabla}{}^2 \phi) + \text{h.c.} \right) + \frac{e\kappa}{4} \phi^\dagger \phi^\dagger \phi \phi \triangle A^0 \tag{1.100}$$

$$+ \quad \text{higher order terms with derivative couplings,}$$

where $\triangle$ is the Laplacian and $a\overset{\leftrightarrow}{\nabla}b = \frac{1}{2}(a\nabla b - b\nabla a)$. Further, the constant C_R determines the single-particle form factor and C_0, C_2 are related to the s-wave phase-shift. Finally, κ determines the contact interaction.

At leading order in this framework, only the contact interaction coupling must be extracted from the lattice in order to compute the RFF. To do this, an extension of the Lüscher's method in the case of external sources must be derived, leading to the determination of the missing Lagrangian parameter, κ.

List of publications

The present thesis is based on the following publications in international peer-reviewed journals:

- **J. Lozano**, A. Agadjanov, J. Gegelia, U.-G. Meißner, and A. Rusetsky, Phys. Rev. **D 103**, 034507 (2021).

- **Lozano, J.**, Meißner, U.-G., Romero-López, F., Rusetsky, A., Schierholz, G. Resonance form factors from finite-volume correlation functions with the external field method. J. High Energ. Phys. **2022**, 106 (2022).

Conference proceedings:

- **J. Lozano**, "Finite volume corrections to forward Compton scattering off the nucleon," PoS LATTICE2021, 307 (2022).

Compton scattering in a finite volume

Summary

The content of this chapter is based on the publication

- J. Lozano, A. Agadjanov, J. Gegelia, U.-G. Meißner, and A. Rusetsky, Phys. Rev. **D 103**, 034507 (2021).

This work deals with the forward doubly virtual Compton scattering amplitude off nucleons. In recent years, the calculation of this amplitude has regained attention, as it is a crucial part in the analysis of fundamental problems such as, for example, the study of the muonic Lamb shift or evaluation of the proton-neutron mass difference. Thus, a model-independent calculation of this amplitude would certainly aid in the solution of these problems. Lattice Quantum Chromodynamics (LQCD) is a well-suited approach to examine this issue. This approach provides necessary tools to investigate these problems from first principles in Quantum Chromodynamics (QCD). Nevertheless, these calculations are afflicted by finite-volume artifacts, which must be removed from lattice results. The objective of this work is to estimate these finite-volume corrections to the Compton amplitude for a certain kinematical configuration.

An appropriate way to calculate the Compton amplitude in the low-energy regime is to make use of Effective Field Theories. For this reason, the calculations were done in the low-energy effective theory of QCD known as Baryon Chiral Perturbation Theory (BChPT). The results are computed up-to-and-including $O(p^4)$, where p is a small momentum/mass. Our study focused on the calculation of the so-called subtraction function, which is related to the Compton amplitude in a particular kinematics. To achieve this, we evaluated the forward doubly virtual Compton scattering amplitude off nucleons and investigated the behavior of the subtraction function at small values of the photon momentum, both in the infinite and in a finite volume. Furthermore, the finite-volume corrections to the subtraction function were evaluated up-to-and-including $O(p^4)$.

As a first step, which was performed by the author of this thesis in close collaboration with J. Gegelia, all diagrams contributing to the forward doubly virtual Compton scattering amplitude are calculated following the Feynman rules obtained from the effective Lagrangian of order $O(p^4)$. In this study, there exist two sets of diagrams: one set for the proton and another one for the neutron. In the infinite volume, the final result after the summation of all contributions is a second-order tensor that can be written in terms of two invariant amplitudes. These are quantities that must be analyzed in

order to determine the nature of the subtraction function. The subtraction function can be defined through the 11-component of the Compton tensor. For this reason, we only compute the Compton amplitude for this component in a certain kinematics.

Until now, all the analysis of the subtraction function was done in the infinite volume. As a next step, the infinite-volume integrals are replaced by sums and the amplitude is again calculated in a finite volume. The result of this calculation leads to an estimation of the finite-volume corrections to the Compton amplitude. Note also that, in a finite volume, the Lorentz-invariance does not hold anymore, and the Compton amplitude cannot be written down in terms of two kinematic structures only. Hence, one has to compare certain components of this amplitude (11 component, in our case) directly in a finite and in the infinite volume. For convenience, a ratio of these is taken. With this, one can easily estimate the discrepancy between the two as a function of the dimensionless parameter $M_\pi L$, where M_π is the mass of the pion. Finally, one can estimate how big the side of the box should be so that these corrections can be safely ignored.

The results of this work can be summarized as follows:

- The forward doubly virtual Compton scattering amplitude is evaluated both in the infinite and in a finite volume.

- The subtraction function at small values of the momentum transfer is obtained in the infinite volume.

- The evaluation of exponentially small finite-volume corrections to the Compton amplitude is performed.

- It is concluded that the infinite-volume subtraction function can be extracted from the lattice with a good precision for sufficiently large cubic box of length L.

Finite volume corrections to forward Compton scattering off the nucleon

J. Lozano,[1,*] A. Agadjanov,[2,†] J. Gegelia [ORCID],[3,4,‡] U.-G. Meißner [ORCID],[1,5,4,§] and A. Rusetsky [ORCID][1,4,‖]

[1]*Helmholtz-Institut für Strahlen- und Kernphysik (Theorie) and Bethe Center for Theoretical Physics,
Universität Bonn, 53115 Bonn, Germany*
[2]*PRISMA⁺ Cluster of Excellence and Institut für Kernphysik, Johannes Gutenberg-Universität Mainz,
D-55099 Mainz, Germany*
[3]*Ruhr-University Bochum, Faculty of Physics and Astronomy, Institute for Theoretical Physics II,
D-44870 Bochum, Germany*
[4]*Tbilisi State University, 0186 Tbilisi, Georgia*
[5]*Institute for Advanced Simulation, Institut für Kernphysik and Jülich Center for Hadron Physics,
Forschungszentrum Jülich, D-52425 Jülich, Germany*

We calculate the spin-averaged amplitude for doubly virtual forward Compton scattering off nucleons in the framework of manifestly Lorentz-invariant baryon chiral perturbation theory at complete one-loop order $O(p^4)$. The calculations are carried out both in the infinite and in a finite volume. The obtained results allow for a detailed estimation of the finite-volume corrections to the amplitude which can be extracted on the lattice using the background field technique.

I. INTRODUCTION

Recent years have observed a rapidly increasing interest in calculations of nucleon structure functions on the lattice. Different algorithms, which enable one to extract these quantities from lattice measurements, have been proposed. For example, in Ref. [1] a method for a direct calculation of the quark and gluon distribution functions on Euclidean lattices by Lorentz boosting of the nucleons was suggested. A lattice calculation of the Euclidean four-point function, describing the virtual Compton amplitude, and its relation to the leptoproduction cross section has been considered [2–5]. A similar method has been applied to the study of the hadronic tensor with charged vector currents in Ref. [6]. In the present paper we shall concentrate on an alternative proposal which is based on the use of the background field technique (or the Feynman-Hellmann method) for measuring the forward doubly virtual Compton scattering amplitude off nucleons; see Refs. [7–13]. This amplitude is directly related to the moments of the structure functions.

*lozano@hiskp.uni-bonn.de
†agadjanov@uni-mainz.de
‡jambul.gegelia@ruhr-uni-bochum.de
§meissner@hiskp.uni-bonn.de
‖rusetsky@hiskp.uni-bonn.de

For a review of the present status of lattice studies of the structure functions, see, e.g., Ref. [14].

In Refs. [7–13] a comprehensive theoretical assessment of the feasibility of the extraction of the Compton amplitude has been carried out. Here, one has to note that a similar technique has been already successfully used for the extraction of the magnetic moments and polarizabilities of certain hadrons [15–17]. The study of Compton scattering, however, implies another level of sophistication. Namely, whereas the static characteristics of the nucleon can be measured in constant background magnetic and electric fields, the dependence of the forward Compton amplitude on the photon virtuality, $q^2 = -Q^2$, cannot be studied similarly. Therefore, one has to use periodic background fields (in space), which enable one to consider nonzero values of the photon three-momentum, while the time component of the photon momentum q stays zero. Several subtle issues had to be addressed in this context, for example, a consistent realization of the periodic background field on a finite lattice [18], or the zero-frequency limit [13]. It must also be mentioned that, according to Ref. [19], the interpretation of the lattice measurements, which are done in a finite volume, might be ambiguous for both constant and periodic fields. More precisely, the quantity that is obtained as a result of such a measurement (for instance, the polarizability) could be different from what one has previously identified as a finite-volume counterpart of the polarizability. This point of view has been countered in Ref. [13], where it has been argued that the finite-volume lattice results allow for a unique

interpretation in terms of well-defined physical quantities (at least when the photon virtuality is not zero). Since this issue is important in the context of the problem considered here, we shall briefly address it later.

It should be stressed that the measurement of the forward Compton amplitude on the lattice is a useful endeavor by itself, even beyond its relation to the nucleon structure functions. Indeed, let us point out that the forward Compton amplitude represents an important building block in many long-standing fundamental problems that have recently come under a renewed scrutiny. In particular, the knowledge of this amplitude is needed for the evaluation of the Lamb shift in muonic hydrogen [20], as well as the proton-neutron mass difference. The study of the latter problem has a decades-long history [21,22], but still continues to attract quite some interest that is reflected in a string of recent publications [23–28]. To a large part, this upsurge of interest can be related to the fact that the present lattice studies are in a position to address the calculation of the purely electromagnetic proton-neutron mass shift in QCD plus QED, and hence the results of phenomenological determinations can be directly confronted with lattice data. Further, in Refs. [27,28], under the assumption that the high-energy behavior of the Compton amplitude is fully determined by Reggeon exchange (the so-called Reggeon dominance hypothesis), a sum rule has been derived that involves this amplitude in a particular kinematics (a variant of this sum rule has been known in the literature already for 50 years [29]). Notably, the latter enables one to express the Compton amplitude through the experimentally measured electroproduction cross sections. Calculations on the basis of the above sum rule have been performed recently [28], where the uncertainties emerging from the use of all presently available experimental input have been thoroughly analyzed. A direct evaluation of the Compton amplitude on the lattice would allow one to compare the outcomes of these two different theoretical calculations. Should it happen that the results are very different, this could be attributed to the failure of the Reggeon dominance hypothesis, i.e., to the existence of so-called fixed poles in the Compton amplitude. At present, we are not aware of any mechanism within QCD that would lead to such poles. Hence, their discovery would challenge our understanding of the asymptotic behavior of QCD and stimulate a quest for new mechanisms, which are responsible for this behavior.

One of the most important questions, which so far has not been addressed in the context of the extraction of the Compton amplitude from lattice data, is the issue of the finite-volume corrections to the physical quantities of interest. It is very important to estimate, prior to performing any calculations on the lattice, how large lattices should be used to suppress the unwanted finite-volume artifacts. Note that, even though on general grounds these artifacts are

exponentially small, due to possible large prefactors they might still be substantial for the presently used lattice sizes. The systematic study of this problem that is carried out in what follows within the framework of baryon chiral perturbation theory (BChPT) at order $O(p^4)$ is intended to fill this gap.[1]

The layout of the paper is the following. In Sec. II we collect all definitions and input, which will be needed later. This concerns both purely infinite-volume calculations as well as the finite-volume setting used on the lattice for the extraction of the Compton amplitude. Further, the calculation of the Compton amplitude is carried out in the infinite as well as in a finite volume. Namely, Sec. III contains the full expression of the infinite-volume Compton amplitude at $O(p^4)$ in BChPT. Also, a comparison to the results available in the literature is carried out. The expression of the finite-volume amplitude at the same order is given in Sec. IV. In Sec. IV B, the results of the numerical estimations of the finite-volume artifacts are discussed. Section V contains our conclusions.

II. BASIC DEFINITIONS AND NOTATIONS

A. Doubly virtual Compton scattering in forward direction in the infinite volume

In this paper we follow the notations of Ref. [24]. In order to render the paper self-contained, below we collect all formulas that will be used in the infinite-volume calculations. The Compton scattering amplitude is defined as

$$
\hat{T}^{\mu\nu}(p', s', q'|p, s, q)
= \frac{i}{2} \int d^4x \, e^{iq \cdot x} \langle p', s'|Tj^\mu(x)j^\nu(0)|p, s\rangle, \quad (1)
$$

where (p', s') and (p, s) are the four-momenta and spin projections of incoming and outgoing nucleons, respectively, and q and q' are the momenta of the (virtual) photons in the initial and final states, respectively. Further, j^μ denotes the electromagnetic current. The state vectors of the nucleon are normalized as

$$
\langle p', s'|p, s\rangle = 2p^0(2\pi)^3\delta^{(3)}(\mathbf{p}' - \mathbf{p})\delta_{s's}. \quad (2)
$$

We define the unpolarized forward scattering amplitude as an average over the nucleon spins:

$$
T^{\mu\nu}(p, q) = \frac{1}{2}\sum_s \hat{T}^{\mu\nu}(p, s, q|p, s, q). \quad (3)
$$

Using Lorentz invariance, current conservation, and parity, this amplitude can be expressed through two invariant amplitudes:

---

[1]For brevity, we shall often refer to the calculations up-to-and-including order p^4 as to the calculations at $O(p^4)$.

$$T^{\mu\nu}(p,q) = T_1(\nu,q^2)K_1^{\mu\nu} + T_2(\nu,q^2)K_2^{\mu\nu},$$
$$K_1^{\mu\nu} = q^\mu q^\nu - g^{\mu\nu}q^2,$$
$$K_2^{\mu\nu} = \frac{1}{m^2}\{(p^\mu q^\nu + p^\nu q^\mu)p\cdot q - g^{\mu\nu}(p\cdot q)^2 - p^\mu p^\nu q^2\},$$

$$(4)$$

where $\nu = p\cdot q/m$ and m is the nucleon mass.

At this place we mention that the choice of the invariant amplitudes is not unique. In the literature, another choice is often made, using the set $\hat{T}_1, \hat{T}_2$ with $\hat{T}_1 = q^2 T_1 + \nu^2 T_2$ and $\hat{T}_2 = -\nu^2 T_2$. This alternative choice, however, produces kinematic singularities, which complicate the discussion of the asymptotic behavior of these amplitudes. As a result, the issue with the fixed poles may become obscure. For further details on this subject we refer the reader to Refs. [24,28] and also to [30,31]. Further, in Refs. [27,28], another set of invariant amplitudes $\bar{T} = T_1 + \frac{1}{2}T_2$, T_2 has been introduced instead of T_1, T_2. The advantage of using this set consists in the fact that the leading asymptotic behavior of $\bar{T}$ at large values of Q^2 is governed by spin-0 operators, whereas the contribution from the spin-2 operators in the operator product expansion cancels in this particular linear combination. A thorough discussion of this question is given in Ref. [28]. Here, we only mention that the set $\bar{T}, T_2$ is obviously free from the kinematic singularities, as well as the set T_1, T_2.

Further, the invariant amplitudes can be split into the elastic and inelastic (or, equivalently, into the Born and non-Born) parts. Again note that such a splitting is not uniquely defined and the definition of Ref. [24] differs from the ones used in Refs. [32,33].[2] Here we would like to mention only that the definition, which will be used in the following, unambiguously follows from the requirement that the elastic amplitude vanishes in the limit $\nu \to \infty$, for fixed q^2, and thus obeys an unsubtracted dispersion relation in the variable ν. Under this requirement, the elastic part is given by

$$T_1^{\text{el}}(\nu, q^2) = \frac{4m^2 q^2\{G_E^2(q^2) - G_M^2(q^2)\}}{(4m^2\nu^2 - q^4)(4m^2 - q^2)},$$
$$T_2^{\text{el}}(\nu, q^2) = -\frac{4m^2\{4m^2 G_E^2(q^2) - q^2 G_M^2(q^2)\}}{(4m^2\nu^2 - q^4)(4m^2 - q^2)}, \quad (5)$$

where G_E and G_M denote the electric and magnetic (Sachs) form factors of the nucleon.

The inelastic invariant amplitudes are defined as $T_i^{\text{inel}} = T_i - T_i^{\text{el}}$, with $i = 1, 2$. The amplitudes T_i^{inel} obey dispersion relations in the variable ν:

$$T_1^{\text{inel}}(\nu, q^2) = T_1^{\text{inel}}(\nu_0, q^2) + 2(\nu^2 - \nu_0^2)$$
$$\times \int_{\nu_{\text{th}}}^\infty \frac{\nu' d\nu' V_1(\nu', q^2)}{(\nu'^2 - \nu_0^2)(\nu'^2 - \nu^2 - i\varepsilon)},$$
$$T_2^{\text{inel}}(\nu, q^2) = 2\int_{\nu_{\text{th}}}^\infty \frac{\nu' d\nu' V_2(\nu', q^2)}{\nu'^2 - \nu^2 - i\varepsilon}. \quad (6)$$

Here, one has already taken into account the fact that, according to Regge theory, the dispersion relations for T_1^{inel} and T_2^{inel} require one subtraction and no subtractions, respectively. The lower integration limit is equal to $\nu_{\text{th}} = (W_{\text{th}}^2 - m^2 - q^2)/(2m)$, with $W_{\text{th}} = m + M_\pi$, where M_π is the pion mass. The quantities V_1, V_2 denote the absorptive parts of $T_1^{\text{inel}}, T_2^{\text{inel}}$. They can be expressed through the experimentally observed total (transverse, longitudinal) electroproduction cross sections $\sigma_T(\nu, q^2), \sigma_L(\nu, q^2)$.

The choice of the subtraction point ν_0 is arbitrary. In the literature, the choice $\nu_0 = 0$ is often used. The quantity $S_1^{\text{inel}}(q^2) = T_1^{\text{inel}}(0, q^2)$ is usually referred to as the subtraction function. Analogously, one can define the full subtraction function that includes the elastic part as well: $S_1(q^2) = S_1^{\text{el}}(q^2) + S_1^{\text{inel}}(q^2) = T_1(0, q^2)$. At $q^2 = 0$ the inelastic part of the subtraction function is given by

$$S_1^{\text{inel}}(0) = -\frac{\kappa^2}{4m^2} - \frac{m}{\alpha}\beta_M, \quad (7)$$

where κ and β_M denote the anomalous magnetic moment and the magnetic polarizability of the nucleon, respectively, and $\alpha \simeq 1/137$ is the electromagnetic fine-structure constant.

Recently, a different subtraction function was introduced in Refs. [27,28]. The subtraction point has been chosen at $\nu_0 = iQ/2$, where $Q = \sqrt{-q^2}$. The new subtraction function is expressed through the amplitude $\bar{T}$:

$$\bar{S}(q^2) = \bar{T}^{\text{inel}}(\nu_0, q^2). \quad (8)$$

At $Q^2 = 0$ one has

$$\bar{S}(0) = -\frac{\kappa^2}{4m^2} + \frac{m}{2\alpha}(\alpha_E - \beta_M). \quad (9)$$

The two subtraction functions are closely related to each other. Namely, the difference $S_1^{\text{inel}}(q^2) - \bar{S}(q^2)$ is given through a convergent integral over the experimentally measured electroproduction cross sections. Hence, it suffices to calculate one of these subtraction functions. Since the choice $\nu_0 = 0$, in contrast to $\nu_0 = iQ/2$, can be implemented on the lattice in a straightforward manner [12,13], we stick to this choice.

---

[2]See, e.g., Refs. [28,34] for a general discussion of the issue of nonuniqueness of the Born part of the Compton scattering amplitude.

B. Extraction of the subtraction function on the lattice

Below, we shall collect all formulas which are needed for the extraction of the subtraction function on the lattice with the use of the background field method. More details are contained in the original papers [12,13]. Here, we consider the nucleon placed in a periodic magnetic field on the lattice with a spatial size L (the temporal size of the lattice is assumed to be much larger and is effectively set to infinity). The configuration of the magnetic field is chosen as

$$\mathbf{B} = (0, 0, -eB\cos(\omega \mathbf{n}\mathbf{x})), \quad \mathbf{n} = (0, 1, 0), \quad (10)$$

where e denotes the proton charge. Because of the periodic boundary conditions, the available values of ω are quantized,[3]

$$\omega = \frac{2\pi n}{L}. \quad (11)$$

The energy levels of a nucleon in the magnetic field depend on the projection of the nucleon spin along the z axis. In Ref. [13] it has been shown that the spin-averaged level shift in the magnetic field with a given configuration is given by

$$\delta E = -\frac{1}{4m}\left(\frac{eB}{\omega}\right)^2 T_L^{11}(p, q) + O(B^3), \qquad p^\mu = (m, \mathbf{0}),$$

$$q^\mu = (0, 0, \omega, 0). \quad (12)$$

Note that here $T_L^{11}(p, q)$ denotes the 11-component of the full Compton scattering amplitude in a finite volume [in other words, $T_L^{11}(p, q)$ includes both inelastic and elastic parts]. Further, $q^2 = -\omega^2$. Hence, placing a nucleon in the periodic magnetic field enables one to extract the amplitude at nonzero (albeit discrete) values of $q^2 < 0$. The other variable is $\nu = p \cdot q/m = 0$ in the given kinematics. Thus, in order to obtain a nonzero value of ν, one has to put the nucleon in a moving frame.

Note also that due to the lack of Lorentz invariance on a finite hypercubic lattice, the decomposition of this amplitude into invariant amplitudes in a form given in Eq. (4) does in general not hold. However, all quantities in Eq. (12) are well-defined in a finite volume. For example, in perturbation theory, $T^{11}(p, q)$ is given by a sum of all diagrams at a given order, where all momentum integrations are replaced by finite-volume momentum sums. In the infinite-volume limit one has

$$\lim_{L\to\infty} T_L^{11}(p, q) = T^{11}(p, q) = -\omega^2 S_1(q^2). \quad (13)$$

---

[3]In fact, this is one of the possible realizations of the external field on the lattice. An alternative implies the quantization of the magnitude of the field, rather than its frequency [18]. However, as was demonstrated in Ref. [13], the present realization provides an optimal framework for the extraction of the subtraction function at nonzero values of the momentum transfer.

The finite-volume corrections in the above formula are suppressed by a factor of $\exp(-M_\pi L)$, multiplied by powers of L. As already mentioned in the Introduction, despite the exponential factor, the corrections can still be sizable for the present-day lattices. Last but not least, let us stress once more that, for all values of L, Eq. (12) enables one to extract a perfectly well-defined quantity $T_L^{11}(p, q)$, which in the infinite volume limit yields the quantity $S_1(q^2)$ that we are after. This demonstrates explicitly that in this setup one could avoid any ambiguous interpretation of the results as mentioned in Ref. [19].

We conclude this section by briefly specifying the scope and aims of the present paper. It is clear that the extraction of the Compton amplitude on the lattice can be carried out only in a restricted kinematical domain. For instance, if the variable ν lies above the pion production threshold $\nu_{\text{th}} = (2m)^{-1}(W_{\text{th}}^2 - m^2 - q^2)$, then the extracted matrix element does not possess an infinite-volume limit. This can be seen immediately since, in the infinite-volume limit, the corresponding amplitude is complex, whereas the amplitude extracted from an Euclidean lattice is always real. Hence, in order to arrive at the infinite-volume amplitude, one has either to take into account the proper Lellouch-Lüscher factor in analogy with Ref. [35] (see also Refs. [36–42]; a first step in this direction has been made in Ref. [43]) or to use an approach that resembles the optical potential method of Ref. [44] (see also Refs. [45,46]). All of this is very complicated and not even needed to achieve the goals we have stated in the beginning. Indeed, given the subtraction function, which is obtained from the Compton amplitude at $\nu = 0$, one may restore the whole Compton amplitude by using dispersion relations. The whole uncertainty related to the fixed poles then resides in the subtraction function, and the rest is uniquely determined by analyticity, unitarity, and the experimental input.

C. Effective Lagrangian

In this paper the forward Compton scattering amplitude will be calculated in BChPT at order p^4, both in the infinite and in a finite volume. Below we specify the effective Lagrangian with the pions and nucleons, which is needed for such a calculation. The leading-order effective Lagrangian of pions interacting with external sources has the form [47]:

$$\mathcal{L}_\pi^{(2)} = \frac{F^2}{4}\langle D_\mu U(D^\mu U)^\dagger \rangle + \frac{F^2}{4}\langle \chi U^\dagger + U\chi^\dagger \rangle, \quad (14)$$

where $\chi = 2B(s + ip)$, $D_\mu U = \partial_\mu U - ir_\mu U + iUl_\mu$, and the 2×2 matrix U represents the pion field. The parameter B is related to the quark condensate, F is the pion decay constant in the two-flavor chiral limit, and s, p, $l_\mu = v_\mu - a_\mu$ and $r_\mu = v_\mu + a_\mu$ are external sources. The notation $\langle \cdots \rangle$ denotes the trace in flavor space.

The full order four effective Lagrangian of nucleons interacting with pions and external fields is given in Ref. [48]. Below we specify only those terms, which contribute in our calculations,[4]

$$\mathcal{L}_{\pi N} = \mathcal{L}_1 + \mathcal{L}_2 + \mathcal{L}_3 + \mathcal{L}_4 + \cdots,$$

$$\mathcal{L}_1 = \bar{\Psi} i \gamma^\mu D_\mu \Psi - \overset{\circ}{m} \bar{\Psi} \Psi + \frac{\overset{\circ}{g}_A}{2} \bar{\Psi} \gamma^\mu \gamma_5 u_\mu \Psi,$$

$$\mathcal{L}_2 = c_1 \langle \chi_+ \rangle \bar{\Psi} \Psi - \frac{c_2}{8 \overset{\circ}{m}^2} \langle u^\alpha u^\beta \rangle (\bar{\Psi} \{D_\alpha, D_\beta\} \Psi + \text{H.c.}) + \frac{c_3}{2} \langle u^\mu u_\mu \rangle \bar{\Psi} \Psi$$
$$+ i \frac{c_4}{4} \bar{\Psi} [u_\mu, u_\nu] \sigma^{\mu\nu} \Psi + \frac{c_6}{2} \bar{\Psi} \sigma^{\mu\nu} \tilde{F}^+_{\mu\nu} \Psi + \frac{c_7}{8} \bar{\Psi} \sigma^{\mu\nu} \langle F^+_{\mu\nu} \rangle \Psi + \cdots,$$

$$\mathcal{L}_3 = \left(\frac{i d_6}{2 \overset{\circ}{m}} \bar{\Psi} [D^\mu, \tilde{F}^+_{\mu\nu}] D^\nu \Psi + \text{H.c.} \right) + \left(\frac{i d_7}{2 \overset{\circ}{m}} \bar{\Psi} [D^\mu, \langle F^+_{\mu\nu} \rangle] D^\nu \Psi + \text{H.c.} \right) + \cdots,$$

$$\mathcal{L}_4 = -\frac{e_{54}}{2} \bar{\Psi} [D^\lambda, [D_\lambda, \langle F^+_{\mu\nu} \rangle]] \sigma^{\mu\nu} \Psi - \frac{e_{74}}{2} \bar{\Psi} [D^\lambda, [D_\lambda, \tilde{F}^+_{\mu\nu}]] \sigma^{\mu\nu} \Psi + e_{89} \bar{\Psi} \langle F^+_{\mu\nu} \rangle \langle F^{+\mu\nu} \rangle \Psi$$
$$- \left(\frac{e_{90}}{4 \overset{\circ}{m}^2} \bar{\Psi} \langle F^+_{\lambda\mu} \rangle \langle F^{+\lambda\alpha} \rangle g_{\alpha\nu} D^{\mu\nu} \Psi + \text{H.c.} \right) + e_{91} \bar{\Psi} \tilde{F}^+_{\mu\nu} \langle F^{+\mu\nu} \rangle \Psi$$
$$- \left(\frac{e_{92}}{4 \overset{\circ}{m}^2} \bar{\Psi} \tilde{F}^+_{\lambda\mu} \langle F^{+\lambda\alpha} \rangle g_{\alpha\nu} D^{\mu\nu} \Psi + \text{H.c.} \right) + e_{93} \bar{\Psi} \langle \tilde{F}^+_{\mu\nu} \tilde{F}^{+\mu\nu} \rangle \Psi$$
$$- \left(\frac{e_{94}}{4 \overset{\circ}{m}^2} \bar{\Psi} \langle \tilde{F}^+_{\lambda\mu} F^{+\lambda\alpha} \rangle g_{\alpha\nu} D^{\mu\nu} \Psi + \text{H.c.} \right) - \frac{e_{105}}{2} \bar{\Psi} \langle F^+_{\mu\nu} \rangle \langle \chi_+ \rangle \sigma^{\mu\nu} \Psi$$
$$- \frac{e_{106}}{2} \bar{\Psi} \tilde{F}^+_{\mu\nu} \langle \chi_+ \rangle \sigma^{\mu\nu} \Psi - \left(\frac{e_{117}}{8 \overset{\circ}{m}^2} \bar{\Psi} \langle F^-_{\lambda\mu} F^{-\lambda\alpha} + F^+_{\lambda\mu} F^{+\lambda\alpha} \rangle g_{\alpha\nu} D^{\mu\nu} \Psi + \text{H.c.} \right)$$
$$+ \frac{e_{118}}{2} \bar{\Psi} \langle F^-_{\mu\nu} F^{-\mu\nu} + F^+_{\mu\nu} F^{+\mu\nu} \rangle \Psi + \cdots, \tag{15}$$

where

$$\sigma^{\mu\nu} = \frac{i}{2} (\gamma^\mu \gamma^\nu - \gamma^\nu \gamma^\mu),$$

$$\tilde{X} = X - \frac{1}{2} \langle X \rangle,$$

$$D_\mu \Psi = \partial_\mu \Psi + (\Gamma_\mu - i v^{(s)}_\mu) \Psi,$$

$$\Gamma_\mu = \frac{1}{2} [u^\dagger \partial_\mu u + u \partial_\mu u^\dagger - i (u^\dagger r_\mu u + u l_\mu u^\dagger)],$$

$$D^{\mu\nu} = D^\mu D^\nu + D^\nu D^\mu,$$

$$u_\mu = i [u^\dagger \partial_\mu u - u \partial_\mu u^\dagger - i (u^\dagger r_\mu u - u l_\mu u^\dagger)],$$

$$F^\pm_{\mu\nu} = u F_{L\mu\nu} u^\dagger \pm u^\dagger F_{R\mu\nu} u,$$

$$F_{R\mu\nu} = \partial_\mu r_\nu - \partial_\nu r_\mu - i [r_\mu, r_\nu],$$

$$F_{L\mu\nu} = \partial_\mu l_\nu - \partial_\nu l_\mu - i [l_\mu, l_\nu],$$

$$\chi_+ = u^\dagger \chi u^\dagger + u \chi^\dagger u. \tag{16}$$

In the above expressions, Ψ denotes the nucleon field, $u = \sqrt{U}$ contains pion fields, $v^{(s)}_\mu$ is the part of the vector current that is proportional to the unit matrix in the flavor space, $\overset{\circ}{m}$ and $\overset{\circ}{g}_A$ denote the nucleon mass and the axial-vector coupling

---

[4]Note that our definitions of the low-energy constants agree with those of Ref. [48] except for c_6 and c_7, which are related as $c_6 = c_6^{\text{FMMS}}/4\overset{\circ}{m}$ and $c_7 = (c_6^{\text{FMMS}} + c_7^{\text{FMMS}})/2\overset{\circ}{m}$ (here c_6^{FMMS} and c_7^{FMMS} denote the corresponding couplings of Ref. [48]); see Ref. [49]. Here, FMMS denotes the authors of Ref. [48] (Fettes-Meißner-Mojžiš-Steininger). EOMS stands for extended on-mass-shell.

constant in the chiral limit, and c_i, d_i, and e_i are the low-energy constants at $O(p^2)$, $O(p^3)$, and $O(p^4)$, respectively. It is assumed that the above Lagrangian is used to generate Feynman diagrams, which will be evaluated by using the EOMS renormalization scheme. Acting in this manner, there is no need to explicitly display the counterterms of the effective Lagrangian that remove the power-counting breaking contributions from the loop diagrams. Hence, the numerical values of the finite parts of the low-energy constants (LECs) correspond to the EOMS scheme.

To obtain the expressions that correspond to diagrams with external photons, we need to substitute $s = \mathcal{M}$, $p = a_\mu = 0$, $v_\mu = -e\tau_3\mathcal{A}_\mu/2$, and $v_\mu^{(s)} = -e\mathcal{A}_\mu/2$, where $\mathcal{A}_\mu$ is the electromagnetic field. We work in the isospin limit $m_u = m_d = \hat{m}$, and $M^2 = 2B\hat{m}$ is the pion mass at leading order.

III. INFINITE VOLUME

A. The workflow

We calculate doubly virtual Compton scattering on the proton and on the neutron separately up-to-and-including $O(p^4)$. There are tree and one-loop diagrams contributing to this process at the given accuracy. Standard power-counting rules of low-energy chiral effective field theory apply to these diagrams [50,51]. More specifically, we are assigning chiral order -2 to pion propagators, nucleon propagators count as of order -1, the interaction vertices originating from the effective Lagrangian of the order N count also as of order N, and the integrations over loop momenta are assigned order 4. While the power-counting rules are directly applicable to the tree diagrams, the loop diagrams of our manifestly Lorentz-invariant formalism contain pieces that violate the counting rules. However, power-counting violating terms are polynomials in the quark masses and external momenta and thus can be systematically absorbed in the redefinition of the parameters of the effective Lagrangian. In our calculations, we use dimensional regularization supplemented with the EOMS scheme [52,53]. In this scheme, the polynomials in quark masses and external momenta which break the power counting up to a given chiral order, are dropped from each diagram. This naturally guarantees that the renormalized one-loop diagrams satisfy power counting.[5] Note that, in contrast to the results of the heavy baryon formalism [56,57], our expressions for loop diagrams contain an infinite number of higher-order terms.

In the calculations of the diagrams we used the programs FeynCalc [58,59] and X-package [60]. We have verified that the sum of all tree and one-loop diagrams

---

[5]The terms which break power counting can also be systematically removed by using the heat kernel method; see Refs. [54,55].

satisfies current conservation. This guarantees that the whole unpolarized amplitude is parametrized in terms of two invariant functions T_1 and T_2. However, this does not apply to the individual diagrams. In order to extract the contributions of separate diagrams to T_1 and T_2, we single out the contributions to the coefficients of the structures $q^\mu q^\nu$ and $-q^2 p^\mu p^\nu/m^2$, since these appear exclusively in $K_1^{\mu\nu}$ and $K_2^{\mu\nu}$, respectively; see Eq. (4). The individual contributions, which are listed below, should be interpreted in this sense. Finally, using the Lehmann-Symanzik-Zimmermann scheme, we add these contributions and multiply the result with the residue of the nucleon propagator at the pole corresponding to the one-nucleon state. Acting in this manner, one gets the full expressions of $T_1(\nu, q^2)$ and $T_2(\nu, q^2)$ we are interested in.

Next, we need an algorithm for the separation of the elastic contributions from T_1 and T_2. For instance, let us first extract the s-channel pole. To this end, we multiply the full expressions for $T_1(\nu, q^2)$, $T_2(\nu, q^2)$ by $2m\nu + q^2$ and then substitute $\nu = -q^2/(2m)$. Apparently, as a result of this procedure, one obtains the residue of the s-channel pole. In order to determine the residue of the u-channel pole, we multiply the amplitudes by $2m\nu - q^2$. Finally, adding both pole terms together, we arrive at the elastic amplitudes $T_1^{\text{el}}(\nu, q^2)$ and $T_2^{\text{el}}(\nu, q^2)$. These vanish in the limit when $\nu \to \infty$ and q^2 stays fixed. This exactly coincides with our definition of the elastic amplitudes.

B. The amplitude in the infinite volume

The invariant amplitudes T_1 and T_2 up-to-and-including $O(p^4)$ are given as sums over the contributions of the diagrams shown in Figs. 1–4:
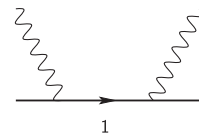

FIG. 1. Tree diagram contributing at $O(p)$. Solid and wiggly lines denote nucleons and photons, respectively. The crossed diagram is not shown.
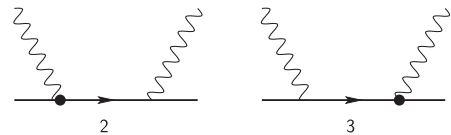

FIG. 2. Tree diagrams contributing at $O(p^2)$. Solid and wiggly lines denote nucleons and photons, respectively. The filled circles are vertices from the second-order Lagrangian $\mathcal{L}_2$. Crossed diagrams are not shown.
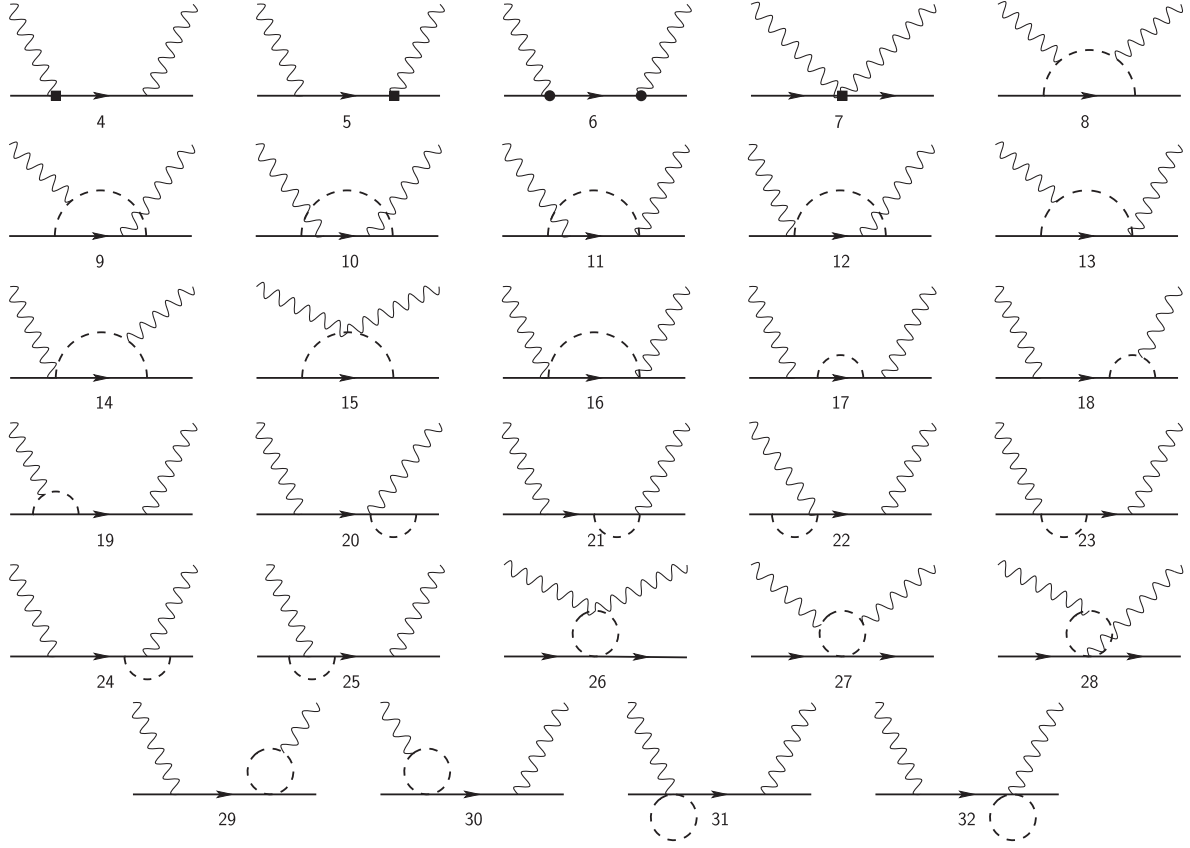
FIG. 3.　Tree and loop diagrams contributing at $O(p^3)$. Solid, dashed, and wiggly lines denote nucleons, pions, and photons, respectively. Filled circles and squares represent vertices from $\mathcal{L}_2$ and $\mathcal{L}_3$, respectively. Crossed diagrams are not shown.

$$T_i(\nu, q^2) = Z_N \left(T_i^1(\nu, q^2) + \sum_{a=2}^{3} T_i^a(\nu, q^2) \right.$$
$$\left. + \sum_{a=4}^{32} T_i^a(\nu, q^2) + \sum_{a=33}^{67} T_i^a(\nu, q^2) \right), \quad i = 1, 2.$$
$$(17)$$

The different terms in the above equation are the contributions at $O(p)$, $O(p^2)$, $O(p^3)$, and $O(p^4)$, respectively. The enumeration of the contributions corresponds to the one of the diagrams shown in Figs. 1–4. Here, we remind the reader that, under the individual contributions to the invariant amplitudes T_1 and T_2, we understand the scalar factors that multiply the structures $q^\mu q^\nu$ and $-q^2 p^\mu p^\nu / m^2$, respectively. Further, Z_N is the residue of the nucleon propagator at the pole,

$$Z_N = 1 - \frac{3g_A^2}{4F^2} (2m^2(2M^2 B_0'(m^2, M, m) + B_1(m^2, M, m))$$
$$+ M^2 B_0(m^2, M, m) + A_0(m))$$
$$+ \frac{6c_2}{mF^2} A_{00}(M) + O(p^5), \qquad (18)$$

which counts as $Z_N = 1 + O(p^2)$. For this reason, one has to take this factor into account only together with the tree-level diagrams at $O(p)$ and $O(p^2)$. Note also that, to this accuracy, one may replace $\mathring{g}_A$, $\mathring{m}$, F by their physical values g_A, m, F_π. The loop functions which enter the above expression are tabulated in the Appendix A. The derivative in the function B_0 (denoted by the prime) is taken with respect to the first argument.

In Appendixes B and C we list the individual contributions to $T_1(\nu, q^2)$ and $T_2(\nu, q^2)$ for $\nu = 0$. The full expressions for a generic ν are much more complicated, and we do not display them here explicitly. These can be extracted from the *Mathematica* notebook [61]. Note also that the expressions, given in these Appendixes, should be understood as 2×2 matrices in the isospin space, folded by the isospin wave functions of a proton or a neutron (not shown separately). For example, the factor $1 + \tau^3$ is equal to 2 and 0 for the proton and the neutron, respectively.

C. Numerical input

In order to make numerical predictions, one has to fix the values of the LECs that enter the amplitudes. It should be noted that, albeit these LECs do not depend on the quark
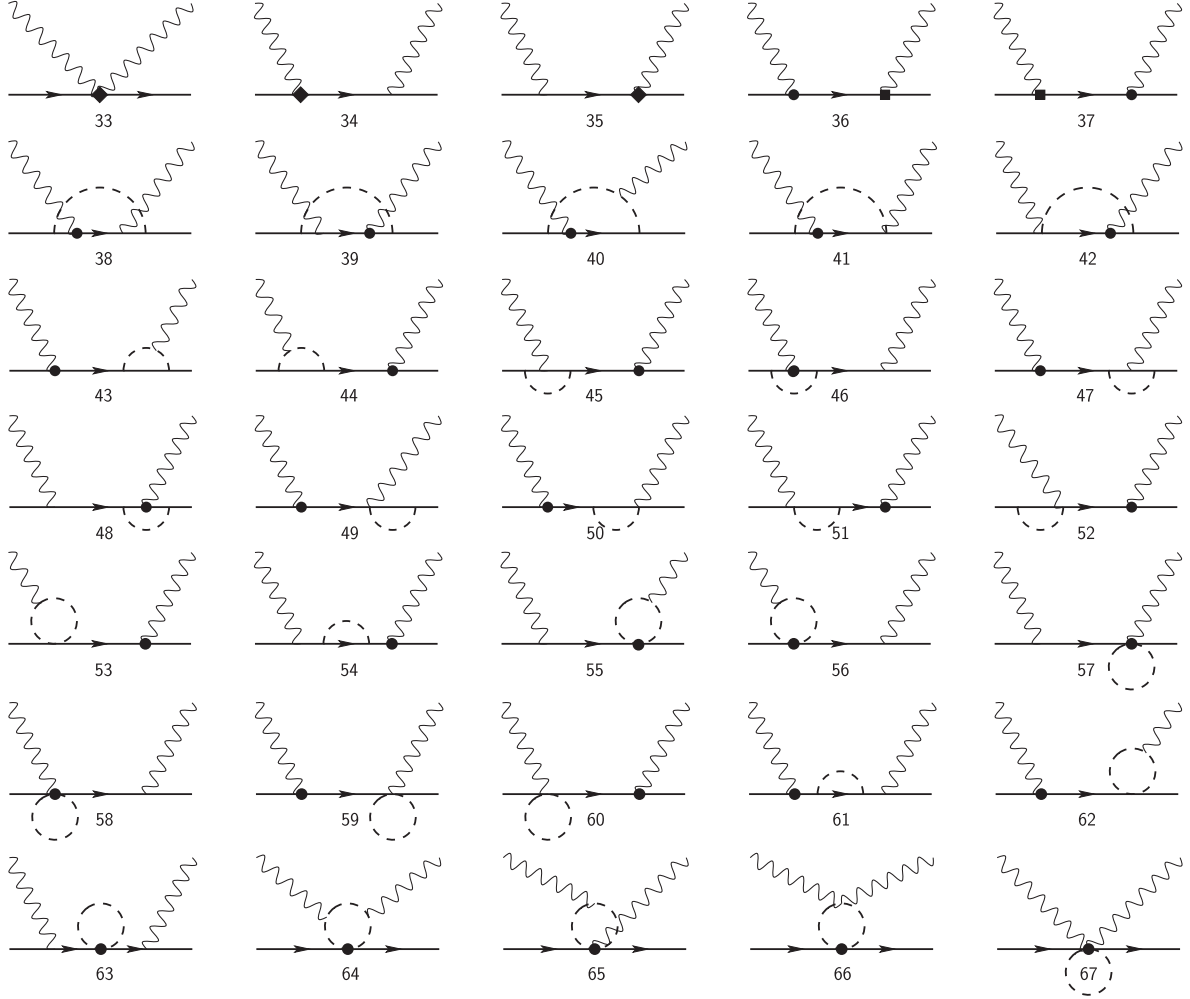
FIG. 4. Tree and loop diagrams contributing at $O(p^4)$. Solid, dashed, and wiggly lines denote nucleons, pions, and photons, respectively. Filled circles, squares, and diamonds represent vertices from $\mathcal{L}_2$, $\mathcal{L}_3$, and $\mathcal{L}_4$, respectively. Crossed diagrams are not shown.

masses by definition, such a dependence sneaks in when these are determined through the fit of the amplitudes calculated in a given chiral order to the experimental data. In certain cases, such remnant quark mass dependence can be numerically significant and, in addition, lead to the different results when different schemes, say, the infrared regularization (IR) or the EOMS scheme, are used. This fact should be kept in mind once input from different fits is used in the amplitudes.

The LECs that appear in the amplitudes fall into different groups. We shall use $g_A = 1.2672$ and $F_\pi = 92.3$ MeV throughout the paper, and M_π, m will be identified with the charged pion and the proton masses, respectively. The order p^2 LECs c_i are studied in the most detail, and rather precise values for these are available in the literature. Moreover, different fits (see, e.g., Refs. [62–64]) yield results which are compatible with each other at an accuracy that is sufficient for our purposes. The recent and very precise determination of

$c_{1,2,3,4}$ from πN input has been performed in Ref. [65] using the matching of the chiral representation to the solution of the Roy-Steiner equations:

$$c_1 = (-1.11 \pm 0.03)\,\text{GeV}^{-1}, \quad c_2 = (3.13 \pm 0.03)\,\text{GeV}^{-1},$$
$$c_3 = (-5.61 \pm 0.06)\,\text{GeV}^{-1}, \quad c_4 = (4.26 \pm 0.04)\,\text{GeV}^{-1}.$$
$$(19)$$

In the following calculations, we shall use these values. Owing to the fact that the quoted uncertainties are so small, one may neglect their impact on the total uncertainty and safely stick to the central values.

Turning to the LECs $c_{6,7}$, we note that these appear in the amplitudes in combination with the $O(p^4)$ LECs:

$$\tilde{c}_6 = c_6 - 4M^2 e_{106}, \qquad \tilde{c}_7 = c_7 - 4M^2 e_{105}, \quad (20)$$

where $M^2 = M_\pi^2$ at this order. These are exactly the contributions which appear in the anomalous magnetic moments of the proton and the neutron, $\kappa_p = 1.793$, $\kappa_n = -1.913$, and can be fitted to the latter. A consistent extraction of these couplings has been performed in Ref. [66], which gives the results for the IR and EOMS schemes separately (no errors are attached to their results). Here, we quote the result for the EOMS scheme only, as this is used in our calculation:

$$\tilde{c}_6 = 1.26 \text{ GeV}^{-1}, \qquad \tilde{c}_7 = -0.13 \text{ GeV}^{-1}. \quad (21)$$

Next, the $O(p^3)$ LECs $d_{6,7}$ and $O(p^4)$ LECs $e_{54,74}$ enter the expression of the electric and magnetic radii of the proton and the neutron, and can be fitted by using experimental data on the nucleon electromagnetic form factors. This was done in Ref. [66], where the values of these LECs are given, again separately for different schemes and with no uncertainties attached:

$$d_6 = -0.69 \text{ GeV}^{-2}, \qquad d_7 = -0.50 \text{ GeV}^{-2}, \quad (22)$$

and

$$e_{54} = 0.19 \text{ GeV}^{-3}, \qquad e_{74} = 1.59 \text{ GeV}^{-3}. \quad (23)$$

Note that the values for d_6, d_7 are consistent with the earlier determination in Ref. [67].

Let us now turn to the last group of the $O(p^4)$ LECs, which are related to the nucleon polarizabilities. At order p^3, the polarizabilities are predictions free of LECs [68]. The $O(p^4)$ LECs that contribute to the amplitudes at $q^2 = 0$ can be related to the polarizabilities, and we use (experimental or lattice) input for the latter. This allows one to determine four linearly independent combinations of the $O(p^4)$ LECs which, according to Ref. [49], can be defined as

$$e_x^\pm = 2e_{90} + e_{94} + e_{117} \pm e_{92},$$
$$e_y^\pm = 2e_{89} + e_{93} + e_{118} \pm e_{91}. \quad (24)$$

In Ref. [49] the results of three different fits for e_x^+, e_y^+ are presented. In the following, however, we shall not use these results.

In order to carry out the comparison with the results from the literature, we perform a numerical evaluation of the subtraction functions $S_1^{\text{inel}}(q^2)$ and $\bar{S}(q^2)$ which, using Eqs. (7) and (9), can be written as

$$S_1^{\text{inel}}(q^2) = -\frac{\kappa^2}{4m^2} - \frac{m}{\alpha}\beta_M + (S_1^{\text{inel}}(q^2) - S_1^{\text{inel}}(0)),$$
$$\bar{S}(q^2) = -\frac{\kappa^2}{4m^2} + \frac{m}{2\alpha}(\alpha_E - \beta_M) + (\bar{S}(q^2) - \bar{S}(0)). \quad (25)$$

In other words, in order to minimize the uncertainty, we aim at a description of the q^2-dependence of the subtraction functions only; their values at $q^2 = 0$ are considered as input. Stated differently, up-to-and-including order p^4, the q^2-dependence of the subtraction functions $S_1(q^2)$ and $\bar{S}(q^2)$ (but not their normalization at $q^2 = 0$) is determined by the LECs, which are rather well known from the fit to the data on the low-energy πN scattering and nucleon electromagnetic form factors. Thus, the q^2-dependence can be determined very accurately from BChPT.

The experimental values for the electric and magnetic polarizabilities are summarized in the recent paper by Melendez *et al.* [69] (see, e.g., Refs. [70–73] for some earlier work):

$$\text{proton}: \alpha_E^p + \beta_M^p = 14.0 \pm 0.2, \quad \alpha_E^p - \beta_M^p = 7.5 \pm 0.9,$$
$$\text{neutron}: \alpha_E^n + \beta_M^n = 15.2 \pm 0.4, \quad \alpha_E^n - \beta_M^n = 7.9 \pm 3.0. \quad (26)$$

For the difference proton-neutron one gets

$$\alpha_E^{p-n} + \beta_M^{p-n} = -1.20 \pm 0.45,$$
$$\alpha_E^{p-n} - \beta_M^{p-n} = -0.4 \pm 3.1, \quad \beta_M^{p-n} = -0.4 \pm 1.6. \quad (27)$$

All quantities are given in units of 10^{-4} fm^3.

In Ref. [24], using Reggeon dominance, the isovector electric and magnetic polarizabilities have been predicted with an accuracy that supersedes the experimental precision. For instance, the value for the electric polarizability, extracted from the recent Review of Particle Physics [74], is given by $\alpha_E^{p-n} = -0.6(1.2)$. On the other hand, using Reggeon dominance and the experimental value for $\alpha_E^{p-n} + \beta_M^{p-n}$ from Ref. [69], which was determined by using the Baldin sum rule, one gets

$$\alpha_E^{p-n} = -1.7 \pm 0.4, \qquad \beta_M^{p-n} = 0.5 \pm 0.6,$$
$$\alpha_E^{p-n} - \beta_M^{p-n} = -2.2 \pm 0.9. \quad (28)$$

Finally, recently a very accurate lattice calculation of the magnetic polarizability has become available [75]:

$$\beta_M^p = 2.79 \pm 0.22_{-18}^{+13}, \qquad \beta_M^n = 2.06 \pm 0.26_{-20}^{+15},$$
$$\beta_M^{p-n} = 0.80 \pm 0.28 \pm 0.04. \quad (29)$$

One can combine this with the experimental result for $\alpha_E^{p-n} + \beta_M^{p-n}$ from Eq. (27) in order to get a more accurate estimate:

$$\alpha_E^{p-n} - \beta_M^{p-n} = -2.80 \pm 0.72, \qquad \beta_M^{p-n} = 0.80 \pm 0.28. \quad (30)$$
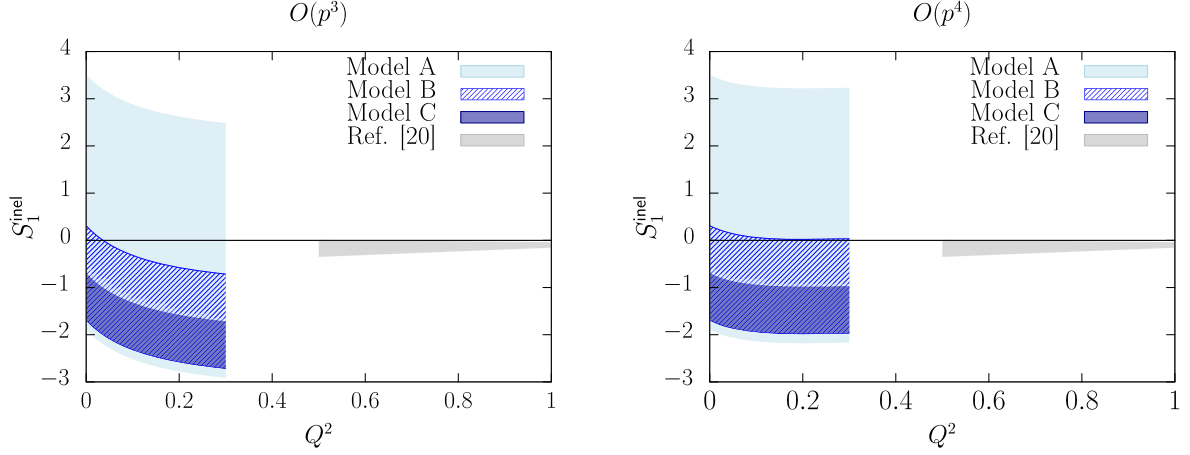
FIG. 5.   The subtraction function $S_1^{\text{inel}}(q^2)$ for proton minus neutron, at order p^3 and p^4 in the left panel and right panel, respectively. Here, $Q^2 = -q^2$. The light blue, dashed and dark blue bands show the results of Models A, B, and C, respectively. The result of Ref. [24], which is obtained with the use of the Reggeon dominance hypothesis, is shown by the gray band. GeV units are used everywhere.

To summarize, we now have three sets of polarizabilities, referred to as Model A [Eq. (27)], Model B [Eq. (28)], and Model C [Eq. (30)]. These correspond to the purely experimental input, the Reggeon dominance hypothesis and the combination of the lattice results with experimental data. Below, we shall evaluate the difference of the subtraction functions for the proton and the neutron[6] using the input from the three distinct models:

$$\text{Model A} : S_1^{\text{inel}}(0) = (0.8 \pm 2.7) \text{ GeV}^{-2},$$
$$\bar{S}(0) = (-0.2 \pm 2.6) \text{ GeV}^{-2},$$
$$\text{Model B} : S_1^{\text{inel}}(0) = (-0.7 \pm 1.0) \text{ GeV}^{-2},$$
$$\bar{S}(0) = (-1.7 \pm 0.8) \text{ GeV}^{-2},$$
$$\text{Model C} : S_1^{\text{inel}}(0) = (-1.2 \pm 0.5) \text{ GeV}^{-2},$$
$$\bar{S}(0) = (-2.2 \pm 0.6) \text{ GeV}^{-2}. \quad (31)$$

D. The subtraction function

The main goal of the present paper is to evaluate the finite-volume corrections to the Compton amplitude. However, having the expression of the infinite-volume amplitude at hand, one may compare it to the known results from the literature. For instance, here we shall discuss the comparison to the subtraction functions $S_1^{\text{inel}}(q^2)$ and $\bar{S}(q^2)$ for proton minus neutron, obtained from the experimental input by using the Reggeon dominance hypothesis in Refs. [24,28], respectively. Note that the experimental input, used in these papers, leads to a very large uncertainty

at small values of Q^2, which comes mainly from the resonance region above the Δ resonance. On the other hand, the results of the chiral perturbation theory become generally unreliable at higher values of Q^2. Thus, combining both calculations, one can get a coherent picture of the Q^2-dependence of the subtraction function in a wide interval and check the consistency of the Reggeon dominance hypothesis: Should it turn out that there is an apparent mismatch between the low-Q^2 and high-Q^2 regions, this might cast doubt on the above hypothesis.

In order to reduce the error, which stems from the poor knowledge of the higher-order LECs, in our calculations we have attempted to evaluate the Q^2-dependence of the subtraction functions by subtracting their values at the origin. Eventually, the latter quantity is expressed in terms of the electric and magnetic polarizabilities [see Eq. (25)]. The polarizabilities can be fixed from the different inputs, leading to what we term Models A, B, and C [see Eq. (31)]. The corresponding results in the interval $0 < Q^2 < 0.3 \text{ GeV}^2$ are displayed in Fig. 5 for the function $S_1^{\text{inel}}(q^2)$ and in Fig. 6 for the function $\bar{S}(q^2)$. Note that the uncertainty, which is displayed here, comes entirely from the poor knowledge of the polarizabilities. In other words, we assume that the uncertainties coming from other LECs are much smaller and do not contribute significantly to the error (it is clear that even attaching a reasonable uncertainty to other LECs and adding uncertainties in quadrature, the changes will barely be visible due to the huge uncertainty in the polarizabilities). Note also that, in this scheme, the subtraction functions at $O(p^3)$ are no more considered as a parameter-free prediction, but contain polarizabilities as input.

From Figs. 5 and 6 one may conclude that the results obtained in BChPT and by using the Reggeon dominance are reasonably consistent with each other within the error

---

[6]In order to ease the notations, we do not attach the superscript $p - n$ to the subtraction functions, corresponding to the difference proton minus neutron. From the context it is always clear which subtraction function is meant.
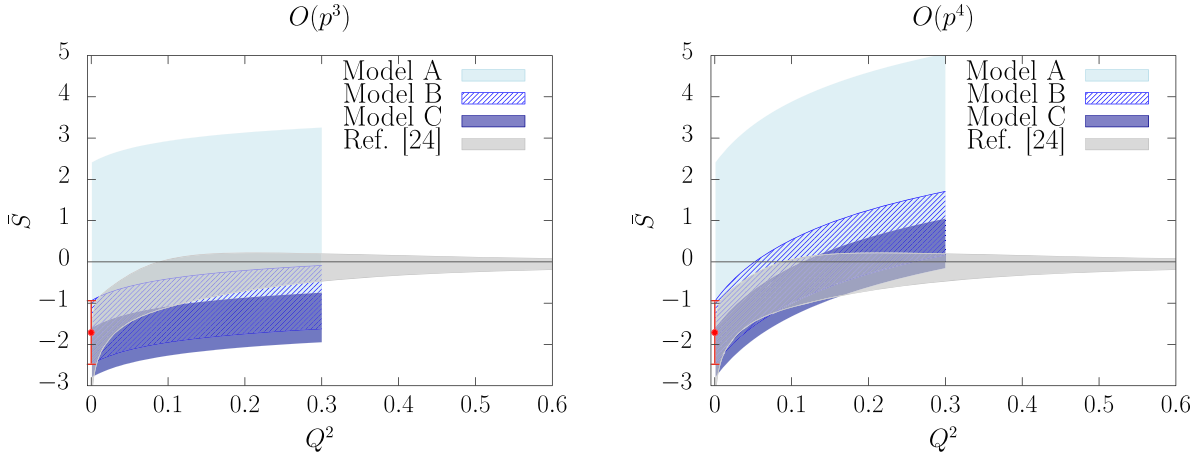
FIG. 6.   Results for the subtraction function $\bar{S}(q^2)$ for proton minus neutron. The notations are the same as in Fig. 5. The gray band shows the result of Ref. [28], obtained with the use of the Reggeon dominance. GeV units are used everywhere. The data point at the origin shows the prediction of the $\bar{S}(0)$ in Model B with Reggeon dominance; see Eq. (31).

bars. In case of the subtraction function $\bar{S}(q^2)$ this can be seen more clearly, since the results of the calculations, based on the Reggeon dominance, are available for all values of Q^2 down to $Q^2 = 0$; see Ref. [28] [in the case of $S_1^{\mathrm{inel}}(q^2)$, the calculations extend down to $Q^2 = 0.5$ GeV^2; see Ref. [24]]. Note, however, that the uncertainty in different models, considered in the present paper, lead to very large error bars in these plots. This concerns, especially, the results of Model A, which completely overlap with the results of Models B and C, thus bringing no independent constraints. What is more important in our opinion is that the amplitudes calculated in the effective field theory show a smooth behavior in the vicinity of $Q^2 = 0$; stated differently, no rapid variations are observed. Note also that the convergence is quite poor, and the picture changes significantly when going from $O(p^3)$ to $O(p^4)$. Still, we do not observe any apparent disagreement to the Reggeon dominance. Also, it should be noted that both the $O(p^3)$ and the $O(p^4)$ contributions are part of the complete one-loop amplitude, so a true test of convergence could only be achieved by going to the two-loop level. This, however, is beyond the scope of this paper.

We finish this section by briefly mentioning related calculations in the literature. Our result for the polarizabilities fully agrees with that of Ref. [76], where the calculations were done in the relativistic BChPT at $O(p^3)$. Next, our subtraction function $S_1^{\mathrm{inel}}(q^2)$ coincides with the one from Ref. [33] at order p^3. Moreover, in the recent paper [77], these calculations were extended up-to-and-including order p^4. However, at $O(p^4)$, the contribution from the Δ-resonance comes into play, and this renders the direct comparison more complicated (note, however, that for proton minus neutron the leading contribution of the Δ drops out, as already noted in Ref. [78]). For this reason, in this paper we restricted ourselves to $O(p^3)$ and verified that

the sum of the polarizabilities $\alpha_E + \beta_M$ is algebraically reproduced in our calculations, for both the proton and the neutron. Further, expanding our result in inverse powers of m, one should reproduce the nonanalytic pieces of the heavy baryon ChPT (HBChPT). The result of Ref. [79] is written down in a form of expansion in Q^2. However, the coefficient of the expansion at $O(Q^4)$, which is given in Eq. (12) of that paper, cannot be obtained from our result in this way. Moreover, since the difference stems from the $O(p^3)$ part of the relativistic amplitude, one could use Ref. [77] for a check, expanding their amplitude in powers of Q^2. The result of this expansion reproduces our result. Note also that in Ref. [80], where the calculations were carried out within HBChPT at $O(p^4)$, the polarizabilities were extracted from the real Compton scattering amplitude that corresponds to the $O(Q^2)$ term in the expansion of the virtual amplitude. At this order, there are no disagreements. Finally, note the calculation of the subtraction function, carried out in Refs. [81,82] in the framework of HBChPT. In particular, the contribution of the Δ-resonance has been studied. Here, we do not present an explicit comparison to these papers.

Another group of the papers deals with the calculation of the subtraction function by using dispersion relations and experimental input (see, e.g., Ref. [83]), or modeling it, taking into account the constraints at $Q^2 = 0$ and at Q^2 tending to infinity [23,25,26]. This work has been discussed in great detail in Refs. [24,28], to which the interested reader is referred.

IV. FINITE VOLUME CORRECTIONS

A. Analytic expression for the finite-volume amplitude

The diagrams that contribute to the Compton amplitude are the same in the infinite and in a finite volume. The only

difference consists in replacing the three-dimensional integrals with the sums over discrete lattice momenta (we take that the effects related to a finite size of a lattice in the temporal direction are already taken into account during the measurement of the energy levels). Assuming periodic boundary conditions, in the loop integrals one has to replace

$$\int \frac{d^4k}{(2\pi)^4 i} \rightarrow \int_V \frac{d^4k}{(2\pi)^4 i} \equiv \int \frac{dk_0}{2\pi i} \frac{1}{L^3} \sum_{\mathbf{k}},$$

$$\mathbf{k} = \frac{2\pi}{L}\mathbf{n}, \quad \mathbf{n} = \mathbb{Z}^3. \qquad (32)$$

Some of the loop integrals in the infinite volume diverge. In a finite volume, this divergence can be dealt with using dimensional regularization in the same manner as in the infinite volume. The counterterms that remove the divergences are the same in both cases. In the following, we shall use this fact and write down the finite-volume sums in a dimensionally regularized fashion, without specifying how this is done. These sums will be further split into the infinite-volume parts and the corrections. The regularization is relevant only for the first parts, where the standard prescription can be applied. The finite-volume corrections are ultraviolet finite and can be calculated in four dimensions.

A closely related question concerns the presence of the power-counting breaking terms in the covariant BChPT. It must be stressed that there are no such terms in the finite-volume part of the amplitude, as all such terms are suppressed by a factor $\exp(-mL)$ containing the nucleon mass. On the contrary, in the infinite-volume part these terms are present and can be dealt with, e.g., by using the EOMS prescription, as described above. The reason for this is, of course, that the breaking of the power-counting rules is a high-energy phenomenon that emerges for loop momenta of the order of the nucleon mass. On the other hand, the large-L behavior is governed by the momenta of the order of the pion mass. This region does not contribute to the breaking of the power counting.

In order to carry out the calculations, one needs the expression of the nucleon Z-factor in a finite volume. This quantity is defined in the rest frame of the nucleon, where the nucleon propagator is given by

$$S_L(p) = i \int_L d^4x\, e^{ip_0 x_0} \langle 0|T\Psi(x)\bar{\Psi}(0)|0\rangle, \quad p^\mu = (p^0, \mathbf{0}). \qquad (33)$$

In the above expression, the integration is carried out in a finite box. Further,

$$S_L(p) = \frac{1}{\overset{\circ}{m} - \gamma^0 p^0 - \Sigma_L(p)}, \qquad (34)$$

where $\Sigma_L(p)$ denotes the self-energy of the nucleon in a finite volume and

$$\Sigma_L(p) = A_L(p_0) + \gamma^0 p^0 B_L(p^0). \qquad (35)$$

The finite-volume mass of the nucleon is implicitly given through the solution of the equation that contains the scalar functions $A_L(p^0), B_L(p^0)$:

$$m_L = \frac{\overset{\circ}{m} - A_L(m_L)}{1 + B_L(m_L)} = \overset{\circ}{m} - A_L(m_L) - m_L B_L(m_L) + \cdots. \qquad (36)$$

This equation can be solved by iteration, expressing m_L order by order through the infinite-volume parameters. Further, the Z-factor in a finite volume is given by the residue of the nucleon propagator at the pole $p^0 = m_L$. It can also be expressed in terms of the functions $A_L(p^0), B_L(p^0)$ and the derivatives thereof with respect to the variable p^0:

$$Z_L = (1 + A'_L(m_L) + B_L(m_L) + m_L B'(m_L))^{-1}$$
$$= 1 - A'_L(m_L) - B_L(m_L) - m_L B'(m_L) + \cdots. \qquad (37)$$

The explicit expression for this quantity is given by

$$Z_L = -\frac{3m g_A^2 \tilde{\mathcal{B}}_{(1,1)}^0(m, M; m)}{2F^2}$$
$$+ \frac{3M^2 g_A^2 (3M^2 - 8m^2) \tilde{\mathcal{B}}_{(1,1)}(m, M; m)}{4F^2(M^2 - 4m^2)}$$
$$- \frac{3g_A^2 \tilde{\mathcal{A}}_{(1)}(m)(4m^2 + 3M^2)}{4F^2(4m^2 - M^2)}$$
$$+ \frac{3g_A^2 \tilde{\mathcal{A}}_{(1)}(M)(M^2 - 2m^2)}{F^2(4m^2 - M^2)} + \frac{6c_2 \tilde{\mathcal{A}}_{(1)}^{00}(M)}{F^2 m}. \qquad (38)$$

The loop functions are specified in Appendix D. Their derivatives have been reduced again to loop functions, utilizing the algebraic identities that are specified in Refs. [49,84].

Finally, note that Lorentz symmetry is broken in a cubic box and one can no more use the decomposition of the Compton amplitude into two scalar amplitudes. This is, in fact, not needed, because the energy shift of a nucleon in the periodic field is directly given by the 11-component of the Compton tensor [12,13]. Putting together all contributions, one can write

$$T_L^{11}(\text{neutron}) = \tilde{\mathcal{T}}_n^{(1)} + \tilde{\mathcal{T}}_n^{(2)} + \tilde{\mathcal{T}}_n^{(3)} + \tilde{\mathcal{T}}_n^{(4)} + O(p^5),$$
$$T_L^{11}(\text{proton}) = \tilde{\mathcal{T}}_p^{(1)} + \tilde{\mathcal{T}}_p^{(2)} + \tilde{\mathcal{T}}_p^{(3)} + \tilde{\mathcal{T}}_p^{(4)} + O(p^5). \qquad (39)$$

The individual contributions are given by

$O(p)$: neutron

$$\tilde{T}_n^{(1)} = 0. \tag{40}$$

$O(p)$: proton

$$\tilde{T}_p^{(1)} = 0. \tag{41}$$

$O(p^2)$: neutron

$$\tilde{T}_n^{(2)} = 0. \tag{42}$$

$O(p^2)$: proton

$$\tilde{T}_p^{(2)} = 2m(2c_6 + c_7). \tag{43}$$

$O(p^3)$: neutron

$$
\begin{aligned}
\tilde{T}_n^{(3)} =\ & m^2(2c_6 - c_7)^2 + \frac{2g_A^2 m^2}{F^2}\{-4M^2\tilde{\mathcal{D}}_{(1,1,1,1)}^{11}(m,M,m,M;p,q,p+q) - 4M^2\tilde{\mathcal{C}}_{(2,1,1)}^{11}(M,m,M;-p,q) \\
& - 4M^2\tilde{\mathcal{C}}_{(2,1,1)}^{11}(m,M,m;-p,q) + M^2q^2\tilde{\mathcal{C}}_{(2,1,1)}(m,M,m;-p,q) - q^2\tilde{\mathcal{C}}_{(1,1,1)}(m,M,m;-p,q) \\
& - 4\tilde{\mathcal{B}}_{(2,1)}^{11}(m,m;q) - M^2\tilde{\mathcal{B}}_{(1,2)}(m,M;p) - M^2\tilde{\mathcal{B}}_{(2,1)}(m,M;p) + q^2\tilde{\mathcal{B}}_{(2,1)}(m,m;q) - \tilde{\mathcal{A}}_{(2)}(m)\}.
\end{aligned}
\tag{44}
$$

$O(p^3)$: proton

$$
\begin{aligned}
\tilde{T}_p^{(3)} =\ & m^2(2c_6 + c_7)^2 + 2q^2(d_6 + 2d_7) \\
& + \frac{m^2 g_A^2}{F^2}\Bigg\{ 4\tilde{\mathcal{C}}_{(1,1,1)}^{11}(m,M,m;-p,q) - 8\tilde{\mathcal{C}}_{(1,1,1)}^{11}(M,m,M;-p,q) - 8M^2\tilde{\mathcal{C}}_{(2,1,1)}^{11}(M,m,M;-p,q) \\
& - 4M^2\tilde{\mathcal{C}}_{(2,1,1)}^{11}(m,M,m;-p,q) + M^2q^2\tilde{\mathcal{C}}_{(2,1,1)}(m,M,m;-p,q) - (q^2 - 2M^2)\tilde{\mathcal{C}}_{(1,1,1)}(m,M,m;-p,q) \\
& - 4\tilde{\mathcal{B}}_{(2,1)}^{11}(m,m;q) + \frac{3}{2m^2}p_\alpha\tilde{\mathcal{B}}_{(1,1)}^{\alpha}(M,m;p+q) - 2M^2\tilde{\mathcal{B}}_{(1,2)}(M,m;p) - M^2\tilde{\mathcal{B}}_{(2,1)}(M,m;p) \\
& + q^2\tilde{\mathcal{B}}_{(2,1)}(m,m;q) + 2\tilde{\mathcal{B}}_{(1,1)}(m,m;q) - \tilde{\mathcal{B}}_{(1,1)}(m,M;p) + \tilde{\mathcal{B}}_{(1,1)}(M,m;p+q) - \tilde{\mathcal{A}}_{(2)}(m) \Bigg\} \\
& + \frac{3g_A^2}{F^2 q^2}\Bigg\{ -p_\alpha q_\beta\tilde{\mathcal{B}}_{(1,1)}^{\alpha\beta}(M,m;p+q) - p_\alpha p_\beta\tilde{\mathcal{B}}_{(1,1)}^{\alpha\beta}(M,m;p+q) + \frac{M^2}{2}p_\alpha\tilde{\mathcal{B}}_{(1,1)}^{\alpha}(M,m;p+q) \\
& - 2m^2 q_\alpha\tilde{\mathcal{B}}_{(1,1)}^{\alpha}(M,m;p+q) - m^2 M^2\tilde{\mathcal{B}}_{(1,1)}(m,M;p) + m^2 M^2\tilde{\mathcal{B}}_{(1,1)}(M,m;p+q) + \frac{m^2}{2}\tilde{\mathcal{A}}_{(1)}(m) \Bigg\}.
\end{aligned}
\tag{45}
$$

$O(p^4)$: neutron

$$
\begin{aligned}
\tilde{T}_n^{(4)} =\ & 8m(2e_{89} + e_{93} + e_{118} - e_{91})q^2 \\
& + \frac{mg_A^2}{F^2}\{-4(2c_6 + c_7)q^2 m^2\tilde{\mathcal{D}}_{(1,1,1,1)}^{11}(m,M,m,M;p,-q,p-q) - 8m^2(2c_6 - c_7)\tilde{\mathcal{C}}_{(1,1,1)}^{11}(m,M,m;p,q) \\
& - 8m^2(2c_6 - c_7)\tilde{\mathcal{C}}_{(1,1,1)}^{11}(M,m,M;-p,q) + 4(2c_6 + c_7)q^2 M^2 m^2\tilde{\mathcal{C}}_{(2,1,1)}(m,M,m;p,q) \\
& - 2(4c_6 m^2 M^2 - c_7(q^2(M^2 - 2m^2) + 2m^2 M^2))\tilde{\mathcal{C}}_{(1,1,1)}(m,M,m;p,q) \\
& + (2c_6 - c_7)q_\alpha(\tilde{\mathcal{B}}_{(1,1)}^{\alpha}(M,m;p+q) - \mathcal{B}_{(1,1)}^{\alpha}(M,m;p-q)) + 4m^2 q^2(2c_6 + c_7)\tilde{\mathcal{B}}_{(2,1)}(m,m;q) \\
& - (c_7(q^2 + 4m^2 - M^2) + 2c_6(q^2 + M^2))\tilde{\mathcal{B}}_{(1,1)}(M,m;p+q) \\
& + 4c_7 m^2\tilde{\mathcal{B}}_{(1,1)}(m,M;p) - 2(4c_6 m^2 - c_7(q^2 + 2m^2))\tilde{\mathcal{B}}_{(1,1)}(m,m;q) \\
& - 2(2c_6 - c_7)\tilde{\mathcal{B}}_{(1,1)}^{11}(M,M;q) + 2(2c_6 - c_7)p_\alpha\tilde{\mathcal{B}}_{(1,1)}^{\alpha}(M,m;p+q) - (2c_6 - c_7)\tilde{\mathcal{A}}_{(1)}(m)\} \\
& + \frac{4}{mF^2}\Bigg\{ (2c_6 - c_7)m^2\left(\tilde{\mathcal{B}}_{(1,1)}^{11}(M,M;q) + \frac{1}{2}\tilde{\mathcal{A}}_{(1)}(M)\right) - c_2 p_\alpha p_\beta(4\tilde{\mathcal{B}}_{(2,1)}^{11\alpha\beta}(M,M;q) + \tilde{\mathcal{A}}_{(2)}^{\alpha\beta}(M)) \\
& + (2c_1 - c_3)M^2 m^2(4\tilde{\mathcal{B}}_{(2,1)}^{11}(M,M;q) + \tilde{\mathcal{A}}_{(2)}(M)) \Bigg\}.
\end{aligned}
\tag{46}
$$

$O(p^4)$: proton

$$
\begin{aligned}
\tilde{T}_p^{(4)} = {} & 8m(2e_{89} + e_{93} + e_{118} + e_{91})q^2 + 4m((2e_{54} + e_{74})q^2 - 4(2e_{105} + e_{106})M^2) \\
& + \frac{mg_A^2}{F^2}\Bigg\{ 4(c_7 - 2c_6)q^2m^2\tilde{\mathcal{D}}_{(1,1,1,1)}^{11}(m,M,m,M;p,-q,p-q) + 16c_7m^2\tilde{\mathcal{C}}_{(1,1,1)}^{11}(m,M,m;p,q) \\
& - 8m^2(2c_6 + c_7)\tilde{\mathcal{C}}_{(1,1,1)}^{11}(M,m,M;-p,q) + 2(2c_6 + c_7)m^2M^2q^2\tilde{\mathcal{C}}_{(2,1,1)}(m,M,m;p,q) \\
& + (2c_6q^2(M^2 - 2m^2) + c_7(q^2(M^2 - 2m^2) + 8m^2M^2))\tilde{\mathcal{C}}_{(1,1,1)}(m,M,m;p,q) \\
& - \frac{1}{4}(2c_6 + c_7)q_\alpha(\tilde{\mathcal{B}}_{(1,1)}^\alpha(M,m;p-q) - \tilde{\mathcal{B}}_{(1,1)}^\alpha(M,m;p+q)) - 3(2c_6 + c_7)p_\alpha\tilde{\mathcal{B}}_{(1,1)}^\alpha(M,m;p) \\
& + 8(c_6 + c_7)p_\alpha\tilde{\mathcal{B}}_{(1,1)}^\alpha(M,m;p+q) - 6(2c_6 + c_7)M^2p_\alpha\tilde{\mathcal{B}}_{(2,1)}^\alpha(M,m;p) \\
& + (4c_6(m^2 - M^2) + 2c_7m^2)\tilde{\mathcal{B}}_{(1,1)}(m,M;p) + (c_7(8m^2 + q^2) + 2c_6q^2)\tilde{\mathcal{B}}_{(1,1)}(m,m;q) \\
& - 2(2c_6 + c_7)\tilde{\mathcal{B}}_{(1,1)}^{11}(M,M;q) - \frac{1}{2}(2c_6 + c_7)(4m^2 - M^2 + q^2)\tilde{\mathcal{B}}_{(1,1)}(M,m;p+q) \\
& + 2(2c_6 + c_7)m^2q^2\tilde{\mathcal{B}}_{(2,1)}(m,m;q) + \frac{3}{2}(2c_6 + c_7)M^2\tilde{\mathcal{B}}_{(1,1)}(M,m;p) + \left(3c_6 + \frac{7c_7}{2}\right)\tilde{\mathcal{A}}_{(1)}(m) \Bigg\} \\
& + \frac{mg_A^2}{F^2q^2}\Bigg\{ \frac{9}{4}(2c_6 + c_7)p_\alpha q_\beta\tilde{\mathcal{B}}_{(1,1)}^{\alpha\beta}(M,m;p-q) - \frac{3}{4}(2c_6 + c_7)(8p_\alpha p_\beta + 9p_\alpha q_\beta + 4q_\alpha q_\beta)\tilde{\mathcal{B}}_{(1,1)}^{\alpha\beta}(M,m;p+q) \\
& + \frac{1}{8}(c_6(32m^2 - 6M^2) + 3c_7(16m^2 - M^2))q_\alpha\tilde{\mathcal{B}}_{(1,1)}^\alpha(M,m;p-q) \\
& + \left(c_6\left(\left(\frac{9M^2}{4} - 4m^2\right)q_\alpha + 6M^2p_\alpha\right) + \frac{3}{8}c_7(8M^2p_\alpha + (3M^2 - 16m^2))q_\alpha\right)\tilde{\mathcal{B}}_{(1,1)}^\alpha(M,m;p+q) \\
& + 3(2c_6 + c_7)m^2(2M^2(\tilde{\mathcal{B}}_{(1,1)}(M,m;p+q) - \tilde{\mathcal{B}}_{(1,1)}(M,m;p)) + \tilde{\mathcal{A}}_{(1)}(m)) \Bigg\} \\
& + \frac{4}{mF^2}\Bigg\{ (2c_6 - c_7)m^2\left(\tilde{\mathcal{B}}_{(1,1)}^{11}(M,M;q) + \frac{1}{2}\tilde{\mathcal{A}}_{(1)}(M)\right) - c_2p_\alpha p_\beta(4\tilde{\mathcal{B}}_{(2,1)}^{11\alpha\beta}(M,M;q) + \tilde{\mathcal{A}}_{(2)}^{\alpha\beta}(M)) \\
& + (2c_1 - c_3)M^2m^2(4\tilde{\mathcal{B}}_{(2,1)}^{11}(M,M;q) + \tilde{\mathcal{A}}_{(2)}(M)) + \frac{3}{q^2}c_2q_\alpha q_\beta\tilde{\mathcal{A}}_{(1)}^{\alpha\beta}(M) + m^2c_6\tilde{\mathcal{A}}_{(1)}(M) \\
& + c_7m^2(\tilde{\mathcal{B}}_{(1,1)}^{11}(M,M;q) + \tilde{\mathcal{A}}_{(1)}(M)) - c_4m^2\tilde{\mathcal{B}}_{(1,1)}^{11}(M,M;q) \Bigg\}.
\end{aligned}
\tag{47}
$$

Note that in the above expressions, we have replaced m_L, emerging from the kinematics, by the infinite-volume nucleon mass, m. Up to the chiral order we are working, this is a perfectly valid procedure. Finally, the expressions for the various finite-volume sums, which enter the above formulas, are listed in Appendix D.

B. Numerical results

In this section, we evaluate the finite-volume corrections to the 11-component of the Compton tensor, which enters the expression of the energy shift in the periodic background field. The quantity, which will be calculated here, is given by

$$
\Delta = \frac{T_L^{11}(p,q) - T^{11}(p,q)}{T^{11}(p,q)}.
\tag{48}
$$

We calculate this quantity for the physical value of the pion mass and for several different values of q^2, separately for the proton and the neutron. Having explicit expressions for the amplitude, it is straightforward to carry out the calculations for unphysical quark masses as well, if needed. It should be stressed that we are mainly interested in the order-of-magnitude estimate of the correction, which is needed to answer the following question: How large should the box size L be so that one can safely neglect the finite-volume artifacts?

The results at $O(p^3)$ can be obtained directly from Eqs. (40)–(47), since these contain no unknown LECs.

At $O(p^4)$, however, the LECs $e_y^\pm$, defined in Eq. (24), appear. We fit these to the magnetic polarizability β_M:

$$\text{Model A}: e_y^+ = (0.42 \pm 0.10) \text{ GeV}^{-3},$$
$$e_y^- = (0.56 \pm 0.34) \text{ GeV}^{-3},$$
$$\text{Model C}: e_y^+ = (0.53 \pm 0.06) \text{ GeV}^{-3},$$
$$e_y^- = (0.91 \pm 0.07) \text{ GeV}^{-3} \qquad (49)$$

(note that we do not have separate inputs for the proton and neutron for Model B). For further calculations, we use the following values of the $O(p^4)$ LECs:

$$e_y^+ = (0.46 \pm 0.14) \text{ GeV}^{-3}, \quad e_y^- = (0.60 \pm 0.38) \text{ GeV}^{-3}. \qquad (50)$$

This choice covers Model A, as well as Model C.

The finite-volume corrections to the Compton amplitude are shown in Figs. 7 and 8 for the following values of the variable Q^2:

$$Q^2 = 0.001 M_\pi^2, \quad 0.01 M_\pi^2, \quad 0.1 M_\pi^2, \quad 0.5 M_\pi^2, \quad M_\pi^2, \quad 2 M_\pi^2. \qquad (51)$$

These figures contain our main result, answering the question about the feasibility of the extraction of the
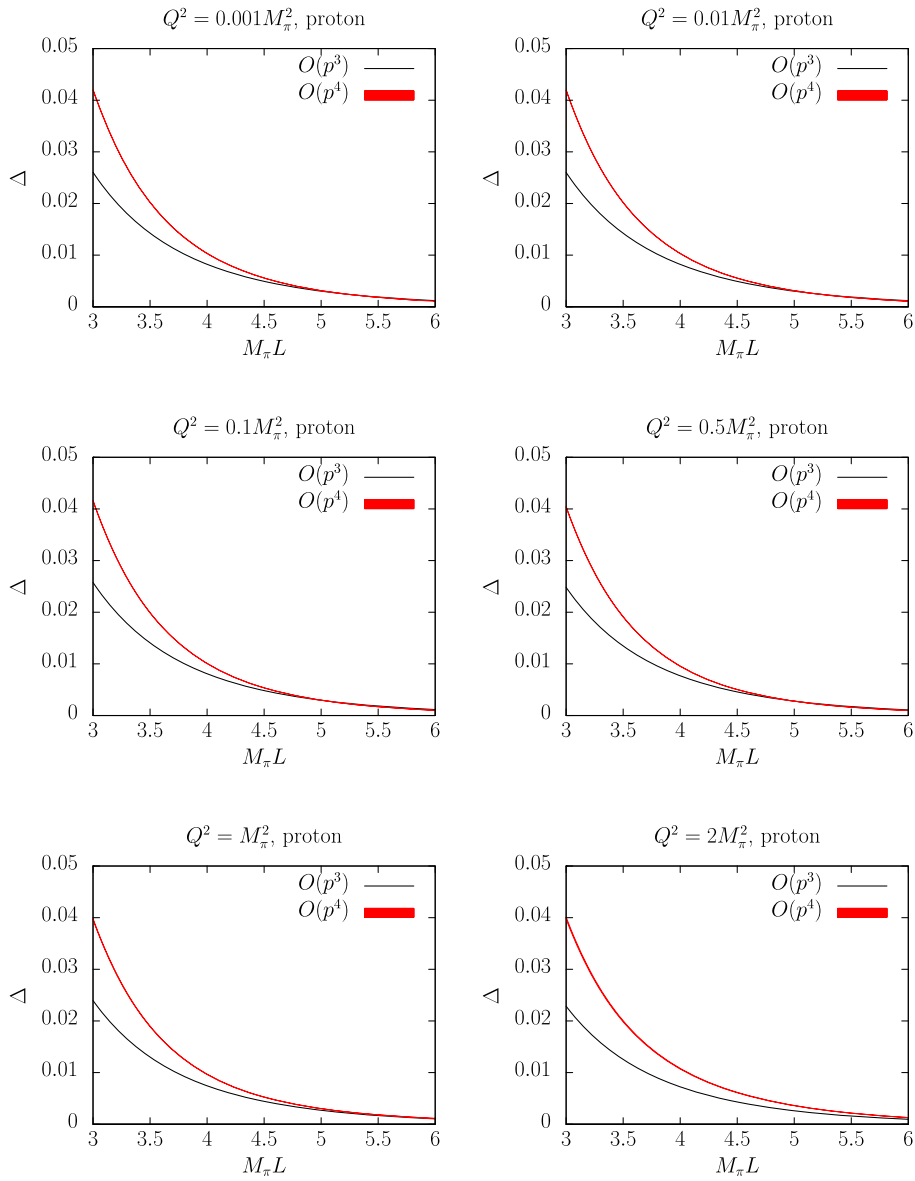

FIG. 7.   The finite-volume effect in the proton amplitude versus the dimensionless variable $M_\pi L$. The uncertainty in the knowledge of e_y^+ does not translate into a large uncertainty in the final results, and the width of the red band is barely visible by eye.
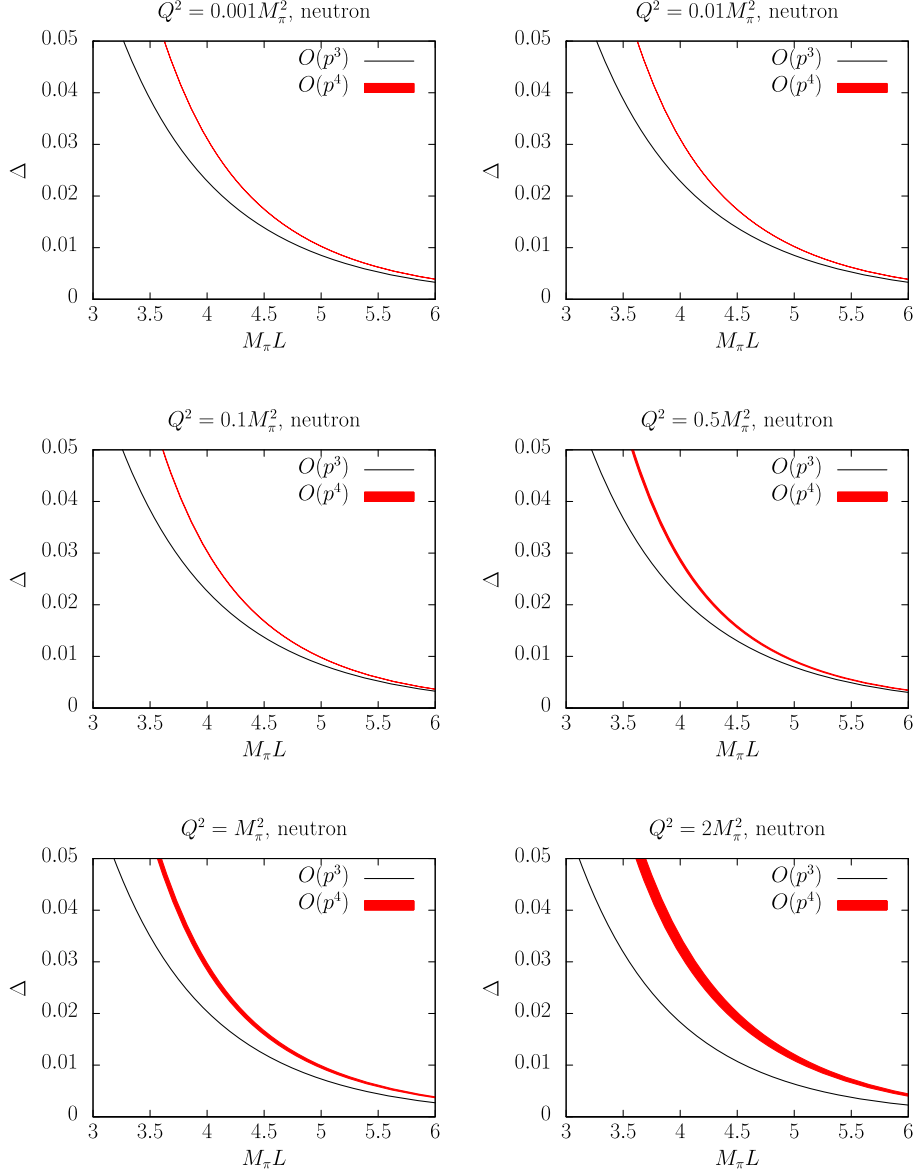
FIG. 8.   The same as in Fig. 7 for the neutron.

subtraction function on the lattice. It is seen that, for both the proton and the neutron, the finite-volume corrections are encouragingly small for $M_\pi L \geq 4$ (the fact that they are slightly smaller for the proton than for the neutron stems from the presence of the large second-order pole term proportional to the combination $2c_6 + c_7$, in the infinite-volume proton amplitude). Further, it is very comforting to see that the convergence of the result at fourth order is reasonable. Moreover, the uncertainty caused by the poor knowledge of the $O(p^4)$ LECs is indeed moderate in the final results (for example, in case of the proton, it is hardly visible by the bare eye). Taking this fact into account, one might wonder whether the uncertainty in the LECs at lower orders might play a more significant role. Following our expectation, a 20%–30% error in a final result generously

covers the effect coming from these LECs. Another easy way to estimate the uncertainty of calculations (not limited necessarily to the poorly determined LECs) is to compare the results at $O(p^3)$ and $O(p^4)$. Taking into account the fact that the present study was primarily intended to serve as a rough estimate of the size of the exponentially suppressed corrections to the amplitude, we did not try to investigate this question further.

Finally, note that the relative correction stays almost constant from $Q^2 \simeq 0$ to $Q^2 \simeq 2M_\pi^2$ and, possibly, even for higher values of Q^2. In other words, the finite-volume artifacts do not hinder an accurate extraction of the amplitude at large Q^2. Here we remind the reader that an accurate measurement of the inelastic part on the lattice becomes more difficult as $Q^2 \to 0$, because the elastic

contribution dominates in this limit [12,13]. Hence, the finite-volume artifacts do not further restrict an interval in Q^2, where an accurate calculation of the subtraction function is possible.

V. SUMMARY

(i) Using baryon chiral perturbation theory and the EOMS renormalization scheme of Refs. [52,53], which guarantees that the renormalized expressions satisfy the standard power counting, we have evaluated the doubly virtual spin-averaged Compton scattering amplitude off nucleons up to $O(p^4)$ in the infinite volume. We have further calculated finite-volume corrections to the so-called subtraction function at the same chiral order.

(ii) The inelastic parts of the infinite-volume subtraction functions $S_1^{\mathrm{inel}}(q^2)$ and $\bar{S}(q^2)$ show a rather regular behavior at small values of q^2 that is of the order of the pion mass squared. None of the loop diagrams up-to-and-including order p^4 leads to a rapid variation of the calculated subtraction functions at small scales. Note that in these calculations we have fixed the numerical values of some of the $O(p^4)$ LECs through the proton and neutron magnetic polarizabilities which, at present, are not known to high accuracy (especially, the one for the neutron).

(iii) The main result of this work is the calculation of the finite-volume corrections in the Compton scattering amplitude. These calculations are interesting, first and foremost, in view of the perspective of a measurement of the subtraction function on the lattice using periodic external fields. Note also that, since the cubic lattice does not preserve Lorentz invariance, the definition of the subtraction function in a finite volume is ambiguous. On the other hand, what is extracted from the nucleon mass shift, measured on the lattice, is a particular component of the second-rank Compton tensor T_L^{11}, which is a well-defined quantity and which tends to $S_1(q^2)$ (modulo an overall kinematic factor) in the infinite-volume limit. The numerical results quoted in this work refer to this quantity.

(iv) At this stage, we do not know, on the one hand, how the other subtraction function $\bar{S}(q^2)$ can be measured on the lattice. On the other hand, the two subtraction functions are related to each other: Their difference is a convergent integral containing experimentally measured electroproduction cross sections.

(v) Our results show that the exponentially vanishing finite-volume corrections to the quantity T_L^{11} amount up to 2%–3% percent or less at $M_\pi L \simeq 4$ for both the proton and the neutron. This means that one can extract the infinite-volume subtraction function with a good accuracy already using reasonably large lattices. We also note that the convergence of our results is rather good, and the poor knowledge of the $O(p^4)$ LECs does not pose a real obstacle as the resulting uncertainty is very small.

(vi) As pointed out in Refs. [12,13], the large elastic part renders the extraction of the subtraction function at low q^2 problematic. Having the finite-volume corrections well under control might help one to carry out the analysis at lower values of q^2. On the other hand, the observed q^2-behavior of the quantity Δ is very mild up to $-q^2 = 2M_\pi^2$, and one may try to push the upper limit in q^2 higher, allowing for the extraction of the subtraction function in a larger interval of q^2. Such an extrapolation, however, comes with a grain of salt, since it implicitly assumes a good convergence of chiral perturbation theory at higher values of q^2. In general, one might consider the results for $-q^2 < 0.1M_\pi^2$ relatively safe. Beyond this value, a reliable calculation should include an estimate of the higher-order corrections that is very difficult and clearly lies beyond the scope of the present paper. Note also that the finite-volume corrections (which are the main output of this paper) are quite small, so even a large uncertainty in their calculation does not critically affect the extraction of the Compton tensor on the lattice. As seen from Figs. 5 and 6, in the calculation of the infinite-volume quantities, such as the subtraction functions, the situation is quite different. Here, the modification from $O(p^3)$ to $O(p^4)$ is rather significant for higher absolute values of q^2.

APPENDIX A: DEFINITION OF THE LOOP INTEGRALS

The one-loop integrals appearing in our calculations are defined as follows:
One factor in the denominator:

$$\int \frac{d^n k}{k^2 - m^2 + i\epsilon} = A_0(m),$$

$$\int \frac{d^n k}{[k^2 - m^2 + i\epsilon]^N} = A_0^{(N)}(m),$$

$$\int \frac{d^n k\, k^\mu k^\nu}{k^2 - m^2 + i\epsilon} = g^{\mu\nu} A_{00}(m). \tag{A1}$$

Two factors in the denominator:

$$\int \frac{d^n k}{[k^2 - M^2 + i\epsilon][(p+k)^2 - m^2 + i\epsilon]} = B_0(p^2; M, m),$$

$$\int \frac{d^n k}{[k^2 - M^2 + i\epsilon]^M[(p+k)^2 - m^2 + i\epsilon]^N} = B_0^{(M,N)}(p^2; M, m),$$

$$\int \frac{d^n k\, k^\mu}{[k^2 - M^2 + i\epsilon][(p+k)^2 - m^2 + i\epsilon]} = p^\mu B_1(p^2; M, m),$$

$$\int \frac{d^n k\, k^\mu}{[k^2 - M^2 + i\epsilon]^M[(p+k)^2 - m^2 + i\epsilon]^N} = p^\mu B_1^{(M,N)}(p^2; M, m),$$

$$\int \frac{d^n k\, k^\mu k^\nu}{[k^2 - M^2 + i\epsilon][(p+k)^2 - m^2 + i\epsilon]} = g^{\mu\nu} B_{00}(p^2; M, m) + p^\mu p^\nu B_{11}(p^2; M, m),$$

$$\int \frac{d^n k\, k^\mu k^\nu}{[k^2 - M^2 + i\epsilon]^M[(p+k)^2 - m^2 + i\epsilon]^N} = g^{\mu\nu} B_{00}^{(M,N)}(p^2; M, m) + p^\mu p^\nu B_{11}^{(M,N)}(p^2; M, m),$$

$$\int \frac{d^n k\, k^\mu k^\nu k^\alpha}{(k^2 - M^2 + i\epsilon)^2[(k-q)^2 - M^2 + i\epsilon]} = -q^\alpha q^\mu q^\nu B_{111}^{(2,1)}(q^2; M, M) - (q^\nu g^{\alpha\mu} + q^\mu g^{\alpha\mu} + q^\alpha g^{\mu\nu}) B_{001}^{(2,1)}(q^2; M, M),$$

$$\int \frac{d^n k\, k^\mu k^\nu k^\alpha k^\beta}{(k^2 - M^2 + i\epsilon)^2[(k-q)^2 - M^2 + i\epsilon]} = (g^{\alpha\nu} g^{\beta\mu} + g^{\alpha\mu} g^{\beta\nu} + g^{\alpha\beta} g^{\mu\mu}) B_{0000}^{(2,1)}(q^2; M, M) + q^\mu q^\nu q^\alpha q^\beta B_{1111}^{(2,1)}(q^2; M, M)$$

$$+ (q^\beta q^\nu g^{\alpha\mu} + q^\mu q^\nu g^{\alpha\beta} + q^\mu q^\beta g^{\alpha\nu} + q^\alpha q^\beta g^{\mu\nu} + q^\mu q^\alpha g^{\beta\nu}$$

$$+ q^\nu q^\alpha g^{\mu\beta}) B_{0011}^{(2,1)}(q^2; M, M). \tag{A2}$$

Three factors in the denominator:

$$\int \frac{d^n k}{[k^2 - M^2 + i\epsilon][(p+k)^2 - m_1^2 + i\epsilon][(q+k)^2 - m_2^2 + i\epsilon]} = C_0(p^2, (p-q)^2, q^2; M, m_1, m_2),$$

$$\int \frac{d^n k}{[k^2 - M^2 + i\epsilon]^M[(p+k)^2 - m_1^2 + i\epsilon]^N[(q+k)^2 - m_2^2 + i\epsilon]^K} = C_0^{(M,N,K)}(p^2, (p-q)^2, q^2; M, m_1, m_2),$$

$$\int \frac{d^n k\, k^\mu}{[k^2 - M^2 + i\epsilon][(p+k)^2 - m_1^2 + i\epsilon][(q+k)^2 - m_2^2 + i\epsilon]}$$

$$= q^\mu C_2(p^2, (p-q)^2, q^2; M, m_1, m_2) + p^\mu C_1(p^2, (p-q)^2, q^2; M, m_1, m_2),$$

$$\int \frac{d^n k\, k^\mu}{[k^2 - M^2 + i\epsilon]^M[(p+k)^2 - m_1^2 + i\epsilon]^N[(q+k)^2 - m_2^2 + i\epsilon]^K}$$

$$= q^\mu C_2^{(M,N,K)}(p^2, (p-q)^2, q^2; M, m_1, m_2) + p^\mu C_1^{(M,N,K)}(p^2, (p-q)^2, q^2; M, m_1, m_2),$$

$$\int \frac{d^n k k^\mu k^\nu}{[k^2 - M^2 + i\epsilon][(p + k)^2 - m_1^2 + i\epsilon][(q + k)^2 - m_2^2 + i\epsilon]}$$

$$= g^{\mu\nu} C_{00}(p^2, (p - q)^2, q^2; M, m_1, m_2) + q^\mu q^\nu C_{22}(p^2, (p - q)^2, q^2; M, m_1, m_2)$$

$$+ p^\mu p^\nu C_{11}(p^2, (p - q)^2, q^2; M, m_1, m_2) + (p^\nu q^\mu + p^\mu q^\nu) C_{12}(p^2, (p - q)^2, q^2; M, m_1, m_2),$$

$$\int \frac{d^n k k^\mu k^\nu}{[k^2 - M^2 + i\epsilon]^M [(p + k)^2 - m_1^2 + i\epsilon]^N [(q + k)^2 - m_2^2 + i\epsilon]^K}$$

$$= g^{\mu\nu} C_{00}^{(M,N,K)}(p^2, (p - q)^2, q^2; M, m_1, m_2) + q^\mu q^\nu C_{22}^{(M,N,K)}(p^2, (p - q)^2, q^2; M, m_1, m_2)$$

$$+ p^\mu p^\nu C_{11}^{(M,N,K)}(p^2, (p - q)^2, q^2; M, m_1, m_2) + (p^\mu q^\nu + p^\nu q^\mu) C_{12}^{(M,N,K)}(p^2, (p - q)^2, q^2; M, m_1, m_2). \tag{A3}$$

APPENDIX B: TREE-LEVEL EXPRESSIONS—INDIVIDUAL DIAGRAMS

Below we list the tree-order contributions to the quantities $T_1(0, q^2)$ and $T_2(0, q^2)$, coming from the individual diagrams in Figs. 1–4. At the order we are working, one may safely replace $\mathring{m}$ by m, M by M_π, and F by F_π everywhere.

$O(p)$ *contributions:*

$$T_1^1 = 0, \qquad T_2^1 = 2m^2(\tau^3 + 1)\frac{1}{q^4}. \tag{B1}$$

$O(p^2)$ *contributions:*

$$T_1^{2,3} = \frac{m}{q^2}(2c_6 + c_7)(\tau^3 + 1), \qquad T_2^{2,3} = 0. \tag{B2}$$

$O(p^3)$ *contributions:*

$$T_1^{4,5} = 0,$$

$$T_2^{4,5} = -4\frac{m^2}{q^2}(d_6 + 2d_7)(\tau^3 + 1),$$

$$T_1^6 = \frac{m^2}{q^2}(4c_7 c_6 \tau^3 + 4c_6^2 + c_7^2),$$

$$T_2^6 = -\frac{m^2}{q^2}(4c_7 c_6 \tau^3 + 4c_6^2 + c_7^2),$$

$$T_1^7 = (d_6 + 2d_7)(\tau^3 + 1),$$

$$T_2^7 = 0. \tag{B3}$$

$O(p^4)$ *contributions:*

$$T_1^{33} = 8m(2e_{89} + e_{93} + e_{118} + \tau^3 e_{91}),$$

$$T_2^{33} = 4m(2e_{90} + e_{94} + e_{117} + \tau^3 e_{92}),$$

$$T_1^{34,35} = \frac{2m}{q^2}(\tau^3 + 1)((2e_{54} + e_{74})q^2 - 4(2e_{105} + e_{106})M^2),$$

$$T_2^{34,35} = 0,$$

$$T_1^{36,37} = 0,$$

$$T_2^{36,37} = -2m(c_7(d_6 \tau^3 + 2d_7) + 2c_6(2d_7 \tau^3 + d_6)). \tag{B4}$$

APPENDIX C: ONE-LOOP EXPRESSIONS—INDIVIDUAL DIAGRAMS

Below one finds the one-loop contributions to the amplitudes $T_1(0, q^2)$ and $T_2(0, q^2)$:
$O(p^3)$ *contributions:*

$$T_1^8 = -\frac{m^2 g_A^2}{8\pi^2 F^2} \{M^2(4(C_{22}^{(2,1,1)}(m^2, m^2 + q^2, q^2; M, m, M) + C_2^{(2,1,1)}(m^2, m^2 + q^2, q^2; M, m, M))$$
$$+ C_0^{(2,1,1)}(m^2, m^2 + q^2, q^2; M, m, M)) + 4C_{22}(m^2, m^2 + q^2, q^2; M, m, M)$$
$$+ C_0(m^2, m^2 + q^2, q^2; M, m, M) + 4C_2(m^2, m^2 + q^2, q^2; M, m, M)\}, \tag{C1}$$

$$T_2^8 = \frac{m^4 g_A^2}{2\pi^2 F^2 q^2}(M^2 C_{11}^{(2,1,1)}(m^2, m^2 + q^2, q^2; M, m, M) + C_{11}(m^2, m^2 + q^2, q^2; M, m, M)),$$

$$T_1^9 = \frac{m^2(\tau^3 - 1)g_A^2}{16\pi^2 F^2} \{M^2(4(C_{22}^{(2,1,1)}(m^2, q^2, m^2 + q^2; M, m, m) - C_{22}^{(2,1,1)}(m^2, m^2 + q^2, q^2; M, m, M)$$
$$+ C_{22}^{(2,1,1)}(m^2 + q^2, m^2, q^2; M, m, M) + 2C_{12}^{(2,1,1)}(m^2 + q^2, m^2, q^2; M, m, M)$$
$$+ C_{11}^{(2,1,1)}(m^2 + q^2, m^2, q^2; M, m, M) + C_2^{(2,1,1)}(m^2, q^2, m^2 + q^2; M, m, m)$$
$$- C_2^{(2,1,1)}(m^2, m^2 + q^2, q^2; M, m, M) + C_2^{(2,1,1)}(m^2 + q^2, m^2, q^2; M, m, M)$$
$$+ C_1^{(2,1,1)}(m^2 + q^2, m^2, q^2; M, m, M)) + C_0^{(2,1,1)}(m^2, q^2, m^2 + q^2; M, m, m)$$
$$- C_0^{(2,1,1)}(m^2, m^2 + q^2, q^2; M, m, M) + C_0^{(2,1,1)}(m^2 + q^2, m^2, q^2; M, m, M))$$
$$+ 4C_{22}(m^2, q^2, m^2 + q^2; M, m, m) - 2C_{22}(m^2, m^2 + q^2, q^2; M, m, M) + 2C_{22}(m^2 + q^2, m^2, q^2; M, m, M)$$
$$+ 4C_{12}(m^2 + q^2, m^2, q^2; M, m, M) + 2C_{11}(m^2 + q^2, m^2, q^2; M, m, M) + C_0(m^2, q^2, m^2 + q^2; M, m, m)$$
$$- C_0(m^2, m^2 + q^2, q^2; M, m, M) + C_0(m^2 + q^2, m^2, q^2; M, m, M) + 4C_2(m^2, q^2, m^2 + q^2; M, m, m)$$
$$- 3C_2(m^2, m^2 + q^2, q^2; M, m, M) + 3C_2(m^2 + q^2, m^2, q^2; M, m, M) + 3C_1(m^2 + q^2, m^2, q^2; M, m, M)\},$$

$$T_2^9 = -\frac{m^4(\tau^3 - 1)g_A^2}{8\pi^2 F^2 q^2}(2M^2 C_{22}^{(2,1,1)}(m^2, q^2, m^2 + q^2; M, m, m) + 4M^2 C_{12}^{(2,1,1)}(m^2, q^2, m^2 + q^2; M, m, m)$$
$$+ 2M^2 C_{11}^{(2,1,1)}(m^2, q^2, m^2 + q^2; M, m, m) - 2M^2 C_{11}^{(2,1,1)}(m^2, m^2 + q^2, q^2; M, m, M)$$
$$+ 2M^2 C_{11}^{(2,1,1)}(m^2 + q^2, m^2, q^2; M, m, M) + 2M^2 C_1^{(2,1,1)}(m^2, q^2, m^2 + q^2; M, m, m)$$
$$- 2M^2 C_1^{(2,1,1)}(m^2, m^2 + q^2, q^2; M, m, M) + 2M^2 C_1^{(2,1,1)}(m^2 + q^2, m^2, q^2; M, m, M)$$
$$+ (2M^2 - q^2)C_2^{(2,1,1)}(m^2, q^2, m^2 + q^2; M, m, m) - q^2 C_1^{(2,1,1)}(m^2, q^2, m^2 + q^2; M, m, m)$$
$$+ q^2 C_1^{(2,1,1)}(m^2, m^2 + q^2, q^2; M, m, M) - q^2 C_1^{(2,1,1)}(m^2 + q^2, m^2, q^2; M, m, M)$$
$$+ 2C_{22}(m^2, q^2, m^2 + q^2; M, m, m) + 4C_{12}(m^2, q^2, m^2 + q^2; M, m, m) + 2C_{11}(m^2, q^2, m^2 + q^2; M, m, m)$$
$$- C_{11}(m^2, m^2 + q^2, q^2; M, m, M) + C_{11}(m^2 + q^2, m^2, q^2; M, m, M) + 2C_2(m^2, q^2, m^2 + q^2; M, m, m)$$
$$+ 2C_1(m^2, q^2, m^2 + q^2; M, m, m) - C_1(m^2, m^2 + q^2, q^2; M, m, M) + C_1(m^2 + q^2, m^2, q^2; M, m, M)),$$

$$T_1^{10} = \frac{m^2(\tau^3 - 3)g_A^2}{8\pi^2 F^2} \{B_{11}^{(2,1)}(q^2; m, m) + B_1^{(2,1)}(q^2; m, m) + M^2(C_{22}^{(1,2,1)}(m^2, q^2, m^2 + q^2; M, m, m)$$
$$+ C_2^{(1,2,1)}(m^2, q^2, m^2 + q^2; M, m, m))\},$$

$$T_2^{10} = \frac{m^2(\tau^3 - 3)g_A^2}{32\pi^2 F^2 q^2}(-4m^2 M^2(C_{22}^{(1,2,1)}(m^2, q^2, m^2 + q^2; M, m, m)$$
$$+ 2(C_{12}^{(1,2,1)}(m^2, q^2, m^2 + q^2; M, m, m) + C_1^{(1,2,1)}(m^2, q^2, m^2 + q^2; M, m, m))$$
$$+ C_{11}^{(1,2,1)}(m^2, q^2, m^2 + q^2; M, m, m) + C_0^{(1,2,1)}(m^2, q^2, m^2 + q^2; M, m, m)$$
$$+ 2C_2^{(1,2,1)}(m^2, q^2, m^2 + q^2; M, m, m)) + B_0(m^2 + q^2; M, m) + B_1(m^2 + q^2; M, m)),$$

$$T_1^{11,12} = -\frac{m^2(\tau^3 - 1)g_A^2(C_{22}(m^2, q^2, m^2 + q^2; M, m, m) + C_2(m^2, q^2, m^2 + q^2; M, m, m))}{4\pi^2 F^2},$$

$$T_2^{11,12} = -\frac{m^2(\tau^3 - 1)g_A^2}{8\pi^2 F^2 q^2}(B_0(m^2 + q^2; M, m) + B_1(m^2 + q^2; M, m) - 2m^2(C_{22}(m^2, q^2, m^2 + q^2; M, m, m)$$
$$+ 2C_{12}(m^2, q^2, m^2 + q^2; M, m, m) + C_{11}(m^2, q^2, m^2 + q^2; M, m, m) + C_2(m^2, q^2, m^2 + q^2; M, m, m)$$
$$+ C_1(m^2, q^2, m^2 + q^2; M, m, m))),$$

$$T_1^{13,14} = \frac{m^2 g_A^2(2C_{22}(m^2, m^2 + q^2, q^2; M, m, M) + C_2(m^2, m^2 + q^2, q^2; M, m, M))}{4\pi^2 F^2},$$

$$T_2^{13,14} = -\frac{m^4 g_A^2}{2\pi^2 F^2 q^2}C_{11}(m^2, m^2 + q^2, q^2; M, m, M),$$

$$T_1^{15} = 0,$$

$$T_2^{15} = 0,$$

$$T_1^{16} = 0,$$

$$T_2^{16} = -\frac{m^2 g_A^2}{8\pi^2 F^2 q^2}(B_0(m^2 + q^2; M, m) + B_1(m^2 + q^2; M, m)),$$

$$T_1^{17} = 0,$$

$$T_2^{17} = -\frac{3m^2(\tau^3 + 1)g_A^2}{32\pi^2 F^2(q^2)^3}((2m^2 + q^2)(M^2 B_1(m^2 + q^2; M, m) + 2((m^2 + q^2)B_{11}(m^2 + q^2; M, m)$$
$$+ B_{00}(m^2 + q^2; M, m))) + M^2(-(4m^2 + q^2))B_0(m^2 + q^2; M, m) - 2(3m^2 + q^2)A_0(m)),$$

$$T_1^{18,19} = -\frac{m^2(\tau^3 + 1)g_A^2}{8\pi^2 F^2 q^2}\{B_0(m^2 + q^2; m, M) + 2B_1(m^2 + q^2; m, M) + M^2 C_0(m^2, m^2 + q^2, q^2; M, m, M)$$
$$+ (2M^2 + q^2)C_2(m^2, m^2 + q^2, q^2; M, m, M) + 2q^2 C_{22}(m^2, m^2 + q^2, q^2; M, m, M)\},$$

$$T_2^{18,19} = \frac{m^2(\tau^3 + 1)g_A^2}{4\pi^2 F^2(q^2)^2}(m^2(B_0(m^2 + q^2; m, M) + B_1(m^2 + q^2; m, M) - B_1(m^2; M, m)$$
$$+ (q^2 - 2M^2)C_1(m^2, m^2 + q^2, q^2; M, m, M) + q^2 C_{11}(m^2, m^2 + q^2, q^2; M, m, M)) + B_{00}(q^2; M, M)),$$

$$T_1^{20-23} = 0,$$

$$T_2^{20-23} = -\frac{m^2(\tau^3 + 1)g_A^2}{8\pi^2 F^2(q^2)^2}(M^2 B_0(m^2 + q^2; M, m) + q^2 B_1(m^2 + q^2; M, m) - 2m^2 B_1(m^2; M, m) + A_0(m) + A_0(M)),$$

$$T_1^{24,25} = \frac{m^2(\tau^3 + 1)g_A^2}{8\pi^2 F^2 q^2}(B_1(m^2 + q^2; M, m) - B_1(q^2; m, m) + (q^2 - M^2)C_2(m^2, q^2, m^2 + q^2; M, m, m)$$
$$+ q^2 C_{22}(m^2, q^2, m^2 + q^2; M, m, m)),$$

$$T_2^{24,25} = -\frac{m^2(\tau^3 + 1)g_A^2}{16\pi^2 F^2(q^2)^2}(-q^2(B_0(m^2 + q^2; M, m) + B_1(m^2 + q^2; M, m)$$
$$- 2m^2(C_{22}(m^2, q^2, m^2 + q^2; M, m, m) + 2C_{12}(m^2, q^2, m^2 + q^2; M, m, m)$$
$$+ C_{11}(m^2, q^2, m^2 + q^2; M, m, m))) - 4m^2 M^2(C_0(m^2, q^2, m^2 + q^2; M, m, m)$$
$$+ C_2(m^2, q^2, m^2 + q^2; M, m, m) + C_1(m^2, q^2, m^2 + q^2; M, m, m)) + A_0(M)),$$

$$T_1^{29-32} = 0,$$

$$T_2^{29-32} = \frac{m^2(\tau^3 + 1)(A_0(M) - 2B_{00}(q^2; M, M))}{4\pi^2 F^2(q^2)^2}. \tag{C2}$$

$O(p^4)$ contributions:

$$T_1^{38,39} = -\frac{(2c_6 + c_7)g^2 m(\tau^3 - 3)}{64\pi^2 F^2}\{4m^2(B_0^{(2,1)}(q^2; m, m) + M^2 C_0^{(1,2,1)}(m^2, q^2, m^2 + q^2; M, m, m))$$
$$- B_0(m^2 + q^2; M, m) - B_1(m^2 + q^2; M, m) + 2B_0(q^2; m, m) + 2B_1(q^2; m, m)$$
$$+ 2M^2(C_0(m^2, q^2, m^2 + q^2; M, m, m) + C_2(m^2, q^2, m^2 + q^2; M, m, m))\},$$

$$T_2^{38,39} = 0,$$

$$T_1^{40} = -\frac{m^3 g_A^2(2c_6 - c_7\tau^3)}{16\pi^2 F^2}\{4q^2 C_{22}^{(2,1,1)}(q^2, m^2, m^2 + q^2; m, m, M) + 8q^2 C_{12}^{(2,1,1)}(q^2, m^2, m^2 + q^2; m, m, M)$$
$$+ 4q^2 C_{11}^{(2,1,1)}(q^2, m^2, m^2 + q^2; m, m, M) - 4q^2 C_{11}^{(2,1,1)}(q^2, m^2 + q^2, m^2; m, m, M)$$
$$+ 4q^2 C_{11}^{(2,1,1)}(m^2 + q^2, q^2, m^2; m, M, M) + q^2 C_0^{(2,1,1)}(q^2, m^2, m^2 + q^2; m, m, M)$$
$$- q^2 C_0^{(2,1,1)}(q^2, m^2 + q^2, m^2; m, m, M) + q^2 C_0^{(2,1,1)}(m^2 + q^2, q^2, m^2; m, M, M)$$
$$+ 4q^2 C_2^{(2,1,1)}(q^2, m^2, m^2 + q^2; m, m, M) + 4q^2 C_1^{(2,1,1)}(q^2, m^2, m^2 + q^2; m, m, M)$$
$$- 4q^2 C_1^{(2,1,1)}(q^2, m^2 + q^2, m^2; m, m, M) + 4q^2 C_1^{(2,1,1)}(m^2 + q^2, q^2, m^2; m, M, M)$$
$$+ C_0(q^2, m^2, m^2 + q^2; m, m, M) - C_0(q^2, m^2 + q^2, m^2; m, m, M) + 2C_2(q^2, m^2, m^2 + q^2; m, m, M)$$
$$+ 2C_1(q^2, m^2, m^2 + q^2; m, m, M) - 2C_1(q^2, m^2 + q^2, m^2; m, m, M)\},$$

$$T_2^{40} = \frac{m^3 g_A^2(2c_6 - c_7\tau^3)}{16F^2\pi^2 q^2}(-4B_1^{(2,1)}(m^2; m, M)m^2 - 4B_1^{(2,1)}(m^2 + q^2; m, M)m^2 - 2B_{11}^{(2,1)}(m^2; m, M)m^2$$
$$- 2B_{11}^{(2,1)}(m^2 + q^2; m, M)m^2 + 4q^2 C_0^{(2,1,1)}(q^2, m^2, m^2 + q^2; m, m, M)m^2$$
$$- 4q^2 C_0^{(2,1,1)}(q^2, m^2 + q^2, m^2; m, m, M)m^2 + 4q^2 C_0^{(2,1,1)}(m^2 + q^2, q^2, m^2; m, M, M)m^2$$
$$+ 8q^2 C_2^{(2,1,1)}(q^2, m^2, m^2 + q^2; m, m, M)m^2 - 8q^2 C_2^{(2,1,1)}(q^2, m^2 + q^2, m^2; m, m, M)m^2$$
$$+ 8q^2 C_2^{(2,1,1)}(m^2 + q^2, q^2, m^2; m, M, M)m^2 + 4q^2 C_{22}^{(2,1,1)}(q^2, m^2, m^2 + q^2; m, m, M)m^2$$
$$- 4q^2 C_{22}^{(2,1,1)}(q^2, m^2 + q^2, m^2; m, m, M)m^2 + 4q^2 C_{22}^{(2,1,1)}(m^2 + q^2, q^2, m^2; m, M, M)m^2$$
$$+ 8q^2 C_1^{(2,1,1)}(m^2 + q^2, q^2, m^2; m, M, M)m^2 + 8q^2 C_{12}^{(2,1,1)}(m^2 + q^2, q^2, m^2; m, M, M)m^2$$
$$+ 4q^2 C_{11}^{(2,1,1)}(m^2 + q^2, q^2, m^2; m, M, M)m^2 + 2A_0^{(2)}(m) - 3B_0(m^2; m, M) + B_0(m^2 + q^2; m, M)$$
$$- 3B_1(m^2; m, M) + B_1(m^2 + q^2; m, M) + (M^2 - 2m^2)B_0^{(2,1)}(m^2; m, M)$$
$$+ (-2m^2 + M^2 - q^2)B_0^{(2,1)}(m^2 + q^2; m, M) + M^2 B_1^{(2,1)}(m^2; m, M) + M^2 B_1^{(2,1)}(m^2 + q^2; m, M)$$
$$- 3q^2 B_1^{(2,1)}(m^2 + q^2; m, M) - 2q^2 B_{11}^{(2,1)}(m^2 + q^2; m, M) - 2(B_{00}^{(2,1)}(m^2; m, M)$$
$$+ B_{00}^{(2,1)}(m^2 + q^2; m, M)) + q^2 C_0(q^2, m^2, m^2 + q^2; m, m, M) - q^2 C_0(q^2, m^2 + q^2, m^2; m, m, M)$$
$$+ 2q^2 C_0(m^2 + q^2, q^2, m^2; m, M, M) + q^2 C_2(q^2, m^2, m^2 + q^2; m, m, M) - q^2 C_2(q^2, m^2 + q^2, m^2; m, m, M)$$
$$+ 2q^2 C_2(m^2 + q^2, q^2, m^2; m, M, M) + 2q^2 C_1(m^2 + q^2, q^2, m^2; m, M, M)),$$

$$T_1^{41,42} = -\frac{m g_A^2(2c_6 - c_7\tau^3)}{16\pi^2 F^2}\{-B_1(m^2 + q^2; M, m) + B_0(q^2; m, m) + 2B_1(q^2; m, m)$$
$$+ M^2 C_0(m^2, q^2, m^2 + q^2; M, m, m) + 2(M^2 - 2m^2)C_2(m^2, q^2, m^2 + q^2; M, m, m)\},$$

$$T_2^{41,42} = -\frac{m^3 g_A^2(2c_6 - c_7\tau^3)}{8\pi^2 F^2 q^2}(-B_0(m^2 + q^2; M, m) - B_1(m^2 + q^2; M, m) + B_0(m^2; M, m) + B_1(m^2; M, m)$$
$$- q^2(C_0(m^2, q^2, m^2 + q^2; M, m, m) + C_2(m^2, q^2, m^2 + q^2; M, m, m) + C_1(m^2, q^2, m^2 + q^2; M, m, m))),$$

$$T_1^{43,44} = -\frac{g_A^2 m(2c_6(\tau^3+3)+c_7(3\tau^3+1))}{128\pi^2 F^2 q^2}\{4m^2(B_0(m^2+q^2;m,M)+2B_1(m^2+q^2;m,M)$$
$$-B_0(m^2;M,m)+q^2(4(C_{22}(m^2,m^2+q^2,q^2;M,m,M)+C_2(m^2,m^2+q^2,q^2;M,m,M))$$
$$+C_0(m^2,m^2+q^2,q^2;M,m,M)))+q^2(4(B_{11}(q^2;M,M)+B_1(q^2;M,M))+B_0(q^2;M,M))$$
$$-2A_0(M)\},$$

$$T_2^{43,44} = -\frac{m^3 g_A^2(2c_6(\tau^3+3)+c_7(3\tau^3+1))}{32\pi^2 F^2 q^2}(B_0(m^2+q^2;m,M)+B_1(m^2+q^2;m,M)+B_1(m^2;M,m)$$
$$-4m^2 C_{11}(m^2,m^2+q^2,q^2;M,m,M)-q^2 C_1(m^2,m^2+q^2,q^2;M,m,M)),$$

$$T_1^{45,47} = \frac{g_A^2 m(2c_6(3\tau^3-1)+c_7(3-\tau^3))}{64\pi^2 F^2 q^2}\{-M^2 B_0(m^2;M,m)+(6m^2+q^2)B_1(m^2+q^2;M,m)$$
$$+(4m^2+q^2)B_0(q^2;m,m)+M^2(4m^2+q^2)C_0(m^2,q^2,m^2+q^2;M,m,m)$$
$$+8m^2 q^2(C_{22}(m^2,q^2,m^2+q^2;M,m,m)+C_2(m^2,q^2,m^2+q^2;M,m,m))-A_0(m)\},$$

$$T_2^{45,47} = \frac{m^3 g_A^2}{8\pi^2 F^2(q^2)^2}(c_6(\tau^3-1)+c_7)(q^2(3B_1(m^2+q^2;M,m)-B_1(m^2;M,m)$$
$$-4m^2(C_{22}(m^2,q^2,m^2+q^2;M,m,m)+2C_{12}(m^2,q^2,m^2+q^2;M,m,m)$$
$$+C_{11}(m^2,q^2,m^2+q^2;M,m,m))+q^2(C_0(m^2,q^2,m^2+q^2;M,m,m)$$
$$+C_2(m^2,q^2,m^2+q^2;M,m,m)+C_1(m^2,q^2,m^2+q^2;M,m,m)))+(M^2-q^2)B_0(m^2;M,m)$$
$$+(M^2+2q^2)B_0(m^2+q^2;M,m)+2m^2(B_1(m^2+q^2;M,m)+B_1(m^2;M,m))+2A_0(m)-2A_0(M)),$$

$$T_1^{46,48} = -\frac{(2c_6-3c_7)g_A^2 m(\tau^3+1)}{64\pi^2 F^2 q^2}\{M^2 B_0(m^2;M,m)+(6m^2+q^2)B_1(m^2+q^2;M,m)$$
$$+(4m^2-q^2)B_0(q^2;m,m)-2q^2 B_1(q^2;m,m)+2q^2((4m^2-M^2)C_2(m^2,q^2,m^2+q^2;M,m,m)$$
$$+4m^2 C_{22}(m^2,q^2,m^2+q^2;M,m,m))+M^2(4m^2-q^2)C_0(m^2,q^2,m^2+q^2;M,m,m)+A_0(m)\},$$

$$T_2^{46,48} = -\frac{(2c_6-3c_7)m^3(\tau^3+1)g_A^2}{32\pi^2 F^2(q^2)^2}(q^2(3B_1(m^2+q^2;M,m)-B_1(m^2;M,m)$$
$$-4m^2(C_{22}(m^2,q^2,m^2+q^2;M,m,m)+2C_{12}(m^2,q^2,m^2+q^2;M,m,m)$$
$$+C_{11}(m^2,q^2,m^2+q^2;M,m,m))+q^2(C_0(m^2,q^2,m^2+q^2;M,m,m)+C_2(m^2,q^2,m^2+q^2;M,m,m)$$
$$+C_1(m^2,q^2,m^2+q^2;M,m,m)))+(M^2-q^2)B_0(m^2;M,m)+(M^2+2q^2)B_0(m^2+q^2;M,m)$$
$$+2m^2(B_1(m^2+q^2;M,m)+B_1(m^2;M,m))+2A_0(m)-2A_0(M)),$$

$$T_1^{49-52} = -\frac{mg_A^2}{16\pi^2 F^2 q^2}(2c_6+c_7\tau^3)(M^2(B_0(m^2+q^2;M,m)+B_0(m^2;M,m))+q^2 B_1(m^2+q^2;M,m)+2A_0(m)),$$

$$T_2^{49-52} = 0,$$

$$T_1^{53,62} = \frac{m(c_7+2c_6\tau_3)B_{00}(q^2;M,M)}{4\pi^2 F^2 q^2},$$

$$T_2^{53,62} = 0,$$

$$T_1^{54,61} = -\frac{3(2c_6+c_7)g^2 m(\tau^3+1)}{64\pi^2 F^2(q^2)^2}\{(2m^2+q^2)(M^2 B_1(m^2+q^2;M,m)+2((m^2+q^2)B_{11}(m^2+q^2;M,m)$$
$$+B_{00}(m^2+q^2;M,m)))+M^2(-(4m^2+q^2))B_0(m^2+q^2;M,m)-2(3m^2+q^2)A_0(m)\},$$

$$T_2^{54,61} = 0,$$

$$T_1^{55,56} = \frac{c_4 m(\tau^3+1)B_{00}(q^2;M,M)}{8\pi^2 F^2 q^2},$$

$$T_2^{55,56} = 0,$$

$$T_1^{57,58} = \frac{(\tau^3 + 1)(c_6 m^2 A_0(M) + 3c_2 A_{00}(M))}{8\pi^2 F^2 m q^2},$$

$$T_2^{57,58} = -\frac{3c_2 m(\tau^3 + 1)A_{00}(M)}{2\pi^2 F^2 (q^2)^2},$$

$$T_1^{59,60} = -\frac{m(c_7 + 2c_6\tau_3)A_0(M)}{8\pi^2 F^2 q^2},$$

$$T_2^{59,60} = 0,$$

$$T_1^{63} = 0,$$

$$T_2^{63} = -\frac{3m^2(\tau^3 + 1)}{4\pi^2 F^2 m(q^2)^3}(2c_1 m^2 M^2 A_0(M) - A_{00}(M)(c_3 dm^2 + c_2(m^2 + q^2))),$$

$$T_1^{64} = -\frac{m}{4\pi^2 F^2}\{-2c_1 M^2(4(B_{11}^{(2,1)}(q^2; M, M) + B_1^{(2,1)}(q^2; M, M)) + B_0^{(2,1)}(q^2; M, M))$$
$$+ c_3(M^2(4(B_{11}^{(2,1)}(q^2; M, M) + B_1^{(2,1)}(q^2; M, M)) + B_0^{(2,1)}(q^2; M, M)) + 4B_{11}(q^2; M, M)$$
$$+ B_0(q^2; M, M) + 4B_1(q^2; M, M)) + c_2(B_{00}^{(2,1)}(q^2; M, M) + 4(B_{001}^{(2,1)}(q^2; M, M) + B_{0011}^{(2,1)}(q^2; M, M)))\},$$

$$T_2^{64} = \frac{2c_2 m}{\pi^2 F^2 q^2}B_{0000}^{(2,1)}(q^2; M, M),$$

$$T_1^{65,66} = -\frac{c_3 m(B_0(q^2; M, M) - 4B_{11}(q^2; M, M))}{4\pi^2 F^2},$$

$$T_2^{65,66} = -\frac{c_2 m}{\pi^2 F^2 q^2}B_{00}(q^2; M, M),$$

$$T_1^{67} = 0,$$

$$T_2^{67} = \frac{c_2 m}{4\pi^2 F^2 q^2}A_0(M). \tag{C3}$$

Contributions of tree diagrams to the elastic parts of $T_1(0, q^2)$ *and* $T_2(0, q^2)$:

$$T_{1,\text{el}}^1 = 0,$$

$$T_{2,\text{el}}^1 = 2m^2(\tau^3 + 1)\frac{1}{q^4},$$

$$T_{1,\text{el}}^{2-3} = m(2c_6 + c_7)(\tau^3 + 1)\frac{1}{q^2},$$

$$T_{2,\text{el}}^{2-3} = 0,$$

$$T_{1,\text{el}}^{4-5} = (\tau^3 + 1)(2d_7 + d_6),$$

$$T_{2,\text{el}}^{4-5} = -4m^2(\tau^3 + 1)(2d_7 + d_6)\frac{1}{q^2},$$

$$T_{1,\text{el}}^6 = (2c_6\tau^3 + c_7)^2\frac{q^2 + 4m^2}{4q^2},$$

$$T_{2,\text{el}}^6 = -m^2(2c_6\tau^3 + c_7)^2\frac{1}{q^2},$$

$$T_{1,\text{el}}^{34-35} = 2m(\tau^3 + 1)\frac{((2e_{54} + e_{74})q^2 - 4(2e_{105} + e_{106})M^2)}{q^2},$$

$$T_{2,\text{el}}^{34-35} = 0,$$

$$T_{1,\text{el}}^{36-37} = \frac{q^2}{2m}(2c^6\tau^3 + c_7)(d_6\tau^3 + 2d_7),$$

$$T_{2,\text{el}}^{36-37} = -2m(2c^6\tau^3 + c_7)(d_6\tau^3 + 2d_7). \tag{C4}$$

Contributions of $O(p^3)$ one-loop diagrams to the elastic parts of $T_1(0, q^2)$ and $T_2(0, q^2)$:

$$T_{1,\text{el}}^{18,19} = -\frac{m^2(\tau^3 + 1)g_A^2}{8\pi^2 F^2 q^2}\{B_0(m^2; m, M) + 2B_1(m^2; m, M) + M^2 C_0(m^2, m^2, q^2; M, m, M)$$
$$+ (2M^2 + q^2)C_2(m^2, m^2, q^2; M, m, M) + 2q^2 C_{22}(m^2, m^2, q^2; M, m, M)\},$$

$$T_{2,\text{el}}^{18,19} = \frac{m^2(\tau^3 + 1)g_A^2}{4\pi^2 F^2(q^2)^2}\{m^2(B_0(m^2; m, M) + B_1(m^2; m, M) - B_1(m^2; M, m)$$
$$+ (q^2 - 2M^2)C_1(m^2, m^2, q^2; M, m, M) + q^2 C_{11}(m^2, m^2, q^2; M, m, M)) + B_{00}(q^2; M, M)\},$$

$$T_{1,\text{el}}^{20-23} = 0,$$

$$T_{2,\text{el}}^{20-23} = -\frac{m^2(\tau^3 + 1)g_A^2(M^2 B_0(m^2; M, m) - 2m^2 B_1(m^2; M, m) + A_0(m) + A_0(M))}{8\pi^2 F^2(q^2)^2},$$

$$T_{1,\text{el}}^{24,25} = \frac{m^2(\tau^3 + 1)g_A^2}{8\pi^2 F^2 q^2}\{B_1(m^2; M, m) - B_1(q^2; m, m) + M^2(-C_2(m^2, q^2, m^2; M, m, m))$$
$$+ q^2 C_{22}(m^2, q^2, m^2; M, m, m)\},$$

$$T_{2,\text{el}}^{24,25} = -\frac{m^2(\tau^3 + 1)g_A^2}{16\pi^2 F^2(q^2)^2}\{2m^2(q^2(C_{22}(m^2, q^2, m^2; M, m, m) + 2C_{12}(m^2, q^2, m^2; M, m, m)$$
$$+ C_{11}(m^2, q^2, m^2; M, m, m)) - 2M^2(C_0(m^2, q^2, m^2; M, m, m) + C_2(m^2, q^2, m^2; M, m, m)$$
$$+ C_1(m^2, q^2, m^2; M, m, m))) + A_0(M)\},$$

$$T_{1,\text{el}}^{29-32} = 0,$$

$$T_{2,\text{el}}^{29-32} = \frac{m^2(\tau^3 + 1)(A_0(M) - 2B_{00}(q^2; M, M))}{4\pi^2 F^2(q^2)^2}. \tag{C5}$$

Contributions of $O(p^4)$ one-loop diagrams to the elastic parts of $T_1(0, q^2)$ and $T_2(0, q^2)$:

$$T_{1,\text{el}}^{43,44} = -\frac{mg_A^2(c_7\tau^3 + 2c_6)}{32\pi^2 F^2 q^2}\{4m^2(B_0(m^2; m, M) - B_0(m^2; M, m) + 2B_1(m^2; m, M)$$
$$+ q^2(4(C_{22}(m^2, m^2, q^2; M, m, M) + C_2(m^2, m^2, q^2; M, m, M)) + C_0(m^2, m^2, q^2; M, m, M)))$$
$$+ q^2(4B_{11}(q^2; M, M) + 3B_0(q^2; M, M) + 8B_1(q^2; M, M)) - 2A_0(M)\},$$

$$T_{2,\text{el}}^{43,44} = \frac{m^5 g_A^2(c_7\tau^3 + 2c_6)C_{11}(m^2, m^2, q^2; M, m, M)}{2\pi^2 F^2 q^2},$$

$$T_{1,\text{el}}^{45,47} = \frac{mg_A^2}{64\pi^2 F^2 q^2}\{c_7(8m^2(3B_1(m^2; M, m) + 2B_0(q^2; m, m) + 2M^2 C_0(m^2, q^2, m^2; M, m, m)$$
$$+ 4q^2 C_{22}(m^2, q^2, m^2; M, m, m)) + M^2(3\tau^3 - 1)B_0(m^2; M, m) + (3\tau^3 - 1)A_0(m))$$
$$+ 2c_6(4m^2(\tau^3 - 1)(3B_1(m^2; M, m) + 2B_0(q^2; m, m) + 2M^2 C_0(m^2, q^2, m^2; M, m, m)$$
$$+ 4q^2 C_{22}(m^2, q^2, m^2; M, m, m)) + M^2(1 - 3\tau^3)B_0(m^2; M, m) + (1 - 3\tau^3)A_0(m))\},$$

$$T_{2,\text{el}}^{45,47} = \frac{m^3 g_A^2 (c_6(\tau^3-1)+c_7)}{4\pi^2 F^2 (q^2)^2} \{2m^2 (B_1(m^2;M,m) - q^2(C_{22}(m^2,q^2,m^2;M,m,m)$$

$$+ 2C_{12}(m^2,q^2,m^2;M,m,m) + C_{11}(m^2,q^2,m^2;M,m,m))) + M^2 B_0(m^2;M,m) + A_0(m) - A_0(M)\},$$

$$T_{1,\text{el}}^{46,48} = -\frac{(2c_6-3c_7)m(\tau^3+1)g_A^2}{64\pi^2 F^2 q^2} \{2m^2 (3B_1(m^2;M,m) + 2B_0(q^2;m,m) + 2M^2 C_0(m^2,q^2,m^2;M,m,m)$$

$$+ 4q^2 C_{22}(m^2,q^2,m^2;M,m,m)) + M^2 B_0(m^2;M,m) + A_0(m)\},$$

$$T_{2,\text{el}}^{46,48} = \frac{(2c_6-3c_7)m^3(\tau^3+1)g_A^2}{16\pi^2 F^2 (q^2)^2} \{2m^2 (q^2(C_{22}(m^2,q^2,m^2;M,m,m) + 2C_{12}(m^2,q^2,m^2;M,m,m)$$

$$+ C_{11}(m^2,q^2,m^2;M,m,m)) - B_1(m^2;M,m)) - M^2 B_0(m^2;M,m) - A_0(m) + A_0(M)\},$$

$$T_{1,\text{el}}^{49-52} = -\frac{m g_A^2 (c_7\tau^3+2c_6)(M^2 B_0(m^2;M,m)+A_0(m))}{8\pi^2 F^2 q^2},$$

$$T_{2,\text{el}}^{49-52} = 0,$$

$$T_{1,\text{el}}^{53,62} = \frac{m(c_7+2c_6\tau_3)B_{00}(q^2;M,M)}{4\pi^2 F^2 q^2},$$

$$T_{2,\text{el}}^{53,62} = 0,$$

$$T_{1,\text{el}}^{55,56} = \frac{c_4 m(\tau^3+1)B_{00}(q^2;M,M)}{8\pi^2 F^2 q^2},$$

$$T_{2,\text{el}}^{55,56} = 0,$$

$$T_{1,\text{el}}^{57,58} = \frac{(\tau^3+1)(c_6 m^2 A_0(M) + 3c_2 A_{00}(M))}{8\pi^2 F^2 m q^2},$$

$$T_{2,\text{el}}^{57,58} = -\frac{3c_2 m(\tau^3+1)A_{00}(M)}{2\pi^2 F^2 (q^2)^2},$$

$$T_{1,\text{el}}^{59,60} = -\frac{m(c_7+2c_6\tau_3)A_0(M)}{8\pi^2 F^2 q^2},$$

$$T_{2,\text{el}}^{59,60} = 0. \tag{C6}$$

APPENDIX D: FINITE-VOLUME SUMS

$$\int_V \frac{d^n k}{(2\pi)^n} \frac{\{1, k^\mu, k^\mu k^\nu\}}{(k^2-m^2)^M} \equiv \tilde{\mathcal{A}}_{(M)}^{\{,\mu,\mu\nu\}}(m^2),$$

$$\int_V \frac{d^n k}{(2\pi)^n} \frac{\{1, k^\mu, k^\mu k^\nu, k^\mu k^\nu k^\alpha, k^\mu k^\nu k^\alpha k^\beta\}}{(k^2-m_1^2)^M((k-p)^2-m_2^2)^N} \equiv \tilde{\mathcal{B}}_{(M,N)}^{\{,\mu,\mu\nu,\mu\nu\alpha,\mu\nu\alpha\beta\}}(m_1,m_2;p),$$

$$\int_V \frac{d^n k}{(2\pi)^n} \frac{\{1, k^\mu, k^\mu k^\nu\}}{(k^2-m_1^2)^M((k-p)^2-m_2^2)^N((k-q)^2-m_3^2)^R} \equiv \tilde{\mathcal{C}}_{(M,N,R)}^{\{,\mu,\mu\nu\}}(m_1,m_2,m_3;p,q),$$

$$\int_V \frac{d^n k}{(2\pi)^n} \frac{\{1, k^\mu, k^\mu k^\nu\}}{(k^2-m_1^2)^M((k-p)^2-m_2^2)^N((k-q)^2-m_3^2)^R((k-r)^2-m_4^2)^S} \equiv \tilde{\mathcal{D}}_{(M,N,R,S)}^{\{,\mu,\mu\nu\}}(m_1,m_2,m_3,m_4;p,q,r). \tag{D1}$$

Here, $\int_V$ denotes an integral in the finite volume, which really is a sum. The calculation of these sums by using the Poisson formula is considered in Appendix E.

APPENDIX E: EVALUATION OF THE FINITE-VOLUME SUMS USING POISSON'S FORMULA

The calculation of finite-volume sums with the use of Poisson's formula is nowadays a standard procedure. For a detailed introduction, we refer the reader, e.g., to Ref. [85], and list only the final results here.

The following notations are used:

$$
\mathcal{D}x_n = \delta(1 - x_1 - \cdots - x_n)dx_1 \cdots dx_n,
$$

$$
\int \mathcal{D}x_n f(x_1, \ldots, x_n)
$$

$$
= \int_0^1 dx_1 \int_0^{1-x_1} dx_2 \cdots
$$

$$
\times \int_0^{1-\cdots-x_{n-2}} dx_{n-1} f(x_1, \ldots, x_{n-1}, 1 - x_1 - \cdots - x_{n-1}),
$$

$$(E1)$$

where $n^\mu = (0, \mathbf{n})$ is a unit spacelike vector, whose components take integer values. Further, $K_\nu(z)$ denote the modified Bessel functions of the second kind.

The finite-volume sums, which are displayed in Appendix D, contain an infinite-volume piece and finite-volume correction. The ultraviolet divergences are contained only in the former, while the latter is ultraviolet convergent and vanishes exponentially for large values of L. In order to ease the notation, we list only the finite-volume corrections. The following notation is used:

$$
\overline{\int}_V \frac{d^n k}{(2\pi)^n i} = \int_V \frac{d^n k}{(2\pi)^n i} - \int \frac{d^n k}{(2\pi)^n i}. \qquad (E2)
$$

The full list of the finite-volume sums entering the amplitude at $O(p^4)$ is given below. Note that in the expressions, which contain only nucleon propagators, the finite-volume corrections are extremely small [proportional to the factor $\exp(-mL)$] and can therefore be neglected. We shall indicate these quantities by writing ≈ 0 at the end. Also, note that the structure of the integrands, which appear in the infinite and in a finite volume, is in general different. This is related to the fact that Lorentz invariance is used in the infinite volume to reduce tensor integrals to scalar ones. Some factors in the denominator get canceled during this procedure. One cannot apply the same trick in a finite volume.

One factor in the denominator:

$$
I_1 = \overline{\int}_V \frac{d^n k}{(2\pi)^n i} \frac{1}{k^2 - m^2} = -\frac{m}{4\pi^2 L} \sum_{\mathbf{n} \neq 0} \frac{1}{|\mathbf{n}|} K_1(|\mathbf{n}|mL) \approx 0,
$$

$$(E3)$$

$$
I_2 = \overline{\int}_V \frac{d^n k}{(2\pi)^n i} \frac{1}{(k^2 - m^2)^2} = \frac{1}{8\pi^2} \sum_{\mathbf{n} \neq 0} K_0(|\mathbf{n}|mL) \approx 0,
$$

$$(E4)$$

$$
I_3 = \overline{\int}_V \frac{d^n k}{(2\pi)^n i} \frac{1}{k^2 - M^2} = -\frac{M}{4\pi^2 L} \sum_{\mathbf{n} \neq 0} \frac{1}{|\mathbf{n}|} K_1(|\mathbf{n}|ML),
$$

$$(E5)$$

$$
I_4 = \overline{\int}_V \frac{d^n k}{(2\pi)^n i} \frac{1}{(k^2 - M^2)^2} = \frac{1}{8\pi^2} \sum_{\mathbf{n} \neq 0} K_0(|\mathbf{n}|ML), \qquad (E6)
$$

$$
I_5^{\mu\nu} = \overline{\int}_V \frac{d^n k}{(2\pi)^n i} \frac{k^\mu k^\nu}{k^2 - M^2} = \frac{M^2}{4\pi^2 L^2} \sum_{\mathbf{n} \neq 0} \left\{ \frac{1}{\mathbf{n}^2} K_2(|\mathbf{n}|ML)g^{\mu\nu} + \frac{ML}{|\mathbf{n}|^3} K_3(|\mathbf{n}|ML)n^\mu n^\nu \right\}, \qquad (E7)
$$

$$
I_6^{\mu\nu} = \overline{\int}_V \frac{d^n k}{(2\pi)^n i} \frac{k^\mu k^\nu}{(k^2 - M^2)^2} = -\frac{M}{8\pi^2 L} \sum_{\mathbf{n} \neq 0} \left\{ \frac{1}{|\mathbf{n}|} K_1(|\mathbf{n}|ML)g^{\mu\nu} + \frac{ML}{\mathbf{n}^2} K_2(|\mathbf{n}|ML)n^\mu n^\nu \right\}. \qquad (E8)
$$

Two factors in the denominator:

$$
I_7 = \overline{\int}_V \frac{d^n k}{(2\pi)^n i} \frac{1}{(k^2 - m^2)((k - q)^2 - m^2)} = \frac{1}{8\pi^2} \sum_{\mathbf{n} \neq 0} \int_0^1 dx e^{iLx\mathbf{n}\mathbf{q}} K_0(|\mathbf{n}|L\sqrt{g}) \approx 0,
$$

$$
g = m^2 - x(1 - x)q^2.
$$

$$(E9)$$

$$
I_8 = \overline{\int}_V \frac{d^n k}{(2\pi)^n i} \frac{1}{(k^2 - m^2)((k - p)^2 - M^2)^2} = -\frac{L}{16\pi^2} \sum_{\mathbf{n} \neq 0} \int_0^1 dx x e^{iLx\mathbf{p}\mathbf{n}} \frac{|\mathbf{n}|}{\sqrt{g}} K_1(|\mathbf{n}|L\sqrt{g}),
$$

$$
g = (1 - x)m^2 + xM^2 - x(1 - x)p^2.
$$

$$(E10)$$

$$I_9 = \overline{\int}_V \frac{d^n k}{(2\pi)^n i} \frac{1}{(k^2 - m^2)^2((k-p)^2 - M^2)} = -\frac{L}{16\pi^2} \sum_{\mathbf{n} \neq 0} \int_0^1 dx (1-x) e^{iLx\mathbf{n}\mathbf{p}} \frac{|\mathbf{n}|}{\sqrt{g}} K_1(|\mathbf{n}|L\sqrt{g}),$$

$$g = (1-x)m^2 + xM^2 - x(1-x)p^2. \tag{E11}$$

$$I_{10} = \overline{\int}_V \frac{d^n k}{(2\pi)^n i} \frac{1}{(k^2 - m^2)^2((k-q)^2 - m^2)} = -\frac{L}{16\pi^2} \sum_{\mathbf{n} \neq 0} \int_0^1 dx (1-x) e^{iLx\mathbf{n}\mathbf{q}} \frac{|\mathbf{n}|}{\sqrt{g}} K_1(|\mathbf{n}|L\sqrt{g}) \approx 0,$$

$$g = m^2 - x(1-x)q^2. \tag{E12}$$

$$I_{11} = \overline{\int}_V \frac{d^n k}{(2\pi)^n i} \frac{1}{(k^2 - M^2)((k-p-q)^2 - m^2)} = \frac{1}{8\pi^2} \sum_{\mathbf{n} \neq 0} \int_0^1 dx\, e^{iL(1-x)\mathbf{n}(\mathbf{p+q})} K_0(|\mathbf{n}|L\sqrt{g}),$$

$$g = m^2(1-x) + M^2 x - x(1-x)(p+q)^2. \tag{E13}$$

$$I_{12} = \overline{\int}_V \frac{d^n k}{(2\pi)^n i} \frac{1}{(k^2 - M^2)((k-q)^2 - M^2)} = \frac{1}{8\pi^2} \sum_{\mathbf{n} \neq 0} \int_0^1 dx\, e^{iLx\mathbf{n}\mathbf{q}} K_0(|\mathbf{n}|L\sqrt{g}),$$

$$g = M^2 - x(1-x)q^2. \tag{E14}$$

$$I_{13} = \overline{\int}_V \frac{d^n k}{(2\pi)^n i} \frac{1}{(k^2 - m^2)((k-p)^2 - M^2)} = \frac{1}{8\pi^2} \sum_{\mathbf{n} \neq 0} \int_0^1 dx\, e^{iLx\mathbf{n}\mathbf{p}} K_0(|\mathbf{n}|L\sqrt{g}),$$

$$g = m^2(1-x) + M^2 x - x(1-x)p^2. \tag{E15}$$

$$I_{14}^\mu = \overline{\int}_V \frac{d^n k}{(2\pi)^n i} \frac{k^\mu}{(k^2 - m^2)((k-p)^2 - M^2)} = \frac{1}{8\pi^2} \sum_{\mathbf{n} \neq 0} \int_0^1 dx\, e^{iLx\mathbf{n}\mathbf{p}} \left\{ x p^\mu K_0(|\mathbf{n}|L\sqrt{g}) + i n^\mu \frac{\sqrt{g}}{|\mathbf{n}|} K_1(|\mathbf{n}|L\sqrt{g}) \right\},$$

$$g = m^2(1-x) + M^2 x - x(1-x)p^2. \tag{E16}$$

$$I_{15}^\mu = \overline{\int}_V \frac{d^n k}{(2\pi)^n i} \frac{k^\mu}{(k^2 - M^2)((k-p-q)^2 - m^2)}$$

$$= \frac{1}{8\pi^2} \sum_{\mathbf{n} \neq 0} \int_0^1 dx\, e^{iL(1-x)\mathbf{n}(\mathbf{p+q})} \left\{ (1-x)(p+q)^\mu K_0(|\mathbf{n}|L\sqrt{g}) + i n^\mu \frac{\sqrt{g}}{|\mathbf{n}|} K_1(|\mathbf{n}|L\sqrt{g}) \right\},$$

$$g = m^2(1-x) + M^2 x - x(1-x)(p+q)^2. \tag{E17}$$

$$I_{16}^\mu = \overline{\int}_V \frac{d^n k}{(2\pi)^n i} \frac{k^\mu}{(k^2 - M^2)^2((k-p)^2 - m^2)}$$

$$= -\frac{L}{16\pi^2} \sum_{\mathbf{n} \neq 0} \int_0^1 dx\, x\, e^{-iL(1-x)\mathbf{n}\mathbf{p}} \left\{ (1-x)p^\mu \frac{|\mathbf{n}|}{\sqrt{g}} K_1(|\mathbf{n}|L\sqrt{g}) - i n^\mu K_0(|\mathbf{n}|L\sqrt{g}) \right\},$$

$$g = m^2(1-x) + M^2 x - x(1-x)p^2. \tag{E18}$$

$$I_{17}^{\mu\nu} = \overline{\int}_V \frac{d^n k}{(2\pi)^n i} \frac{k^\mu k^\nu}{(k^2 - m^2)^2((k-q)^2 - m^2)}$$

$$= -\frac{1}{16\pi^2} \sum_{\mathbf{n} \neq 0} \int_0^1 dx (1-x) e^{iLx\mathbf{n}\mathbf{q}} \left\{ x^2 q_\mu q_\nu \frac{|\mathbf{n}|L}{\sqrt{g}} K_1(|\mathbf{n}|L\sqrt{g}) + ixL(q_\mu n_\nu + n_\mu q_\nu) K_0(|\mathbf{n}|L\sqrt{g}) \right.$$

$$\left. - n_\mu n_\nu \frac{L\sqrt{g}}{|\mathbf{n}|} K_1(|\mathbf{n}|L\sqrt{g}) - g_{\mu\nu} K_0(|\mathbf{n}|L\sqrt{g}) \right\},$$

$$g = m^2 - x(1-x)q^2. \tag{E19}$$

$$I_{18}^{\mu\nu} = \overline{\int}_V \frac{d^n k}{(2\pi)^n i} \frac{k^\mu k^\nu}{(k^2 - M^2)((k-p-q)^2 - m^2)}$$

$$= \frac{1}{8\pi^2} \sum_{\mathbf{n} \neq 0} \int_0^1 dx e^{iL(1-x)\mathbf{n}(\mathbf{p+q})} \left\{ (1-x)^2 (p+q)^\mu (p+q)^\nu K_0(|\mathbf{n}|L\sqrt{g}) - g^{\mu\nu} \frac{\sqrt{g}}{|\mathbf{n}|L} K_1(|\mathbf{n}|L\sqrt{g}) \right.$$

$$\left. + i((p+q)^\mu n^\nu + n^\mu (p+q)^\nu) \frac{(1-x)\sqrt{g}}{|\mathbf{n}|} K_1(|\mathbf{n}|L\sqrt{g}) - n^\mu n^\nu \frac{g}{|\mathbf{n}|^2} K_2(|\mathbf{n}|L\sqrt{g}) \right\},$$

$$g = m^2(1-x) + M^2 x - x(1-x)(p+q)^2. \tag{E20}$$

$$I_{19}^{\mu\nu} = \overline{\int}_V \frac{d^n k}{(2\pi)^n i} \frac{k^\mu k^\nu}{(k^2 - M^2)((k-q)^2 - M^2)}$$

$$= \frac{1}{8\pi^2} \sum_{\mathbf{n} \neq 0} \int_0^1 dx e^{iLx\mathbf{n}\mathbf{q}} \left\{ x^2 q^\mu q^\nu K_0(|\mathbf{n}|L\sqrt{g}) + \frac{ix\sqrt{g}}{|\mathbf{n}|} (q^\mu n^\nu + q^\nu n^\mu) K_1(|\mathbf{n}|L\sqrt{g}) \right.$$

$$\left. - g^{\mu\nu} \frac{\sqrt{g}}{L|\mathbf{n}|} K_1(|\mathbf{n}|L\sqrt{g}) - \frac{g}{|\mathbf{n}|^2} n^\mu n^\nu K_2(|\mathbf{n}|L\sqrt{g}) \right\},$$

$$g = M^2 - x(1-x)q^2. \tag{E21}$$

$$I_{20}^{\mu\nu} = \overline{\int}_V \frac{d^n k}{(2\pi)^n i} \frac{k^\mu k^\nu}{(k^2 - M^2)^2((k-q)^2 - M^2)}$$

$$= -\frac{1}{16\pi^2} \sum_{\mathbf{n} \neq 0} \int_0^1 dx x e^{-iL(1-x)\mathbf{n}\mathbf{q}} \left\{ \left((1-x)^2 q^\mu q^\nu \frac{|\mathbf{n}|}{\sqrt{g}} - \frac{\sqrt{g}}{|\mathbf{n}|} n^\mu n^\nu \right) L K_1(|\mathbf{n}|L\sqrt{g}) \right.$$

$$\left. - (g^{\mu\nu} + iL(1-x)(q^\mu n^\nu + n^\mu q^\nu)) K_0(|\mathbf{n}|L\sqrt{g}) \right\},$$

$$g = M^2 - x(1-x)q^2. \tag{E22}$$

$$I_{21}^{\mu\nu\alpha\beta} = \overline{\int}_V \frac{d^n k}{(2\pi)^n i} \frac{k^\mu k^\nu k^\alpha k^\beta}{(k^2 - M^2)^2((k-q)^2 - M^2)}$$

$$= -\frac{1}{16\pi^2} \sum_{\mathbf{n} \neq 0} \int_0^1 dx x e^{-iL(1-x)\mathbf{n}\mathbf{q}} \{ (1-x)^4 J_0^{\mu\nu\alpha\beta} + (1-x)^3 J_1^{\mu\nu\alpha\beta} + (1-x)^2 J_2^{\mu\nu\alpha\beta} + (1-x) J_3^{\mu\nu\alpha\beta} + J_4^{\mu\nu\alpha\beta} \},$$

$$J_0^{\mu\nu\alpha\beta} = q^\mu q^\nu q^\alpha q^\beta \frac{L|\mathbf{n}|}{\sqrt{g}} K_1(|\mathbf{n}|L\sqrt{g}),$$

$$J_1^{\mu\nu\alpha\beta} = (q^\mu q^\nu q^\alpha n^\beta + \text{perm})(-iL) K_0(|\mathbf{n}|L\sqrt{g}),$$

$$J_2^{\mu\nu\alpha\beta} = (q^\mu q^\nu g^{\alpha\beta} + \text{perm})(-K_0(|\mathbf{n}|L\sqrt{g})) + (q^\mu q^\nu n^\alpha n^\beta + \text{perm}) \left(-\frac{L\sqrt{g}}{|\mathbf{n}|} K_1(|\mathbf{n}|L\sqrt{g}) \right),$$

$$J_3^{\mu\nu\alpha\beta} = (q^\mu n^\nu g^{\alpha\beta} + \text{perm}) \left(\frac{i\sqrt{g}}{|\mathbf{n}|} K_1(|\mathbf{n}|L\sqrt{g}) \right) + (q^\mu n^\nu n^\alpha n^\beta + \text{perm}) \left(\frac{iLg}{\mathbf{n}^2} K_2(|\mathbf{n}|L\sqrt{g}) \right),$$

$$J_4^{\mu\nu\alpha\beta} = (g^{\mu\nu} g^{\alpha\beta} + \text{perm}) \left(\frac{\sqrt{g}}{L|\mathbf{n}|} K_1(|\mathbf{n}|L\sqrt{g}) \right) + (g^{\alpha\beta} n^\mu n^\nu + \text{perm}) \left(\frac{g}{\mathbf{n}^2} K_2(|\mathbf{n}|L\sqrt{g}) \right) + n^\mu n^\nu n^\alpha n^\beta \left(\frac{Lg^{3/2}}{|\mathbf{n}|^{3/2}} K_3(|\mathbf{n}|L\sqrt{g}) \right),$$

$$g = M^2 - x(1-x)q^2. \tag{E23}$$

In the above equations, "perm" stands for all permutations of the indices μ, ν, α, β.

Three factors in the denominator:

$$I_{22} = \overline{\int}_V \frac{d^n k}{(2\pi)^n i} \frac{1}{(k^2 - m^2)^2((k+p)^2 - M^2)((k-q)^2 - m^2)} = \frac{L^2}{32\pi^2} \sum_{\mathbf{n} \neq 0} \int \mathcal{D}x_3 e^{iL\mathbf{n}\mathbf{r}} \frac{\mathbf{n}^2}{g} K_2(|\mathbf{n}|L\sqrt{g})x_1,$$

$$g = (x_1 + x_3)m^2 + x_2 M^2 - x_1 x_2 p^2 - x_1 x_3 q^2 - x_2 x_3 (p+q)^2. \tag{E24}$$

$$I_{23} = \overline{\int}_V \frac{d^n k}{(2\pi)^n i} \frac{1}{(k^2 - m^2)((k+p)^2 - M^2)((k-q)^2 - m^2)} = -\frac{1}{16\pi^2} \sum_{\mathbf{n} \neq 0} \int \mathcal{D}x_3 e^{iL\mathbf{n}\mathbf{r}} \frac{|\mathbf{n}|L}{\sqrt{g}} K_1(|\mathbf{n}|L\sqrt{g}),$$

$$g = (x_1 + x_3)m^2 + x_2 M^2 - x_1 x_2 p^2 - x_1 x_3 q^2 - x_2 x_3 (p+q)^2. \tag{E25}$$

$$I_{24}^{\mu\nu} = \overline{\int}_V \frac{d^n k}{(2\pi)^n i} \frac{k^\mu k^\nu}{(k^2 - m^2)((k-p)^2 - M^2)((k-q)^2 - m^2)}$$

$$= -\frac{1}{16\pi^2} \sum_{\mathbf{n} \neq 0} \int \mathcal{D}x_3 e^{iL\mathbf{n}\mathbf{r}} \left\{ \frac{|\mathbf{n}|L}{\sqrt{g}} r^\mu r^\nu K_1(|\mathbf{n}|L\sqrt{g}) + iL(r^\mu n^\nu + n^\mu r^\nu) K_0(|\mathbf{n}|L\sqrt{g}) - g^{\mu\nu} K_0(|\mathbf{n}|L\sqrt{g}) \right.$$

$$\left. - \frac{L\sqrt{g}}{|\mathbf{n}|} n^\mu n^\nu K_1(|\mathbf{n}|L\sqrt{g}) \right\},$$

$$r^\mu = x_2 q^\mu + x_3 p^\mu,$$

$$g = (x_1 + x_2)m^2 + x_3 M^2 - x_3 x_1 p^2 - x_2 x_1 q^2 - x_2 x_3 (p-q)^2. \tag{E26}$$

$$I_{25}^{\mu\nu} = \overline{\int}_V \frac{d^n k}{(2\pi)^n i} \frac{k^\mu k^\nu}{(k^2 - M^2)^2((k+p)^2 - m^2)((k-q)^2 - M^2)}$$

$$= \frac{L^2}{32\pi^2} \sum_{\mathbf{n} \neq 0} \int \mathcal{D}x_3 x_1 e^{iL\mathbf{n}\mathbf{r}} \left\{ r^\mu r^\nu \frac{\mathbf{n}^2}{g} K_2(|\mathbf{n}|L\sqrt{g}) + i(r^\mu n^\nu + n^\mu r^\mu) \frac{|\mathbf{n}|}{\sqrt{g}} K_1(|\mathbf{n}|L\sqrt{g}) \right.$$

$$\left. - g^{\mu\nu} \frac{|\mathbf{n}|}{L\sqrt{g}} K_1(|\mathbf{n}|L\sqrt{g}) - n^\mu n^\nu K_0(|\mathbf{n}|L\sqrt{g}) \right\},$$

$$r_\mu = x_3 q_\mu - x_2 p_\mu,$$

$$g = (x_1 + x_3)M^2 + x_2 m^2 - x_1 x_2 p^2 - x_1 x_3 q^2 - x_2 x_3 (p+q)^2. \tag{E27}$$

$$I_{26}^{\mu\nu} = \overline{\int}_V \frac{d^n k}{(2\pi)^n i} \frac{k^\mu k^\nu}{(k^2 - m^2)^2((k+p)^2 - M^2)((k-q)^2 - m^2)}$$

$$= \frac{L^2}{32\pi^2} \sum_{\mathbf{n} \neq 0} \int \mathcal{D}x_3 e^{iL\mathbf{n}\mathbf{r}} x_1 \left\{ \frac{\mathbf{n}^2}{g} r_\mu r_\nu K_2(|\mathbf{n}|L\sqrt{g}) + i(r_\mu n_\nu + n_\mu r_\nu) \frac{|\mathbf{n}|}{\sqrt{g}} K_1(|\mathbf{n}|L\sqrt{g}) \right.$$

$$\left. - g_{\mu\nu} \frac{|\mathbf{n}|}{L\sqrt{g}} K_1(|\mathbf{n}|L\sqrt{g}) - n_\mu n_\nu K_0(|\mathbf{n}|L\sqrt{g}) \right\},$$

$$r^\mu = x_3 q^\mu - x_2 p^\mu,$$

$$g = (x_1 + x_3)m^2 + x_2 M^2 - x_1 x_2 p^2 - x_1 x_3 q^2 - x_2 x_3 (p+q)^2. \tag{E28}$$

$$I_{27}^{\mu\nu} = \overline{\int}_V \frac{d^n k}{(2\pi)^n i} \frac{k^\mu k^\nu}{(k^2 - M^2)((k+p)^2 - m^2)((k-q)^2 - M^2)}$$

$$= -\frac{1}{16\pi^2} \sum_{\mathbf{n} \neq 0} \int \mathcal{D}x_3 e^{iL\mathbf{n}\mathbf{r}} \left\{ r^\mu r^\nu \frac{|\mathbf{n}|L}{\sqrt{g}} K_1(|\mathbf{n}|L\sqrt{g}) + iL(r^\mu n^\nu + n^\mu r^\nu) K_0(|\mathbf{n}|L\sqrt{g}) \right.$$

$$\left. - g^{\mu\nu} K_0(|\mathbf{n}|L\sqrt{g}) - n^\mu n^\nu \frac{L\sqrt{g}}{|\mathbf{n}|} K_1(|\mathbf{n}|L\sqrt{g}) \right\},$$

$$r^\mu = x_3 q^\mu - x_2 p^\mu,$$

$$g = (x_1 + x_3)M^2 + x_2 m^2 - x_1 x_2 p^2 - x_1 x_3 q^2 - x_2 x_3 (p+q)^2. \tag{E29}$$

$$I_{28}^{\mu\nu} = \overline{\int}_V \frac{d^n k}{(2\pi)^n i} \frac{k_\mu k_\nu}{(k^2 - m^2)((k+p)^2 - M^2)((k-q)^2 - m^2)}$$

$$= -\frac{1}{16\pi^2} \sum_{\mathbf{n} \neq 0} \int \mathcal{D}x_3 e^{iL\mathbf{n}\mathbf{r}} \left\{ r^\mu r^\nu \frac{|\mathbf{n}|L}{\sqrt{g}} K_1(|\mathbf{n}|L\sqrt{g}) + iL(r^\mu n^\nu + n^\mu r^\nu) K_0(|\mathbf{n}|L\sqrt{g}) \right.$$

$$\left. - g^{\mu\nu} K_0(|\mathbf{n}|L\sqrt{g}) - n^\mu n^\nu \frac{\sqrt{g}L}{|\mathbf{n}|} K_1(|\mathbf{n}|L\sqrt{g}) \right\},$$

$$r^\mu = x_3 q^\mu - x_2 p^\mu,$$

$$g = (x_1 + x_3)m^2 + x_2 M^2 - x_1 x_2 p^2 - x_1 x_3 q^2 - x_2 x_3 (p+q)^2. \tag{E30}$$

Four factors in the denominator:

$$I_{29}^{\mu\nu} = \overline{\int}_V \frac{d^n k}{(2\pi)^n i} \frac{k^\mu k^\nu}{(k^2 - m^2)((k-p)^2 - M^2)((k-q)^2 - m^2)((k-p-q)^2 - M^2)}$$

$$= \frac{L^2}{32\pi^2} \sum_{\mathbf{n} \neq 0} \int \mathcal{D}x_4 e^{iL\mathbf{n}\mathbf{r}} \left\{ r^\mu r^\nu \frac{\mathbf{n}^2}{g} K_2(|\mathbf{n}|L\sqrt{g}) + i(r^\mu n^\nu + n^\mu r^\nu) \frac{|\mathbf{n}|}{\sqrt{g}} K_1(|\mathbf{n}|L\sqrt{g}) \right.$$

$$\left. - g^{\mu\nu} \frac{|\mathbf{n}|}{L\sqrt{g}} K_1(|\mathbf{n}|L\sqrt{g}) - n^\mu n^\nu K_0(|\mathbf{n}|L\sqrt{g}) \right\},$$

$$r^\mu = (x_2 + x_4)p^\mu + (x_3 + x_4)q^\mu,$$

$$g = (x_1 + x_3)m^2 + (x_2 + x_4)M^2 + ((x_2 + x_4)p + (x_3 + x_4)q)^2 - x_2 p^2 - x_3 q^2 - x_4 (p+q)^2. \tag{E31}$$

[1] X. Ji, Phys. Rev. Lett. **110**, 262002 (2013).

[2] K. F. Liu and S. J. Dong, Phys. Rev. Lett. **72**, 1790 (1994).

[3] K. F. Liu, Phys. Rev. D **62**, 074501 (2000).

[4] J. Liang, T. Draper, K.-F. Liu, A. Rothkopf, and Y.-B. Yang (XQCD Collaboration), Phys. Rev. D **101**, 114503 (2020).

[5] H. Fukaya, S. Hashimoto, T. Kaneko, and H. Ohki, Phys. Rev. D **102**, 114516 (2020).

[6] J. Liang *et al.* (χQCD Collaboration), *Proc. Sci.*, LAT-TICE2019 (2020) 046 [arXiv:2008.12389].

[7] R. Horsley, R. Millo, Y. Nakamura, H. Perlt, D. Pleiter, P. E. L. Rakow, G. Schierholz, A. Schiller, F. Winter, and J. M. Zanotti (QCDSF and UKQCD Collaborations), Phys. Lett. B **714**, 312 (2012).

[8] A. Chambers *et al.* (CSSM and QCDSF/UKQCD Collaborations), Phys. Rev. D **90**, 014510 (2014).

[9] A. Chambers, R. Horsley, Y. Nakamura, H. Perlt, D. Pleiter, P. Rakow, G. Schierholz, A. Schiller, H. Stüben, R. Young, and J. Zanotti, Phys. Rev. D **92**, 114517 (2015).

[10] A. Chambers, R. Horsley, Y. Nakamura, H. Perlt, P. Rakow, G. Schierholz, A. Schiller, K. Somfleth, R. Young, and J. Zanotti, Phys. Rev. Lett. **118**, 242001 (2017).

[11] K. U. Can, A. Hannaford-Gunn, R. Horsley, Y. Nakamura, H. Perlt, P. E. L. Rakow, G. Schierholz, K. Y. Somfleth, H. Stüben, R. D. Young, and J. M. Zanotti, Phys. Rev. D **102**, 114505 (2020).

[12] A. Agadjanov, U.-G. Meißner, and A. Rusetsky, Phys. Rev. D **95**, 031502 (2017).

[13] A. Agadjanov, U.-G. Meißner, and A. Rusetsky, Phys. Rev. D **99**, 054501 (2019).

[14] H. W. Lin *et al.*, Prog. Part. Nucl. Phys. **100**, 107 (2018).

[15] M. J. Savage, P. E. Shanahan, B. C. Tiburzi, M. L. Wagman, F. Winter, S. R. Beane, E. Chang, Z. Davoudi, W. Detmold, and K. Orginos, Phys. Rev. Lett. **119**, 062002 (2017).

[16] E. Chang, W. Detmold, K. Orginos, A. Parreño, M. J. Savage, B. C. Tiburzi, and S. R. Beane (NPLQCD Collaboration), Phys. Rev. D **92**, 114502 (2015).

[17] W. Detmold, B. Tiburzi, and A. Walker-Loud, Phys. Rev. D **73**, 114505 (2006).

[18] Z. Davoudi and W. Detmold, Phys. Rev. D **92**, 074506 (2015).

[19] J. Hu, F. J. Jiang, and B. C. Tiburzi, Phys. Rev. D **77**, 014502 (2008).

[20] C. E. Carlson and M. Vanderhaeghen, Phys. Rev. A **84**, 020102 (2011).

[21] W. Cottingham, Ann. Phys. (N.Y.) **25**, 424 (1963).

[22] J. Gasser and H. Leutwyler, Nucl. Phys. **B94**, 269 (1975).

[23] A. Walker-Loud, C. E. Carlson, and G. A. Miller, Phys. Rev. Lett. **108**, 232301 (2012).

[24] J. Gasser, M. Hoferichter, H. Leutwyler, and A. Rusetsky, Eur. Phys. J. C **75**, 375 (2015).

[25] F. Erben, P. Shanahan, A. Thomas, and R. Young, Phys. Rev. C **90**, 065205 (2014).

[26] A. W. Thomas, X. G. Wang, and R. D. Young, Phys. Rev. C **91**, 015209 (2015).

[27] J. Gasser, H. Leutwyler, and A. Rusetsky, Phys. Lett. B **814**, 136087 (2021).

[28] J. Gasser, H. Leutwyler, and A. Rusetsky, Eur. Phys. J. C **80**, 1121 (2020).

[29] M. Elitzur and H. Harari, Ann. Phys. (N.Y.) **56**, 81 (1970).

[30] H. Leutwyler, *Proc. Sci.*, CD15 (2015) 022 [arXiv:1510.07511].

[31] M. Hoferichter, *Proc. Sci.*, CD2018 (2019) 028.

[32] D. Drechsel, B. Pasquini, and M. Vanderhaeghen, Phys. Rep. **378**, 99 (2003).

[33] J. M. Alarcón, V. Lensky, and V. Pascalutsa, Eur. Phys. J. C **74**, 2852 (2014).

[34] S. Scherer, A. Korchin, and J. Koch, Phys. Rev. C **54**, 904 (1996).

[35] L. Lellouch and M. Lüscher, Commun. Math. Phys. **219**, 31 (2001).

[36] M. T. Hansen and S. R. Sharpe, Phys. Rev. D **86**, 016007 (2012).

[37] R. A. Briceño and Z. Davoudi, Phys. Rev. D **88**, 094507 (2013).

[38] R. A. Briceño, M. T. Hansen, and A. Walker-Loud, Phys. Rev. D **91**, 034501 (2015).

[39] R. A. Briceño and M. T. Hansen, Phys. Rev. D **92**, 074509 (2015).

[40] V. Bernard, D. Hoja, U.-G. Meißner, and A. Rusetsky, J. High Energy Phys. 09 (2012) 023.

[41] A. Agadjanov, V. Bernard, U.-G. Meißner, and A. Rusetsky, Nucl. Phys. **B886**, 1199 (2014).

[42] A. Agadjanov, V. Bernard, U.-G. Meißner, and A. Rusetsky, Nucl. Phys. **B910**, 387 (2016).

[43] R. A. Briceño, Z. Davoudi, M. T. Hansen, M. R. Schindler, and A. Baroni, Phys. Rev. D **101**, 014509 (2020).

[44] D. Agadjanov, M. Döring, M. Mai, U.-G. Meißner, and A. Rusetsky, J. High Energy Phys. 06 (2016) 043.

[45] M. T. Hansen, H. B. Meyer, and D. Robaina, Phys. Rev. D **96**, 094513 (2017).

[46] J. Bulava and M. T. Hansen, Phys. Rev. D **100**, 034521 (2019).

[47] J. Gasser and H. Leutwyler, Ann. Phys. (N.Y.) **158**, 142 (1984).

[48] N. Fettes, U.-G. Meißner, M. Mojžiš, and S. Steininger, Ann. Phys. (N.Y.) **283**, 273 (2000); **288**, 249(E) (2001).

[49] D. Djukanovic, Ph.D thesis, University of Mainz, 2008.

[50] S. Weinberg, Nucl. Phys. **B363**, 3 (1991).

[51] G. Ecker, Prog. Part. Nucl. Phys. **35**, 1 (1995).

[52] J. Gegelia and G. Japaridze, Phys. Rev. D **60**, 114038 (1999).

[53] T. Fuchs, J. Gegelia, G. Japaridze, and S. Scherer, Phys. Rev. D **68**, 056005 (2003).

[54] M. L. Du, F. K. Guo, and U.-G. Meißner, J. Phys. G **44**, 014001 (2017).

[55] M. L. Du, F. K. Guo, and U.-G. Meißner, J. High Energy Phys. 10 (2016) 122.

[56] E. E. Jenkins and A. V. Manohar, Phys. Lett. B **255**, 558 (1991).

[57] V. Bernard, N. Kaiser, J. Kambor, and U.-G. Meißner, Nucl. Phys. **B388**, 315 (1992).

[58] R. Mertig, M. Bohm, and A. Denner, Comput. Phys. Commun. **64**, 345 (1991).

[59] V. Shtabovenko, R. Mertig, and F. Orellana, Comput. Phys. Commun. **207**, 432 (2016).

[60] H. H. Patel, Comput. Phys. Commun. **218**, 66 (2017).

[61] See Supplemental Material at http://link.aps.org/supplemental/10.1103/PhysRevD.103.034507 for the results given in Appendices B and C for generic ν.

[62] T. Becher and H. Leutwyler, J. High Energy Phys. 06 (2001) 017.

[63] U.-G. Meißner, *Proc. Sci.*, LAT2005 (2006) 009 [arXiv:hep-lat/0509029].

[64] H. Krebs, A. Gasparyan, and E. Epelbaum, Phys. Rev. C **85**, 054006 (2012).

[65] M. Hoferichter, J. Ruiz de Elvira, B. Kubis, and U.-G. Meißner, Phys. Rep. **625**, 1 (2016).

[66] T. Fuchs, J. Gegelia, and S. Scherer, J. Phys. G **30**, 1407 (2004).

[67] B. Kubis and U.-G. Meißner, Nucl. Phys. **A679**, 698 (2001).

[68] V. Bernard, N. Kaiser, and U.-G. Meißner, Phys. Rev. Lett. **67**, 1515 (1991).

[69] J. A. Melendez, R. J. Furnstahl, H. W. Grießhammer, J. A. McGovern, D. R. Phillips, and M. T. Pratola, arXiv:2004.11307.

[70] J. A. McGovern, D. R. Phillips, and H. W. Grießhammer, Eur. Phys. J. A **49**, 12 (2013).

[71] L. S. Myers *et al.* (COMPTON@MAX-lab Collaboration), Phys. Rev. Lett. **113**, 262506 (2014).

[72] V. O. de León *et al.*, Eur. Phys. J. A **10**, 207 (2001).

[73] M. I. Levchuk and A. I. L'vov, Nucl. Phys. **A674**, 449 (2000).

[74] P. A. Zyla *et al.* (Particle Data Group), Prog. Theor. Exp. Phys. **2020**, 083C01 (2020).

[75] R. Bignell, W. Kamleh, and D. Leinweber, Phys. Rev. D **101**, 094502 (2020).

[76] V. Bernard, N. Kaiser, and U.-G. Meißner, Nucl. Phys. **B373**, 346 (1992).

[77] J. M. Alarcón, F. Hagelstein, V. Lensky, and V. Pascalutsa, Phys. Rev. D **102**, 014006 (2020).

[78] V. Bernard, N. Kaiser, A. Schmidt, and U.-G. Meißner, Phys. Lett. B **319**, 269 (1993).

[79] M. C. Birse and J. A. McGovern, Eur. Phys. J. A **48**, 120 (2012).

[80] V. Bernard, N. Kaiser, U.-G. Meißner, and A. Schmidt, Z. Phys. A **348**, 317 (1994).

[81] D. Nevado and A. Pineda, Phys. Rev. C **77**, 035202 (2008).

[82] C. Peset and A. Pineda, Nucl. Phys. **B887**, 69 (2014).

[83] O. Tomalak, Eur. Phys. J. Plus **135**, 411 (2020).

[84] G. Devaraj and R. G. Stuart, Nucl. Phys. **B519**, 483 (1998).

[85] J. Bijnens, E. Boström, and T. A. Lähde, J. High Energy Phys. 01 (2014) 019.

Resonance form factors

Summary

The content of this chapter is based on the publication

- Lozano, J., Meißner, UG., Romero-López, F., Rusetsky, A., Schierholz, G. Resonance form factors from finite-volume correlation functions with the external field method. *J. High Energ. Phys.* **2022**, 106 (2022).

It is well-known that the decay matrix element of an unstable state, calculated in the framework of lattice QCD, has an ill-defined limit at $L \to \infty$ (here, L is the spacial extension of a cubic lattice). In the case of the so-called resonance form factors, this irregular behavior persists even after multiplying each external leg with the pertinent Lellouch-Lüscher factor and arises from the so-called triangle diagram, in which one of the resonance constituents couples to an external current while the other propagates without interacting with such a field. For simplicity, the case of a resonance that arises from the scattering of two particles is considered here.

In this work, we proposed a novel method to tackle this problem, in which the difficulty, related to the presence of the triangle diagram, is circumnavigated. The approach is based on the study of two-particle scattering in a static, spatially periodic external field by using a generalization of the Lüscher method in the presence of such a field. In addition, it was demonstrated that the resonance form factor in the Breit frame is given by the derivative of a resonance pole position in the complex plane with respect to the coupling constant of the external field. This result is a generalization of the well-known Feynman-Hellmann theorem for the form factor of a stable particle.

To achieve this, we made use of the non-relativistic effective field theory (NREFT), which is well suited to study the case at hand, where the two-particle system, from which the resonance emerges, is under investigation. An advantage of this framework is that the number of diagrams needed to determine the resonance form factor is drastically reduced. This simplifies the calculations considerably and allows for a rather straightforward computation of the form factor for both the one- and two-particle cases. Moreover, the couplings of the NREFT Lagrangian are related to already known quantities, such as the scattering phase shift and the single-particle form factor. At lowest order, there exists one coupling in the Lagrangian that has to be fitted to the data. We demonstrated that determining such a coupling on the lattice is equivalent to extracting the resonance form factor. To this end, we have first derived the Lüscher equation in the presence of an external field. The unknown

coupling is determined by solving this equation. This procedure allows one to extract the parameter from the finite-volume two-particle energy spectrum. Next, an expression for the resonance form factor can be evaluated in the infinite volume. The only piece missing to fully evaluate the derived form factor is the one that was previously fitted to the data. In this way, the resonance form factor can be fully calculated as no other quantities are needed for its determination.

We have also made an attempt to extend the already-known result that relates the form factor and the mass of a stable particle. In collaboration with Romero-Lopez F., the author of this thesis was responsible of carrying out this task. In the case at hand, the complex pole position of the resonance will play the role of the particle mass. The position of such a pole can be obtained by solving the previously-derived Lüscher equation in the presence of an external field with the extracted values of the couplings in the infinite volume. We showed that, for the case of a resonance in the Breit frame, taking the derivative of the pole position with respect to the coupling of the external field, one can obtain the form factor. This finding extends the Feynman-Hellmann theorem to the case of resonances.

The results of this work can be summarized as follows:

- A generalization of the Lüscher equation in the presence of an external field is obtained.

- Based on the above equation, a procedure for the extraction of the resonance form factor from lattice calculations of the two-particle spectrum in the external field is formulated.

- Additionally, the Feynman-Hellmann theorem is extended to the case of unstable particles.

Resonance form factors from finite-volume correlation functions with the external field method

Jonathan Lozano,[a] Ulf-G. Meißner,[a,b,c] Fernando Romero-López,[d] Akaki Rusetsky[a,c] and Gerrit Schierholz[e]

[a] *Helmholtz-Institut für Strahlen- und Kernphysik (Theorie) and*
Bethe Center for Theoretical Physics, Universität Bonn,
53115 Bonn, Germany

[b] *Institute for Advanced Simulation and Institut für Kernphysik, Forschungszentrum Jülich,*
D-52425 Jülich, Germany

[c] *Tbilisi State University,*
0186 Tbilisi, Georgia

[d] *Center for Theoretical Physics, Massachusetts Institute of Technology,*
Cambridge, MA 02139, U.S.A.

[e] *Deutsches Elektronen-Synchrotron DESY,*
Notkestr. 85, 22607 Hamburg, Germany

E-mail: lozano@hiskp.uni-bonn.de, meissner@hiskp.uni-bonn.de,
fernando@mit.edu, rusetsky@hiskp.uni-bonn.de,
gerrit.schierholz@desy.de

ABSTRACT: A novel method for the extraction of form factors of unstable particles on the lattice is proposed. The approach is based on the study of two-particle scattering in a static, spatially periodic external field by using a generalization of the Lüscher method in the presence of such a field. It is shown that the resonance form factor is given by the derivative of the resonance pole position in the complex plane with respect to the coupling constant to the external field. Unlike the standard approach, this proposal does not suffer from problems caused by the presence of the triangle diagram.

Contents

1   Introduction

The study of the form factors of unstable particles from lattice field theory provides plenty of information about the structure of these particles. This study is however complicated by a non-trivial mapping of the results of lattice calculations — performed in a finite volume — onto the relevant infinite-volume form factors.[1]

Such a mapping is rather trivial in case of a stable particle. Namely, let $|p\rangle$ be an infinite-volume state, which describes a single particle moving with the on-shell momentum p^μ. The infinite-volume form factor $\langle p|J(0)|q\rangle$ is defined as the matrix element of some current $J(x)$ between one-particle states (in order to ease the notations, we consider the

---

[1]Discretization effects are neglected throughout this paper.

spinless particles and the scalar currents here). Due to the Lorentz-invariance, the form factor is a function of a single variable $t = (p - q)^2$. Furthermore, on the lattice, the spectrum contains the one-particle states $|p\rangle_L$. Here, L denotes the spatial extension of a cubic lattice, while, for simplicity, the time extension is assumed to be infinite. The finite-volume form factor is given by the matrix element between these states, $\langle p|J(0)|q\rangle_L$. Then, in the limit $L \to \infty$, one has

$$\langle p|J(0)|q\rangle_L = \langle p|J(0)|q\rangle + O(e^{-\mu L}), \tag{1.1}$$

where μ is a characteristic mass scale — typically a multiple of the mass of lightest particle in the system. Furthermore, recall that three-momenta in a finite volume are discretized, $\mathbf{p} = (2\pi/L)\,\mathbf{n}$ and $\mathbf{n} \in \mathbb{Z}^3$. Hence, in order to have a fixed $\mathbf{p}$ in infinite volume, one cannot keep $\mathbf{n}$ constant. One could, for example, choose a monotonic sequence of discrete values of $L \in \{L_i\}$, such that $\mathbf{p}$ and $\mathbf{q}$ are allowed finite-volume momenta. Equation (1.1) must be interpreted exactly in this sense.

The situation is far less trivial in case of unstable particles. First, a one-particle state describing a resonance does not exist in the infinite-volume spectrum. Let us, for simplicity, consider a situation in which the resonance emerges in the scattering of two identical spinless particles. In order to define the resonance form factor in the infinite volume, one has to start from the five-point Green function $\langle p_1, p_2; out|J(0)|q_1, q_2; in\rangle$. Defining the total momenta of the outgoing and incoming particle pair by $P = p_1 + p_2$ and $Q = q_1 + q_2$, respectively, it can be shown that, if a resonance in a given channel exists, this five-point function possesses a double pole in the complex plane,

$$\langle p_1, p_2; out|J(0)|q_1, q_2; in\rangle \sim \frac{1}{(M_R^2 - P^2)(M_R^2 - Q^2)}, \tag{1.2}$$

located on some unphysical Riemann sheet for the variables P^2, Q^2. The infinite-volume resonance form factor can be expressed through the residue at this double pole (for more details, see e.g, ref. [1]). This (complex-valued) form factor is a function of a single variable $t = (P - Q)^2$ and, in case of the conserved currents, obeys the usual Ward identities — for example, it is properly normalized at $t = 0$.

In a finite volume, one can access the spectrum of a Hamiltonian having the quantum number of two particle states. Let us denote the eigenstates of the Hamiltonian by $|\alpha, \mathbf{P}\rangle_L$ (the so-called scattering states). Here, $\mathbf{P}$ is the total three-momentum of two particles and α labels different states having the same $\mathbf{P}$. If one varies L while keeping the $\mathbf{P}$ constant, the energies $E_\alpha(\mathbf{P}, L)$ exhibit power-law corrections in L with respect to the sum of the energies of one-particle states. Furthermore, one can evaluate the matrix elements of a current $\langle \alpha, \mathbf{P}|J(0)|\beta, \mathbf{Q}\rangle_L$ on the lattice for any α, β. Interpreting an infinite-volume limit of such a matrix element, as well as performing the analytic continuation to the resonance pole is however a delicate task. As in case of a stable particle, the momenta $\mathbf{P}, \mathbf{Q}$ are discretized and the limit $L \to \infty$ has to be treated accordingly (namely, the pertinent integer vectors $\mathbf{n}, \mathbf{m}$ cannot be considered fixed, see the discussion above). Furthermore, even for a fixed $\mathbf{P}$, the eigenvalues $E_\alpha(\mathbf{P}, L)$ collapse toward the threshold, as $L \to \infty$. Therefore, in order to stay in the vicinity of a fixed infinite-volume center-of-mass (CM)

energy E (or, equivalently, $E_\alpha(\mathbf{P}, L) \simeq \sqrt{E^2 + \mathbf{P}^2}$), one cannot treat α as fixed anymore.[2] Higher excited states should be considered in the limit $L \to \infty$ and fixed E.

After fixing carefully the kinematics, one might ask oneself, how the infinite-volume limit should be carried out in the matrix elements. For instance, it is well known that the corrections are no more exponentially suppressed for unstable particles. Even for a much simpler case of the finite-volume decay matrix element of an unstable state, this limit is not well defined mathematically and can be performed only after removing the factor that corresponds to the interactions of the decay products in the final state, the well-known the Lellouch-Lüscher factor [3]. This approach works perfectly for the transition form factors of resonances into stable states, as well as for timelike form factors of stable particles, see [4–13]. Recently, a three-particle analog of the Lellouch-Lüscher formula has been also derived [14, 15]. The situation, however, becomes more complicated in case of the resonance matrix elements which is studied in the present paper. The problem is that, even after explicitly removing the Lellouch-Lüscher factors that correspond to the unstable particles, the remaining expression still does not exhibit a regular behavior in L and, hence, the infinite-volume limit cannot be performed [1, 16–18]. Additional developments concerning the evaluation of the resonance matrix elements can be found in refs. [2, 19, 20].

To summarize the findings of refs. [1, 16–18], a consistent procedure for the analytic continuation of the obtained result into the complex plane, which is needed to define a resonance form factor rigorously, cannot be straightforwardly formulated for the whole finite-volume matrix element. The culprit is the so-called triangle diagram, in which one of the "constituent particles" of a resonance couples to the external current J, whereas the second acts as a spectator, see figure 1a (for simplicity, we consider the resonance emerging in two-particle scattering). Such a triangle diagram is more singular in the finite volume than a loop diagram with two propagators, which corresponds to the Lüscher zeta-function. In refs. [1, 16–18] the problem was addressed in different frameworks, but from a very similar physics perspective. Schematically, the proper procedure could be described as follows. It is proposed to single out the contribution of the triangle diagram in a finite volume. The infinite-volume limit and the analytic continuation in the remainder of the amplitude can be performed without further ado. The triangle contribution, calculated analytically in the infinite volume and at the resonance pole, can be added back at the final stage. Even if the above procedure is absolutely consistent, the necessity of subtracting/adding the triangle diagram, to our taste, may turn the extraction of the resonance form factors into quite a challenging endeavor, with hard-to-control systematic errors.

On the other hand, the Feynman-Hellmann theorem [21, 22] has been successfully used to compute form factors of *stable* hadrons in a static, spatially periodic external field [23].[3]

---

[2]Note that in ref. [2], the finite-volume matrix elements at a fixed α, β are considered. For instance, the ground-state matrix element can be expanded in $1/L$, which gives only access to the form factor at zero-momentum transfer. By contrast, matrix elements at fixed energy have irregular behavior as a function of L, "jumping" over the poles of the one-loop diagrams in a finite volume.

[3]Note however that the study of the limit of zero-momentum transfer in this approach requires further scrutiny and is by no means trivial. The structure of the energy levels changes in this limit — the Landau levels emerge in the constant field. More discussion of this subtle issue is given in ref. [24].
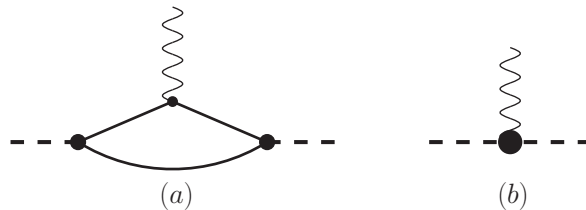
Figure 1. a) The triangle diagram which leads to an irregular behavior of the matrix element in a finite volume, and b) a local vertex that has a regular behavior. The dashed, single and wiggled lines denote the resonance, its constituents and the external current, respectively.

Moreover, the same method has been applied to the study of baryon structure functions and doubly virtual Compton scattering amplitude on the lattice [24–27]. In case of the form factor, one computes the two-point function *in an external field* in the Breit frame,[4] and determines the mass of a particle in the external field. It can then be shown that the derivative of the particle mass with respect to the coupling constant to the external field gives, at leading order in this coupling constant, the form factor in the Breit frame.

It is natural to ask, whether one can generalize this method to the calculation of the form factors of unstable particles. The role of the particle mass in this case is played by the resonance pole position in the complex plane. In this paper we shall demonstrate that, at leading order, the derivative of the pole position with respect to the coupling constant to the external field gives the resonance form factor. It will also be shown that, in order to compute the resonance form factor, performing analytic continuation and finding a pole in the presence of the external field is even superfluous. It suffices to determine the local contribution to the form factor, see figure 1b, which can be extracted directly on the real axis. Then, the analytic continuation can be performed in the explicit expressions, evaluated in the infinite volume and in the absence of the external field. This does not cause any problems and hence, the problem related to the triangle diagram, does not show up in this approach. Note that the local contribution, unlike the matrix element itself, contains only exponentially suppressed corrections in a finite volume, which are easy to handle. Finally, note that applying the Feynman-Hellmann theorem to resonances is not new. In particular, this theorem has been used to define the sigma-terms for the resonances in ref. [28]. In the present paper, the approach of ref. [28] is generalized to the case of spatially periodic fields.[5]

---

[4]Since the external field breaks translational invariance, the three-momentum is not conserved. The two-point function in the Breit frame is then defined as the one whose initial and final three-momenta $\mathbf{p}, \mathbf{q}$ are opposite in direction and have the same magnitude $|\mathbf{p}| = |\mathbf{q}| = \omega/2$, where $2\pi/\omega$ defines the period of the external field.

[5]Here, we mention in addition an application of the Feynman-Hellmann theorem to the calculation of the matrix element of a current between the two-body scattering states, which was carried out in ref. [2]. However, as already mentioned, the results of that paper cannot be directly compared to ours. First, in our calculations, the CM energies of the incoming/outgoing pairs and not the labels α, β are fixed. Second, the Feynman-Hellmann theorem in ref. [2] is used for the energies on the real axis and not in the complex plane. Lastly, the method of ref. [2] is restricted to the scalar current which can be obtained through the differentiation of the Lagrangian over the particle mass, whereas the method, described in the present paper, can be applied to a generic current.

The material of the present paper is rather technical. In order to make the argument easier to follow, here we present a brief synopsis with the focus on the physics content.

i) In our derivation, we make use of the framework of the non-relativistic effective field theory (NREFT). As already mentioned, the contributions to the form factor fall into two classes. This is shown in figure 1, where the triangle diagram causes difficulties in the infinite-volume limit, and the local contribution does not. Note also that all ingredients needed to construct the triangle diagram are assumed to be known in advance: the external field coupling to a single constituent, and a resonance coupling to the constituents (described by the elastic phase shift at the energies close to the resonance mass). By contrast, the contact contribution is unknown and should be determined. Such a splitting can be naturally described in an NREFT framework, with a Lagrangian similar to the one given below in eq. (2.1). Here, the coupling $C_R, \ldots$ determines the single particle form factor, the couplings C_0, C_2 describe the S-wave elastic scattering phase shift near threshold, and the quantity κ characterizes the lowest-order contact interaction. Higher-order terms are not displayed explicitly. At this order, determining κ on the lattice is equivalent to extracting the form factor, which can be straightforwardly calculated from the known analytic expression in the infinite volume that contains κ (as well as other constants) as free parameters.

ii) In order to describe the form factor, one has to inject a non-zero momentum transfer between the initial and final states. This can be achieved by placing a system in a spatially periodic external field, whose frequency is equal to the momentum transfer. The details are considered in section 3, where the result of ref. [23] concerning the determination of the form factor of a stable particle using the Feynman-Hellmann method has been re-derived and extended (see section 3.2).

iii) The central result of the paper is the derivation of the generalized Lüscher equation in the periodic external field. Symbolically, this can be written as

$$\det\left(X^{-1} - \frac{1}{2}\Pi \right) = 0 \, , \tag{1.3}$$

see eqs. (4.8) and (4.9) for more details. Here, the matrix X^{-1} is a counterpart of the inverse K-matrix, $p \cot \delta(p)$, and the loop function Π corresponds to the Lüscher zeta-function Z_{00}, when the external periodic field is turned on. This equation enables one to extract the contact contribution κ from the two-particle energy spectrum in the external field, provided the single particle form factor and the phase shift have been computed in advance. The extraction of κ can be performed at real energies, an analytic continuation is not needed. The infinite-volume limit is trivial since, by definition, the contact terms can contain only exponentially suppressed corrections for the large box sizes.

iv) The Feynman-Hellmann theorem in quantum mechanics deals with the Hamiltonians, linearly depending on a parameter λ:

$$H = H_0 + \lambda \mathcal{O} \, , \tag{1.4}$$

where $\mathcal{O}$ is some operator. The eigenstates of the Hamiltonian, $|n(\lambda)\rangle$, and the eigenvalues, $E_n(\lambda)$, also depend on λ. The Feynman-Hellmann theorem states that

$$\frac{dE_n(\lambda)}{d\lambda} = \langle n(\lambda)|\mathcal{O}|n(\lambda)\rangle. \tag{1.5}$$

We generalize this result for unstable states. One can namely extract the resonance pole position P_R^0 in the complex energy plane, also for a non-vanishing external field, see section 4.5. The derivative of P_R^0 with respect to the coupling to the external field, e (which plays the role of λ here), at $e = 0$ is proportional to the resonance form factor, evaluated at the (complex) resonance pole:

$$\left.\frac{dP_R^0(e)}{de}\right|_{e=0} \propto F. \tag{1.6}$$

For more details, see section 4.6 and, in particular, eq. (4.36).

The layout of the paper is as follows: in section 2 we consider the problem exclusively in the infinite volume and give a consistent definition of the resonance form factor. Section 3 contains a collection of the formulae that describe the motion of a single spinless particle in a periodic external field. Here, we derive an exact expression for the one-particle propagator as well as the modified Lüscher zeta-function in the external field. Section 4 is directly dedicated to the extraction of the local contribution to the form factor. The proof of the Feynman-Hellman theorem for the resonance form factor within the NREFT framework is also described here. Finally, section 5 contains the results of the numerical study of the quantization condition in an external field, which was carried out within a toy model. Note also that this paper provides a proof of principle only. For this reason, we have simplified the physical problem as much as possible. For example, we consider a non-relativistic case in detail, neglecting relativistic corrections whatsoever in the beginning. Moreover, to avoid clutter of indices, we restrict ourselves to the case of a single scalar field and neglect all partial waves other than the S-wave. All these effects can be taken into account in a rather straightforward fashion, see a very brief discussion in section 4.7.

2 Resonance form factor in the infinite volume

Let us consider a scalar non-relativistic particle with mass m, moving in an external electromagnetic field $A^\mu(x)$. We shall further assume that only $A^0(x)$ is different from zero, and that it corresponds to the static field, i.e., $A^0(x) = A^0(\mathbf{x})$. The Lagrangian which describes particles in this field consists of an infinite tower of operators with increasing mass dimension that respect all symmetries, namely rotational invariance, the discrete symmetries, and gauge invariance. In the following, we shall restrict ourselves to at most two particles in the initial and final states. Hence, the operators in the Lagrangian should contain at most two fields ϕ and two conjugated fields. Furthermore, only terms up to first order in the coupling e will be included in the Lagrangian, since we are exclusively interested in the linear shift in the external field.

We shall start from the Lagrangian[6]

$$\mathcal{L} = \phi^\dagger \left(i\partial_t - m + eA^0 + \frac{eC_R}{6m^2} \triangle A^0 + \frac{\nabla^2}{2m} \right) \phi + C_0 \phi^\dagger \phi^\dagger \phi\phi$$

$$+ C_2 \left(\phi^\dagger \phi^\dagger (\phi \overset{\leftrightarrow}{\nabla}^2 \phi) + \text{h.c.} \right) + \frac{e\kappa}{4} \phi^\dagger \phi^\dagger \phi\phi \triangle A^0 \,, \tag{2.1}$$

where the Galilei-invariant derivative is defined as $a\overset{\leftrightarrow}{\nabla}b = \frac{1}{2}(a\nabla b - b\nabla a)$ and $\triangle$ denotes the Laplacian. Note that in the above Lagrangian we did not make an attempt to write down all possible terms up to a given order in the expansion in the inverse powers of m. Hence, the theory, defined by it, is only a model that nevertheless possesses all essential ingredients of the full theory. For the sake of clarity, we shall consider the proof on the basis of this model first, and address the general case very briefly only at the end.[7]

The main aim of this section is to set up the framework for the evaluation of the resonance form factor in a theory described by the Lagrangian (2.1). The final result, given in eq. (2.23), can be derived in few steps. We start from the two-particle scattering amplitude for the process $q_1 + q_2 \to p_1 + p_2$ at $e = 0$ (no external field). In the non-relativistic effective theory, this amplitude is given by a sum of bubble diagrams (we remind the reader that, for simplicity, we focus on S-wave scattering only):

$$T(\mathbf{p}, \mathbf{q}; \mathbf{P}; P^0) = \frac{8\pi}{m} \left\{ K(p,q) + K(p,q_0) \frac{iq_0}{1 - iq_0 K(q_0, q_0)} K(q_0, q) \right\}, \tag{2.2}$$

where $p = |\mathbf{p}|$, $q = |\mathbf{q}|$, and

$$q_0^2 = m\left(P^0 - 2m - \frac{\mathbf{P}^2}{4m} \right), \qquad K(p,q) = \frac{m}{8\pi} \left(4C_0 - 4C_2(p^2 + q^2) \right). \tag{2.3}$$

Note that P^0 has an infinitesimal positive imaginary part $P^0 \to P^0 + i\varepsilon$ which, for brevity, is never shown explicitly. External particles are on mass shell: $p_i^0 = m + \mathbf{p}_i^2/(2m)$ and $q_i^0 = m + \mathbf{q}_i^2/(2m)$ for $i = 1, 2$. Furthermore, the center-of-mass and relative momenta are given by

$$\mathbf{P} = \mathbf{p}_1 + \mathbf{p}_2 = \mathbf{q}_1 + \mathbf{q}_2 \,, \qquad \mathbf{p} = \frac{\mathbf{p}_1 - \mathbf{p}_2}{2} \,, \qquad \mathbf{q} = \frac{\mathbf{q}_1 - \mathbf{q}_2}{2} \,. \tag{2.4}$$

On the energy shell, $\mathbf{p}^2 = \mathbf{q}^2 = q_0^2$ and the total energy P^0 is given by

$$P^0 = 2m + \frac{\mathbf{P}^2}{4m} + \frac{q_0^2}{m} \,. \tag{2.5}$$

---

[6]For a review of the non-relativistic effective theories for hadrons see, e.g., ref. [29].

[7]A brief comment about gauge invariance is in order. The restrictions $A^0 = A^0(\mathbf{x})$ and $\mathbf{A} = 0$ do not leave room for gauge transformations except a trivial shift of A^0 by a constant. In order to arrive at the Lagrangian given in eq. (2.1), one has first to write down the most general gauge-invariant Lagrangian for arbitrary A^μ, and choose a particular configuration of the external field afterwards. Note also that $\triangle A^0$ in eq. (2.1) emerges from the gauge-invariant expression $-\nabla\mathbf{E}$, which reduces to $\triangle A^0$ for $\mathbf{A} = 0$.

The on-shell scattering amplitude takes the form

$$T(q_0) = \frac{8\pi/m}{K^{-1}(q_0, q_0) - iq_0} = \frac{8\pi/m}{-1/a + rq_0^2/2 + \cdots - iq_0}\,, \tag{2.6}$$

where

$$C_0 = -\frac{2\pi a}{m}\,, \qquad C_2 = \frac{\pi r a^2}{2m}\,, \tag{2.7}$$

and a, r denote the S-wave scattering length and effective range, respectively.

Let us now adjust the parameters a, r so that there is a low-lying resonance in the S-wave. In this case, the resonance pole position is determined from the equation:

$$-\frac{1}{a} + \frac{1}{2} r q_R^2 - \sqrt{-q_R^2} = 0\,. \tag{2.8}$$

The choice of the minus sign in front of the square root corresponds to the second Riemann sheet.

Suppose that a, r are chosen so that the above equation has a solution with $\mathrm{Re}\, q_R^2 > 0$, $\mathrm{Im}\, q_R^2 < 0$, with $|\mathrm{Im}\, q_R^2| \ll |\mathrm{Re}\, q_R^2| \ll m^2$. This solution corresponds to a low-lying resonance in the S wave. In moving frames, the complex resonance energy is then given by

$$P_R^0 = 2m + \frac{\mathbf{P}^2}{4m} + \frac{q_R^2}{m} = \mathrm{Re}\, P_R^0 - \frac{i}{2}\, \Gamma_R\,, \tag{2.9}$$

where Γ_R denotes the width of the resonance.

In the vicinity of the resonance pole, the two-body amplitude behaves as

$$T(q_0) = \frac{8\pi/m}{K^{-1}(q_0, q_0) - \sqrt{-q_0^2}} \rightarrow \frac{Z}{q_0^2 - q_R^2} + \text{regular terms}\,,$$

$$Z = \frac{8\pi/m}{\left[K^{-1}(q_R, q_R)\right]' - \left[\sqrt{-q_R^2}\right]'}\,, \tag{2.10}$$

where primes indicate derivatives with respect to the variable q_0^2, and $q_0^2 = q_R^2$ is set at the end. In the following, Z will be referred to as the wave function renormalization constant of the resonance. It is, in general, a complex quantity.

Let us now turn the coupling to the external field on, and consider the two-point function of a particle in the external field up to $O(e)$:

$$S(\mathbf{p}, \mathbf{q}; p^0) = i \int dt\, d^3\mathbf{x}\, d^3\mathbf{y}\, e^{ip^0 t - i\mathbf{p}\mathbf{x} + i\mathbf{q}\mathbf{y}} \langle 0|T\phi(\mathbf{x}, t)\phi^\dagger(\mathbf{y}, 0)|0\rangle$$

$$= \frac{(2\pi)^3 \delta^3(\mathbf{p} - \mathbf{q})}{m + \frac{\mathbf{p}^2}{2m} - p^0} + \frac{e\Gamma(\mathbf{p}, \mathbf{q})\tilde{A}^0(\mathbf{p} - \mathbf{q})}{\left(m + \frac{\mathbf{p}^2}{2m} - p^0\right)\left(m + \frac{\mathbf{q}^2}{2m} - p^0\right)} + O(e^2)\,, \tag{2.11}$$

where

$$\tilde{A}^0(\mathbf{p} - \mathbf{q}) = \int d^3\mathbf{x}\, e^{-i(\mathbf{p} - \mathbf{q})\mathbf{x}} A^0(\mathbf{x}) \tag{2.12}$$

is the Fourier-transform of the (static) scalar potential. Furthermore, the one-particle form factor $\Gamma(\mathbf{p}, \mathbf{q}; p^0)$ can be directly read off from the Lagrangian,

$$\Gamma(\mathbf{p}, \mathbf{q}) = 1 - \frac{C_R}{6m^2} (\mathbf{p} - \mathbf{q})^2 \,, \tag{2.13}$$

where the quantity C_R is related to the mean charge radius through $C_R = m^2 \langle r^2 \rangle$. Note also that the on-shell condition for the non-relativistic particles is $\mathbf{p}^2/(2m) = \mathbf{q}^2/(2m) = p^0 - m$.

Next, we turn to the definition of the resonance form factor. This quantity can be defined through the expansion of the (equal-time) four-point function in the external field, similarly to the one-particle form factor obtained through the expansion of the two-point function. This four-point function is defined as

$$\tilde{G}(\mathbf{p}, \mathbf{P}; \mathbf{q}, \mathbf{Q}; P^0) = i \int dt \, d^3\mathbf{x}_1 d^3\mathbf{x}_2 d^3\mathbf{y}_1 d^3\mathbf{y}_2 \, e^{iP^0 t - i\mathbf{p}_1\mathbf{x}_1 - i\mathbf{p}_2\mathbf{x}_2 + i\mathbf{q}_1\mathbf{y}_1 + i\mathbf{q}_2\mathbf{y}_2}$$
$$\times \langle 0|T\phi(\mathbf{x}_1, t)\phi(\mathbf{x}_2, t)\phi^\dagger(\mathbf{y}_1, 0)\phi^\dagger(\mathbf{y}_2, 0)|0\rangle \,. \tag{2.14}$$

In the absence of the external field, the equal-time four-point function can be related to the two-particle scattering amplitude, considered above. Writing $\tilde{G} = \tilde{G}_0 + e\tilde{G}_1 + O(e^2)$, we obtain

$$\tilde{G}_0(\mathbf{p}, \mathbf{P}; \mathbf{q}, \mathbf{Q}; P^0) = \frac{(2\pi)^3\delta^3(\mathbf{P} - \mathbf{Q})\,(2\pi)^3\big(\delta^3(\mathbf{p} - \mathbf{q}) + \delta^3(\mathbf{p} + \mathbf{q})\big)}{2m + \frac{\mathbf{P}^2}{4m} + \frac{\mathbf{p}^2}{m} - P_0}$$
$$+ \frac{(2\pi)^3\delta^3(\mathbf{P} - \mathbf{Q})T(\mathbf{p}, \mathbf{q}; \mathbf{P}; P^0)}{\left(2m + \frac{\mathbf{P}^2}{4m} + \frac{\mathbf{p}^2}{m} - P_0\right)\left(2m + \frac{\mathbf{P}^2}{4m} + \frac{\mathbf{q}^2}{m} - P^0\right)} \,, \tag{2.15}$$

where $T(\mathbf{p}, \mathbf{q}; \mathbf{P}; P^0)$ is the two-body amplitude, introduced in eqs. (2.2), (2.3), and $\mathbf{P}$, $\mathbf{Q}$ are the total three-momenta of the particle pairs in the initial and final states, respectively, see eq. (2.4). The four-point function has a simple pole at $P^0 \to P_R^0$,

$$\tilde{G}_0(\mathbf{p}, \mathbf{P}; \mathbf{q}, \mathbf{Q}; P^0) \to (2\pi)^3\delta^3(\mathbf{P} - \mathbf{Q})\frac{\Psi(\mathbf{P}, \mathbf{p})\bar{\Psi}(\mathbf{Q}, \mathbf{q})}{P^0 - P_R^0} \,, \tag{2.16}$$

where

$$\Psi(\mathbf{P}, \mathbf{p}) = \frac{1}{2m + \frac{\mathbf{P}^2}{4m} + \frac{\mathbf{p}^2}{m} - P_0}\sqrt{\frac{Z}{m}}\frac{K(p, q_R)}{K(q_R, q_R)} \,,$$
$$\bar{\Psi}(\mathbf{Q}, \mathbf{q}) = \sqrt{\frac{Z}{m}}\frac{K(q, q_R)}{K(q_R, q_R)}\frac{1}{2m + \frac{\mathbf{Q}^2}{4m} + \frac{\mathbf{q}^2}{m} - P_0} \,. \tag{2.17}$$

In analogy to the case of the two-particle bound states, we shall refer to the quantity Ψ as the "wave function of a resonance." Note that this does not have anything to do with the interpretation of a resonance as a true quantum-mechanical state described by this "wave function", but just represents a convenient brief name.
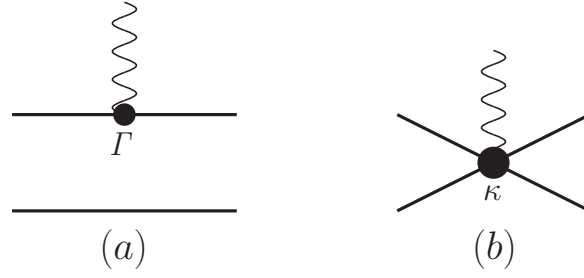
Figure 2. Diagrams contributing to the kernel $\tilde{\Gamma}$ which, convoluted with the wave functions $\bar{\Psi}, \Psi$, yields the resonance form factor, see eq. (2.23). The troublesome triangle diagram (a) in the finite-volume form factor, mentioned in the Introduction, emerges from the disconnected part, where the photon is attached to one of the particles, whereas the second one acts as a spectator. The fully connected diagram (b), where the photon is emanated from the four-particle vertex, is unproblematic.

Next, it can be checked that, like true wave functions, the quantities $\Psi, \bar{\Psi}$ are normalized according to

$$\frac{1}{2!} \int \frac{d^3\mathbf{p}}{(2\pi)^3} \, \bar{\Psi}(\mathbf{P},\mathbf{p}) \Psi(\mathbf{P},\mathbf{p}) = \frac{Z}{2m K^2(q_R, q_R)} \int \frac{d^3\mathbf{p}}{(2\pi)^3} \frac{K^2(p, q_R)}{\left(2m + \frac{\mathbf{P}^2}{4m} + \frac{\mathbf{p}^2}{m} - P_0\right)^2}$$

$$= -\frac{Zm}{8\pi K^2(q_R, q_R)} \frac{d}{dq_0^2} \left(K^2(q_0, q_R)\sqrt{-q_0^2}\right)\Bigg|_{q_0^2 = q_R^2}$$

$$= -\frac{Zm}{8\pi K^2(q_R, q_R)} \left(K'(q_R, q_R) + K^2(q_R, q_R)\left[\sqrt{-q_R^2}\right]'\right) = 1 \,.$$

(2.18)

Here, the factor $1/2!$ emerges from the Bose-symmetry. In the derivation, we have used the fact that the function $K(p, q)$ is real and symmetric (this, in its turn, stems from the hermiticity of the Hamiltonian) and, hence,

$$\frac{d}{dq_0^2} K(q_0, q_R)\Bigg|_{q_0^2 = q_R^2} = \frac{1}{2}\left[K(q_R, q_R)\right]' \,.$$

(2.19)

Up to order e, the equal-time Green function takes the form

$$\tilde{G}_1(\mathbf{p}, \mathbf{P}; \mathbf{q}, \mathbf{Q}; P^0) = \frac{1}{(2!)^2} \int \frac{d^3\mathbf{p}'}{(2\pi)^3} \frac{d^3\mathbf{P}'}{(2\pi)^3} \frac{d^3\mathbf{q}'}{(2\pi)^3} \frac{d^3\mathbf{Q}'}{(2\pi)^3} \tilde{G}_0(\mathbf{p}, \mathbf{P}; \mathbf{p}', \mathbf{P}'; P^0)$$

$$\times \tilde{\Gamma}(\mathbf{p}', \mathbf{P}'; \mathbf{q}', \mathbf{Q}') \tilde{G}_0(\mathbf{q}', \mathbf{Q}'; \mathbf{q}, \mathbf{Q}; P^0) \,.$$

(2.20)

At this order, the vertex $\tilde{\Gamma}$ is given by a sum of a finite number of diagrams, shown in figure 2:

$$\tilde{\Gamma}(\mathbf{p}, \mathbf{P}; \mathbf{q}, \mathbf{Q}) = \bar{\Gamma}(\mathbf{p}, \mathbf{P}; \mathbf{q}, \mathbf{Q}) \tilde{A}^0(\mathbf{P} - \mathbf{Q}) \,,$$

(2.21)

where

$$\bar{\Gamma}(\mathbf{p}, \mathbf{P}; \mathbf{q}, \mathbf{Q}) = -\kappa (\mathbf{P} - \mathbf{Q})^2$$

$$+ \left\{ (2\pi)^3 \delta^3 \left(\frac{(\mathbf{P} - \mathbf{Q})}{2} + (\mathbf{p} - \mathbf{q}) \right) \Gamma \left(\frac{\mathbf{P}}{2} - \mathbf{p}, \frac{\mathbf{Q}}{2} - \mathbf{q} \right) + \left(\begin{matrix} \mathbf{p} \to -\mathbf{p} \\ \mathbf{q} \to -\mathbf{q} \\ \mathbf{p} \to -\mathbf{p}, \mathbf{q} \to -\mathbf{q} \end{matrix} \right) \right\},$$

$$(2.22)$$

and Γ is the one-particle vertex, given in eq. (2.13).

The quantity $\tilde{G}_1$ has a double pole in the variables P^0, Q^0 that is contained in the free Green functions $\tilde{G}_0$. The residue at the double pole defines the form factor of the resonance:

$$F(\mathbf{P}, \mathbf{Q}) = \frac{1}{(2!)^2} \int \frac{d^3\mathbf{p}}{(2\pi)^3} \frac{d^3\mathbf{q}}{(2\pi)^3} \bar{\Psi}(\mathbf{P}, \mathbf{p}) \bar{\Gamma}(\mathbf{p}, \mathbf{P}; \mathbf{q}, \mathbf{Q}) \Psi(\mathbf{Q}, \mathbf{q}), \qquad (2.23)$$

where the energy is fixed at the resonance pole. Using the normalization of the wave functions, given in eq. (2.18), and the fact that, due to the Bose-symmetry, these wave functions are symmetric under $\mathbf{p} \to -\mathbf{p}$ and $\mathbf{q} \to -\mathbf{q}$, respectively, it can be immediately shown that the resonance form factor is properly normalized at zero momentum transfer, as required by the Ward identity (we remind the reader that the charge of the resonance is equal to $2e$). In appendix D we provide the explicit form of eq. (2.23) in dimensional regularization.

All parameters that are present in the Lagrangian (2.1) enter the expression (2.23) as well. Namely, the wave functions $\Psi, \bar{\Psi}$ contain the elastic two-particle scattering parameters C_0, C_2, whereas the kernel $\bar{\Gamma}$ depends on the parameter C_R that describes the single particle form factor, as well as the coupling κ, characterizing the contact term. There will be more couplings, if higher-order derivative terms, higher partial waves, etc., are included, but the general pattern is already clear. All these couplings should be determined on the lattice, on the same configurations. In order to determine the elastic scattering phase, related to C_0, C_2, one may use standard Lüscher approach for the two-body scattering at $e = 0$. The value of C_R can be established by calculating the single particle form factor by using either the standard method or the Feynman-Hellmann theorem. At the order we are working, only a single constant κ remains unknown. Below it will be shown, how this constant can be fixed in the external field.

The framework that we considered in this section is not new and represents a properly adapted version of the Mandelstam formalism [30, 31], which is used to define form factors of *stable* particles. The purpose of such a detailed treatment was to set the stage for a similar calculation in a finite volume. In the following, it will be demonstrated that using the Feynman-Hellmann theorem in a periodic external field, one arrives exactly at the quantity defined by eq. (2.23) in the infinite-volume limit.

3 Single particle in a periodic external field

3.1 Solutions of the Mathieu equation

Up to this point, the discussion was carried out for a generic static external field $A^0(\mathbf{x})$. In order to inject a momentum between the initial and final states on the lattice, it is

convenient to consider a spatially periodic field

$$A^0(\mathbf{x}) = A_0 \cos(\boldsymbol{\omega}\mathbf{x}), \qquad \boldsymbol{\omega} = (0, 0, \omega). \tag{3.1}$$

Here, for convenience, we have chosen the vector $\boldsymbol{\omega}$ in the direction of the z-axis. Furthermore, we project all vectors onto the direction of $\boldsymbol{\omega}$: for instance, the position vector has the components $\mathbf{x} = (\mathbf{x}_\perp, x_\parallel)$, where $\mathbf{x}_\perp, x_\parallel$ denote the components perpendicular and parallel to the z-axis, respectively.

In this section, we shall derive a closed expression of the two-point function of the field ϕ in the external field. We are working here in a cubic box with a spatial elongation L (the time elongation is assumed to be infinite). Periodic boundary conditions are imposed in the spatial directions. As a result, the three-momenta of the particles as well as the frequency ω are quantized:

$$\mathbf{p} = \frac{2\pi}{L}\,\mathbf{n}, \quad \mathbf{n} \in \mathbb{Z}^3, \quad \text{and} \quad \omega = \frac{2\pi}{L}\,N, \quad N \in \mathbb{Z}. \tag{3.2}$$

Let us denote by $|1\rangle$ a state with a single particle in the periodic field. The matrix element of the field operator between the vacuum and the one-particle state defines the Schrödinger wave function

$$\Phi(\mathbf{x}, t) = \langle 0|\phi(\mathbf{x}, t)|1\rangle. \tag{3.3}$$

The wave function obeys a differential equation that can be obtained by using the equations of motion for the field $\phi(\mathbf{x}, t)$:

$$\left(i\partial_t + e\Gamma A_0 \cos(\omega x_\parallel) - m + \frac{\nabla^2}{2m}\right)\Phi(\mathbf{x}, t) = 0. \tag{3.4}$$

Here,

$$\Gamma = \Gamma(\boldsymbol{\omega}) = 1 - \frac{C_R}{6m^2}\,\omega^2 \tag{3.5}$$

is the single-particle form factor evaluated at the three-momentum transfer ω. Note that, after factorizing eq. (3.4) by using an ansatz $\Phi(\mathbf{x}, t) = e^{-iEt + i\mathbf{p}_\perp \mathbf{x}_\perp} f(x_\parallel)$, this equation can be reduced to a so-called Mathieu equation for the function $f(x_\parallel)$. The (unnormalized) solutions of eq. (3.4) that obey periodic boundary conditions are given by

$$\Phi(\mathbf{x}, t) = e^{-iEt + i\mathbf{p}_\perp \mathbf{x}_\perp} \mathrm{me}_{\nu_i + 2n}(z, q),$$
$$z = \frac{\omega x_\parallel}{2}, \qquad q = -\frac{4me\Gamma A_0}{\omega^2}, \tag{3.6}$$

where $\mathrm{me}_{\nu_i + 2n}(z, q)$ denotes the Mathieu function and the index $\nu_i + 2n$, $n \in \mathbb{Z}$, $i = 1, \ldots, N$ labels the eigenfunctions of the Mathieu differential equation corresponding to the eigenvalues $\lambda_{\nu_i + 2n}(q)$ [32].[8] Details are given in appendix A.

The completeness condition for the solutions of the Mathieu equation takes the form:

$$\frac{1}{\pi} \sum_{i=1}^{N} \sum_{n=-\infty}^{\infty} \mathrm{me}_{\nu_i + 2n}(z, q)\mathrm{me}_{\nu_i + 2n}(-z', q) = N \sum_{k=-\infty}^{\infty} \delta(z - z' - \pi k N), \tag{3.7}$$

with the ν_i as given in eq. (A.8).

---

[8]A collection of useful formulae on the properties of the Mathieu functions can be found at https://dlmf.nist.gov/28.

The propagator of the particle ϕ in the external field is defined as:

$$S(\mathbf{x}, \mathbf{y}; E) = i \int_{-\infty}^{+\infty} dt\, e^{iEt} \langle 0|T\phi(\mathbf{x}, t)\phi^{\dagger}(\mathbf{y}, 0)|0\rangle , \qquad (3.8)$$

and it is given by the sum over the eigenfunctions (spectral representation):

$$S(\mathbf{x}, \mathbf{y}; E) = \frac{1}{L^3} \sum_{\mathbf{p}_\perp} \sum_{i=1}^{N} \sum_{n=-\infty}^{\infty} \frac{e^{i\mathbf{p}_\perp(\mathbf{x}_\perp - \mathbf{y}_\perp)}}{m + \frac{\mathbf{p}_\perp^2}{2m} + \frac{\omega^2}{8m}\lambda_{\nu_i+2n}(q) - E}$$
$$\times \mathrm{me}_{\nu_i+2n}\left(\frac{\omega x_\parallel}{2}, q\right)\mathrm{me}_{\nu_i+2n}\left(-\frac{\omega y_\parallel}{2}, q\right). \qquad (3.9)$$

Indeed, it can be directly verified that

$$\left(E + eA_0\cos(\omega x_\parallel) - m + \frac{\nabla^2}{2m}\right)S(\mathbf{x}, \mathbf{y}; E) = -\sum_{\mathbf{m}\in\mathbb{Z}^3} \delta^3(\mathbf{x} - \mathbf{y} - \mathbf{m}L). \qquad (3.10)$$

The propagator can be expanded in powers of e (this corresponds to the Taylor expansion in the parameter q). Up to $O(e)$, the result takes the expected simple form:

$$S(\mathbf{p}, \mathbf{q}; E) = \int_0^L d^3\mathbf{x}\, d^3\mathbf{y}\, e^{-i\mathbf{p}\mathbf{x}+i\mathbf{q}\mathbf{y}} S(\mathbf{x}, \mathbf{y}; E)$$
$$= L^3 \left\{ \frac{\delta_{\mathbf{p}\mathbf{q}}^3}{m + \frac{\mathbf{p}^2}{2m} - E} + \frac{1}{2}\, eA_0\Gamma \frac{\delta_{\mathbf{p}-\boldsymbol{\omega},\mathbf{q}}^3 + \delta_{\mathbf{p}+\boldsymbol{\omega},\mathbf{q}}^3}{\left(m + \frac{\mathbf{p}^2}{2m} - E\right)\left(m + \frac{\mathbf{q}^2}{2m} - E\right)} \right\} + O(e^2). \qquad (3.11)$$

The proof of this equation is given in appendix B.

3.2 The energy shift in the periodic field

The spectrum of a particle in an external periodic field is determined by the poles of the propagator. Performing the Fourier transform using eq. (A.9), the propagator can be rewritten in the following form:

$$S(\mathbf{p}, \mathbf{q}; E) = L^3 \delta_{\mathbf{p}_\perp, \mathbf{q}_\perp}^2 \sum_{i=1}^{N} \sum_{n=-\infty}^{\infty} \sum_{a,b=-\infty}^{\infty} C_{2a}^{\nu_i+2n}(q) C_{2b}^{\nu_i+2n}(q)$$
$$\times \frac{\delta_{-p_\parallel, \frac{\omega}{2}(\nu_i+2n+2a)} \delta_{-q_\parallel, \frac{\omega}{2}(\nu_i+2n+2b)}}{m + \frac{\mathbf{q}_\perp^2}{2m} + \frac{\omega^2}{8m}\lambda_{\nu_i+2n}(q) - E}. \qquad (3.12)$$

Here, the coefficients $C_{2a,2b}^{\nu_i+2n}(q)$ $(a, b \in \mathbb{Z})$ are the same as in eq. (A.9), and their explicit form does not matter here. We see now that, instead of one pole, the propagator in the external field has a tower of poles. This was expected, because the periodic external field carries the momentum $\boldsymbol{\omega}$. Consequently, the three-momentum is not conserved in such a field, and $\mathbf{q} = \mathbf{p} + \ell\boldsymbol{\omega}$, where $\ell \in \mathbb{Z}$ is an integer. In addition, since the particle interacts

– 13 –

with the field, the energies (pole positions) are slightly displaced from the non-interacting values corresponding to $\lambda_{\nu_i+2n}(0) = (\nu_i + 2n)^2$ and are determined through the equation

$$E = m + \frac{\mathbf{p}_\perp^2}{2m} + \frac{\omega^2}{8m}\,\lambda_{\nu_i+2n}(q)\,. \tag{3.13}$$

The crucial point is that $\lambda_{\nu_i+2n}(q) = (\nu_i + 2n)^2 + O(q^2)$ for all values of $\nu_i + 2n$ except $(\nu_i + 2n) = \pm 1$. In this case,

$$\lambda_1(q) = 1 + q + O(q^2)\,, \qquad \lambda_{-1}(q) = 1 - q + O(q^2)\,. \tag{3.14}$$

In the following, for simplicity, we shall take $\mathbf{p}_\perp = \mathbf{q}_\perp = 0$ and determine the *lowest* eigenvalue in the sectors with different values of N. (Note that the integer number N characterizes the momentum transfer in the external field vertex, in units of $2\pi/L$.) The components $p_\parallel, q_\parallel$ are given by $p_\parallel = 2\pi n_\parallel/L$ and $q_\parallel = 2\pi n'_\parallel/L$. In the sectors with $N = 1, 2$ the argument goes as follows:

$N = 1$. In this case, $\nu_i = 0$, and we have

$$- n_\parallel = n + a\,, \qquad -n'_\parallel = n + b\,. \tag{3.15}$$

For any choice of $n_\parallel, n'_\parallel$, we may find a, b so that $n = 0$. Hence, the lowest eigenvalue is $\lambda_{\nu_i+2n}(q) = \lambda_0(q) = O(q^2)$.

$N = 2$. In this case, we have $\nu_i = 0, 1$ and

$$- n_\parallel = \nu_i + 2n + 2a\,, \qquad -n'_\parallel = \nu_i + 2n + 2b\,. \tag{3.16}$$

This means that $n_\parallel, n'_\parallel$ should be either odd or even. If both are chosen to be even, then $\nu_i = 0$ should be fulfilled and $n = 0$ is allowed. Then, the lowest eigenvalue is $\lambda_0(q)$. On the other hand, if $n_\parallel, n'_\parallel$ are odd, then $\nu_i = 1$ is picked up. Since n is integer, $\nu_i + 2n$ is odd and $\lambda_0(q)$ never appears. The lowest eigenvalues are then $\lambda_{\pm 1}(q)$. Assuming $A_0 > 0$ and $q > 0$, we get $\lambda_1(q) < \lambda_1(-q)$ and the lowest energy level will be at

$$E = m + \frac{\omega^2 \lambda_1(q)}{8m} = m + \frac{\omega^2}{8m} - \frac{1}{2}\,eA_0\Gamma\,. \tag{3.17}$$

Hence, differentiating the pole shift with respect to e, one gets the particle form factor $\Gamma = \Gamma(\boldsymbol{\omega})$. This is exactly the case considered in ref. [23]: one places the charged particle in the periodic external field with $\omega = 4\pi/L$, and considers the Breit frame $\mathbf{p} = -\mathbf{q} = -\boldsymbol{\omega}/2$. Then, the linear derivative of the shift of the lowest energy level with respect to the coupling to the external field yields the form factor at the momentum transfer $\boldsymbol{\omega}$. Hence, our result confirms and extends the findings of ref. [23] to different incoming and outgoing momenta, as well as to the higher values of N.

4 Two-particle scattering in the periodic external field

4.1 Lüscher equation

In this section, we shall derive the counterpart of the Lüscher equation in the external field, which allows one to extract the contact coupling, κ, from the finite-volume energy spectrum. To this end, let us consider the two-point function of the composite fields $\phi^2, [\phi^\dagger]^2$:

$$D(\mathbf{P}, \mathbf{Q}; t) = i \int^L d^3\mathbf{x} d^3\mathbf{y} e^{-i\mathbf{P}\mathbf{x}+i\mathbf{Q}\mathbf{y}} \langle 0|T\phi^2(\mathbf{x}, t)[\phi^\dagger(\mathbf{y}, 0)]^2|0\rangle. \qquad (4.1)$$

The diagrams that contribute to this quantity are shown in figure 3. These are reminiscent of the diagrams in the absence of an external field, with two differences: a) the particle propagators in these diagrams are the full ones that include the summation of all external field insertions in these propagators, and b) in addition to the conventional four-particle vertices, there are vertices with the external field attached (the pertinent operator comes with the coupling κ in the Lagrangian). Below, we shall study the implications of these modifications.

First, note that, since the three-momentum is not conserved in the presence of the external field, the two-point function is no more diagonal in the incoming/outgoing total three-momenta $\mathbf{Q}$ and $\mathbf{P}$. Instead of an overall factor $L^3\delta^3_{\mathbf{PQ}}$ it contains a tower of terms with $L^3\delta^3_{\mathbf{P}+\ell\boldsymbol{\omega},\mathbf{Q}}$ and $\ell \in \mathbb{Z}$, $\ell \neq 0$. However, since each momentum flip proceeds through the interaction with the external field and thus adds one power of the coupling e, the terms that multiply $L^3\delta^3_{\mathbf{P}+\ell\boldsymbol{\omega},\mathbf{Q}}$ start at $O(e^\ell)$. Hence, at a given order in e, the quantity $D(\mathbf{P}, \mathbf{Q}; E)$ is a band matrix with the indices $\mathbf{P}, \mathbf{Q}$. Note also that here we do not attempt *a priori* to expand the particle propagator in powers of e, since such an expansion cannot be easily justified on the real axis of the energy.

Let us consider the elementary loop diagram in figure 3. If both four-particle vertices in such a diagram do not contain derivatives of the field ϕ, such a loop is given merely by a convolution of two propagators in the external field
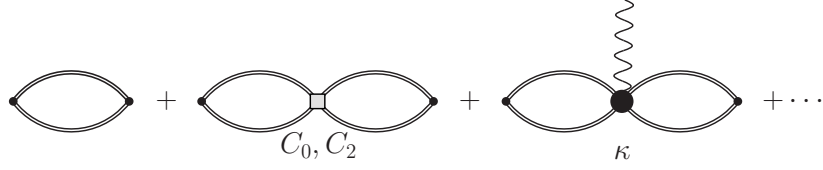
$$\Pi(\mathbf{P}, \mathbf{Q}; E) = \int \frac{dp^0}{2\pi i} \int^L d^3\mathbf{x} d^3\mathbf{y}\, e^{-i\mathbf{P}\mathbf{x}+i\mathbf{Q}\mathbf{y}} S(\mathbf{x}, \mathbf{y}; p^0) S(\mathbf{x}, \mathbf{y}; E - p^0). \qquad (4.2)$$

Here, $S(\mathbf{x}, \mathbf{y}; E)$ is defined by eq. (3.9).

The situation is slightly more complicated in case of vertices with derivatives, e.g., the vertex that is proportional to the coupling C_2 in eq. (2.1). In the case with no external field and using dimensional regularization, it is possible to "pull out" the derivatives acting on the internal lines and transform them into the external momenta. The difference is an off-shell term, which cancels the denominator in the loop, leaving a low-energy polynomial that vanishes after integration in dimensional regularization. The above fact allows one to derive the Lüscher equation in a very simple manner.[9] When the external field is switched on, "pulling out" the derivatives leads to an extra term that depends on the external field.

---

[9]The final result is the same in all regularizations but the use of dimensional regularization makes the derivation particularly simple.

Figure 3. Two-point function of the composite field $\phi^2(x)$. Double lines denote the full one-particle propagator in the external field, see figure 4. The diagrams, in which the external field is attached to the four-particle vertex, are explicitly included.
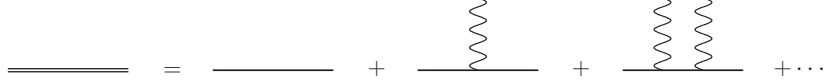
Figure 4. Full one-particle propagator in the external field.

Indeed, using eq. (4.2) together with eq. (A.4), one can easily show that

$$
\int^L d^3\mathbf{x}d^3\mathbf{y}\, e^{-i\mathbf{P}\mathbf{x}+i\mathbf{Q}\mathbf{y}}\bigg\{ S(\mathbf{x},\mathbf{y};p^0)(\overrightarrow{\nabla}_x - \overleftarrow{\nabla}_x)^2 S(\mathbf{x},\mathbf{y};E-p^0)\bigg\}
$$

$$
= \int^L d^3\mathbf{x}d^3\mathbf{y}\, e^{-i\mathbf{P}\mathbf{x}+i\mathbf{Q}\mathbf{y}}
$$

$$
\times \frac{1}{L^3}\sum_{\mathbf{p}_\perp}\sum_{i=1}^{N}\sum_{n=-\infty}^{\infty}\frac{e^{i\mathbf{p}_\perp(\mathbf{x}_\perp-\mathbf{y}_\perp)}\mathrm{me}_{\nu_i+2n}\left(\frac{\omega x_\parallel}{2},q\right)\mathrm{me}_{\nu_i+2n}\left(-\frac{\omega y_\parallel}{2},q\right)}{m+\frac{\mathbf{p}_\perp^2}{2m}+\frac{\omega^2}{8m}\lambda_{\nu_i+2n}(q)-p^0-i\varepsilon} \tag{4.3}
$$

$$
\times \left(-2\mathbf{p}_\perp^2 - 2\mathbf{q}_\perp^2 + \mathbf{P}^2 - \frac{\omega^2}{2}\left(\lambda_{\nu_i+2n}(q)+\lambda_{\nu_j+2m}(q)\right) - 8me\Gamma A^0(\mathbf{x})\right)
$$

$$
\times \frac{1}{L^3}\sum_{\mathbf{q}_\perp}\sum_{j=1}^{N}\sum_{m=-\infty}^{\infty}\frac{e^{i\mathbf{q}_\perp(\mathbf{x}_\perp-\mathbf{y}_\perp)}\mathrm{me}_{\nu_j+2m}\left(\frac{\omega x_\parallel}{2},q\right)\mathrm{me}_{\nu_j+2m}\left(-\frac{\omega y_\parallel}{2},q\right)}{m+\frac{\mathbf{q}_\perp^2}{2m}+\frac{\omega^2}{8m}\lambda_{\nu_j+2m}(q)-E+p^0-i\varepsilon}.
$$

The expression in the brackets, which is present in the numerator, can be rewritten as

$$
-2\mathbf{p}_\perp^2 - 2\mathbf{q}_\perp^2 + \mathbf{P}^2 - \frac{\omega^2}{2}\left(\lambda_{\nu_i+2n}(q)+\lambda_{\nu_j+2m}(q)\right) - 8me\Gamma A^0(\mathbf{x})
$$

$$
= -4m\left(m+\frac{\mathbf{p}_\perp^2}{2m}+\frac{\omega^2}{8m}\lambda_{\nu_i+2n}(q)-p^0\right) - 4m\left(m+\frac{\mathbf{q}_\perp^2}{2m}+\frac{\omega^2}{8m}\lambda_{\nu_j+2m}(q)-E+p^0\right)
$$

$$
- 4m\left(E-2m-\frac{\mathbf{P}^2}{4m}\right) - 8me\Gamma A^0(\mathbf{x})\,. \tag{4.4}
$$

The first two terms cancel with one of the denominators in eq. (4.3). Using dimensional regularization, it can be argued that these two terms give a vanishing contribution to the integral. The third term corresponds to "pulling out" the derivatives on the internal lines. Only the last term is new and shows that, in case of a non-vanishing external field, there is an additional contribution. Physically, this corresponds to the four-particle vertex with the external

field attached (topologically equivalent to the one that contains the coupling κ). In other words, pulling out the derivatives is equivalent to adjusting the coefficients of such terms.[10]

Carrying out this procedure consistently in all loops, it is seen that the full two-point function D obeys the equation

$$\frac{1}{4} D_{\mathbf{PQ}}(E) = \frac{1}{2} \mathit{\Pi}_{\mathbf{PQ}}(E) + \frac{1}{L^6} \sum_{\mathbf{P'Q'}} \frac{1}{2} \mathit{\Pi}_{\mathbf{PP'}}(E) X_{\mathbf{P'Q'}}(E) \frac{1}{4} D_{\mathbf{Q'Q}}(E) \,. \qquad (4.5)$$

Here, for convenience, we have used matrix notation, considering the momenta $\mathbf{P}, \mathbf{Q}, \ldots$ as the indices. The kernel X is given by

$$X_{\mathbf{PQ}}(E) = L^3 \delta_{\mathbf{PQ}}^3 X_{\mathbf{P}}^{(0)}(E) + \frac{e}{2} L^3 (\delta_{\mathbf{P}+\boldsymbol{\omega},\mathbf{Q}}^3 + \delta_{\mathbf{P}-\boldsymbol{\omega},\mathbf{Q}}^3) X_{\mathbf{PQ}}^{(1)}(E) + O(e^2) \,, \qquad (4.6)$$

where

$$X_{\mathbf{P}}^{(0)}(E) = 4C_0 - 8mC_2 \Big(E - 2m - \frac{\mathbf{P}^2}{4m} \Big) + \cdots ,$$
$$X_{\mathbf{PQ}}^{(1)}(E) = -\kappa \omega^2 A_0 - 16mC_2 \mathit{\Gamma} A_0 + \cdots . \qquad (4.7)$$

Note that the second term in $X^{(1)}$ emerges after pulling out the derivatives.

The derivation of the Lüscher equation is now straightforward. The energy levels are determined by the equation

$$\det \mathcal{M} = 0 \,, \qquad \mathcal{M}_{\mathbf{PQ}}(E) = [X_{\mathbf{PQ}}(E)]^{-1} - \frac{1}{2} \mathit{\Pi}_{\mathbf{PQ}}(E) \,. \qquad (4.8)$$

Furthermore, up to first order in e, the inverse of the matrix X is given by

$$[X_{\mathbf{PQ}}(E)]^{-1} = L^3 \delta_{\mathbf{PQ}}^3 k(\mathbf{P}; E) - \frac{e}{2} L^3 (\delta_{\mathbf{P}+\boldsymbol{\omega},\mathbf{Q}}^3 + \delta_{\mathbf{P}-\boldsymbol{\omega},\mathbf{Q}}^3) k(\mathbf{P}; E) X_{\mathbf{PQ}}^{(1)}(E) k(\mathbf{Q}; E)$$
$$+ O(e^2) \,, \qquad (4.9)$$

where

$$k(\mathbf{P}; E) = \Big(4C_0 - 8mC_2 \Big(E - \frac{\mathbf{P}^2}{4m} \Big) + \cdots \Big)^{-1} = \frac{m}{8\pi} \Big(-\frac{1}{a} + \frac{1}{2} r q_0^2(\mathbf{P}; E) + \cdots \Big) ,$$
$$q_0^2(\mathbf{P}; E) = m \Big(E - 2m - \frac{\mathbf{P}^2}{4m} \Big) . \qquad (4.10)$$

As seen from the above equation, at leading order in e, the inverse of the kernel reduces to the well-known expression $q_0 \cot \delta(q_0)$. This was of course expected from the beginning. The $O(e)$ corrections to the kernel can be calculated perturbatively in a consistent manner. At this order, they are characterized by a single unknown effective coupling κ.

---

[10]Note, however, that this additional term does not carry the momenta $\mathbf{P}, \mathbf{Q}$ and, in particular, does not vanish at $(\mathbf{P} - \mathbf{Q})^2 = 0$. This indicates that pulling all derivatives out of the loop, checking Ward identities as well as the normalization of the form factor at zero momentum transfer can become technically complicated, albeit gauge invariance still holds.

Furthermore, if $\mathbf{P} = -\mathbf{Q}$ (Breit frame), the non-diagonal term in eq. (4.9) can be rewritten as

$$k(\mathbf{P}; E) X^{(1)}_{\mathbf{PQ}}(E) k(-\mathbf{P}; E) = -k^2(\mathbf{P}; E)\kappa\omega^2 A_0 - \frac{m^2}{4\pi}\,\Gamma A_0 \frac{dK^{-1}(q_0, q_0)}{dq_0^2} + \cdots$$

$$= -k^2(\mathbf{P}; E)\kappa\omega^2 A_0 - \frac{m^2}{8\pi}\,\Gamma A_0 r + \cdots . \qquad (4.11)$$

In other words, at this order, everything is expressed in terms of the effective-range parameters a, r and the coupling κ.

Equation (4.8) is one of our main results, namely the Lüscher equation in the presence of an external field. In contrast to the conventional Lüscher equation, which reduces to a single equation in the absence of partial-wave mixing, eq. (4.8) results from the matrix equation that connects sectors with different momenta $\mathbf{P}, \mathbf{Q}$. This happens because three-momentum is not a conserved quantity in the case considered here.

In order to make the equations tractable, a truncation should be applied. Let us consider the Breit frame again, with $\mathbf{P} = -\mathbf{Q} = \boldsymbol{\omega}/2$. If $e = 0$, $\mathcal{M}$ is a diagonal matrix, whose matrix elements at $\mathbf{P} = \mathbf{Q} = \pm\boldsymbol{\omega}/2$ linearly vanish at the energies that correspond to the finite-volume spectrum of a system in a frame moving with a momentum $\mathbf{P}$. Turning the external field on, it is seen that the energy levels split and continuously shift from these values.[11] It can be straightforwardly checked that, at order e, it suffices to consider a 2×2 matrix with $\mathbf{P} = \pm\boldsymbol{\omega}/2$ and $\mathbf{Q} = \pm\boldsymbol{\omega}/2$. Adding more rows and columns to this matrix shifts the spectrum in higher orders only.

It is important to realize that the only missing piece in our knowledge of the resonance form factor is the contact contribution, which is proportional to the constant κ in our example. Everything else is known: the form factor in the impulse approximation (this corresponds to the triangle diagram in figure 1a) is determined through the known form factors of individual particles. This way, the coupling κ can be extracted by fitting the data to the energy spectrum obtained from the Lüscher equation in the external field, eq. (4.8). Unlike measured matrix elements of the external current, κ, by definition, may contain only exponentially suppressed contributions in a finite volume. Hence, this method allows one to circumvent the problem of the irregular L-dependence, mentioned in the Introduction.[12]

4.2 The Lüscher zeta-function in the external field; perturbative expansion

We shall now provide an explicit expression for the loop function Π, defined in eq. (4.2). Carrying out the integration over the transverse momenta and the energy, we get

$$\Pi(\mathbf{P}, \mathbf{Q}; E) = L^2 \delta^2_{\mathbf{P}_\perp \mathbf{Q}_\perp} \bar{\Pi}(P_\parallel, Q_\parallel; \mathbf{P}_\perp; E), \qquad (4.12)$$

---

[11]In fact, as we shall see later, the structure of the spectrum at $e \neq 0$ is more complicated. There exist "fake" states which do not have a counterpart at $e = 0$.

[12]This statement should be clarified by an example. Suppose that one calculates the finite-volume energy spectrum in an "exact" theory (be this QCD or relativistic EFT), and then extracts κ from this spectrum by using the NREFT setting described in this paper. The extracted quantity $\kappa = \kappa(L)$ will depend on L. We state that the difference $\kappa(L) - \kappa(\infty) = O(e^{-\mu L})$ (modulo a prefactor that may contain powers of L), where μ is some scale given by a multiple of the lightest mass in the system (here, the only available scale is the particle mass m itself). In this context, one might term this statement, which applies to all effective couplings in NREFT, as the finite-volume counterpart of the Appelquist-Carazzone decoupling theorem.

where

$$
\begin{aligned}
&\bar{\Pi}(P_\parallel, Q_\parallel; \mathbf{P}_\perp; E) \\
&= \frac{1}{L^4} \sum_{\mathbf{P}_\perp} \sum_{i,j=1}^{N} \sum_{n,m=-\infty}^{\infty} \int_0^L dx_\parallel \int_0^L dy_\parallel \, D_{in,jm}(\mathbf{p}_\perp; \mathbf{P}_\perp; E) e^{-iP_\parallel x_\parallel + iQ_\parallel y_\parallel} \\
&\quad \times \mathrm{me}_{\nu_i + 2n}\left(\frac{\omega x_\parallel}{2}, q\right) \mathrm{me}_{\nu_i + 2n}\left(-\frac{\omega y_\parallel}{2}, q\right) \mathrm{me}_{\nu_j + 2m}\left(\frac{\omega x_\parallel}{2}, q\right) \mathrm{me}_{\nu_j + 2m}\left(-\frac{\omega y_\parallel}{2}, q\right), \quad (4.13)
\end{aligned}
$$

and

$$
D_{in,jm}(\mathbf{p}_\perp; \mathbf{P}_\perp; E) = \frac{1}{2m + \frac{\mathbf{p}_\perp^2}{2m} + \frac{(\mathbf{P} - \mathbf{p})_\perp^2}{2m} + \frac{\omega^2}{8m}\left(\lambda_{\nu_i + 2n}(q) + \lambda_{\nu_j + 2m}(q)\right) - E}. \quad (4.14)
$$

Below, we shall consider the perturbative expansion of this expression in powers of the coupling e (or, equivalently, the quantity q). The reason for this is twofold. First, in the standard method of evaluating the resonance form factor, the matrix element between the two-particle scattering states is calculated on the lattice. This corresponds to taking exactly $O(e)$ term in the perturbative expansion. Hence, expanding the result in e, one may establish a closer relation between the "standard" approach and the approach which is proposed in the present paper. The second reason is practical. The full expression of the Lüscher function in the external field is quite cumbersome and is not well suited for numerical evaluation. The expansion allows one to arrive at a much simpler expression. One should be however aware of pitfalls, see below.

In what follows, we shall display the result of the calculation of this quantity at first order in the parameter q. Note that the energy denominator depends on q as well since $\lambda_{\pm 1}(q) = 1 \pm q + O(q^2)$. Hence, the perturbative expansion fails at the energies where the pertinent denominators vanish at $O(q^0)$. For this reason, along with the "perturbative" result, we also present the "exact" one, obtained by expanding the numerator in powers of q but keeping the $O(q)$ terms in the denominator unexpanded. The implications of using the "perturbative" result instead of the "exact" one are also considered in detail.

The initial and final momenta $\mathbf{P}, \mathbf{Q}$ in the above equations are arbitrary. Below, we shall use the notation $P_\parallel = a\omega/2$, $Q_\parallel = b\omega/2$. For simplicity, we shall further restrict ourselves to the 2×2 matrix with $a, b = \pm 1$ (recall that $\mathbf{P}_\perp = \mathbf{Q}_\perp$). The detailed derivation can be found in appendix C. The pertinent elements of the matrix Π_{ab} are denoted as $\tilde{\Pi}_{11} = \tilde{\Pi}_{-1,-1} \doteq \Pi_0$ and $\tilde{\Pi}_{1,-1} = \tilde{\Pi}_{-1,1} \doteq \Pi_1$. The "exact" and "perturbative" results are denoted by $\Pi_{0,1}$ and $\Pi'_{0,1}$, respectively:

$$
\Pi_0 = \Pi_0^{(1)} + \Pi_0^{(2)}, \qquad \Pi_1 = \Pi_1^{(1)} + \Pi_1^{(2)}, \quad (4.15)
$$

where

$$
\begin{aligned}
\Pi_0^{(1)} &= \frac{1}{L^3} \sum_{\mathbf{p}} \frac{1}{2m + \frac{\mathbf{p}^2}{2m} + \frac{(\mathbf{P} - \mathbf{p})^2}{2m} - E}, \\
\Pi_1^{(1)} &= -\frac{\omega^2 q}{4m} \frac{1}{L^3} \sum_{\mathbf{p}} \frac{1}{\left(2m + \frac{\mathbf{p}^2}{2m} + \frac{(\mathbf{P} - \mathbf{p})^2}{2m} - E\right)\left(2m + \frac{\mathbf{p}^2}{2m} + \frac{(\mathbf{Q} - \mathbf{p})^2}{2m} - E\right)},
\end{aligned} \quad (4.16)
$$

and

$$\Pi_0^{(2)} = \frac{1}{L^3} \sum_{\mathbf{P}_\perp} \left\{ \frac{1+\frac{q}{4}}{\frac{\omega^2}{8m}(1+q)+\frac{\omega^2}{2m}-W} + \frac{1-\frac{q}{4}}{\frac{\omega^2}{8m}(1+q)-W} \right.$$

$$\left. + \frac{1-\frac{q}{4}}{\frac{\omega^2}{8m}(1-q)+\frac{\omega^2}{2m}-W} + \frac{1+\frac{q}{4}}{\frac{\omega^2}{8m}(1-q)-W} - \frac{2}{\frac{\omega^2}{8m}+\frac{\omega^2}{2m}-W} - \frac{2}{\frac{\omega^2}{8m}-W} \right\},$$

$$\Pi_1^{(2)} = \frac{1}{L^3} \sum_{\mathbf{P}_\perp} \left\{ \frac{\frac{\omega^2 q}{4m}}{\left(\frac{\omega^2}{8m}-W\right)^2} + \left(\frac{1}{\frac{\omega^2}{8m}(1+q)-W} - \frac{1}{\frac{\omega^2}{8m}(1-q)-W} \right) \right. \tag{4.17}$$

$$+ \frac{q}{4} \left(\frac{1}{\frac{\omega^2}{8m}(1+q)+\frac{\omega^2}{2m}-W} - \frac{2}{\frac{\omega^2}{8m}(1+q)-W} \right.$$

$$\left. \left. + \frac{1}{\frac{\omega^2}{8m}(1-q)+\frac{\omega^2}{2m}-W} - \frac{2}{\frac{\omega^2}{8m}(1-q)-W} - \frac{2}{\frac{\omega^2}{8m}+\frac{\omega^2}{2m}-W} + \frac{4}{\frac{\omega^2}{8m}-W} \right) \right\}.$$

Note also that the following notation is used:

$$W = E - 2m - \frac{\mathbf{p}_\perp^2}{2m} - \frac{(\mathbf{P}-\mathbf{p})_\perp^2}{2m}. \tag{4.18}$$

Some comments are in order now. As already said, the quantities $\Pi_{0,1}^{(1)}$ can be obtained straightforwardly by using the perturbative expansion of the one-particle propagator, see eq. (3.11). Namely, $\Pi_0^{(1)}$ leads to the Lüscher zeta-function, and $\Pi_1^{(1)}$ is nothing but the triangle diagram (or, the so-called G-function, in the approach of refs. [17, 18]). Hence, the relation to the "standard" approach is clearly visible. However, we already know that this expansion fails in the vicinity of the free particle poles. Indeed, instead of one simple pole at $q = 0$, the one-particle propagator possesses two poles at $q \neq 0$, which are located symmetrically on both sides. Expanding the denominator in powers of q, one gets one double pole instead of two single poles, separated by a distance $2q$. This is schematically shown in figure 5. where the names "exact" and "perturbative" refer to $\Pi_{0,1}$ and $\Pi_{0,1}^{(1)}$, respectively. Furthermore, it is worth noting that, formally, $\Pi_{0,1}^{(2)}$ are at least of order q^2 and can be neglected. We have seen, however that such an approximation does not suffice in the vicinity of the singularities. Another observation is that, in the infinite-volume limit, which can be performed for energies below the two-particle threshold, the quantities $\Pi_{0,1}^{(2)}$ behave like L^{-1} for large L modulo exponential corrections.

4.3 "Exact" vs. "perturbative" solution

A very interesting question arises, namely, whether the solutions of the Lüscher equation in the external field are the same up to terms of order e^2, if one replaces $\Pi_{0,1}$ by $\Pi_{0,1}^{(1)}$ (we remind the reader that the difference between these quantities is *formally* of order e^2). The answer to this question is positive, and will be discussed below.

Let us take, for simplicity, $\mathbf{P}_\perp = 0$ and try to obtain a solution in the vicinity of $E = 2m + \omega^2/(8m)$. The quantities $\Pi_{0,1}$ exhibit here the following behavior

$$\Pi_{0,1} = \frac{c_{0,1}^+(q)}{2m + \frac{\omega^2}{8m}(1+q)-E} + \frac{c_{0,1}^-(q)}{2m + \frac{\omega^2}{8m}(1-q)-E} + \bar{\Pi}_{0,1}, \tag{4.19}$$
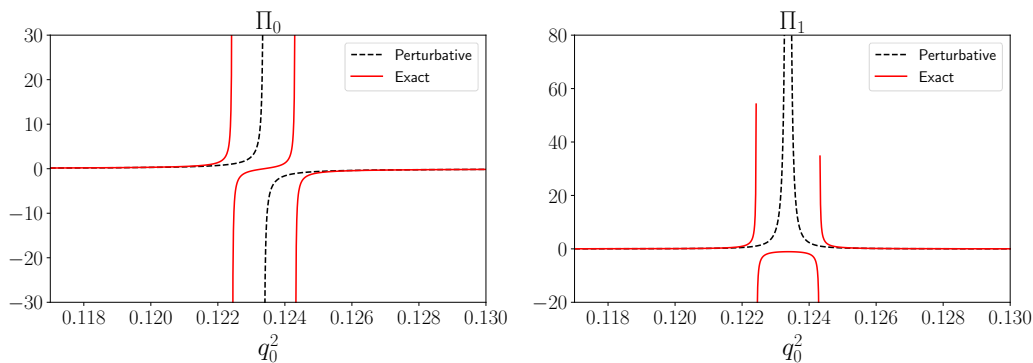
Figure 5. The diagonal and non-diagonal elements of the matrix Π, given in eqs. (4.16) and (4.17). The quantity q_0^2 is given in eq. (2.3). It is seen that the quantity $\Pi_1^{(1)}$ ("perturbative") develops a double pole instead of the two separated simple poles found in Π_1 ("exact"). Since this figure serves illustrative purpose only, we do not specify the values of the parameters in calculations. The units on the vertical axis are arbitrary.

where $\bar{\Pi}_{0,1}$ is a smooth function of E in the vicinity of $E = 2m + \omega^2/(8m)$ and the coefficients

$$c_0^\pm = \frac{1}{L^3}\left(1 \mp \frac{q}{4}\right), \qquad c_1^\pm = \pm\frac{1}{L^3}\left(1 \mp \frac{q}{2}\right), \tag{4.20}$$

can be directly read off from eqs. (4.16) and (4.17). Thus, the Lüscher equation in this case can be reduced to two algebraic equations of the type

$$\mathscr{G}_\pm^{-1}(E) \doteq \frac{c_+(q)}{2m + \frac{\omega^2}{8m}(1+q) - E} + \frac{c_-(q)}{2m + \frac{\omega^2}{8m}(1-q) - E} + f_\pm(E, q) = 0. \tag{4.21}$$

Here, $c_\pm = -\frac{1}{2}\left(c_0^\pm \pm c_1^\pm\right)$ and $f_\pm(E, q)$ are some smooth functions of their arguments which contains $\bar{\Pi}_{0,1}$ as well as the elements of the matrix X, eq. (4.7). Hence, one could expand $f_\pm(E, q)$ in Taylor series in E in the vicinity of the unperturbed level and solve the obtained equations iteratively. At lowest order, $f_\pm(E, q)$ are just constants and one gets quadratic equations for E which can be easily solved. Indeed, rewriting the above equation as

$$\mathscr{G}_\pm^{-1}(E) = \frac{mc_+}{q_+^2 - q_0^2} + \frac{mc_-}{q_-^2 - q_0^2} + f_\pm = 0\,,$$
$$q_\pm^2 = \frac{\omega^2}{16}(1 \pm 2q)\,, \tag{4.22}$$

one gets two roots

$$q_0^2 = q_1^2 + \frac{m(c_+ + c_-)}{2f_\pm} \pm \frac{1}{2f_\pm}\sqrt{D}\,,$$
$$q_1^2 = \frac{1}{2}(q_+^2 + q_-^2) = \frac{\omega^2}{16}\,,$$
$$D = \left(2f_\pm q_1^2 + m(c_+ + c_-)\right)^2 - 4f_\pm(f_\pm q_+^2 q_-^2 + mc_+ q_-^2 + mc_- q_+^2)\,. \tag{4.23}$$

– 21 –

Expanding this solution in powers of q one gets a pair of solutions that differ by the choice of sign in front of the square root

$$q_0^2 = q_1^2 + \frac{m(c_+ + c_-)}{2f_\pm} \pm \frac{m(c_+ + c_-)}{2f_\pm} \left(1 - \frac{f_\pm (q_-^2 - q_+^2)(c_+ - c_-)}{m(c_+ + c_-)^2} \right) + \cdots . \tag{4.24}$$

Choosing the "+" sign, one may verify that one gets exactly the same result as first expanding eq. (4.21) in powers of q and then solving it with respect to E. Higher orders in the expansion in E can be treated in the similar fashion. On the other hand, with the choice of the "−" sign, one arrives at the solution $q_0^2 = q_1^2 + O(q)$. As we shall see below, this corresponds to an unphysical solution.

Albeit the argument, given above, proves that the linear dependence of the energy levels is not altered by using perturbative expansion in $\Pi_{0,1}$, the situation for a finite e is not that clear. It cannot be excluded that the structure of the energy levels is qualitatively different, until e becomes sufficiently small (later, we shall demonstrate this explicitly). For this reason, using the exact solution for $\Pi_{0,1}$ in the fit is preferable.

4.4 Residua

As mentioned earlier, the perturbative expansion contains pitfalls. Here we shall consider one of these. Namely, it will be shown that the use of the *expanded* Lüscher equation might lead to the "fake" poles. The residua of these poles are however of order e^2 and could be thus neglected at the order one is working. In the actual fit to the lattice data, one should carefully identify such poles and exclude them from the analysis.

Below, for simplicity, we restrict ourselves to the case of the 2×2 matrix already considered above. The quantity $\mathscr{G}(E)$, defined in eq. (4.21), contains single poles at $q_0^2 = q_n^2$, which are given, in particular, by eq. (4.24). In the vicinity of such a pole,

$$\mathscr{G}(E) = \frac{\mathscr{Z}_n}{q_n^2 - q_0^2} + \text{regular} . \tag{4.25}$$

Differentiating both sides of the above equation with respect to q_0^2, one may easily ensure that the residuum at the pole, $\mathscr{Z}_n$, is given by the derivative of $\mathscr{G}_\pm^{-1}(E)$ at the pole:

$$\mathscr{Z}_n^{-1} = - \lim_{q_0^2 \to q_n^2} [\mathscr{G}_\pm^{-1}(E)]' . \tag{4.26}$$

On the other hand, from eq. (4.22) one gets

$$[\mathscr{G}_\pm^{-1}(E)]' = \frac{mc_+}{(q_+^2 - q_0^2)^2} + \frac{mc_-}{(q_-^2 - q_0^2)^2} + f_\pm' . \tag{4.27}$$

Equation (4.24) describes two solutions, which differ by the choice of the sign in front of the last term. Taking into account the fact that $c_+ \pm c_- = O(1)$ and $q_\pm^2 - q_1^2 = O(q)$, one immediately gets that the quantity $\mathscr{Z}$ is of order 1 and order q^2 for the first and the second solution, respectively. This demonstrates that the second solution is an artifact of the approximations used, since the terms of order q^2 in the numerators have been systematically neglected.

4.5 Extracting the resonance pole

In the infinite volume momenta are no more quantized. However, the conservation of the three-momentum, $\mathbf{P} = \mathbf{Q} \pm \ell\boldsymbol{\omega}$, implies that the two-point function of the composite fields for a fixed $\boldsymbol{\omega}$ still obeys the matrix equation (4.5). In this equation, however, $\mathbf{P}, \mathbf{Q}, \boldsymbol{\omega}$ are no more restricted to integer multiples of $2\pi/L$. Furthermore, the kernel X is the same (modulo replacing the Kronecker deltas by the Dirac delta-functions), and the loop function Π is replaced by its infinite-volume counterpart that amounts to replacing the sum over the loop momenta by an integral.

A crucial point is that we can use the perturbative expansion (3.11) in the coupling e. The reason is that, in order to find the position of the resonance pole, we are going to solve the infinite-volume analog of eq. (4.5) in the complex plane, where the energy denominator, appearing in the loop, is not singular and the perturbative expansion is justified. However, as seen above, when solving the Lüscher equation on the real axis, the perturbative series diverges in the vicinity of the singularities. Hence, in a finite volume, it is preferable to work with the full expression of the Lüscher zeta-function in the external field.[13]

Up to $O(e)$ terms, the loop function Π in the infinite volume takes the form:

$$
\begin{aligned}
\Pi(\mathbf{P}, \mathbf{Q}; E) = {} & (2\pi)^3 \delta^3(\mathbf{P} - \mathbf{Q}) \Pi_0(\mathbf{P}; E) \\
& + eA_0 \Gamma (2\pi)^3 \big[\delta^3(\mathbf{P} + \boldsymbol{\omega} - \mathbf{Q}) + \delta^3(\mathbf{P} + \boldsymbol{\omega} - \mathbf{Q}) \big] \Pi_1(\mathbf{P}, \mathbf{Q}; E) + O(e^2),
\end{aligned}
\tag{4.28}
$$

where

$$
\begin{aligned}
\Pi_0(\mathbf{P}; E) &= \int \frac{dp^0}{2\pi i} \int \frac{d^3\mathbf{p}}{(2\pi)^3} \frac{1}{\left(m + \frac{\mathbf{p}^2}{2m} - p^0 \right) \left(m + \frac{(\mathbf{P} - \mathbf{p})^2}{2m} - E + p^0 \right)} \\
&= \frac{m}{4\pi} \left[-m \left(E - 2m - \frac{\mathbf{P}^2}{4m} \right) \right]^{1/2}, \\
\Pi_1(\mathbf{P}, \mathbf{Q}; E) &= \int \frac{dp^0}{2\pi i} \int \frac{d^3\mathbf{p}}{(2\pi)^3} \frac{1}{\left(m + \frac{\mathbf{p}^2}{2m} - p^0 \right) \left(m + \frac{(\mathbf{P} - \mathbf{p})^2}{2m} - E + p^0 \right)} \\
&\quad \times \frac{1}{\left(m + \frac{(\mathbf{Q} - \mathbf{p})^2}{2m} - E + p^0 \right)} \\
&= -\frac{m^2}{8\pi} \int_0^1 dx \frac{1}{\sqrt{m(2m + \mathbf{P}^2/(4m) - E) + \frac{1}{4}\omega^2 x(1-x)}} \\
&= -\frac{m^2}{2\pi\omega} \arcsin \frac{\omega}{\sqrt{16m(2m + \mathbf{P}^2/(4m) - E) + \omega^2}} \,.
\end{aligned}
\tag{4.29}
$$

Note that the sign convention in front of the square roots in the above expressions corresponds to the choice of the second Riemann sheet.

---

[13]One should stress here once more that one is forced to exclusively use perturbative expressions within the "standard" approach. From the discussion above it is however clear that both approaches are algebraically equivalent at $O(e)$ (as it should be).

The procedure for determining the position of the pole on the second Riemann sheet is as follows. First, one uses the finite-volume energy levels in the Breit frame, $\mathbf{P} = -\mathbf{Q} = \pm\boldsymbol{\omega}/2$, to extract the parameters of the Lagrangian using the Lüscher equation with an external field, eq. (4.5). In our case, there is a single unknown parameter κ. Next, solving the same equation in the infinite volume, using eq. (4.29), with the extracted values of the couplings, one determines the position of the pole on the second sheet. In this manner, one could study the dependence of the pole position with e. It can be seen that a pair of poles emerges which move in opposite directions as e increases. At first order of e, they move with the same rate.

4.6 Relation to the resonance form factor

From the previous discussion, the infinite-volume two-point function in the external field possesses poles on the second Riemann sheet. In the vicinity of a pole, the residue factorizes. In the Breit frame, one has:

$$D(\mathbf{P}, \mathbf{Q}; E) \to (2\pi)^3 \delta^3(\mathbf{P} - \mathbf{Q} \pm \boldsymbol{\omega}) \frac{\Phi(\mathbf{P})\bar{\Phi}(-\mathbf{P})}{P^0(\mathbf{P}) - P_R^0(\mathbf{P}, e)}. \tag{4.30}$$

Here, we have explicitly indicated the dependence on the parameter e.

Next, we shall differentiate both sides of the above equation with respect to e and set $e = 0$ at the end (because we are interested only in the terms linear in e). The most singular term (a double pole) comes from differentiating the denominator. Hence,

$$\frac{d}{de} D(\mathbf{P}, \mathbf{Q}; E)\bigg|_{e=0} \to (2\pi)^3 \delta^3(\mathbf{P} - \mathbf{Q} \pm \boldsymbol{\omega}) \frac{\Phi(\mathbf{P})\bar{\Phi}(-\mathbf{P})}{(P^0(\mathbf{P}) - P_R^0(\mathbf{P}, 0))^2} \frac{dP_R^0(\mathbf{P}, e)}{de}\bigg|_{e=0}$$
$$+ \text{less singular terms.} \tag{4.31}$$

On the other hand, the quantity D can be identically rewritten as $D = DD^{-1}D$. Differentiating with respect to e, one gets $\frac{d}{de} D = -D\left(\frac{d}{de} D^{-1}\right)D$. The quantity D at $e = 0$ has a pole

$$D(\mathbf{P}, \mathbf{Q}; E) \to (2\pi)^3 \delta^3(\mathbf{P} - \mathbf{Q}) \frac{\Phi(\mathbf{P})\bar{\Phi}(\mathbf{P})}{P^0(\mathbf{P}) - P_R^0(\mathbf{P}, 0)}. \tag{4.32}$$

Taking into account the definition (2.14) and comparing with eq. (2.16), one can straightforwardly read off the relation between the quantity $\Phi(\mathbf{P})$ and the wave function $\Psi(\mathbf{P}, \mathbf{p})$, introduced in section 2:

$$\Phi(\mathbf{P}) = \int \frac{d^3\mathbf{p}}{(2\pi)^3} \Psi(\mathbf{P}, \mathbf{p}). \tag{4.33}$$

An important remark is in order. In the limit $e = 0$, the three-momentum is conserved and, hence, one can establish the relation between Ψ and Φ only for $\mathbf{P} = \mathbf{Q}$. However, the fact that the residue at the pole factorizes, enables one to write down the residue for $\mathbf{P} \neq \mathbf{Q}$ as well. In simple cases like the one considered here, the factorization at the pole can be verified explicitly, carrying out the truncation in the $\mathbf{P}, \mathbf{Q}$ space and inverting the resulting matrix.

Finally, using $D^{-1} = \frac{1}{2}\Pi^{-1} - \frac{1}{4}X$ and taking into account eqs. (4.6) and (4.28), one gets

$$\frac{d}{de}D(\mathbf{P}, \mathbf{Q}; E) \to -(2\pi)^3\delta^3(\mathbf{P} - \mathbf{Q} \pm \boldsymbol{\omega})\frac{\Phi(\mathbf{P})\bar{\Phi}(\mathbf{P})\,\Phi(-\mathbf{P})\bar{\Phi}(-\mathbf{P})}{(P^0(\mathbf{P}) - P_R^0(\mathbf{P}, 0))^2}$$
$$\times \left[-\frac{1}{2}A_0\Pi_0^{-1}(\mathbf{P}, E_R)\Gamma\Pi_1(\mathbf{P}, -\mathbf{P}; E_R)\Pi_0^{-1}(-\mathbf{P}; E_R) - \frac{1}{8}X_{\mathbf{P},-\mathbf{P}}^{(1)}(E_R) \right].$$
(4.34)

Comparing eqs. (4.31) and (4.34), we finally obtain:

$$\left.\frac{dP_R^0(\mathbf{P})}{de}\right|_{e=0}$$
$$= \frac{1}{2}\bar{\Phi}(\mathbf{P})\left[\Pi_0^{-1}(\mathbf{P}, E_R)A_0\Gamma\Pi_1(\mathbf{P}, -\mathbf{P}; E_R)\Pi_0^{-1}(-\mathbf{P}; E_R) + \frac{1}{4}X_{\mathbf{P},-\mathbf{P}}^{(1)}(E_R)\right]\Phi(-\mathbf{P}). \quad (4.35)$$

In order to prove that this expression is the same as eq. (2.23), let us first assume that $C_2 = 0$ and use $\tilde{A}^0(\mathbf{P} - \mathbf{Q}) = \frac{1}{2}(2\pi)^3(\delta^3(\mathbf{P} - \mathbf{Q} + \boldsymbol{\omega}) + \delta^3(\mathbf{P} - \mathbf{Q} - \boldsymbol{\omega})$. When $C_2 = 0$, the integration over the relative momenta in eq. (2.23) is performed trivially, yielding eq. (4.35) (note that eq. (4.33) should be used to prove this relation). If $C_2 \neq 0$, in analogy to what was done before, one has to pull out the derivatives acting on the internal lines. Then, the expression for $X^{(1)}$ will be modified and one arrives again at eq. (4.7). Equations (2.23) and (4.35) are also equivalent in this case. Finally, we arrive at our final result that looks remarkably simple:

$$\frac{1}{2}A_0F(\mathbf{P}, -\mathbf{P}) = \left.\frac{dP_R^0(\mathbf{P})}{de}\right|_{e=0}. \quad (4.36)$$

In other words, in the Breit frame the resonance form factor is given by the derivative of the resonance pole position with respect to the coupling constant with the external field.[14]

To summarize, all what is needed to compute the resonance form factor is the contact contribution (at the lowest order, this is parameterized by a single coupling constant, κ). The latter can be determined by fitting directly the energy levels in the external field.[15] The resonance form factor can be then calculated using eqs. (2.22) and (2.23). Hence, extracting the resonance pole first and using then a Feynman-Hellmann theorem is even superfluous. However, the direct analogy with the Feynman-Hellmann theorem for the form factors of stable particles is still remarkable.

Extracting the contact contribution could, however, be complicated, since this contribution contains suppression factors. For example, from eq. (4.11) it is seen that the contribution containing κ is multiplied by a factor $k^2(\mathbf{P}; E)$. In the case of a shallow and narrow resonance, this approximately equals to q_0^2. In addition, owing to gauge invariance, a factor ω^2 is present. This, however, is not an obstacle for the extraction of the form

---

[14]As already mentioned, each pole $e = 0$ splits into two, moving in the opposite direction at equal speed, when the external field is turned on. Choosing another pole yields just a different sign in eq. (4.36).

[15]For instance, it could be advantageous to fit the quantity $\Delta \doteq \langle E \rangle_{\phi^2} - 2\langle E \rangle_\phi$, calculated on the lattice in the presence of the external field. This quantity describes the energy shift of the two-particle state caused by the interactions between them and might be more sensitive to the small effects coming from contact interactions parameterized by κ.

factor, since the same suppression factors also emerge in the expression of the latter in the infinite volume. In other words, if the quantity κ, determined on the lattice, is zero within the error bars, this simply means that the form factor at this accuracy is given only by the impulse approximation.

4.7 Relativistic corrections, higher partial waves and all that

In this section we briefly consider the generalization of the above approach to higher orders in the momentum expansion. This is needed, in particular, to render the approach applicable to the study of the problems where relativistic effects cannot be neglected. The inclusion of the higher-derivative interaction terms (an analog of the term with C_2), which also describe higher partial waves, as well as derivative four-particle interaction with the external field (similar to the coupling κ), proceeds relatively straightforwardly and will not be considered here. A single non-trivial piece is the modification of the Lagrangian in the single particle sector. As it is known, derivative insertions in the non-relativistic propagators should be summed up to all orders, in order to arrive at a correct dispersion relation. We shall try to do the same in presence of the external field below.

In general, writing down all terms in the one-particle sector is a complicated task (in higher orders) and can be carried out order by order in the expansion in the inverse mass. Matching should be performed in the same setting, order by order in the expansion. The situation simplifies dramatically, if we additionally restrict ourselves to terms that are linear in e. These should be matched to the relativistic form factor $F_\mu(p', p) = ie(p'_\mu + p_\mu)F(t)$, with $t = (p' - p)^2$. In this case, the form of the Lagrangian can be read off directly from the matching condition and takes the form (the differential operators act on everything right to them):

$$\mathcal{L} = \phi^\dagger \left(i\partial_t - W + e\Gamma \frac{1}{\sqrt{2W}} \left(W A^0(\mathbf{x}) + A^0(\mathbf{x})W \right) \frac{1}{\sqrt{2W}} \right) \phi$$

$$+ \text{ terms with four fields} . \tag{4.37}$$

Here, $W = \sqrt{m^2 - \triangle}$ denotes the relativistic energy operator, and $\Gamma(\boldsymbol{\omega}) = F(-\omega^2)$. The equation for the one-particle wave function takes the form

$$\left(i\partial_t - W + e\Gamma \frac{1}{\sqrt{2W}} \left(W A^0(\mathbf{x}) + A^0(\mathbf{x})W \right) \frac{1}{\sqrt{2W}} \right) \Phi(\mathbf{x}, t) = 0 . \tag{4.38}$$

Using eq. (A.1), this equation can be rewritten as

$$\left(E - W_\perp + e\Gamma \frac{1}{\sqrt{2W_\perp}} \left(W_\perp A^0(\mathbf{x}) + A^0(\mathbf{x})W_\perp \right) \frac{1}{\sqrt{2W_\perp}} \right) \bar{\Phi}(z) = 0 , \tag{4.39}$$

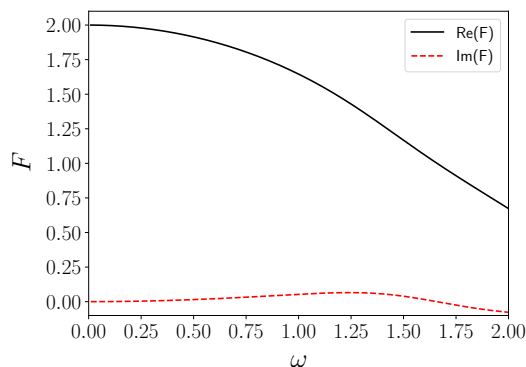where

$$W_\perp = \sqrt{m^2 + \mathbf{p}_\perp^2 + \frac{4}{\omega^2} \frac{d^2}{dz^2}} . \tag{4.40}$$

Albeit eq. (4.39) does not have the form of the Mathieu equation, at first order in e it can be reduced to it through the redefinition of the wave function:

$$\bar{\Phi}(z) = \sqrt{2W_\perp} \left(1 - \frac{e\Gamma}{\sqrt{2W_\perp}} A^0(\mathbf{x}) \right) \bar{\Phi}'(z) . \tag{4.41}$$

Figure 6. Real and imaginary parts of the resonance form factor.

The equation for the transformed wave function can then be rewritten as:

$$\left(E - W_\perp + e\Gamma A^0(\mathbf{x}) + O(e^2) \right) \bar{\Phi}'(z) = 0 \,, \tag{4.42}$$

or similarly,

$$\left((E + e\Gamma A^0(\mathbf{x}))^2 - W_\perp^2 + O(e^2) \right) \bar{\Phi}'(z)$$
$$= \left(E^2 - m^2 - \mathbf{p}_\perp^2 + \frac{4}{\omega^2} \frac{d^2}{dz^2} + \frac{2Ee\Gamma}{\omega} \cos 2z + O(e^2) \right) \Phi'(z) = 0 \,. \tag{4.43}$$

This is an equation of the Mathieu type, where the non-relativistic dispersion law (as in eq. (A.2)) is replaced by the relativistic expression $E^2 - m^2 + \mathbf{p}_\perp^2$. Note, however, that the parameter q in this equation depends on the eigenvalue E, so the solutions can be found only numerically with an iterative procedure. Once this is done, one can construct the eigenvectors, using eq. (4.41). These eigenvectors, in turn, can be used to construct the one-particle propagators and to calculate the Lüscher zeta-function in the periodic external field. Since the primary aim of the present paper is the proof of principle, we shall not consider all these rather straightforward issues here, which form a separate piece of work for the future.

5 Numerical implementation

In this section, we shall test our theoretical predictions numerically. Since this test serves an illustrative purpose only, we have not made an attempt to choose realistic values of the different parameters in the toy model. In particular, we choose $m = 1$ from the beginning and show everything in mass units. The values of other parameters are $a = -1.5$, $r = -9$, $\kappa = 10$ and $C_R = 0.9$. Without loss of generality, one may set $A_0 = 1$. With this choice of parameters, there exist a couple of poles on the second Riemann sheet located at $q_R^2 = 0.123 \pm i\, 0.082$. The resonance form factor, evaluated with the help of eqs. (2.22) and (2.23), is shown in figure 6. Note that, owing to the Ward identity, the form factor is normalized as $F(0) = 2$ at $\omega = 0$.
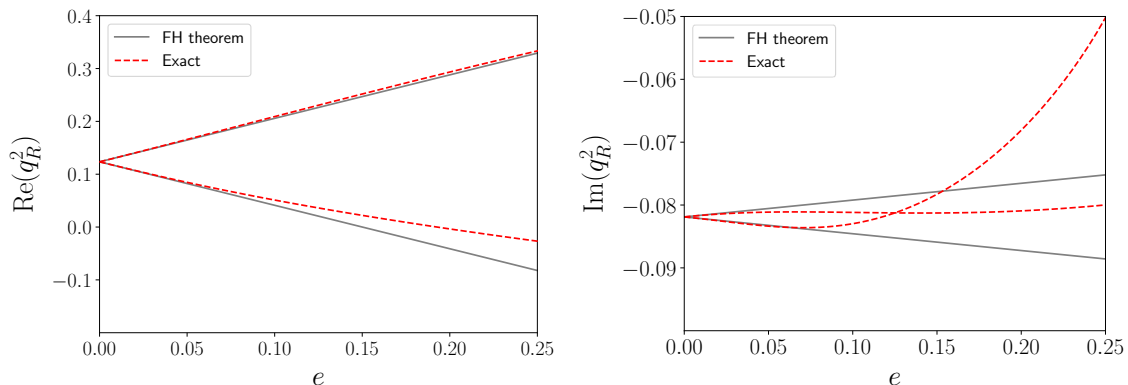
Figure 7. Verification of the Feynman-Hellmann theorem for the real and imaginary parts of the pole position in the complex plane at $\omega = 1$. Thin black lines depict the prediction of the theorem.

Furthermore, when $e \neq 0$, the pole in the complex plane splits into two that move in the opposite direction from the initial location. In figure 7 we plot the real and imaginary parts of these poles versus e. It is seen that at small values of e this dependence is almost linear and is determined by the Feynman-Hellmann theorem. For this example with $\omega = 1$, we obtain

$$F(\mathbf{P}, \mathbf{Q}) = 1.6454 + i0.0535, \qquad 2\frac{dP_R^0}{de}\bigg|_{e=0} = 1.6455 + i0.0534. \tag{5.1}$$

The second number has been obtained by numerically differentiating the pole trajectory in the complex plane. The explicit expression of the form factor in this model is written down in appendix D.

In figure 8, we display the spectrum in a finite volume at different values of e and for a fixed L (In order to discuss the qualitative behavior of the spectrum we used an arbitrarily chosen value $L = 20$). The structure of the levels turns out to be rather complicated. In the absence of field, there is a set of doubly degenerate energy levels (black filled dots) corresponding to states with momentum $\mathbf{P}$ and $-\mathbf{P}$, which are related by a time-reversal transformation. When $e \neq 0$, time-reversal invariance is broken and these two levels split symmetrically at $O(e)$. Moreover, there are additional energy levels which do not have a zero-field counterpart. This is attributed to the fact that, at $e \neq 0$, the poles in the functions Π_0, Π_1 also split (see figure 5), and the determinant in the Lüscher equation can cross the real axis at more places, e.g., between the poles. However, it can be easily checked that these solutions correspond to the "artifacts" that were discussed in the previous section. Namely, the residua corresponding to these levels are of order e^2 and have a different sign as compared to the physical levels. We have also checked that the unphysical levels, in difference with the physical ones, are not stable if the dimension of the matrix in the quantization condition is increased. This fact further supports the conclusion that these levels emerge due to the approximations that were made during the derivation of the quantization condition. Hence, in the analysis of data, such unphysical levels should be merely discarded.
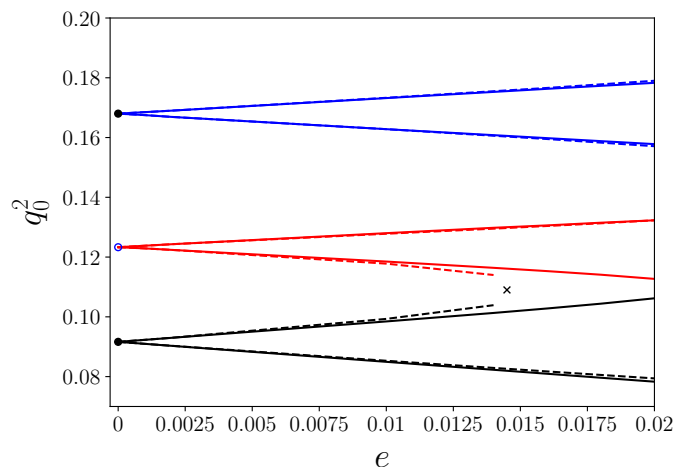
Figure 8. Qualitative structure of the energy levels in the external field. The levels at $e = 0$ are denoted by black filled dots. These are split when $e \neq 0$. There are additional levels (red curves) that do not have counterparts at $e = 0$. On the figure, they emanate from the empty blue dot. The solid and dotted lines denote the "exact" and "perturbative" solutions, respectively, depending on the use of the "exact" and "perturbative" expressions for the loop function. The approximate location where two "perturbative" levels merge and disappear is marked by a cross.
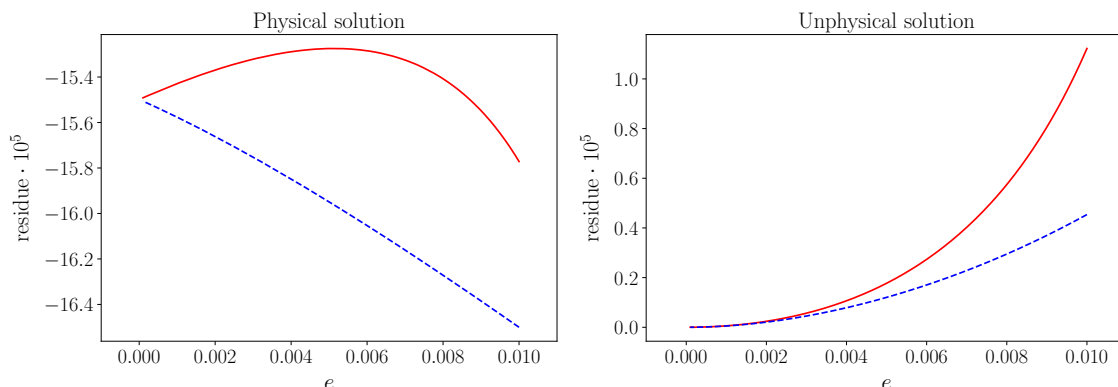
Figure 9. The e-dependence of the residua for the physical and unphysical levels. The blue and red curves correspond to the two different solutions of the quantization condition.

Furthermore, figure 8 nicely demonstrates the limitations of the use of the perturbative approach to the calculation of Π_0, Π_1. In the vicinity of $e = 0.015$, two "perturbative" levels merge and disappear (the determinant does not cross the real axis anymore), whereas the "exact" levels still exist. Note that this happens already at rather small values of e, for which other levels are very well described by the perturbative solution.

In figure 9, the difference between the physical and unphysical levels is clearly seen. Here, we plot the e-dependence of the residua, calculated using eq. (4.26) (blue and red lines correspond to the two roots of the quantization condition that merge in the limit $e = 0$). For the physical levels, the residua converge to a non-zero limit and exhibit a linear dependence on e for small e. In contrast to this, the residua for the unphysical levels behave as e^2 and vanish for $e = 0$. This agrees with our theoretical findings.
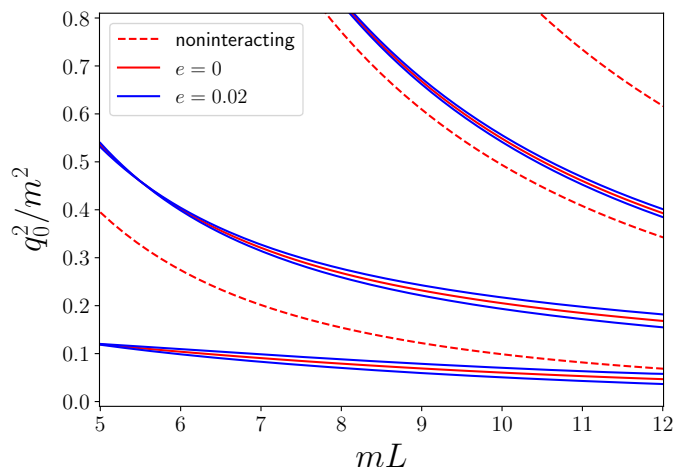
Figure 10. The *L*-dependence of the energy levels for $e = 0$, as well as for $e \neq 0$. For comparison, we plot the non-interacting energy levels as well, corresponding to the two free particles in a box. A single energy level at $e = 0$ splits into two nearby levels, when the external field is turned on.

In addition to this, in figure 10 we show the *L*-dependence of the energy levels ("exact" solutions only). Finally, note that, with our choice of parameters, the contribution from the contact interaction, parameterized by the coupling κ, is negligibly small. This could be expected, since the first term in eq. (4.11) is much smaller that the second. However, as already discussed, this cannot pose an obstacle for the calculation of the resonance form factor, the goal we are after.

6 Conclusions

i) A novel method for the computation of the resonance form factors on the lattice has been proposed. Within this approach, one circumvents the calculation of the three-point function on the lattice, measuring instead the finite-volume energy spectrum in an external periodic field in space.

ii) It is known that the finite-volume three-point function, figure 1a, has an irregular dependence of the box size *L* that complicates the extraction of the infinite-volume form factor considerably. On the other hand, with this method, one merely needs to extract the parameters of the contact interaction with the external field from the fit to the energy levels at $e \neq 0$. These parameters, by definition, can only contain exponentially suppressed corrections in *L*.

iii) If the lattice simulations are performed at a non-zero external field, the formalism that is used to analyze the data should be also set in the presence of the external field. In order to match this objective, a generalization of the Lüscher equation in the presence of an external periodic field is obtained in this paper.

iv) Since in the vicinity of the free-particle poles the use of perturbation theory is questionable, an expression for the modified Lüscher function has been derived that

avoids the expansion of the energy denominators. The limits of the use of perturbation theory in this context have been discussed in detail. On the other hand, for consistency, one is forced to use a strictly perturbative framework to analyze data on the matrix elements in the "standard" approach [1, 16–18]. Of course, in the limit $e \to 0$, the matrix elements extracted within two different approaches, agree.

v) The Feynman-Hellmann theorem, which has been so far proven for stable particles only, is generalized to the case of resonances. It has been demonstrated that, finding the (complex) resonance pole position in the external field and in the Breit frame, and differentiating this quantity with respect to e, one arrives at the form factor. The theoretical arguments have been checked numerically, see eq. (5.1).

vi) A numerical implementation of the framework is considered for a toy model. The qualitative structure of the energy levels is discussed.

vii) The present work provides a proof of principle only. Different improvements and generalizations will have to be considered. For example, it will be crucial to take into account relativistic corrections to all orders and write down a framework that is explicitly Lorentz-invariant. Furthermore, higher orders in the effective theory should be systematically included in order to write down the result in a form that does not explicitly rely on the effective-range expansion, and is also valid away from the elastic threshold. Partial-wave mixing should also be addressed appropriately. Finally, the numerical implementation should be considered for realistic values of the parameters that resemble the cases of existing low-lying resonances. All these technical issues will be addressed in the future.

Acknowledgments

A Mathieu equation: essentials

The differential equation (3.4) admits variable separation by using the ansatz

$$\Phi(\mathbf{x}, t) = e^{-iEt + i\mathbf{p}_\perp \mathbf{x}_\perp} \bar{\Phi}(z), \qquad z = \frac{\omega x_\parallel}{2}, \tag{A.1}$$

where the function $\bar{\bar{\Phi}}(z)$ obeys the differential equation

$$\left(\frac{d^2}{dz^2} + \frac{8m}{\omega^2}\left(E - m - \frac{\mathbf{p}_\perp^2}{2m}\right) + \frac{8me\Gamma A_0}{\omega^2}\cos 2z\right)\bar{\bar{\Phi}}(z) = 0\,. \tag{A.2}$$

This coincides with the Mathieu equation [32].[8] Note that the potential in the above equation is periodic, and hence the solutions are given by Bloch's wave functions that have the property

$$\bar{\bar{\Phi}}(z + \pi) = e^{i\nu\pi}\bar{\bar{\Phi}}(z)\,, \qquad -1 < \nu \le 1\,. \tag{A.3}$$

The solutions corresponding to a particular ν (the so-called ν-periodic solutions) are denoted by $\mathrm{me}_{\nu+2n}(z, q)$ (with an integer n) and obey the equation

$$\left(\frac{d^2}{dz^2} + \lambda_{\nu+2n}(q) - 2q\cos 2z\right)\mathrm{me}_{\nu+2n}(z, q) = 0\,. \tag{A.4}$$

From the comparison of eqs. (A.2) and (A.4) it follows that

$$\lambda_{\nu+2n}(q) = \frac{8m}{\omega^2}\left(E - m - \frac{\mathbf{p}_\perp^2}{2m}\right)\,. \tag{A.5}$$

In case when ν becomes integer, one has

$$\lambda_n(q) = \begin{cases} a_n(q)\,, & n = 0, 1, \cdots \\ b_{-n}(q)\,, & n = -1, -2, \cdots \end{cases} \tag{A.6}$$

and

$$me_n(z, q) = \begin{cases} \sqrt{2}\,ce_n(z, q), & n = 0, 1, \cdots \\ -\sqrt{2}i\,se_{-n}(z, q), & n = -1, -2, \cdots \end{cases} \tag{A.7}$$

Due to the periodic boundary conditions, the parameter ν will be quantized. Indeed, from $\Phi(x_\parallel + L) = \Phi(x_\parallel)$ we get $\bar{\bar{\Phi}}(z + \pi N) = e^{i\nu\pi N}\bar{\bar{\Phi}}(z) = \bar{\bar{\Phi}}(z)$, leading to the condition $e^{i\nu\pi N} = 1$. Together with the requirement $-1 < \nu \le 1$ this leads to the conclusion that ν can take the following values

$$\begin{aligned} N = 1: \quad & \nu = 0 \\ N = 2: \quad & \nu = 0, 1 \\ N = 3: \quad & \nu = -\frac{2}{3}, 0, \frac{2}{3} \\ N = 4: \quad & \nu = -\frac{1}{2}, 0, \frac{1}{2}, 1 \end{aligned} \tag{A.8}$$

and so on.

The Fourier expansion of the Mathieu functions takes the form

$$\mathrm{me}_\nu(z, q) = \sum_{a=-\infty}^{\infty} C_{2a}^\nu(q)e^{i(\nu+2a)z}\,. \tag{A.9}$$

The coefficients of this expansion, $C_{2a}^\nu(q)$, are known.[8]

B Expansion of the propagator in powers of q

The expansion of Mathieu functions $me_\nu(z, q)$ in powers of q for the non-integer (ν) and integer $(k \geq 2)$ values of the index is given by

$$\mathrm{me}_\nu(z,q) = e^{i\nu z} - \frac{q}{4}\left(\frac{1}{\nu+1}e^{i(\nu+2)z} - \frac{1}{\nu-1}e^{i(\nu-2)z}\right) + O(q^2),$$

$$\mathrm{me}_k(z,q) = \sqrt{2}\left\{\cos kz - \frac{q}{4}\left(\frac{1}{k+1}\cos(k+2)z - \frac{1}{k-1}\cos(k-2)z\right) + O(q^2)\right\},$$

$$\mathrm{me}_{-k}(z,q) = -i\sqrt{2}\left\{\sin kz - \frac{q}{4}\left(\frac{1}{k+1}\sin(k+2)z - \frac{1}{k-1}\sin(k-2)z\right) + O(q^2)\right\}. \quad (B.1)$$

If $k = 1, 0, -1$, the pertinent expressions take the form

$$\mathrm{me}_1(z,q) = \sqrt{2}\left\{\cos z - \frac{q}{8}\cos 3z + O(q^2)\right\},$$

$$\mathrm{me}_0(z,q) = 1 - \frac{q}{2}\cos 2z + O(q^2),$$

$$\mathrm{me}_{-1}(z,q) = -i\sqrt{2}\left\{\sin z - \frac{q}{8}\sin 3z + O(q^2)\right\}. \quad (B.2)$$

In order to perform the expansion of the two-point function $S(\mathbf{x}, \mathbf{y}; E)$, given by eq. (3.9), one should consider the cases of odd and even N separately. In case of the odd N, the only integer value of the parameter ν in the interval $\nu \in]-1, 1]$ is $\nu = 0$. In case of the even N, there are two integer values $\nu = 0, 1$. In the sum over all eigenvectors, one should separate the integer and non-integer values of ν, and carry out the expansion in q in each term.

Let us start from the more simple case of the odd N. Here, $i = 1$ corresponds to the value $\nu_i = 0$. The eigenvalues are given by $\lambda_{\nu_i+2n} = (\nu_i + 2m)^2 + O(q^2)$. The original expression of the propagator can be split into three terms $S = S_1 + S_2 + S_3$, where, at $O(q^2)$,

$$S_1 = \frac{1}{L^3}\sum_{\mathbf{p}_\perp}\sum_{i=2}^{N}\sum_{n=-\infty}^{\infty}\frac{e^{i\mathbf{p}_\perp(\mathbf{x}_\perp-\mathbf{y}_\perp)}}{m + \frac{\mathbf{p}_\perp^2}{2m} + \frac{\omega^2}{8m}(\nu_i+2n)^2 - E}$$
$$\times\left[e^{i(\nu_i+2n)\frac{\omega x_\parallel}{2}} - \frac{q}{4}\left(\frac{e^{i(\nu_i+2n+2)\frac{\omega x_\parallel}{2}}}{\nu_i+2n+1} - \frac{e^{i(\nu_i+2n-2)\frac{\omega x_\parallel}{2}}}{\nu_i+2n-1}\right)\right]$$
$$\times\left[e^{-i(\nu_i+2n)\frac{\omega y_\parallel}{2}} - \frac{q}{4}\left(\frac{e^{-i(\nu_i+2n+2)\frac{\omega y_\parallel}{2}}}{\nu_i+2n+1} - \frac{e^{-i(\nu_i+2n-2)\frac{\omega y_\parallel}{2}}}{\nu_i+2n-1}\right)\right],$$

$$= \frac{1}{L^3}\sum_{\mathbf{p}_\perp}\sum_{i=2}^{N}\sum_{n=-\infty}^{\infty}\frac{e^{i\mathbf{p}_\perp(\mathbf{x}_\perp-\mathbf{y}_\perp)}}{m + \frac{\mathbf{p}_\perp^2}{2m} + \frac{\omega^2}{8m}(\nu_i+2n)^2 - E}e^{i(\nu_i+2n)\frac{\omega(x_\parallel-y_\parallel)}{2}}$$
$$\times\left[1 - \frac{q}{4}\left(\frac{e^{i\omega x_\parallel}}{\nu_i+2n+1} - \frac{e^{-i\omega x_\parallel}}{\nu_i+2n-1} + \frac{e^{-i\omega y_\parallel}}{\nu_i+2n+1} - \frac{e^{i\omega y_\parallel}}{\nu_i+2n-1}\right)\right], \quad (B.3)$$

$$S_2 = \frac{1}{L^3}\sum_{\mathbf{p}_\perp}\sum_{n=0}^{\infty}\frac{e^{i\mathbf{p}_\perp(\mathbf{x}_\perp-\mathbf{y}_\perp)}}{m + \frac{\mathbf{p}_\perp^2}{2m} + \frac{\omega^2}{8m}(2n)^2 - E}\left[2\mathrm{ce}_{2n}\left(\frac{\omega x_\parallel}{2}, q\right)\mathrm{ce}_{2n}\left(-\frac{\omega y_\parallel}{2}, q\right)\right], \quad (B.4)$$

– 33 –

and

$$S_3 = \frac{1}{L^3} \sum_{\mathbf{p}_\perp} \sum_{n=-\infty}^{-1} \frac{e^{i\mathbf{p}_\perp(\mathbf{x}_\perp - \mathbf{y}_\perp)}}{m + \frac{p_\perp^2}{2m} + \frac{\omega^2}{8m}(2n)^2 - E} \left[-2\mathrm{se}_{2n}\left(\frac{\omega x_\parallel}{2}, q\right) \mathrm{se}_{2n}\left(-\frac{\omega y_\parallel}{2}, q\right) \right]. \qquad \text{(B.5)}$$

Using eq. (B.2), one could rewrite the last two terms at $O(q)$ in the following form:

$$S_2 + S_3 == \sum_{n=-\infty}^{\infty} \sum_{\mathbf{p}_\perp} \frac{e^{i\mathbf{p}_\perp(\mathbf{x}_\perp - \mathbf{y}_\perp)}}{m + \frac{\mathbf{p}_\perp^2}{2m} + \frac{\omega^2 n^2}{2m} - E} e^{in\omega(x_\parallel - y_\parallel)}$$
$$\times \left\{ 1 - \frac{q}{4}\left(\frac{e^{-i\omega y_\parallel}}{2n+1} - \frac{e^{i\omega y_\parallel}}{2n-1} + \frac{e^{i\omega x_\parallel}}{2n+1} - \frac{e^{-i\omega x_\parallel}}{2n-1} \right) \right\}. \qquad \text{(B.6)}$$

It is easy to see that eq. (B.6) follows from eq. (B.3) for $\nu_i = 0$. Hence, one could lump together these two expressions, extending the sum in eq. (B.3) from $i = 1$ to $i = N$. Furthermore, defining $p_\parallel = \frac{\omega}{2}(\nu_i + 2n)$, it is easily seen that the sum over all i, n is equivalent to sum over all $p_\parallel = \frac{2\pi}{L} k$, where $k \in \mathbb{Z}$. Defining further $\mathbf{p} = (\mathbf{p}_\perp, p_\parallel)$ and $\mathbf{px} = \mathbf{p}_\perp \mathbf{x}_\perp - p_\parallel x_\parallel$, the two-point function can be rewritten in a more compact form:

$$S(\mathbf{x}, \mathbf{y}; E) = \frac{1}{L^3} \sum_{\mathbf{p}} \frac{e^{i\mathbf{p}(\mathbf{x}-\mathbf{y})}}{m + \frac{\mathbf{p}^2}{2m} - E}$$
$$\times \left\{ 1 - \frac{\omega q}{8}\left(\frac{e^{i\omega x_\parallel}}{p_\parallel + \frac{\omega}{2}} - \frac{e^{-i\omega x_\parallel}}{p_\parallel - \frac{\omega}{2}} + \frac{e^{-i\omega y_\parallel}}{p_\parallel + \frac{\omega}{2}} - \frac{e^{i\omega y_\parallel}}{p_\parallel - \frac{\omega}{2}} \right) \right\}. \qquad \text{(B.7)}$$

One can now shift $p_\parallel \to p_\parallel - \omega$ and $p_\parallel \to p_\parallel + \omega$ in the third and fourth terms in the brackets, respectively. Then, we have

$$S(\mathbf{x}, \mathbf{y}, E) = \frac{1}{L^3} \sum_{\mathbf{p}} \frac{e^{i\mathbf{p}(\mathbf{x}-\mathbf{y})}}{m + \frac{\mathbf{p}^2}{2m} - E}$$
$$- \left\{ \frac{\omega q}{8} \frac{1}{L^3} \sum_{\mathbf{p}} \frac{e^{i(\mathbf{p}+\omega)\mathbf{x} - i\mathbf{p}\mathbf{y}}}{p_\parallel + \frac{\omega}{2}} \left(\frac{1}{m + \frac{\mathbf{p}^2}{2m} - E} - \frac{1}{m + \frac{(\mathbf{p}+\omega)^2}{2m} - E} \right) + (\omega \to -\omega) \right\}$$
$$= \frac{1}{L^3} \sum_{\mathbf{p}} \frac{e^{i\mathbf{p}(\mathbf{x}-\mathbf{y})}}{m + \frac{\mathbf{p}^2}{2m} - E}$$
$$- \frac{\omega^2 q}{8} \frac{1}{L^3} \sum_{\mathbf{p}} \left\{ \frac{e^{i(\mathbf{p}+\omega)\mathbf{x} - i\mathbf{p}\mathbf{y}}}{\left(m + \frac{\mathbf{p}^2}{2m} - E\right)\left(m + \frac{(\mathbf{p}+\omega)^2}{2m} - E\right)} + (\omega \to -\omega) \right\}. \qquad \text{(B.8)}$$

Performing the Fourier transform and using eq. (3.6), we finally arrive at eq. (3.11).

The calculations in case of an even N are slightly more complicated. Now, the eigenvalue corresponding to $\nu_i = 1$ is also present, with $\lambda_{\pm 1}(q) = 1 \pm q + O(q^2)$. Hence, the denominators corresponding to this eigenvalue, should be expanded:

$$\frac{1}{m + \frac{\mathbf{p}_\perp^2}{2m} + \frac{\omega^2}{8m}\lambda_{\pm 1}(q) - E} = \frac{1}{m + \frac{\mathbf{p}_\perp^2}{2m} + \frac{\omega^2}{8m} - E}$$
$$\mp \frac{\omega^2 q}{8m} \frac{1}{\left(m + \frac{\mathbf{p}_\perp^2}{2m} + \frac{\omega^2}{8m} - E\right)^2} + O(q^2). \qquad \text{(B.9)}$$

Otherwise, the calculations follow exactly the same path. Adding all contributions carefully, one finally verifies that eq. (3.11) holds in case of the even N as well.

C The Lüscher function at $e \neq 0$

Taking into account the fact that $\omega = 2\pi N/L$ and performing the variable transformation $x_\parallel = 2u/\omega$, $y_\parallel = 2v/\omega$ in eq. (4.13), we get

$$\bar{\Pi}(P_\parallel, Q_\parallel; \mathbf{P}_\perp; E) = \frac{1}{\pi^2 L^2 N^2} \sum_{\mathbf{P}_\perp} \sum_{i,j=1}^{N} \sum_{n,m=-\infty}^{\infty} \int_0^{N\pi} du \int_0^{N\pi} dv \, D_{in,jm}(\mathbf{p}_\perp; \mathbf{P}_\perp; E)$$
$$\times e^{-iau+ibv} \, \mathrm{me}_{\nu_i+2n}(u,q) \mathrm{me}_{\nu_i+2n}(-v,q) \mathrm{me}_{\nu_j+2m}(u,q) \mathrm{me}_{\nu_j+2m}(-v,q) \,.$$
$$\text{(C.1)}$$

Here, $a = 2P_\parallel/\omega$ and $b = 2Q_\parallel/\omega$. Furthermore, using the periodicity property of the Mathieu functions, the integration over the variables u, v can be restricted to the interval from 0 to π:

$$\int_0^{N\pi} du \int_0^{N\pi} dv \, e^{-iau+ibv} \, \mathrm{me}_{\nu_i+2n}(u,q) \mathrm{me}_{\nu_i+2n}(-v,q) \mathrm{me}_{\nu_j+2m}(u,q) \mathrm{me}_{\nu_j+2m}(-v,q)$$
$$= \sum_{k,l=1}^{N-1} e^{i\pi(\nu_i+2n+\nu_j+2m-a)(k-1)-i\pi(\nu_i+2n+\nu_j+2m-b)(l-1)}$$
$$\times \int_0^{\pi} du \int_0^{\pi} dv \, e^{-iau+ibv} \, \mathrm{me}_{\nu_i+2n}(u,q) \mathrm{me}_{\nu_i+2n}(-v,q) \mathrm{me}_{\nu_j+2m}(u,q) \mathrm{me}_{\nu_j+2m}(-v,q)$$
$$= N^2 \sum_{k,l=-\infty}^{\infty} \delta_{a-b,2k} \, \delta_{\nu_i+2n+\nu_j+2m-a,2l}$$
$$\times \int_0^{\pi} du \int_0^{\pi} dv \, e^{-iau+ibv} \, \mathrm{me}_{\nu_i+2n}(u,q) \mathrm{me}_{\nu_i+2n}(-v,q) \mathrm{me}_{\nu_j+2m}(u,q) \mathrm{me}_{\nu_j+2m}(-v,q) \,.$$
$$\text{(C.2)}$$

Hence,

$$\bar{\Pi}(P_\parallel, Q_\parallel; \mathbf{P}_\perp; E) = \sum_{\ell=-\infty}^{\infty} L \delta_{P_\parallel-Q_\parallel, \ell\omega} \tilde{\Pi}(P_\parallel, Q_\parallel; \mathbf{P}_\perp; E) \,, \tag{C.3}$$

where

$$\tilde{\Pi}(P_\parallel, Q_\parallel; \mathbf{P}_\perp; E) = \frac{1}{\pi^2 L^3} \sum_{\mathbf{P}_\perp} \sum_{i,j=1}^{N} \sum_{n,m=-\infty}^{\infty} \sum_{k=-\infty}^{\infty} \delta_{\nu_i+2m+\nu_j+2m-a,2k}$$
$$\times \int_0^{\pi} du \int_0^{\pi} dv \, D_{in,jm}(\mathbf{p}_\perp; \mathbf{P}_\perp; E) e^{-iau+ibv}$$
$$\times \mathrm{me}_{\nu_i+2n}(u,q) \mathrm{me}_{\nu_i+2n}(-v,q) \mathrm{me}_{\nu_j+2m}(u,q) \mathrm{me}_{\nu_j+2m}(-v,q) \,. \tag{C.4}$$

Since $\nu_i, \nu_j \in]-1, 1]$, the sum over k in the above equation has a finite number of non-zero terms. Finally, one can carry out the summation over k, which yields

$$\tilde{\Pi}(P_\parallel, Q_\parallel; \mathbf{P}_\perp; E) = \frac{1}{\pi^2 L^3} \sum_{\mathbf{P}_\perp} \sum_{i,j=1}^{N} \sum_{n,m=-\infty}^{\infty} \int_0^\pi du \int_0^\pi dv \, D_{in,jm}(\mathbf{p}_\perp; \mathbf{P}_\perp; E) e^{-iau+ibv}$$
$$\times \mathrm{me}_{\nu_i+2n}(u,q) \mathrm{me}_{\nu_i+2n}(-v,q) \mathrm{me}_{\nu_j+2m}(u,q) \mathrm{me}_{\nu_j+2m}(-v,q) \,. \tag{C.5}$$

Note that the conservation of the "longitudinal momentum" takes the form

$$\frac{\omega}{2}(\nu_i + 2n) + \frac{\omega}{2}(\nu_j + 2m) - P_\parallel = k\omega \,. \tag{C.6}$$

Equation (C.5) is still too complicated for using it in the analysis of data. Here, we are interested in the shift of the energy levels that are linear in e. It would be therefore useful to get a simplified expression that allows one to extract the levels at this precision. To this end, one first expands the numerator, using the eqs. (B.1) and (B.2). Furthermore, as we already know, the eigenvalues $\lambda_{\nu_i+2n}(q)$ up to the order q^2 correspond to those in the free theory, whereas the case $\nu_i + 2n = \pm 1$ is an exception, see eq. (3.14). Expanding the denominator in $D_{in,jm}(\mathbf{p}_\perp; \mathbf{P}_\perp; E)$ up to the first order in q corresponds to the "perturbative" expression, whereas leaving the denominator intact leads to the "exact" one. The final result is displayed in eqs. (4.15), (4.16), (4.17).

D Explicit expression for the form factor

An explicit expression for the form factor in the toy model considered here can be straightforwardly obtained by evaluating the expression given in eq. (2.23). Below, we give the final result without derivation:

$$F(\mathbf{P}, \mathbf{Q}) = F(\omega) = \frac{\sqrt{-q_R^2}}{4\pi\left(1 + r\sqrt{-q_R^2}\right)} \left\{ -\kappa\omega^2 q_R^2 + 8\pi\Gamma\left(r + \frac{4}{\omega}\arcsin\frac{\omega}{\sqrt{\omega^2 - 16q_R^2}}\right) \right\} \,. \tag{D.1}$$

References

[1] D. Hoja, U.G. Meissner and A. Rusetsky, *Resonances in an external field: The $1+1$ dimensional case*, *JHEP* **04** (2010) 050 [`arXiv:1001.1641`] [INSPIRE].

[2] R.A. Briceño, M.T. Hansen and A.W. Jackura, *Consistency checks for two-body finite-volume matrix elements: II. Perturbative systems*, *Phys. Rev. D* **101** (2020) 094508 [`arXiv:2002.00023`] [INSPIRE].

[3] L. Lellouch and M. Lüscher, *Weak transition matrix elements from finite volume correlation functions*, *Commun. Math. Phys.* **219** (2001) 31 [hep-lat/0003023] [INSPIRE].

[4] M.T. Hansen and S.R. Sharpe, *Multiple-channel generalization of Lellouch-Lüscher formula*, *Phys. Rev. D* **86** (2012) 016007 [arXiv:1204.0826] [INSPIRE].

[5] R.A. Briceño, M.T. Hansen and A. Walker-Loud, *Multichannel $1 \to 2$ transition amplitudes in a finite volume*, *Phys. Rev. D* **91** (2015) 034501 [arXiv:1406.5965] [INSPIRE].

[6] R.A. Briceño and M.T. Hansen, *Multichannel $0 \to 2$ and $1 \to 2$ transition amplitudes for arbitrary spin particles in a finite volume*, *Phys. Rev. D* **92** (2015) 074509 [arXiv:1502.04314] [INSPIRE].

[7] R.A. Briceño, J.J. Dudek and L. Leskovec, *Constraining $1 + \mathcal{J} \to 2$ coupled-channel amplitudes in finite-volume*, *Phys. Rev. D* **104** (2021) 054509 [arXiv:2105.02017] [INSPIRE].

[8] R.A. Briceño, J.J. Dudek, R.G. Edwards, C.J. Shultz, C.E. Thomas and D.J. Wilson, *The $\pi\pi \to \pi\gamma^\star$ amplitude and the resonant $\rho \to \pi\gamma^\star$ transition from lattice QCD*, *Phys. Rev. D* **93** (2016) 114508 [*Erratum ibid.* **105** (2022) 079902] [arXiv:1604.03530] [INSPIRE].

[9] R.A. Briceno, J.J. Dudek, R.G. Edwards, C.J. Shultz, C.E. Thomas and D.J. Wilson, *The resonant $\pi^+\gamma \to \pi^+\pi^0$ amplitude from Quantum Chromodynamics*, *Phys. Rev. Lett.* **115** (2015) 242001 [arXiv:1507.06622] [INSPIRE].

[10] A. Agadjanov, V. Bernard, U.-G. Meißner and A. Rusetsky, *The $B \to K^*$ form factors on the lattice*, *Nucl. Phys. B* **910** (2016) 387 [arXiv:1605.03386] [INSPIRE].

[11] A. Agadjanov, V. Bernard, U.G. Meißner and A. Rusetsky, *A framework for the calculation of the $\Delta N\gamma^*$ transition form factors on the lattice*, *Nucl. Phys. B* **886** (2014) 1199 [arXiv:1405.3476] [INSPIRE].

[12] H.B. Meyer, *Lattice QCD and the Timelike Pion Form Factor*, *Phys. Rev. Lett.* **107** (2011) 072002 [arXiv:1105.1892] [INSPIRE].

[13] K.H. Sherman, F.G. Ortega-Gama, R.A. Briceño and A.W. Jackura, *Two-current transition amplitudes with two-body final states*, *Phys. Rev. D* **105** (2022) 114510 [arXiv:2202.02284] [INSPIRE].

[14] F. Müller and A. Rusetsky, *On the three-particle analog of the Lellouch-Lüscher formula*, *JHEP* **03** (2021) 152 [arXiv:2012.13957] [INSPIRE].

[15] M.T. Hansen, F. Romero-López and S.R. Sharpe, *Decay amplitudes to three hadrons from finite-volume matrix elements*, *JHEP* **04** (2021) 113 [arXiv:2101.10246] [INSPIRE].

[16] V. Bernard, D. Hoja, U.G. Meissner and A. Rusetsky, *Matrix elements of unstable states*, *JHEP* **09** (2012) 023 [arXiv:1205.4642] [INSPIRE].

[17] R.A. Briceño and M.T. Hansen, *Relativistic, model-independent, multichannel $2 \to 2$ transition amplitudes in a finite volume*, *Phys. Rev. D* **94** (2016) 013008 [arXiv:1509.08507] [INSPIRE].

[18] A. Baroni, R.A. Briceño, M.T. Hansen and F.G. Ortega-Gama, *Form factors of two-hadron states from a covariant finite-volume formalism*, *Phys. Rev. D* **100** (2019) 034511 [arXiv:1812.10504] [INSPIRE].

[19] R.A. Briceño, M.T. Hansen and A.W. Jackura, *Consistency checks for two-body finite-volume matrix elements: I. Conserved currents and bound states*, *Phys. Rev. D* **100** (2019) 114505 [arXiv:1909.10357] [INSPIRE].

[20] R.A. Briceño, A.W. Jackura, F.G. Ortega-Gama and K.H. Sherman, *On-shell representations of two-body transition amplitudes: Single external current*, *Phys. Rev. D* **103** (2021) 114512 [arXiv:2012.13338] [INSPIRE].

[21] H. Hellmann, *Einführung in die Quantenchemie*, Deuticke, Leipzig und Wien (1937).

[22] R.P. Feynman, *Forces in Molecules*, *Phys. Rev.* **56** (1939) 340 [INSPIRE].

[23] QCDSF, UKQCD and CSSM collaborations, *Electromagnetic form factors at large momenta from lattice QCD*, *Phys. Rev. D* **96** (2017) 114509 [arXiv:1702.01513] [INSPIRE].

[24] A. Agadjanov, U.-G. Meißner and A. Rusetsky, *Nucleon in a periodic magnetic field: Finite-volume aspects*, *Phys. Rev. D* **99** (2019) 054501 [arXiv:1812.06013] [INSPIRE].

[25] K.U. Can et al., *Lattice QCD evaluation of the Compton amplitude employing the Feynman-Hellmann theorem*, *Phys. Rev. D* **102** (2020) 114505 [arXiv:2007.01523] [INSPIRE].

[26] CSSM/QCDSF/UKQCD collaboration, *Generalized parton distributions from the off-forward Compton amplitude in lattice QCD*, *Phys. Rev. D* **105** (2022) 014502 [arXiv:2110.11532] [INSPIRE].

[27] A. Agadjanov, U.-G. Meißner and A. Rusetsky, *Nucleon in a periodic magnetic field*, *Phys. Rev. D* **95** (2017) 031502 [arXiv:1610.05545] [INSPIRE].

[28] J. Ruiz de Elvira, U.G. Meißner, A. Rusetsky and G. Schierholz, *Feynman-Hellmann theorem for resonances and the quest for QCD exotica*, *Eur. Phys. J. C* **77** (2017) 659 [arXiv:1706.09015] [INSPIRE].

[29] J. Gasser, V.E. Lyubovitskij and A. Rusetsky, *Hadronic atoms in QCD + QED*, *Phys. Rept.* **456** (2008) 167 [arXiv:0711.3522] [INSPIRE].

[30] S. Mandelstam, *Dynamical variables in the Bethe-Salpeter formalism*, *Proc. Roy. Soc. Lond. A* **233** (1955) 248 [INSPIRE].

[31] K. Huang and H.A. Weldon, *Bound State Wave Functions and Bound State Scattering in Relativistic Field Theory*, *Phys. Rev. D* **11** (1975) 257 [INSPIRE].

[32] N.W. McLachlan, *Theory and Application of Mathieu Functions*, Dover Publications, Reprint edition (1964).

Summary

The study of hadronic processes in a finite volume plays an important role in the extraction of hadronic properties from lattice data. For instance, here we have focused on Compton scattering and resonance form factors. This motivates us to analyze these phenomena in a more detailed manner, particularly through the use of non-perturbative tools.

The theory in which is work is mainly based is known as Quantum Chronodynamics (QCD), and it is an excellent model that describes the dynamics of elementary particles and its interactions through the strong force. Nonetheless, there are certain calculations within this framework that are better tackled by the use of lattice QCD, the main numerical tool for studying non-perturbative QCD. This is a first-principle method based on the path integral formulation of QCD in Euclidean space-time. Due to the introduction of the momentum cut-off by the lattice spacing, the theory is regularized.

In particular, we are interested in the dynamics of hadrons at low energies. These low-energy regimes are usually inaccessible due to the large coupling constant present here. Instead, we make use of lattice QCD. More specifically, our attention is put into the analysis of unstable hadrons, i.e., resonances and the stable hadrons, such as, for example, the nucleon. In the first case, contrary to the one of stable particles, the study turns out to be rather complicated. Namely, final-state interactions of resonances render the standard lattice approaches ineffective. Nevertheless, there exist methods which are able to extract information from the finite-volume spectrum and latter be taken into the infinite-volume limit. The extraction of finite-volume observables in the two-particle sector is well-understood and it is performed through the so-called Lüscher method. In our case, this allows us to calculate the matrix elements of unstable particles which are an essential part in the computation of form factors.

In the case of stable hadrons, we investigated the properties of the nucleon by making use of an effective field theory of QCD, known as Chiral Perturbation Theory, together with the external field method, which is well suited for this endeavor. In our first work, we focused on the determination of the nucleon structure functions from the Compton amplitude, both in the infinite volume and in a finite volume. This further allowed us to compute the so-called subtraction function by considering the Compton amplitude in a particular kinematics. The main objective of this study was to estimate the finite-volume corrections to the subtraction function when the system was placed in a periodic magnetic external field. To accomplish this, a ratio of the infinite- and finite-volume results was obtained from the calculation of the Compton tensor. This ratio, as a function of the lattice size L, dictates at which length the finite-volume corrections to the subtraction function can be safely ignored.

In this study, we demonstrated that the finite-volume corrections to the Compton tensor are negligible for sufficiently small boxes. This result allows one to safely investigate the subtraction function on the lattice.

One could also try to extract the properties of unstable composite particles from the lattice. For example, the computation of the form factors provides us with information about the structure of such particles. In order to perform these calculations, one must consider that the states under investigation are not stable and will eventually decay. This is not as straightforward as in the case of the stable hadrons, as the mapping of the finite-volume results into the infinite volume is not a trivial endeavor. This is due to the presence of contributions that have an ill-defined behavior when the infinite-volume is considered.

To tackle this issue, we made use of a non-relativistic effective field theory (NREFT) and considered the case of a resonance that emerges in the scattering of two identical particles. Furthermore, the external field method was also employed in this study, as such a procedure leads to the extraction of the form factor for stable particles in a particular frame; we aimed to extend this result to the case of resonances. To demonstrate this, we computed the resonance form factor in the infinite volume in the NREFT. In this case, the parameters needed to fully determine the form factor are already known, except for one coupling that was later extracted from the lattice data. This extraction was achieved by deriving and then solving the Lüscher equation in an external field. By fitting to the energy levels, the unknown coupling was determined. With this, we fully computed the form factor of the resonance considered here. As a check to this result, we invoked the Feynman-Hellmann theorem. Namely, we determined the complex pole position of the resonance and took its derivative with respect to the coupling of the external field. As we expected, this yielded the resonance form factor.

These results open the possibility to study more complex systems in such a framework. For instance, the case of particles with spin should also be considered. In the future, the inclusion of higher-order terms in the NREFT Lagrangian should be performed. In addition, it would be very interesting to numerically implement realistic values, resembling a low-lying resonance.

The findings of this thesis are summarized as follows:

- In Chapter 2, we studied the low-energy doubly virtual forward nucleon Compton scattering in a finite volume. In particular, we were interested in the finite-volume correction to the Compton tensor for a certain kinematics. We were also able to calculate infinite-volume quantities, such as the electric and magnetic polarizabilities to different orders in Chiral Perturbation Theory. The results show that these exponentially suppressed corrections are rather small and do not significantly influence the extraction of this quantity from lattice calculations

- In Chapter 3, we computed the form factor of an unstable particle. This was done for a toy model in the case of two-body scattering of a scalar field in the presence of an external field, from which we were able to define the resonance form factor. To fully determine this quantity, only one unknown parameter had to be extracted from the lattice. To perform the extraction, an extension of the Lüscher's method in the presence of an external source was derived. Furthermore, we also showed that the resonance form factor can be obtained by first determining the pole position of the particle and then taking the derivative with respect to the external fields coupling constant.

4.1 Outlook

The future of hadron particle physics is promising. For example, the recent observations of exotic states in experiments calls for a better and deeper understanding of QCD in the hadron sector. As most of the hadrons decay through the strong force, particular effort is exercised here. In particular, we are interested in resonances, which are unstable composite particles. Due to its peculiar properties, the extraction of hadronic information from the lattice poses an stimulating challenge. Nowadays, the study of such particles has been crucial in the further development of our understanding of QCD.

Recent advances in computational techniques had made lattice QCD one of the most viable ways to study the dynamics of strongly interacting particles. Most of the focus has been put on the study of particles that are stable within QCD. More recently, the attention shifted to determining the properties of resonances. The two-body sector case is well understood. Namely, the Lüscher's method proves to be an indispensable tool to study these kind of processes. However, there are final states that contain more than two particles, such as the $a_1(1260) \rightarrow \pi\pi\pi$. Recently, extensions of Lüscher's method to many-particle states have been on the spotlight. Nowadays, there are three main approaches that were developed to study the three-body sector a finite volume: the Relativistic Field Theory, Non-Relativistic Effective Field Theory and Finite Volume Unitarity. Despite being derived from different principles, it can be shown that the approaches are conceptually equivalent. Regardless of their differences, these methods are able to extract the finite-volume information from the lattice in a successful manner.

In this thesis we focused in extracting data from the lattice for different hadron processes. By applying the finite-volume procedure to our infinite-volume data, we were able to obtain several interesting results reported throughout this work. Nonetheless, there are still certain aspects of our research that can be further investigated. In the following, we suggest extensions to the works presented in this thesis. The further development of these ideas is left as future research projects.

- *Finite-volume corrections to the Compton tensor with twisted-boundary conditions.* After considering the case of periodic boundary conditions in the analysis of the Compton amplitude, the implementation of twisted-boundary conditions is straightforward. Namely, a continuous phase factor is added at the boundary leading to a shift of the loop momenta. This allows for a continuous change of the momentum transfer, Q^2. In particular, access to smaller spatial momenta is achieved with this method. The aim is to perform this procedure in a particular component of the Compton tensor and investigate the dependence of the finite-volume corrections on the so-called twisting angle.

- *Relativistic extension to the Lüscher equation in an external field.* The pioneering study, carried out in [125], was performed in a toy model and served the proof of principle only. In the context of the Non-Relativistic Effective Field Theories, several improvements can be done. For instance, relativistic corrections to all orders should be included in this framework. Moreover, terms of higher orders in the Lagrangian should also be considered here. Furthermore, partial-wave mixing should be implemented accordingly.

Bibliography

[1] S. L. Glashow, *Partial-symmetries of weak interactions*, Nuclear Physics **22** (1961) 579,
     ISSN: 0029-5582, URL:
     https://www.sciencedirect.com/science/article/pii/0029558261904692.

[2] F. Englert and R. Brout, *Broken Symmetry and the Mass of Gauge Vector Mesons*,
     Phys. Rev. Lett. **13** (9 1964) 321,
     URL: https://link.aps.org/doi/10.1103/PhysRevLett.13.321.

[3] P. W. Higgs, *Broken Symmetries and the Masses of Gauge Bosons*,
     Phys. Rev. Lett. **13** (16 1964) 508,
     URL: https://link.aps.org/doi/10.1103/PhysRevLett.13.508.

[4] G. S. Guralnik, C. R. Hagen and T. W. B. Kibble,
     Global Conservation Laws and Massless Particles, Phys. Rev. Lett. **13** (20 1964) 585,
     URL: https://link.aps.org/doi/10.1103/PhysRevLett.13.585.

[5] A. Salam, *Weak and Electromagnetic Interactions*, Conf. Proc. C **680519** (1968) 367.

[6] S. Weinberg, *A Model of Leptons*, Phys. Rev. Lett. **19** (21 1967) 1264,
     URL: https://link.aps.org/doi/10.1103/PhysRevLett.19.1264.

[7] A. Einstein, *The Field Equations of Gravitation*,
     Sitzungsber. Preuss. Akad. Wiss. Berlin (Math. Phys.) **1915** (1915) 844.

[8] A. Einstein, *The Foundation of the General Theory of Relativity*,
     Annalen Phys. **49** (1916) 769, ed. by J.-P. Hsu and D. Fine.

[9] C. Rovelli, "Notes for a brief history of quantum gravity",
     *9th Marcel Grossmann Meeting on Recent Developments in Theoretical and Experimental
     General Relativity, Gravitation and Relativistic Field Theories (MG 9)*, 2000 742,
     arXiv: gr-qc/0006061.

[10] A. Ashtekar,
     "Loop Quantum Gravity: Four Recent Advances and a Dozen Frequently Asked Questions",
     11th Marcel Grossmann Meeting on General Relativity, 2007 126,
     arXiv: 0705.2222 [gr-qc].

[11] J. H. Schwarz, *String theory: Progress and problems*, Prog. Theor. Phys. Suppl. **170**
     (2007) 214, ed. by R. Ikeda, Y. Kanada-Enyo, T. Kugo, M. Saski and N. Sasao,
     arXiv: hep-th/0702219.

[12] B. P. Abbott et al., *Observation of Gravitational Waves from a Binary Black Hole Merger*,
     Phys. Rev. Lett. **116** (2016) 061102, arXiv: 1602.03837 [gr-qc].

[13] B. Abi et al., *Measurement of the Positive Muon Anomalous Magnetic Moment to 0.46 ppm*,
      Phys. Rev. Lett. **126** (14 2021) 141801,
      URL: https://link.aps.org/doi/10.1103/PhysRevLett.126.141801.

[14] T. Albahri et al., *Measurement of the anomalous precession frequency of the muon in the
      Fermilab Muon g − 2 Experiment*, Phys. Rev. D **103** (7 2021) 072002,
      URL: https://link.aps.org/doi/10.1103/PhysRevD.103.072002.

[15] T. Albahri et al.,
      Magnetic-field measurement and analysis for the Muon g − 2 Experiment at Fermilab,
      Phys. Rev. A **103** (4 2021) 042208,
      URL: https://link.aps.org/doi/10.1103/PhysRevA.103.042208.

[16] T. Albahri et al., *Beam dynamics corrections to the Run-1 measurement of the muon
      anomalous magnetic moment at Fermilab*, Phys. Rev. Accel. Beams **24** (4 2021) 044002,
      URL: https://link.aps.org/doi/10.1103/PhysRevAccelBeams.24.044002.

[17] G. Aad et al., *Observation of a new particle in the search for the Standard Model Higgs boson
      with the ATLAS detector at the LHC*, Phys. Lett. B **716** (2012) 1,
      arXiv: 1207.7214 [hep-ex].

[18] S. Chatrchyan et al.,
      Observation of a New Boson at a Mass of 125 GeV with the CMS Experiment at the LHC,
      Phys. Lett. B **716** (2012) 30, arXiv: 1207.7235 [hep-ex].

[19] URL: https://www.quantumdiaries.org/2014/03/14/the-standard-model-a-
      beautiful-but-flawed-theory/.

[20] W. J. Marciano and H. Pagels, *Quantum Chromodynamics: A Review*,
      Phys. Rept. **36** (1978) 137.

[21] G. Ecker, "Quantum chromodynamics", *2005 European School of High-Energy Physics*,
      2006, arXiv: hep-ph/0604165.

[22] Trassiorf, *Eightfold Way*, 2007,
      URL: https://de.wikipedia.org/wiki/Eightfold_Way.

[23] M. Gell-Mann, *A Schematic Model of Baryons and Mesons*, Phys. Lett. **8** (1964) 214.

[24] G. Zweig, *An SU(3) model for strong interaction symmetry and its breaking*, (1964),
      URL: http://inspirehep.net/record/11881/export/hx.

[25] A. Deur, S. J. Brodsky and G. F. de Teramond, *The QCD Running Coupling*,
      Nucl. Phys. **90** (2016) 1, arXiv: 1604.08082 [hep-ph].

[26] R. D. Peccei, *The Strong CP problem and axions*,
      Lect. Notes Phys. **741** (2008) 3, ed. by M. Kuster, G. Raffelt and B. Beltran,
      arXiv: hep-ph/0607268.

[27] S. Bethke, *The 2009 World Average of alpha(s)*,
      Eur. Phys. J. C **64** (2009) 689, ed. by D. H. Beck, D. Haidt and J. W. Negele,
      arXiv: 0908.1135 [hep-ph].

[28] D. J. Gross and F. Wilczek, *Ultraviolet Behavior of Nonabelian Gauge Theories*,
      Phys. Rev. Lett. **30** (1973) 1343, ed. by J. C. Taylor.

[29] H. D. Politzer, *Reliable Perturbative Results for Strong Interactions?*,
Phys. Rev. Lett. **30** (26 1973) 1346,
URL: https://link.aps.org/doi/10.1103/PhysRevLett.30.1346.

[30] C. Patrignani et al., *Review of Particle Physics*, Chin. Phys. **C40** (2016) 100001.

[31] Y. Nambu, *Axial vector current conservation in weak interactions*,
Phys. Rev. Lett. **4** (1960) 380, [,107(1960)].

[32] J. Gasser and H. Leutwyler, *Chiral Perturbation Theory to One Loop*,
Annals Phys. **158** (1984) 142.

[33] J. Gasser and H. Leutwyler,
Chiral Perturbation Theory: Expansions in the Mass of the Strange Quark,
Nucl. Phys. B **250** (1985) 465.

[34] J. Gasser and H. Leutwyler, *Low-Energy Expansion of Meson Form-Factors*,
Nucl. Phys. **B250** (1985) 517.

[35] S. Weinberg, *Phenomenological Lagrangians*, Physica **A96** (1979) 327.

[36] V. Bernard, N. Kaiser and U.-G. Meißner, *Chiral dynamics in nucleons and nuclei*,
Int. J. Mod. Phys. E **4** (1995) 193, arXiv: hep-ph/9501384.

[37] J. Gasser, M. E. Sainio and A. Svarc, *Nucleons with Chiral Loops*,
Nucl. Phys. **B307** (1988) 779.

[38] N. Fettes, U.-G. Meißner, M. Mojzis and S. Steininger,
*The Chiral effective pion nucleon Lagrangian of order p**4*,
Annals Phys. **283** (2000) 273, [Erratum: Annals Phys.288,249(2001)],
arXiv: hep-ph/0001308 [hep-ph].

[39] M. Hoferichter, J. Ruiz de Elvira, B. Kubis and U.-G. Meißner,
Matching pion-nucleon Roy-Steiner equations to chiral perturbation theory,
Phys. Rev. Lett. **115** (2015) 192301, arXiv: 1507.07552 [nucl-th].

[40] V. Bernard, N. Kaiser, J. Kambor and U. G. Meißner, *Chiral structure of the nucleon*,
Nucl. Phys. **B388** (1992) 315.

[41] E. E. Jenkins and A. V. Manohar,
Baryon chiral perturbation theory using a heavy fermion Lagrangian,
Phys. Lett. **B255** (1991) 558.

[42] T. Becher and H. Leutwyler,
Baryon chiral perturbation theory in manifestly Lorentz invariant form,
Eur. Phys. J. **C9** (1999) 643, arXiv: hep-ph/9901384 [hep-ph].

[43] J. Gegelia and G. Japaridze, *Matching heavy particle approach to relativistic theory*,
Phys. Rev. **D60** (1999) 114038, arXiv: hep-ph/9908377 [hep-ph].

[44] T. Fuchs, J. Gegelia, G. Japaridze and S. Scherer,
Renormalization of relativistic baryon chiral perturbation theory and power counting,
Phys. Rev. **D68** (2003) 056005, arXiv: hep-ph/0302117 [hep-ph].

[45] K. G. Wilson, *Confinement of Quarks*, Phys. Rev. **D10** (1974) 2445, [,319(1974)].

[46] K. Symanzik,
*Continuum Limit and Improved Action in Lattice Theories. 1. Principles and phi**4 Theory*,
Nucl. Phys. **B226** (1983) 187.

[47] K. Symanzik, *Continuum Limit and Improved Action in Lattice Theories. 2. O(N) Nonlinear Sigma Model in Perturbation Theory*, Nucl. Phys. **B226** (1983) 205.

[48] Y. Iwasaki, UT-HEP-118 ().

[49] H. B. Nielsen and M. Ninomiya,
Absence of Neutrinos on a Lattice. 1. Proof by Homotopy Theory,
Nucl. Phys. **B185** (1981) 20, [,533(1980)].

[50] M. Lüscher, S. Sint, R. Sommer and P. Weisz,
Chiral symmetry and O(a) improvement in lattice QCD, Nucl. Phys. **B478** (1996) 365,
arXiv: `hep-lat/9605038 [hep-lat]`.

[51] B. Sheikholeslami and R. Wohlert,
Improved Continuum Limit Lattice Action for QCD with Wilson Fermions,
Nucl. Phys. **B259** (1985) 572.

[52] K. Jansen et al., *Nonperturbative renormalization of lattice QCD at all scales*,
Phys. Lett. B **372** (1996) 275, arXiv: `hep-lat/9512009`.

[53] S. Durr et al., *Precision computation of the kaon bag parameter*, Phys. Lett. B **705** (2011) 477,
arXiv: `1106.3230 [hep-lat]`.

[54] N. Ishizuka, K. .-. Ishikawa, A. Ukawa and T. Yoshié,
Calculation of K→ππ decay amplitudes with improved Wilson fermion action in lattice QCD,
Phys. Rev. D **92** (2015) 074503, arXiv: `1505.05289 [hep-lat]`.

[55] R. Frezzotti, P. A. Grassi, S. Sint and P. Weisz, *Lattice QCD with a chirally twisted mass term*,
JHEP **08** (2001) 058, arXiv: `hep-lat/0101001`.

[56] R. Frezzotti and G. C. Rossi, *Chirally improving Wilson fermions. 1. O(a) improvement*,
JHEP **08** (2004) 007, arXiv: `hep-lat/0306014`.

[57] L. Susskind, *Lattice fermions*, Phys. Rev. D **16** (10 1977) 3031,
URL: `https://link.aps.org/doi/10.1103/PhysRevD.16.3031`.

[58] M. Golterman, *QCD with rooted staggered fermions*, PoS **CONFINEMENT8** (2008) 014,
arXiv: `0812.3110 [hep-ph]`.

[59] C. Bernard, *Staggered chiral perturbation theory and the fourth-root trick*,
Phys. Rev. D **73** (2006) 114503, arXiv: `hep-lat/0603011`.

[60] S. R. Sharpe, *Rooted staggered fermions: Good, bad or ugly?*,
PoS **LAT2006** (2006) 022, ed. by T. Blum et al., arXiv: `hep-lat/0610094`.

[61] G. P. Lepage, *Flavor symmetry restoration and Symanzik improvement for staggered quarks*,
Phys. Rev. D **59** (1999) 074502, arXiv: `hep-lat/9809157`.

[62] A. Bazavov et al.,
Nonperturbative QCD Simulations with 2+1 Flavors of Improved Staggered Quarks,
Rev. Mod. Phys. **82** (2010) 1349, arXiv: `0903.3598 [hep-lat]`.

[63] E. Follana et al.,
      Highly improved staggered quarks on the lattice, with applications to charm physics,
      Phys. Rev. D **75** (2007) 054502, arXiv: `hep-lat/0610092`.

[64] C. T. H. Davies et al.,
      Update: Precision D_s decay constant from full lattice QCD using very fine lattices,
      Phys. Rev. D **82** (2010) 114504, arXiv: `1008.4018 [hep-lat]`.

[65] G. C. Donald et al., *Precision tests of the J/ψ from full lattice QCD: mass, leptonic width and radiative decay rate to η_c*, Phys. Rev. D **86** (2012) 094501, arXiv: `1208.2855 [hep-lat]`.

[66] P. H. Ginsparg and K. G. Wilson, *A remnant of chiral symmetry on the lattice*,
      Phys. Rev. D **25** (10 1982) 2649,
      URL: `https://link.aps.org/doi/10.1103/PhysRevD.25.2649`.

[67] P. Hasenfratz, V. Laliena and F. Niedermayer, *The Index theorem in QCD with a finite cutoff*,
      Phys. Lett. B **427** (1998) 125, arXiv: `hep-lat/9801021`.

[68] M. Lüscher, *Exact chiral symmetry on the lattice and the Ginsparg-Wilson relation*,
      Phys. Lett. B **428** (1998) 342, arXiv: `hep-lat/9802011`.

[69] S. Scherer, *Introduction to chiral perturbation theory*,
      Adv. Nucl. Phys. **27** (2003) 277, ed. by J. W. Negele and E. W. Vogt,
      arXiv: `hep-ph/0210398`.

[70] M. J. Savage et al.,
      Proton-Proton Fusion and Tritium β Decay from Lattice Quantum Chromodynamics,
      Phys. Rev. Lett. **119** (2017) 062002, arXiv: `1610.04545 [hep-lat]`.

[71] E. Chang et al., *Magnetic structure of light nuclei from lattice QCD*,
      Phys. Rev. D **92** (2015) 114502, arXiv: `1506.05518 [hep-lat]`.

[72] S. R. Beane et al., *Magnetic moments of light nuclei from lattice quantum chromodynamics*,
      Phys. Rev. Lett. **113** (2014) 252001, arXiv: `1409.3556 [hep-lat]`.

[73] S. R. Beane et al., *Ab initio Calculation of the $np{\to}d\gamma$ Radiative Capture Process*,
      Phys. Rev. Lett. **115** (2015) 132001, arXiv: `1505.02422 [hep-lat]`.

[74] A. J. Chambers et al., *Disconnected contributions to the spin of the nucleon*,
      Phys. Rev. D **92** (2015) 114517, arXiv: `1508.06856 [hep-lat]`.

[75] A. J. Chambers et al., *Feynman-Hellmann approach to the spin structure of hadrons*,
      Phys. Rev. D **90** (2014) 014510, arXiv: `1405.3019 [hep-lat]`.

[76] G. Bali and G. Endrődi,
      Hadronic vacuum polarization and muon $g-2$ from magnetic susceptibilities on the lattice,
      Phys. Rev. D **92** (2015) 054506, arXiv: `1506.08638 [hep-lat]`.

[77] A. J. Chambers et al., *Electromagnetic form factors at large momenta from lattice QCD*,
      Phys. Rev. D **96** (2017) 114509, arXiv: `1702.01513 [hep-lat]`.

[78] A. J. Chambers et al.,
      Nucleon Structure Functions from Operator Product Expansion on the Lattice,
      Phys. Rev. Lett. **118** (2017) 242001, arXiv: `1703.01153 [hep-lat]`.

[79] W. Detmold, B. C. Tiburzi and A. Walker-Loud,
Electromagnetic and spin polarisabilities in lattice QCD, Phys. Rev. D **73** (2006) 114505,
arXiv: `hep-lat/0603026`.

[80] A. Agadjanov, U.-G. Meißner and A. Rusetsky, *Nucleon in a periodic magnetic field*,
Phys. Rev. D **95** (2017) 031502, arXiv: `1610.05545 [hep-lat]`.

[81] A. Agadjanov, U.-G. Meißner and A. Rusetsky,
Nucleon in a periodic magnetic field: Finite-volume aspects, Phys. Rev. D **99** (2019) 054501,
arXiv: `1812.06013 [hep-lat]`.

[82] V. Bernard, N. Kaiser and U. G. Meißner,
Nucleons with chiral loops: Electromagnetic polarizabilities, Nucl. Phys. B **373** (1992) 346.

[83] D. Nevado and A. Pineda,
Forward virtual Compton scattering and the Lamb shift in chiral perturbation theory,
Phys. Rev. C **77** (2008) 035202, arXiv: `0712.1294 [hep-ph]`.

[84] M. C. Birse and J. A. McGovern, *Proton polarisability contribution to the Lamb shift in
muonic hydrogen at fourth order in chiral perturbation theory*, Eur. Phys. J. A **48** (2012) 120,
arXiv: `1206.3030 [hep-ph]`.

[85] C. Peset and A. Pineda,
The two-photon exchange contribution to muonic hydrogen from chiral perturbation theory,
Nucl. Phys. B **887** (2014) 69, arXiv: `1406.4524 [hep-ph]`.

[86] J. M. Alarcón, F. Hagelstein, V. Lensky and V. Pascalutsa,
*Forward doubly-virtual Compton scattering off the nucleon in chiral perturbation theory: the
subtraction function and moments of unpolarized structure functions*,
Phys. Rev. D **102** (2020) 014006, arXiv: `2005.09518 [hep-ph]`.

[87] K. Pachucki, *Proton structure effects in muonic hydrogen*, Phys. Rev. A **60** (5 1999) 3593,
URL: `https://link.aps.org/doi/10.1103/PhysRevA.60.3593`.

[88] W. Cottingham, *The neutron proton mass difference and electron scattering experiments*,
Annals of Physics **25** (1963) 424, ISSN: 0003-4916, URL:
`https://www.sciencedirect.com/science/article/pii/000349166390023X`.

[89] A. Walker-Loud, C. E. Carlson and G. A. Miller, *The Electromagnetic Self-Energy
Contribution to $M_p - M_n$ and the Isovector Nucleon MagneticPolarizability*,
Phys. Rev. Lett. **108** (2012) 232301, arXiv: `1203.0254 [nucl-th]`.

[90] F. B. Erben, P. E. Shanahan, A. W. Thomas and R. D. Young, *Dispersive estimate of the
electromagnetic charge symmetry violation in the octet baryon masses*,
Phys. Rev. C **90** (2014) 065205, arXiv: `1408.6628 [nucl-th]`.

[91] J. Gasser, M. Hoferichter, H. Leutwyler and A. Rusetsky,
Cottingham formula and nucleon polarisabilities,
Eur. Phys. J. C **75** (2015) 375, [Erratum: Eur.Phys.J.C 80, 353 (2020)],
arXiv: `1506.06747 [hep-ph]`.

[92] J. Gasser, H. Leutwyler and A. Rusetsky, *On the mass difference between proton and neutron*,
Phys. Lett. B **814** (2021) 136087, arXiv: `2003.13612 [hep-ph]`.

[93] J. Gasser, H. Leutwyler and A. Rusetsky,
      Sum rule for the Compton amplitude and implications for the proton–neutron mass difference,
      Eur. Phys. J. C **80** (2020) 1121, arXiv: `2008.05806 [hep-ph]`.

[94] R. L. Workman et al., *Review of Particle Physics*, PTEP **2022** (2022) 083C01.

[95] G. Breit and E. Wigner, *Capture of Slow Neutrons*, Phys. Rev. **49** (7 1936) 519,
      URL: `https://link.aps.org/doi/10.1103/PhysRev.49.519`.

[96] A. Badalyan, L. Kok, M. Polikarpov and Y. Simonov,
      Resonances in coupled channels in nuclear and particle physics,
      Physics Reports **82** (1982) 31, ISSN: 0370-1573, URL:
      `https://www.sciencedirect.com/science/article/pii/037015738290014X`.

[97] H. A. Bethe, *Theory of the Effective Range in Nuclear Scattering*, Phys. Rev. **76** (1 1949) 38,
      URL: `https://link.aps.org/doi/10.1103/PhysRev.76.38`.

[98] R. A. Briceno, J. J. Dudek and R. D. Young,
      Scattering processes and resonances from lattice QCD, Rev. Mod. Phys. **90** (2018) 025001,
      arXiv: `1706.06223 [hep-lat]`.

[99] M. Mai, U.-G. Meißner and C. Urbach, *Towards a theory of hadron resonances*, (2022),
      arXiv: `2206.01477 [hep-ph]`.

[100] F.-K. Guo et al., *Hadronic molecules*,
      Rev. Mod. Phys. **90** (2018) 015004, [Erratum: Rev.Mod.Phys. 94, 029901 (2022)],
      arXiv: `1705.00141 [hep-ph]`.

[101] M. Lüscher, *Volume Dependence of the Energy Spectrum in Massive Quantum Field Theories.
      2. Scattering States*, Commun. Math. Phys. **105** (1986) 153.

[102] M. Lüscher, *Two-particle states on a torus and their relation to the scattering matrix*,
      Nuclear Physics B **354** (1991) 531, ISSN: 0550-3213, URL:
      `https://www.sciencedirect.com/science/article/pii/0550321391903666`.

[103] V. Bernard, D. Hoja, U. G. Meißner and A. Rusetsky, *Matrix elements of unstable states*,
      JHEP **09** (2012) 023, arXiv: `1205.4642 [hep-lat]`.

[104] G. Colangelo, J. Gasser, B. Kubis and A. Rusetsky, *Cusps in K —> 3 pi decays*,
      Phys. Lett. B **638** (2006) 187, arXiv: `hep-ph/0604084`.

[105] J. Gasser, B. Kubis and A. Rusetsky, *Cusps in K –> 3pi decays: a theoretical framework*,
      Nucl. Phys. B **850** (2011) 96, arXiv: `1103.4273 [hep-ph]`.

[106] H.-W. Hammer, J.-Y. Pang and A. Rusetsky,
      Three-particle quantization condition in a finite volume: 1. The role of the three-particle force,
      JHEP **09** (2017) 109, arXiv: `1706.07700 [hep-lat]`.

[107] H. .-. Hammer, J. .-. Pang and A. Rusetsky, *Three particle quantization condition in a finite
      volume: 2. general formalism and the analysis of data*, JHEP **10** (2017) 115,
      arXiv: `1707.02176 [hep-lat]`.

[108] C. h. Kim, C. T. Sachrajda and S. R. Sharpe,
      Finite-volume effects for two-hadron states in moving frames, Nucl. Phys. B **727** (2005) 218,
      arXiv: `hep-lat/0507006`.

[109] M. T. Hansen and S. R. Sharpe, *Multiple-channel generalization of Lellouch-Lüscher formula*, Phys. Rev. D **86** (2012) 016007, arXiv: `1204.0826` [`hep-lat`].

[110] R. A. Briceño and M. T. Hansen, *Relativistic, model-independent, multichannel $2 \to 2$ transition amplitudes in a finite volume*, Phys. Rev. D **94** (2016) 013008, arXiv: `1509.08507` [`hep-lat`].

[111] M. T. Hansen and S. R. Sharpe, *Relativistic, model-independent, three-particle quantization condition*, Phys. Rev. D **90** (2014) 116003, arXiv: `1408.5933` [`hep-lat`].

[112] M. T. Hansen and S. R. Sharpe, *Expressing the three-particle finite-volume spectrum in terms of the three-to-three scattering amplitude*, Phys. Rev. D **92** (2015) 114509, arXiv: `1504.04248` [`hep-lat`].

[113] R. A. Briceño, M. T. Hansen and S. R. Sharpe, *Relating the finite-volume spectrum and the two-and-three-particle S matrix for relativistic systems of identical scalar particles*, Phys. Rev. D **95** (2017) 074510, arXiv: `1701.07465` [`hep-lat`].

[114] R. A. Briceño, M. T. Hansen and S. R. Sharpe, *Three-particle systems with resonant subprocesses in a finite volume*, Phys. Rev. D **99** (2019) 014516, arXiv: `1810.01429` [`hep-lat`].

[115] M. Mai and M. Döring, *Three-body Unitarity in the Finite Volume*, Eur. Phys. J. A **53** (2017) 240, arXiv: `1709.08222` [`hep-lat`].

[116] M. Mai and M. Doring, *Finite-Volume Spectrum of $\pi^+\pi^+$ and $\pi^+\pi^+\pi^+$ Systems*, Phys. Rev. Lett. **122** (2019) 062503, arXiv: `1807.04746` [`hep-lat`].

[117] M. T. Hansen and S. R. Sharpe, *Lattice QCD and Three-particle Decays of Resonances*, Ann. Rev. Nucl. Part. Sci. **69** (2019) 65, arXiv: `1901.00483` [`hep-lat`].

[118] F. Müller, J.-Y. Pang, A. Rusetsky and J.-J. Wu, *Relativistic-invariant formulation of the NREFT three-particle quantization condition*, JHEP **02** (2022) 158, arXiv: `2110.09351` [`hep-lat`].

[119] F. Müller, J.-Y. Pang, A. Rusetsky and J.-J. Wu, *Three-particle Lellouch-Lüscher formalism in moving frames*, (2022), arXiv: `2211.10126` [`hep-lat`].

[120] U.-G. Meißner and A. Rusetsky, *Effective Field Theories*, Cambridge University Press, 2022.

[121] D. Hoja, U. .-. Meißner and A. Rusetsky, *Resonances in an external field: The 1+1 dimensional case*, JHEP **04** (2010) 050, arXiv: `1001.1641` [`hep-lat`].

[122] A. Baroni, R. A. Briceño, M. T. Hansen and F. G. Ortega-Gama, *Form factors of two-hadron states from a covariant finite-volume formalism*, Phys. Rev. D **100** (2019) 034511, arXiv: `1812.10504` [`hep-lat`].

[123] H. Hellmann, *Einführung in die Quantenchemie*, Deuticke, Leipzig und Wien (1937).

[124] R. P. Feynman, *Forces in Molecules*, Phys. Rev. **56** (1939) 340.

[125]   J. Lozano, U.-G. Meißner, F. Romero-López, A. Rusetsky and G. Schierholz,
Resonance form factors from finite-volume correlation functions with the external field method,
JHEP **10** (2022) 106, arXiv: 2205.11316 [hep-lat].